Berichte
zur Polar-
und Meeresforschung

668
2013

Reports
on Polar and Marine Research

The Expedition of the Research Vessel "Polarstern" to the Antarctic in 2013 (ANT-XXIX/4)

Edited by
Gerhard Bohrmann
with contributions of the participants

HELMHOLTZ
GEMEINSCHAFT

Alfred-Wegener-Institut
Helmholtz-Zentrum für Polar-
und Meeresforschung
D-27570 BREMERHAVEN
Bundesrepublik Deutschland

ISSN 1866-3192

Hinweis

Die Berichte zur Polar- und Meeresforschung werden vom Alfred-Wegener-Institut Helmholtz-Zentrum für Polar- und Meeresforschung in Bremerhaven* in unregelmäßiger Abfolge herausgegeben.

Sie enthalten Beschreibungen und Ergebnisse der vom Institut (AWI) oder mit seiner Unterstützung durchgeführten Forschungsarbeiten in den Polargebieten und in den Meeren.

Es werden veröffentlicht:

— Expeditionsberichte (inkl. Stationslisten und Routenkarten)

— Expeditions- und Forschungsergebnisse (inkl. Dissertationen)

— wissenschaftliche Berichte der Forschungsstationen des AWI

— Berichte wissenschaftlicher Tagungen

Die Beiträge geben nicht notwendigerweise die Auffassung des Instituts wieder.

Notice

The Reports on Polar and Marine Research are issued by the Alfred-Wegener-Institut Helmholtz-Zentrum für Polar- und Meeresforschung in Bremerhaven*, Federal Republic of Germany. They are published in irregular intervals.

They contain descriptions and results of investigations in polar regions and in the seas either conducted by the Institute (AWI) or with its support.

The following items are published:

— expedition reports (incl. station lists and route maps)

— expedition and research results (incl. Ph.D. theses)

— scientific reports of research stations operated by the AWI

— reports on scientific meetings

The papers contained in the Reports do not necessarily reflect the opinion of the Institute.

The „Berichte zur Polar- und Meeresforschung” continue the former „Berichte zur Polarforschung”

* Anschrift / Address
Alfred-Wegener-Institut
Helmholtz-Zentrum für Polar- und Meeresforschung
D-27570 Bremerhaven
Germany
www.awi.de

Editor:
Dr. Horst Bornemann

Assistant editor:
Birgit Chiaventone

Die "Berichte zur Polar- und Meeresforschung" (ISSN 1866-3192) werden ab 2008 als Open-Access-Publikation herausgegeben (URL: http://epic.awi.de).

Since 2008 the "Reports on Polar and Marine Research" (ISSN 1866-3192) are available as open-access publications (URL: http://epic.awi.de)

The Expedition of the Research Vessel "Polarstern" to the Antarctic in 2013 (ANT-XXIX/4)

Edited by
Gerhard Bohrmann
with contributions of the participants

Please cite or link this publication using the identifier
hdl:10013/epic.41984 or http://hdl.handle.net/10013/epic.41984

ISSN 1866-3192

ANT-XXIX/4

22 March - 16 April 2013

Punta Arenas – Port Stanley
Scotia Sea

Chief Scientist
Gerhard Bohrmann

Coordinator
Rainer Knust

Contents

1.	**Zusammenfassung und Fahrtverlauf**		**3**
	Summary and Itinerary		**4**
	Fahrtverlauf		**5**
	Cruise Narrative		**13**
2.	**Weather Conditions**		**19**
3.	**Multibeam Echo-Sounding and Survey**		**23**
4.	**Subbottom Profiling and Flare Imaging**		**40**
5.	**Ocean Floor Observation System (OFOS)**		**46**
	5.1	**OFOS-1 (PS81/268-1) at Quest caldera**	**50**
	5.2	**OFOS-2 (PS81/268-2) at Quest caldera**	**53**
	5.3	**OFOS-3 (PS81/269-1) at fore-arc**	**56**
	5.4	**OFOS-4 (PS81/270-1) at fore-arc**	**57**
	5.5	**OFOS-5 (PS81/273-1) at fore-arc**	**60**
	5.6	**OFOS-6 (PS81/274-3) at fore-arc**	**63**
	5.7	**OFOS-7 (PS81/275-1) at Protector Shoal**	**65**
	5.8	**OFOS-8 (PS81/276-1) at the rim of Quest caldera**	**68**
	5.9	**OFOS-9 (PS81/278-1) at unnamed submarine volcano**	**71**
	5.10	**OFOS-10 (PS81/285-1) at Cumberland Bay Flare**	**74**
6.	**Late Pleistocene South Georgia and Scotia Sea Marine Sediments**		**80**
7.	**Multi-Sensor Core Logging and Other Physical Properties Measurements**		**87**
8.	**Thermal Properties: *In-situ* Temperature, Bottom Water Temperature and Thermal Conductivity Measurements**		**91**
9.	**Sediment Geochemistry and Biogeochemistry**		**99**
10.	**Biogeochemistry of the Water Column**		**108**
11.	**Molecular Composition of Sedimentary Organic Matter and Radiocarbon Dating**		**115**

12. Late Quaternary Cimatic and Environmental History of South Georgia 117

13. At-Sea Distribution of Sea Birds and Marine Mammals, Representatives of the Oceans Food Chain's Higher Trophic Levels 136

APPENDICES

A.1 Teilnehmende Institute / Participating Institutions 139

A.2 Fahrtteilnehmer / Cruise Participants 142

A.3 Schiffsbesatzung / Ship's Crew 144

A.4 Station List PS 81 146

A.5 PS81 Core Descriptions 157

A.6 CTD Stations, Water Depths and Samples 162

1. ZUSAMMENFASSUNG UND FAHRTVERLAUF

Gerhard Bohrmann MARUM

Der vierte Fahrtabschnitt der 29. *Polarstern*-Expedition in die Antarktis startete am 22. März in Punta Arenas, Chile, und endete auf den Falkland-Inseln in Port Stanley. Südgeorgien wurde nach 5 Tagen Transit erreicht, wobei die Anfahrtszeit zum Test der neuen Software von HYDROSWEEP und zur Kalibrierung des Systems genutzt wurde. Im Bereich Südgeorgien wurde ein international zusammengesetztes Team von sechs Sedimentologen und Geomorphologen in der westlichen Cumberland-Bucht ausgeschifft, die in den kommenden zwei Wochen amphibische Sediment-Beprobungen in Lagunen und tiefen Seen durchführten. Vom Forschungsschiff *Polarstern* wurden parallel dazu bathymetrische und sedimentechographische Vermessungen sowie Beprobungen der glazialen und postglazialen Sedimente in der Cumberland-Bucht durchgeführt.

Nach einem weiteren Tag Transit in östliche Richtung begann das Hauptprogramm im Bereich um die Südsandwich-Inseln. Während ca. 10 Tagen wurden vor allem Vermessungen am Meeresboden mit den schiffseigenen Systemen sowie Beprobungen von Wassersäule und Meeresbodensedimenten und Explorationsbeobachtungen mit dem OFOS (Ocean Floor Observation System) durchgeführt, um Hinweise auf hydrothermale Quellen und Cold Seeps zu explorieren. Die Arbeiten konzentrierten sich auf 3 Regionen. In der 1. Region im Bereich nördlich der Südsandwich-Inseln wurden in drei verschiedenen Vulkanstrukturen Temperaturanomalien von 1 - 3°C nachgewiesen, die zusammen mit der OFOS-Beobachtung von Chimney-Strukturen als deutliche Hinweise auf hydrothermale Aktivität zu interpretieren sind. In einem zweiten Untersuchungsgebiet östlich der Inseln Saunders und Montague in 3.000 - 4.000 m Wassertiefe des Fore-Arcs wurde ein Cold Seep anhand einer akustischen Anomalie in der Wassersäule identifiziert. Aufgrund der Wetterverhältnisse und technischer Schwierigkeiten musste die detaillierte Untersuchung dieses Quellaustritts auf eine zukünftige Reise mit einem ROV verschoben werden. In einem dritten Arbeitsgebiet östlich der südlichsten Südsandwich-Inseln wurden opalreiche Sedimente der Südamerikanischen Platte beprobt, welche die Subduktionsfabrik der ozeanischen Konvergenzzone chemisch als ein Endglied der globalen Subduktionszonen charakterisiert.

Beprobungen der Wassersäule, der Sedimente rundeten das Untersuchungsprogramm ab und während eines weiteren Transittages erreicht *Polarstern* die Südgeorgien Insel, wo sehr erfolgreich Methanemissionen in mehreren glazialen Trögen untersucht werden konnten. Ausgedehnte Kartierungen mit PARASOUND und HYDROSWEEP erbrachten zahlreiche weitere Lokationen von Gas-Seeps, die für zukünftige Untersuchungsprogramme sehr gute Tauchziele mit einem ROV darstellen. Nachdem die Feldgruppe in der westlichen Cumberland-Bucht aufgenommen worden war und ein kurzer Besuch der alten Walfänger-Station Grytviken stattgefunden hatte, dampfte *Polarstern* drei Tage in westliche Richtung nach Port Stanley.

Während der 26 Expeditionstage hat *Polarstern* eine Strecke von 4.819 nautischen Meilen zurückgelegt, wobei die Lotsysteme PARASOUND und HYDROSWEEP kontinuierlich Daten aufgezeichnet haben. Es wurden 18 Schwerlot-Stationen, 12 Multicorer-Stationen, 10 Profile der Wasserschallsonde, 9 OFOS-Profile, 8 CTD-Stationen und 6 Multinetzeinsätze durchgeführt. Zusätzlich wurden biologische Beobachtungen der Vögel und marinen Säugetiere entlang der Fahrtroute durchgeführt.

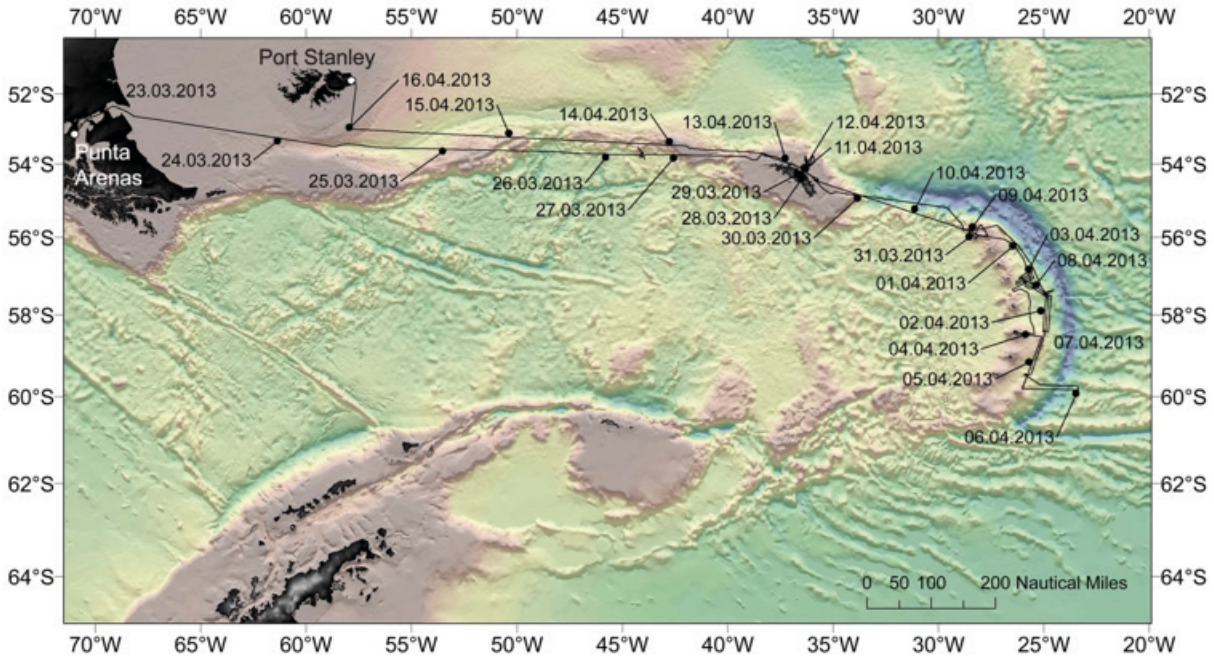

Abb. 1.1: Fahrtroute der Polarstern-Expedition ANT-XXIX/4 im Bereich der Scotia Sea

Fig. 1.1: Cruise track of Polarstern during expedition ANT-XXIX/4 in the Scotia Sea area

SUMMARY AND ITINERARY

Leg 4 of research vessel *Polarstern* cruise 29 started on March 22, 2013 in Punta Arenas, Chile and ended on April 26 in Port Stanley on the Falkland Islands. Five days transit from Punta Arenas to the east brought the vessel to South Georgia. The time was used to test the new upgrade of the HYDROSWEEP and to calibrate this multi-beam system. After *Polarstern* reached South Georgia an international team of six sedimentologists and geo-morphologists was disembarked in the western Cumberland Bay. The group performed amphibian sediment sampling in lagoons and abyssal lakes of the bay during two weeks. *Polarstern* mapped the Cumberland Bay and sampled glacial and post-glacial sediments.

Afterwards *Polarstern* had another day transit to the east to reach the South Sandwich Islands where we performed 10 days of sea-bottom and sediment mapping, sampling of sediments, water column measurements and sea-floor observations by OFOS (Ocean Floor Observation system) in order to find indications

for sea-floor seepage and hydrothermal systems. We worked in 3 different areas: In the northern part of the South Sandwich Islands, submarine volcanoes have been investigated and in total we found 3 places of hydrothermal activities which were indicated by temperature anomalies between 1 - 3°C in the water column and by chimney structures which were observed by OFOS. In a second area of the 3,000 – 4,000 m deep fore-arc basin east of Saunders and Montague Islands a cold seep was pre-investigated, which was found by an acoustic anomaly in the water column. A ROV-survey is needed in order to understand the seepage system in detail. In a third area, east of the southernmost South Sandwich Island, we crossed the deep sea trench and sampled the highly pure diatom ooze of the incoming plate of this zone of convergence.

Water column and sediment sampling completed the program in this area and another day of transit brought us back to South Georgia Island, where we successfully concentrated on the sampling of gas emission sites in two glacial troughs. Extensive mapping by PARASOUND and HYDROSWEEP helped to find several additional gas emission sites, which will be investigated during future cruises. After embarkation of the field group and a short visit of the old whaling station Grytviken *Polarstern* sailed three days back to the west in order to reach the final harbor.

During the 26 days of expedition *Polarstern* covered a distance of 4,819 nm and successfully performed 18 gravity cores, 12 multicorer, 10 sound velocity profiles, 9 OFOS tows, 8 CTD stations and 6 multi-nets. During most of the sailing time continuous measurements of the sediment-echo-sounder PARASOUND and the multi-beam HYDROSWEEP were recorded. In addition, the at-sea distribution of sea birds and marine mammals was worked out by continuous investigation of biologists along the sailing track.

FAHRTVERLAUF

Am Freitag, den 22. März 2013, verließ FS *Polarstern* um 15:00 Uhr Ortszeit ihren Platz an der Bunkerpier Cabo Negro Punta Arenas (Chile) und erreichte nach Durchfahrt der östlichen Magellan Straße das offene Wasser des Südatlantiks. Dem Auslaufen von FS *Polarstern* war eine Liegezeit im Hafen von Punta Arenas vorausgegangen, wobei Mannschaft, Wissenschaftler und wissenschaftliche Geräte der beiden Fahrtabschnitte 3 und 4 der 29. Antarktisreise des Schiffes ausgetauscht wurden. 44 Besatzungsmitglieder und 52 Wissenschaftler und Techniker aus Deutschland, Großbritannien, Belgien, Österreich, USA, China, Australien, Brasilien, Frankreich und Russland wurden am 20. und 21. März auf FS *Polarstern* eingeschifft und nutzten die Zeit, um notwendige Arbeiten an Deck und in den Laboren vorzunehmen. Aufgrund zahlreicher Flugumlegungen verlief die weite Anreise aus Deutschland nach Punta Arenas sehr holprig, wobei fast alle Teilnehmer auf unterschiedliche Art betroffen waren. Nach zwei Tagen Fahrt bei Windstärken 3-6 Beaufort durch recht ruhiges Wasser in östliche Richtung hatten wir schon zwei Fünftel der Transitstrecke nach Südgeorgien geschafft, wo wir die ersten Stationsarbeiten planten. Nach Überschreitung der EEZ Argentiniens wurde gegen 19 Uhr mit der Registrierung und profilierenden Darstellung der akustischen Systeme PARASOUND und HYDROSWEEP begonnen, die von den Wissenschaftlern

durch einen 24-Stunden Wachbetrieb betreut wurden. Zum Fächerecholot HYDROSWEEP wurde im Hafen eine neue und wesentlich erweiterte Software durch einen mitfahrenden Ingenieur der Firma ATLAS installiert.

Auf dem Transitweg nach Südgeorgien wurden am Montag, den 25. März, größere Wassertiefen von 3.000 bis 4.000 m erreicht, wobei erstmals die Qualität des Fächerecholots HYDROSWEEP für diese Wassertiefen getestet werden konnte. Am folgenden Dienstag wurden die Kalibrierungen des Systems für Pitch, Roll und Patch-Test vorgenommen, wozu jeweils drei Fahrtstrecken von 7-8 nautischen Meilen in beiden Richtungen entlang der genau festgelegten Fahrtrouten in sowohl ebenem Gelände als auch in Meeresbereichen mit unterschiedlichen Hangneigungen des Meeresbodens abgefahren wurden. Im gleichen Meeresgebiet wurde eine CTD-Sonde bis 2.200 m Wassertiefe gefahren, um ein möglichst genaues Wasserschallmodell zu ermitteln, dessen Parameter eine Basis der akustischen Tiefenlotungen von HYDROSWEEP darstellt. Gleichzeitig wurden mit der CTD-Sonde erste Wasserproben in unterschiedlichen Tiefen genommen, woraus organische Partikel zur weiteren Untersuchung filtriert wurden.

Am Mittwoch, den 27. März, erreichten wir die Nordwestspitze der Insel Südgeorgien und kartierten einen ca. 400-500 m breiten Streifen des Schelfs indem wir etwa parallel zur Küstenlinie in südöstliche Richtung dampften. Die Biologen aus Belgien, verantwortlich für die Wal- und Vogelbeobachtung, hatten nun alle Hände voll zu tun, um die reichhaltige Fauna im Meer und in der Luft zu registrieren. Die Insel ist etwa 160 km lang, 30 km breit und durch tiefe Fjordsysteme, die sich in die Landmasse einschneiden, gekennzeichnet (Fig. 1.3), wobei die beiden Fjorde der Cumberland Bucht die tiefsten morphologischen Einschnitte Südgeorgiens darstellen. Gegen 18 Uhr Bordzeit erreichten wir die zwischen Larsen und Barff Point etwa 7 km breite Einfahrt der Cumberland Bucht und steuerten zwischen unterschiedlich geformten Eisbergen in den östlichen Arm der Bucht direkt auf den Nordenskjöld Gletscher zu. Dieser Gletscher hat einen Großteil seines Nährgebietes in der höchsten Bergregion Südgeorgiens, die mit dem Gipfel des Mount Paget eine Höhe von 2.934 m erreicht.

Entlang eines Profils von der äußeren in die innere Bucht wurden Sedimentkerne zur Beprobung des Geschiebelehms und der nacheiszeitlichen Ablagerungen genommen und durch Multicorer-Einsätze ergänzt (Fig. 1.5). Sedimentologische Untersuchungen dieser Kerne sind Teil des Untersuchungsprogramms der postglazialen Entwicklung Südgeorgiens. Zusätzliche Untersuchungen der Porenwässer an den gleichen Kernen werden zur Klärung biogeochemischer Stoffkreisläufe der Fjordsysteme herangezogen. In der weiteren Nacht haben wir die Vermessung der westlichen Bucht mit PARASOUND und HYDROSWEEP vorgenommen, um auch dort eine gezielte Beprobung vornehmen zu können.

Am Donnerstag, den 28. März, lag FS *Polarstern* pünktlich um 8:00 Uhr am Eingang zur King Edward Bucht, um dort die Repräsentanten der Regierung von Südgeorgien und den Südsandwich Inseln vor der KEP-Station (King Edward Point) an Bord von FS *Polarstern* zu empfangen.

Die Inselvertreterin der Regierung kam mit dem Stationsleiter an Bord, um die Einklarierung unserer sechsköpfigen Landgruppe vorzunehmen. Eine intensive Einweisung in die Gepflogenheiten und die aktuellen Probleme der Insel waren neben den Umweltschutzbedingungen und vor allem den Verhaltensregeln gegenüber der Tierwelt das Hauptthema. Zurzeit wird in großem Maßstab eine Rattenvernichtungsaktion auf Südgeorgien durchgeführt, da diese Nagetiere,

die schon im 18. Jahrhundert mit den Walfangschiffen zur Insel kamen, sich millionenfach vermehrt haben und einheimische Tiere auszurotten drohen. Die Gespräche waren auch für das Schiff und die Fahrtleitung hoch interessant und alle wichtigen Absprachen waren schnell erledigt, so dass FS *Polarstern* zur westlichen Cumberland Bucht verholen konnte. Dort wurden mit Schlauchboot und einer eigens mitgebrachten schwimmenden Plattform die Geländeausrüstung in der Jason Bucht zum Strand transportiert, wo das international zusammengesetzte Landteam, bestehend aus 6 Glazialsedimentologen und Geomorphologen in den kommenden 2 Wochen amphibische Sedimentkernbeprobungen in der kleinen Jason Lagune und in tieferliegenden Seen der Bucht durchführen konnten. Die Anlandung klappte hervorragend in der windgeschützten Bucht, während im Zentrum der Cumberland Bucht die von den Gletschern kommenden Fallwinde für recht raue Wind- und Seeverhältnisse sorgten.

Am Nachmittag führten wir entlang des PARASOUND-Profils eine Beprobung der postglazialen Sedimente auch in der westlichen Cumberland Bucht durch. Die Ablagerungen, in den PARASOUND-Daten als hervorragend geschichtet in den Senken der Geschiebelehmrücken sichtbar, zeigten neben der Stratifizierung aber auch maskierte Bereiche, sogenanntes Blankening, ein untrüglicher Hinweis auf die Exístenz von freiem Gas. Ein große Überraschung für uns waren die zahlreichen Gas-Flares in der Wassersäule, die akustisch im Echolot durch die Registrierung des 18kHz-Signals in Erscheinung traten und Gas-Austritte am Meeresboden in die Wassersäule dokumentieren. Über 50 solcher Gasaustrittsstellen wurden mit dem PARASOUND registriert und scheinen auf die glazialen Rinnen und Tröge auf dem Kontinentalschelf von Südgeorgien konzentriert zu sein. Unseres Wissens nach sind dies die ersten von FS *Polarstern* registrierten Gas-Flares in der Subantarktis und Antarktis.

Ein weiterer sehr kurzer Besuch zum KEP diente am Karfreitag, den 29. März, der Ausklarierung des HYDROSWEEP Ingenieurs. Er wurde freundlicherweise vom Stationsboot abgeholt und zur KEP-Station an Land transportiert. Von dort führte sein Weg zur MS *Ortelius*, einem Kreuzfahrtschiff, das die alte Walfangstation Grytviken aufsuchte. Mit dem Schiff trat er seine Rückreise über Montevideo an. FS *Polarstern* nahm danach Fahrt auf in östliche Richtung zu den Süd-Sandwich Inseln (Fig. 1.2). Elf vulkanische Inseln und zahlreiche submarine Vulkane bilden infolge der Subduktion im Südsandwich Graben einen vulkanischen Bogen von ca. 300 km Nord-Süd-Erstreckung im zentralen Bereich der Süd-Sandwich Mikroplatte. Besonders im nördlichen Bereich treten Vulkankegel saurer vulkanischer Gesteine auf, die bis zu 400 – 50 m unterhalb der Wasseroberfläche reichen. Acht dieser Vulkanstrukturen haben wir mit PARASOUND und HYDROSWEEP vermessen und vor allem im Hinblick auf mögliche Gas-Emissionen hin untersucht (Fig.1.4). Leider konnten wir keine Gas-Flares im Bereich der Vulkane entdecken, was auf hydrothermale Aktivität hindeuten könnte. Auch ein Beobachtungsprofil mit dem AWI-Video-Schlitten (OFOS = ocean floor observation system) in der QUEST-Caldera zeigte keinerlei optische Hinweise auf Hydrothermalismus. Ein zweiter OFOS-Einsatz über einem vielversprechenden, unbekannten Vulkan konnte aufgrund eines Fischerbootes, das mit Langleinen dort arbeitete, nicht durchgeführt werden und so dampfte FS *Polarstern* am Sonntagnachmittag weiter nach Südwesten, um Untersuchungen im Forearc des Inselbogens durchzuführen (Fig. 1.4).

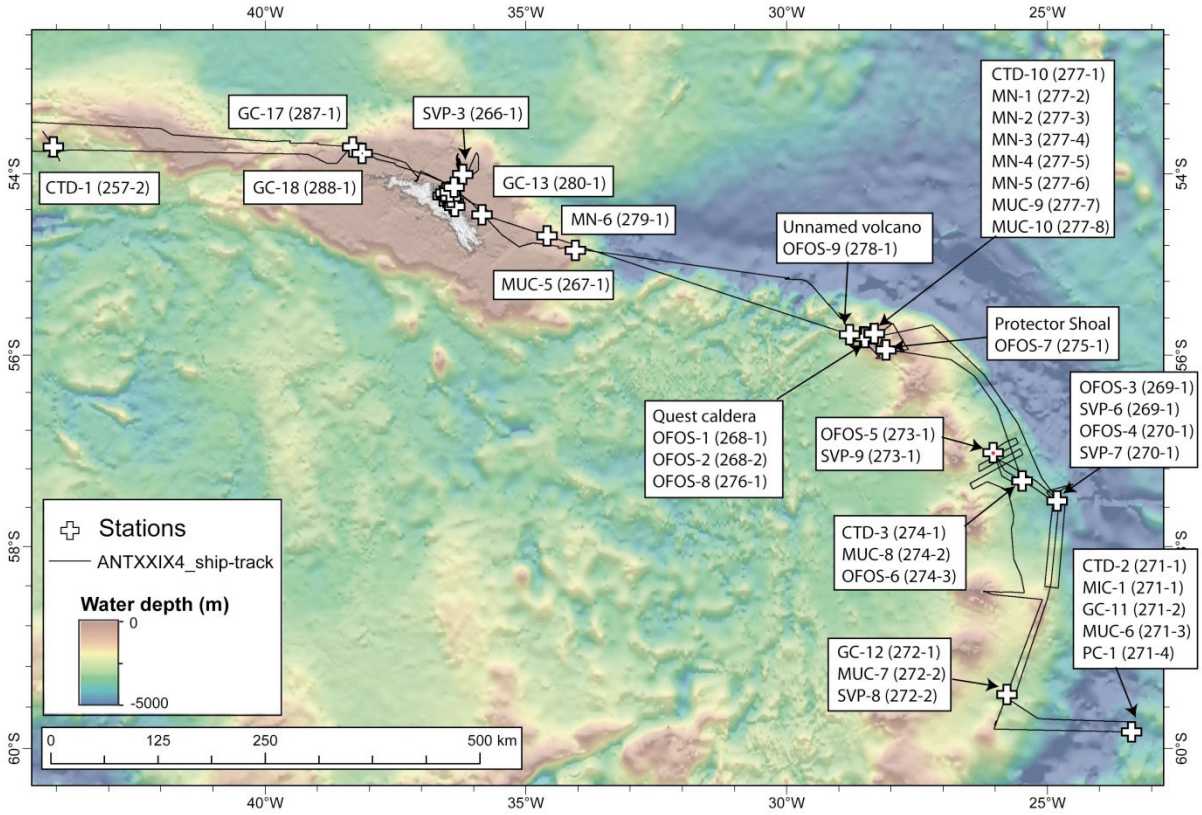

Fig. 1.2: Fahrtroute und Beprobungslokationen der Polarstern-Reise ANT-XXIX/4
Fig. 1.2: Track lines and locations of station work during Polarstern ANT-XXIX/4

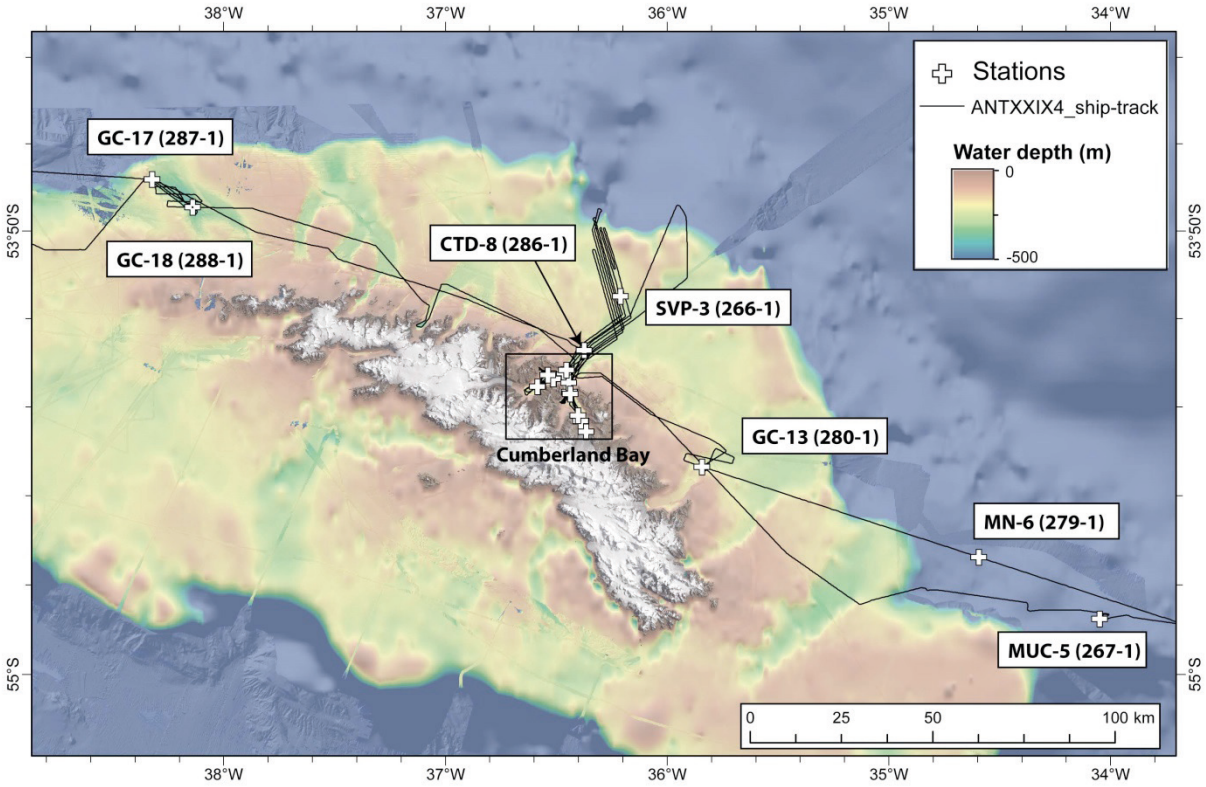

Fig. 1.3: Fahrtverlauf und Beprobungsstationen der Umgebung Süd-Georgiens
Fig. 1.3: Track lines and stations during Polarstern around South Georgia

Nachdem wir am Sonntagabend, den 31. März, die nördlichste Region der submarinen Vulkane der Süd-Sandwich Vulkankette verlassen haben, kartierten wir mit den schiffseigenen Vermessungssystemen PARASOUND und HYDROSWEEP während der Fahrt nach Süden einen unbekannten Rücken, der östlich des vulkanischen Bogens etwa 1.000 m aus dem Forarc-Bereich herausragt. Die oberflächennahen Strukturen lassen diesen Rücken als eine herausgehobene tektonische Scholle der Plattenkonvergenz erscheinen, deren genauere tektonische Position ohne seismische Vermessung nicht zu interpretieren ist. Unser nächstes Zielgebiet war der Forarc-Bereich des nördlichen Sandwichbogens, dessen Meeresbodenbeschaffenheit auf der geographischen Breite der Inseln Visokoi, Candlemas und Saunders im Rahmen einer groß angelegten Untersuchung des BAS vor 18 Jahren exploriert wurde. Damals wurde das tiefgeschleppte System HAWAI MR1 benutzt, um sowohl die Rückstreuung des Meeresbodens als auch die Bathymetrie zu erfassen. Wir haben im Vorfeld diese Daten sehr genau studiert und nach Lokationen gesucht, die erhöhte Rückstreuwerte bei möglichst ebener Bathymetrie zeigen. Aus der Erfahrung mit anderen Regionen können solche Bereiche mit erhöhtem Backscattersignal Lokationen charakterisieren, in denen Fluid- und Gaszirkulation die physikalischen Eigenschaften des Meeresbodens stark verändern. Die auffälligste Backscatter-Anomalie wurde gleich mit einem OFOS-Profil (OFOS = Ocean Floor Observation System) auf der Höhe der Insel Saunders in 3.700 m Wassertiefe überfahren. Leider musste aufgrund eines Problems mit der Winde das OFOS wieder an Bord gehievt werden.

Eine Reparatur der Winde wurde notwendig und so nutzen wir die Zeit mit einer weiteren Vermessung des Forearc-Bereiches, die sowieso auf dieser Reise geplant war. Nach ca. 14 Stunden Vermessung wurde das OFOS wieder eingesetzt und zeichnete hervorragende Bilder des Meeresbodens in hoher Farbqualität auf. Störungen der Bildübertragung nahmen mit der Zeit stark zu und nach einer Stunde musste das OFOS-Profil leider abgebrochen werden. Die Bodenzeit von OFOS reichte aber aus, um den Unterschied der verschiedenen Rückstreuwerte des Meeresbodens zu dokumentieren, welches das Hauptziel des OFOS-Einsatzes war. Nach Bergung des Gerätes stellte sich heraus, dass eine Faser des Glasfaserkabels ca. 40 m vor dessen Endstück einen Defekt hatte. Während das System auf die 2. Glasfaser des Schiffsdrahtes umgelegt wurde, haben wir einen plateauartiger Bereich des oberen Hanges in 2.000 m kartiert, der vorwiegend durch die magmatischen Gesteine der aktiven Sandwichvulkane gebildet wurde. Da die Vorhersagen unseres Bordmeteorologen für den kommenden Tag einen Sturm mit Windstärken von 9-10 auf der Beaufortskala bei einem Seegang von 6 m prognostizierten und die stärkeren Windgeschwindigkeiten im nördlichen Inselbogen sein sollten, haben wir uns entschieden mit FS *Polarstern* unseren Weg weiter nach Süden zum südlichen Sandwichbogen anzutreten.

Dies wurde am Mittwoch, den 3. April, bei weithin kontinuierlicher Aufzeichnung der PARASOUND- und HYDROSWEEP-Signale umgesetzt. Die vorausgesagte Wetterprognose stimmte leider sehr und am späten Abend legte sich das Schiff im Lee der Insel Montague in den Wind, um die z.T. heftigen Windböen abzuwettern (Fig. 1.4). Im Schutz der Insel gab es vor allem einen Wellenschutz, sodass es den seekranken Mitfahrern an Bord etwas angenehmer wurde. Dies war notwendig geworden, da Stationsarbeiten nicht mehr möglich waren und auch die Fächerecholotaufzeichnungen kaum noch nutzbar waren. Am Donnerstagmorgen sahen wir nach Sonnenaufgang, wie nah das Schiff an der Küste von Montague abwetterte, wobei vor allem eine breite Gletscherfront mit scharfer Abbruchkante zu sehen war. Nachdem der Wind nur gering abflaute, entschlossen wir uns, im

Verlauf des Vormittags entlang weiterer Vermessungsprofillinien nach Süden dem Verlauf des Forarc-Bereichs zu folgen. In der Nacht zum Donnerstag erreichten wir unseren südlichsten Punkt auf der geographischen Breite 59° Süd und profilierten weiterhin mit dem Schiff nach Osten über den Südsandwich Tiefsee-Graben hinweg auf die Südamerikanische Platte (Fig. 1.4). Der im Norden über 8.000 m tiefe Tiefseegraben ist im Süden mit 6.000 m nicht ganz so tief eingeschnitten. Etwa 30 Seemeilen weiter östlich waren durch frühere Beprobungen sehr reine Kieselschlämme bekannt. Eine kurze Kartierung zeigte, dass es sich um ein sehr lokales Becken handelt, das durch wunderbar geschichtete Sedimente gefüllt ist.

Am Freitag, den 5. April, führten wir eine Beprobung dieser Lokation mit CTD/ Wasserschöpfern, Multicorer, Schwerelot und 20 m langem Kolbenlot durch (PS81/271-1 bis -4; Fig. 1.4). Das Kolbenlot (PS81/271-4) brachte eine Sequenz sehr reiner Opalschlämme von 18,50 m Mächtigkeit zu Tage, deren Lithologie auf Ablagerungsräume südlich der Polarfront begrenzt ist. Bei einer weiteren Beprobung von Sedimenten im südlichen Forarc zwischen den Inseln Bristol und Thule (PS81/272-1) konnten lediglich stark umgelagerte, kiesreiche Sediment geborgen werden.

Am Sonntag, den 7. April, befanden wir uns wieder auf der geographischen Breite der Candlemas Insel, wo ein hoch spannendes Phänomen in 3.800 m Wassertiefe untersucht wurde. Dort war im PARASOUND-Profil eine Plume-Struktur zu finden, die nur 40 m über den Meeresboden ragt, sich aber sehr klar vom Meeresboden abhebt. Leider konnten wir mit Bordmitteln die Struktur nicht ausreichend untersuchen und beproben. Vor allem die ablaufende Zeit saß uns im Nacken und so wird diese Austrittstelle erst in Zukunft bei einer möglichen Expedition mit einem Tiefseeroboter detailliert untersucht werden können. Die *Polarstern*-Expedition selbst ist als Explorationsreise angelegt, die Tauchziele für eine zukünftige Roboteruntersuchung definieren soll.

Ähnliche Explorationsergebnisse wurden auch am Montag, den 8. April, an drei submarinen Vulkanen (QUEST-Caldera, Protector Shoal und einem unbekannten magmatischen Vulkan) erhoben, an denen das Bodenwasser um mehr als 2°C, in einem Fall sogar 3,5°C erhöht war. Solche Temperaturanomalien sind klare Indikatoren für hydrothermale Quellen. Da das Glasfaserkabel des Schiffes zum Zeitpunkt der Untersuchung nicht zur Verfügung stand, haben wir mit einen Videoschlitten gearbeitet, der über das Koaxkabel mit dem Schiff verbunden war. Obwohl die Bilder auf den Schiffsmonitoren dann nur schwarz/weiß und in deutlich schlechterer Qualität zu sehen waren, konnten wir zumindest einen ersten Eindruck in den Hydrothermalregionen gewinnen. Erste Schornsteine, die sehr wahrscheinlich ehemalige „Schwarze Raucher" darstellen, wurden gesichtet und belegen ebenfalls die hydrothermale Aktivität dieser Vulkane im nördlichen Süd-Sandwich Bogen. Auch dies sind zukünftige Tauchziele, die auf einer kommenden Reise mit dem Tauchroboter QUEST untersucht werden sollen.

Wie Satellitendaten zeigen, ist die Region der nördlichen Süd-Sandwich Inseln durch besonders hohe Planktonproduktivität gekennzeichnet, und zahlreiche Planktonnetzfänge wurden zur Untersuchung der Siliziumisotopie von opalinen Radiolarien-Skeletten durchgeführt. Ergänzt wurden sie durch Multicorer-Proben des Meeresbodens, welche ebenfalls für ein Hälterungsexperiment bentischer Foraminiferen genutzt werden.

Am Mittwoch, den 10. April, verließ FS *Polarstern* die Region der Süd-Sandwich Inseln und dampfte nach Westen in Richtung Südgeorgien, wo wir auf dem Schelf einen glazialen Trog mit Schwerelot und Multicorer beprobten. Mit dem Erreichen der Cumberland Bay haben wir am Ausgang der Bucht mit einem CTD-Profil entlang des Zentrums der östlichen Cumberland Bay begonnen und an dem stärksten Gas-Flare, das mit dem Namen Cumberland Gas-Flare bezeichnet wurde, auch Sedimentkerne genommen. Am folgenden Tag haben wir am frühen Morgen bei herrlichem Sonnenschein die südlichste CTD-Station des Profils unmittelbar am kalbenden Nordenskjöd Gletscher genommen (Fig.1.5). Sodann dampfte FS *Polarstern* in die westliche Cumberland Bucht zur Jason Lagune, wo unsere Feldgruppe schon ihre Ausrüstung auf das Transport- sowie Bohrplattformfloß gepackt hatte und angetrieben durch den Außenbordmotor langsam auf die *Polarstern* zu schipperte. Die Aufnahme der 6-köpfigen Gruppe auf FS *Polarstern* beendete deren 15-tägige Feldarbeit in der Umgebung der Jason Lagune. Das wissenschaftliche Beprobungsprogramm in der Cumberland Bucht ging nach dieser Abwechslung weiter bis zum Freitagmorgen um 08:00, wo wir der alten Walfängerstation Grytviken und der BAS Station King Edward Point (KEP) einen Besuch abstatten konnten. Dieser Ausflug gab dem Schiff und auch einigen Wissenschaftlern die Möglichkeit, das gerade eingelaufene britische Forschungsschiff *James Clark Ross* des BAS zu besuchen und im Rahmen von wissenschaftlichen und technischen Gesprächen sich mit den britischen Kolleginnen und Kollegen auszutauschen.

Mittlerweile hatten wir durch mehrere PARASOUND- und HYDROSWEEP-Profile in der Cumberland Bucht ein sehr genaues Verständnis über die Verteilung der jungen Sedimente und der Gas-Flares bekommen, so dass letzte Beprobungen sehr gezielt in der Bucht durchgeführt werden konnten. Aufgrund der Gas-Flares (Fig. 1.5) waren auch in den Sedimenten hohe Methankonzentrationen zu erwarten, die wir mit unseren GC-Messungen belegen konnten. Ob es sich dabei um mikrobiell-generiertes biogenes oder sogar thermogenes Gas handelt, werden die Isotopenanalysen an Kohlenstoff und Wasserstoff der Methanmoleküle im Heimlabor ergeben. Die Zusammensetzung der Gasfraktion spricht allerdings für eine biogene Gasbildung, die wahrscheinlich sehr oberflächennah in den marinen Ablagerungen stattfindet. In der Nacht von Samstag auf Sonntag (13./14. April) verließ FS *Polarstern* Südgeorgien in Richtung Westen (Fig.1.2).

An einer Kernposition südlich Falkland wurden in 7 m Länge die letzten 70.000 Jahre dokumentiert. Die Analysen des Kerns zeigen, wie sich die Subantarktische Front im Wechsel der Warm- und Kaltzeiten der letzten 70.000 Jahre verändert. Mit einem 20 m langen Kolbenlot wurde in Zusammenarbeit mit dem Britischen Antarktischen Dienst (BAS) ein 12,39 m langer Sedimentkern gezogen mit dem die ozeanographischen Verhältnisse weiter in der Vergangenheit zurückverfolgt werden können. Die *Polarstern*-Reise ANT-XXIX/4 endete am Dienstag, den 16. April, in Port Stanley/Falkland. Es war eine kurze, aber recht erfolgreiche Reise. Innerhalb der 26 Tage haben wir vieles gemessen, beprobt, neu entdeckt und neue Vorstellungen erlangt, die wir zukünftig in wissenschaftlichen Publikationen und Vorträgen veröffentlichen werden. Den Erfolg der wissenschaftlichen Arbeit haben wir auch der hervorragenden und freundlichen Unterstützung durch die Schiffsbesatzung, die Reederei und die AWI Logistik zu verdanken. Dafür danken wir Kapitän Schwarze und seiner gesamten Mannschaft sowie allen weiteren Beteiligten sehr herzlich!

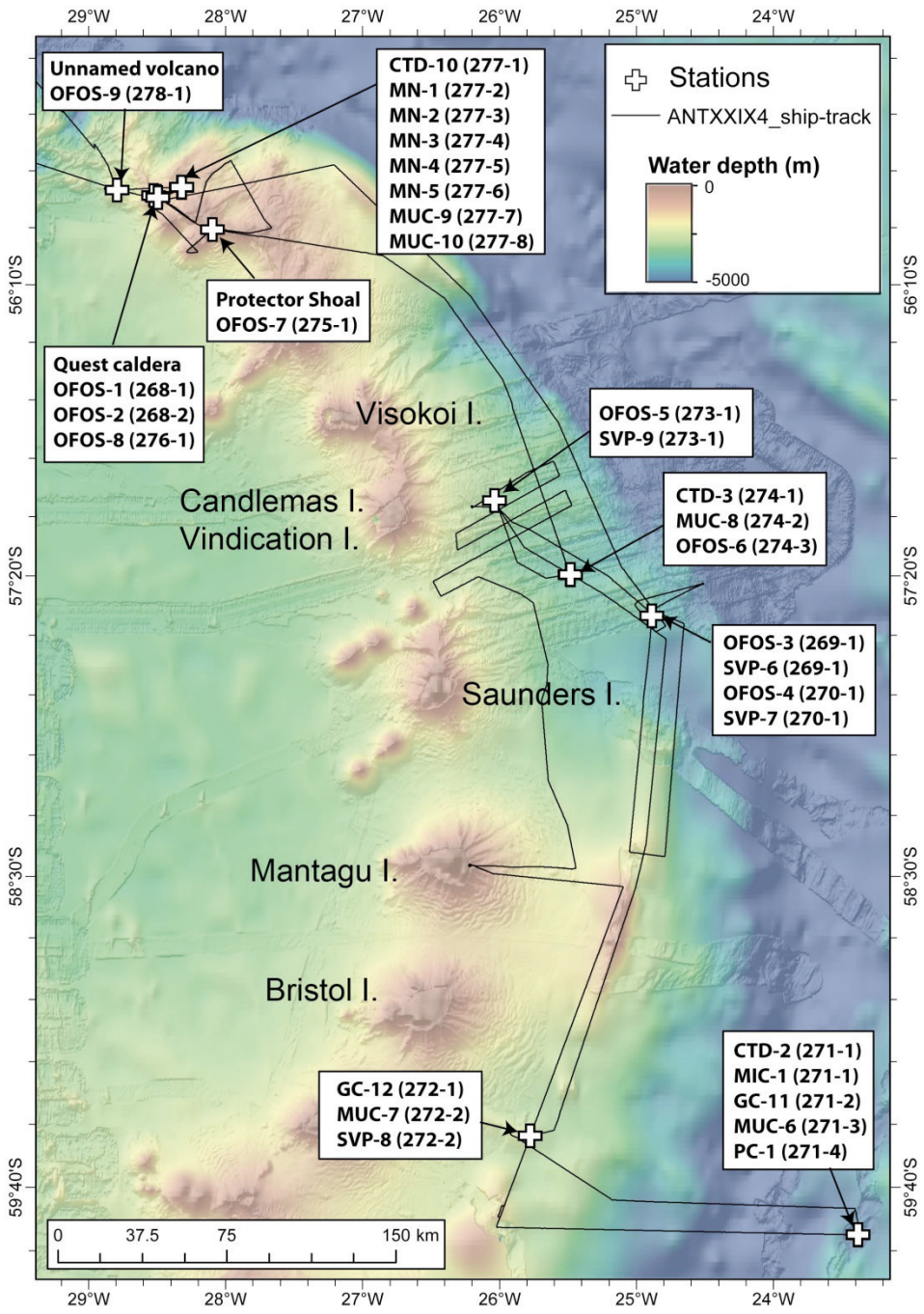

Fig. 1.4: Fahrtroute mit Beprobungen der ANT-XXIX/4 in der Umgebung der Süd-Sandwich Inseln
Fig. 1.4: Track lines of Polarstern cruise ANT-XXIX/4 around the South Sandwich Island Arc

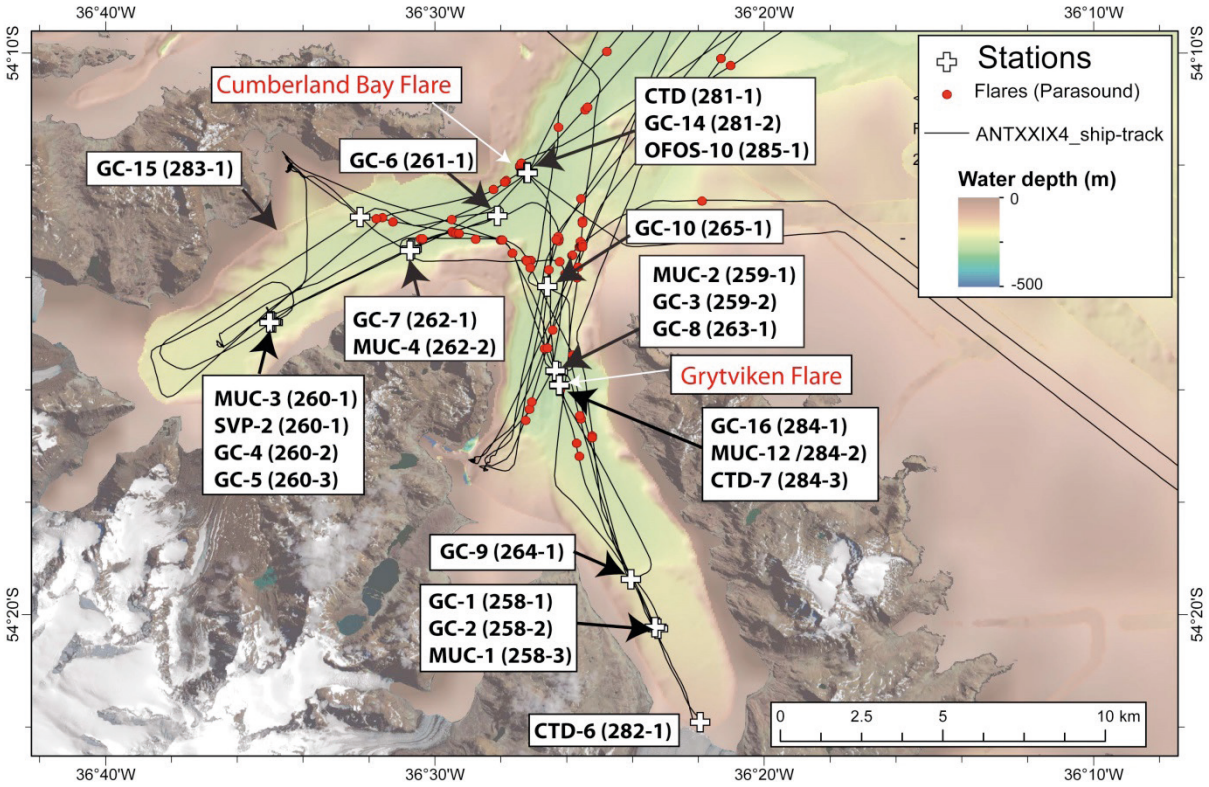

Fig. 1.5: Fahrtverlauf und Stationen in der Cumberland Bucht Ost und West während ANT-XXIX/4
Fig. 1.5: Track lines and stations during ANT-XXIX/4 in the Cumberland Bay West and East

CRUISE NARRATIVE

On Friday 22 February, 2013 *Polarstern* left at 3 p.m. local time her place situated at the bunker pier Cabo Negro Punta Arenas, Chile and reached after the passage through the Strait of Magellan the open water of the South Atlantic. Before sailing *Polarstern* had a demurrage in the port of Punta Arenas while crew members and scientists and scientific devices were exchanged between Legs 3 and 4 of Antarctic cruise no 29. 44 crew members and 52 scientists and technicians from Germany, Great Britain, China, Austria, Brazil, France, Australia, and Russia embarked on 20 and 21 March, and used the time for the necessary work on deck, and also to set up the labs. Because of many changes of flights the arrival of nearly all participants in Punta Arenas was problematic. After two days steaming through more or less calm water with wind 3 - 6 Beaufort to the east we reached already two fifth of the transit distance to South Georgia where we planned to have the first scientific stations. After crossing the EEZ of Argentina we started recording and plotting both hull-mounted acoustic systems, which are the multi-beam HYDROSWEEP and the PARASOUND sediment echo-sounder. Both systems are supervised by scientists working around the clock. For the HYDROSWEEP system new and strongly amplified software was installed in the port of Punta Arenas by *Atlas*.

During our transit to South Georgia we reached greater water depth of 3,000 to 4,000 m on Monday, 25 March, to test the data quality of our multi-beam system HYDROSWEEP at these depths. On the following Tuesday the calibrations of the system for pitch, roll and patch test were done; for each time of calibration a transect of 7 - 8 nautical miles was driven in two directions along set lines, comprising flat seafloor areas as well as slopes with different angles. In the same area a CTD sensor (Station PS81/257-2) was lowered to 2,200 m water depth (Fig. 1.2) to obtain a detailed sound velocity profile, a parameter which forms the basis for the acoustic depth measurements of HYDROSWEEP. At the same time the first water samples were collected at different depths with the water bottles on the CTD, which were then filtered for organic particles for later analysis.

On Wednesday, 27 March, we reached the NW corner of the island of South Georgia and there mapped a ~ 400 - 500 m wide strip of the shelf by steaming in parallel to the shoreline in a southeastern direction. The biologists from Belgium, responsible for the bird and whale observations, were very busy recording the rich bird and sea mammal life at sea and in the air. South Georgia is about 160 km long, 30 km wide and characterized by deep fjords which penetrate into the island (Fig. 1.3), of which those of Cumberland Bay are the longest. At around 6 pm shiptime we reached the 7 km wide entrance of Cumberland Bay between Larsen and Barff Points and steamed between variously shaped icebergs into the eastern arm of the bay, directly in front of the Nordenskjöld glacier. This glacier receives most of its ice from the highest mountain range on South Georgia, topped by Mount Paget at 2,934 m.

We then took a series of sediment cores with the gravity corer and multicorer along a transect from the outer to the inner area of Cumberland Bay East (Fig. 1.5). These cores are for studying of glacial and post-glacial deposits as part of a research program on the post-glacial history of South Georgia. Additional investigations of the pore water from the same sediment cores were used to investigate the biogeochemical cycling of the fjord systems. During the rest of the night we mapped the western bay with PARASOUND and HYDROSWEEP for subsequent targeted sampling. At 8 a.m. on Thursday, 28 March, *Polarstern* arrived at the entrance to King Edward Bay to receive representatives of the Government of South Georgia and the South Sandwich Islands, who live at the King Edward Point (KEP) station.

The Governmental Officer and the base commander came on board to clear customs for our shore-based research team of six people. A detailed introduction to the way of life on the island and its current problems were important parts of the briefing, as well as the regulations for environmental protection and behavior towards the wild life. At present a large-scale rat eradication program is underway. Rats reached South Georgia in the 18th century with the whaling fleets and then, by feasting on the local seabirds and their eggs, multiplied to millions of individuals, threatening to drive the many seabirds (including endemic species) to extinction. The briefing on board was interesting and useful for the ship’s captain and chief scientist, and the official clearing was done in good time so that *Polarstern* was able to steam to Cumberland Bay West. Here a *Polarstern* RIB (Rigid Inflatable Boat) and the purpose-designed, floating drilling platform were launched. These vessels took the cargo of the international shore-based team to the beach of Jason Bay. The team comprised of six glacial sedimentologists and geomorphologists, which took sediment cores in the small Jason Lagoon and further lakes in the vicinity

of the bay. The landing of the team went well in this calm, wind-sheltered bay. These conditions were a stark contrast to those around the corner in the centre of Cumberland Bay West where strong katabatic winds from at the end of the inlet glaciers were responsible for choppy sea conditions.

In the afternoon we followed the earlier PARASOUND profile to sample post-glacial sediments in Cumberland Bay West. The PARASOUND data showed nicely layered sediments in the glacially scoured troughs, but also wipe-out zones, which are unmistakable clues for the presence of free gas. A big, unexpected surprise for us were the numerous gas flares in the water column which appeared as acoustic signals in the 18kHz signal display of the echo-sounder. These documented the exit of gas from the seafloor into the water column. More than 50 of these flares and gas exit points were registered by PARASOUND, and they seem to be concentrated in the glacial channels and troughs along the continental shelf of South Georgia. To our knowledge these are the first gas flares in the sub-Antarctic and Antarctic regions found by *Polarstern*.

A further short visit to KEP on Good Friday was needed to drop off the HYDROSWEEP engineer, who was kindly picked-up by the station's patrol boat and brought to KEP. He boarded the cruise ship M/S *Ortelius* which was visiting the neighboring former whaling station Grytviken to start his home journey back to the office in Germany via Montevideo. *Polarstern* then sailed in easterly direction towards the South Sandwich Islands (Fig. 1.2). Because of subduction in the South Sandwich Trench eleven volcanic islands and several submarine volcanos form an arc of ~300 km from North to South in the centre of the South Sandwich micro-plate. Particularly in the northern area of the arc, acidic volcanic cones reach up to 400 – 50 m below sea level. We measured eight of these volcanic structures by PARASOUND *a*nd HYDROSWEEP, and monitored the screens for interesting submarine structures and potential gas emissions (Fig. 1.4). Unfortunately, we were not able to detect any gas flares in the vicinity of the volcanos, which might have indicated hydrothermal activity. In addition, a dive with the AWI underwater video sled OFOS (Ocean Floor Observation System) in the Quest Caldera found no evidence of hydrothermal activity. A second OFOS dive over a promising, unknown volcano could not go ahead as a long-line fishing vessel was working there (Fig. 1.4). Therefore, *Polarstern* steamed towards the South-West on Easter Sunday afternoon to start investigations in the fore-arc area of the South Sandwich Islands (Fig. 1.4).

After we left the northernmost submarine volcano area of the South Sandwich Island chain last Sunday evening, 31 March we mapped an unknown ridge on the southbound journey with the ship's acoustic survey systems PARASOUND and HYDROSWEEP. To the east of the South Sandwich volcanic arc, this ridge comes up to 1,000 m depth in the fore-arc basin. The near-surface structures indicate that this ridge might be an uplifted plate in a tectonic convergence, but its position and tectonic origin cannot be interpreted without a seismic survey. Our next target was the fore-arc basin of the northern South Sandwich Arc, the seafloor topography of which in the vicinity of Visokoi, Candlemas and Saunders Islands (Fig. 1.4) was explored during a detailed survey of the British Antarctic Survey 18 years ago. At that time the deep-towed HAWAII MR1 system was used to collect bathymetry and backscatter images of the seafloor. In preparation for this expedition we studied these data in detail and looked for locations which showed increased backscatter reflections on a relatively flat seafloor. Our experience from other regions indicated that such areas can be the locations where fluid or gas emissions strongly alter the

physical properties of the seafloor. The most pronounced backscatter anomaly we identified is in the vicinity of Saunders Island in 3,700 m depth and we surveyed this area with OFOS, our deep-sea camera system. Unfortunately, just after seeing the seafloor on the onboard screens we had to bring OFOS back on deck, as a mechanical winch problem occurred.

We then used the winch repair time for a planned further survey in the fore-arc basin. After 14 h of acoustic seafloor surveys OFOS was ready to go again and high quality colour HD images of the seafloor at 3,700 m water depth were obtained for an hour. After these errors in the image transfer along the 6,880 m of fiber-optic cable increased and consequently we had to abort the OFOS dive. Fortunately, OFOS's bottom time and the collected images were enough to characterize the nature of the different backscatter reflections of the seafloor and the main aim of the OFOS dive was achieved. With OFOS back on deck the trouble shooting team found that one fiber of the cable had a fault 40 m after the termination, and they then changed the OFOS data communication to the other fiber. While this work was being undertaken, the acoustic seafloor survey continued on a plateau-like area of the upper slope in 2,000 m depth, which is mostly formed by igneous rocks from the active volcanoes of the South Sandwich Islands. We then decided to continue our southbound voyage with *Polarstern* to the southern part of the arc as our on-board meteorologists forecasted a storm with 9 - 10 Beaufort scale winds and wave heights of 6 m with higher wind speeds in the northern island arc.

On Wednesday, 3 April we steamed to the South while continually gathering PARASOUND and HYDROSWEEP data. The forecast was correct and in the late evening we heaved to in the sheltered side of Montagu Island as heavy gusts surrounded us (Fig. 1.4). The shelter by the island offered protection from the storm and helped those affected by sea-sickness. Due to the high seas no station work was possible and even the multi-beam data were almost unusable. After sunrise on Thursday morning we saw how near the ship was to the coastline of Montagu Island, being only 2 nautical miles away, and this allowed us to see Mount Oceanite and a wide glacier front ending in sharp ice-edge at the sea. After the wind speeds decreased slightly we decided later in the morning to continue the acoustic survey lines towards the south of the fore-arc basin. That night we reached the southernmost position of our expedition at latitude of 59° S and then turned to the East to continue the survey across the South Sandwich Trench onto the South American Plate (Fig. 1.4). While the South Sandwich Trench is over 8,000 m deep in its northern part, the southern sector is less deep at 6,000 m. From the trench we steamed a further 30 nautical miles to the east for a comprehensive coring position where an earlier study found very pure biogenic opal and diatom ooze. Our short mapping survey showed a very localised basin filled with nicely layered sediments.

On Friday, 5 April we sampled the basin with the CTD and water sampler, multi-corer, gravity corer and the 20 m-long piston corer (PS81/271-1 to -4; Fig. 1.4). The piston corer (PS81/271-4) collected a 18.5 m long sequence of very pure biogenic opal ooze, a lithology which is restricted to the areas south of the Polar Front. After travelling back to the southern fore-arc area we had a further sediment coring station between Bristol and Thule Islands (PS272-1), but recovered only a small amount (14 cm) of dark colored sediments covered with a layer of volcanic pumice.

On Sunday, 7 April we were back at the latitude of Candlemas Island where we surveyed a very interesting phenomenon in 3,800 m water depth. PARASOUND data show a plume structure that raised 40 m above the seafloor, which was clearly distinct from the seafloor signal. This structure appeared not to be gas as these usually rise higher in the water column. Unfortunately, we were unable to investigate this structure with the scientific equipment we had on board, so its detailed exploration will have wait for the future when we hope to return with other scientific equipment, including remotely operated vehicles (ROVs). Our recent *Polarstern* expedition was planned as an exploratory cruise to find dive targets for future investigation by ROV.

On Monday 8 April we found more intriguing features on three submarine volcanoes (QUEST Caldera, Protector Shoal and one unnamed; Fig. 1.4), where seafloor temperatures were raised locally by 2°C, and in one area to 3.5°C above the ambient temperature. These thermal anomalies are clear indicators for hydrothermal activity. Unfortunately, the fiber optic cable was unavailable for the dives at these volcanos so we had to use an older, back-up video-sled via the coax cable. Although the video images on the ship-board monitors were black and white and in poorer quality compared to OFOS, we were able to get an impression of the hydrothermal areas. These included some small chimneys formed of white minerals, surrounded by microbial mats, and confirm the presence, for the first time, of hydrothermal activity at the submarine volcanoes of the northern South Sandwich Arc. These are dive targets which we would like to investigate in a future expedition with our ROV QUEST.

Based on satellite data, the region north of the South Sandwich Islands is known to have extremely high phytoplankton productivity. In light of this we used plankton nets to sample the radiolarian element of the phytoplankton for a study of the silicon isotopes in their opaline silica skeletons. We also took multicore samples from the seafloor, which will be used for *in-vivo* experiments on benthic foraminiferans.

On Wednesday, 10 April, we left the South Sandwich Islands and steamed westwards towards South Georgia, where we sampled sediments in one of the glacial shelf troughs using gravity and multi corers. On arrival in Cumberland Bay we started a CTD profile from the entrance of the bay to the center of Cumberland Bay East and sampled sediment cores at the strongest gas flare site, which we named the „Cumberland Bay Flare". In the bright sunshine early next morning we had the southernmost CTD station on the profile in front of the Nordenskjöld Glacier (Fig. 1.5). Then *Polarstern* steamed towards Jason Lagoon in Cumberland Bay West, where our terrestrial field party had already packed their cargo on their sampling platform and sailed slowly over to us powered by an outboard engine. The pick-up by *Polarstern* of the 6 person strong team ended their 15 day long field work in the Jason Lagoon area. After this interruption, the scientific sampling program in Cumberland Bay continued until Friday morning 8 am (Fig. 1.5), when we were able to visit Grytviken, the former whaling station, and the British Antarctic Survey (BAS) station at King Edward Point (KEP) (Fig. 1.4). This trip gave scientists and crew the opportunity to visit the British research vessel RRS *James Clarke Ross* and to talk about science and technical subjects with British colleagues.

We gained a pretty good understanding of the distribution of the young sediments and gas flares in Cumberland Bay, through multiple PARASOUND and HYDROSWEEP profiles, and we used this information to target the last samples. Based on the presence of gas flares (Fig. 1.5) we expected sediments with high methane

concentrations, which were confirmed by our ship-based GC-measurements. Whether this gas has a microbially generated biogenic origin, or possibly a thermogenic origin will be tested in the labs at home based on isotopic analysis of carbon and hydrogen molecules of the methane. The composition of the gas fractions indicates a biogenic gas origin, probably in the uppermost layers of the marine sediments. In the night of Saturday 13 to Sunday 14 April we left South Georgia westwards (Fig. 1.2).

A previous sediment core from the target position was 7 m length and documented the last 70,000 years of time. Analysis of this core showed how the Sub-Antarctic Front changed between cold and warm phases during this time period. In collaboration with our colleagues from BAS, we core by using a 20-m-long piston corer, and recovered 12.39 m sediments. *Polarstern* cruise ANT-XXIX/4 ended on Tuesday 16 April in the port of Port Stanley/Falkland Islands. We had a short but very successful cruise. Over 26 days we measured many parameters, discovered and sampled new things, and gained new ideas, all of which we will publish in future scientific publications and present in lectures. The success of our scientific work is based on the excellent and welcoming support of the *Polarstern* crew, the Laeisz Company and the AWI logistics group. Therefore, we thank Capitan Schwarze and his entire crew with full heart.

2. WEATHER CONDITIONS

Max Miller, Hartmut Sonnabend DWD

On Friday, 22 March 2013 (15:00 p.m.), *Polarstern* left Punta Arenas for the campaign ANT-XXIX/4 at westerly winds 5 to 6 Bft, few clouds and 12°C.

A violent storm had crossed the Drake Passage and weakened. Within the Strait of Magellan some jet like effects up to Bft 8 were observed. But reaching the Atlantic wind veered northwest and abated 3 to 4 Bft. On Saturday, 23 March, *Polarstern* sailed a weak ridge, but swell increased up to 2.5 m. From Sunday on a new low approached. First the warm front caused poor visibility. With the following cold front wind from north to northwest increased and reached its maximum at Bft 7 during the night to Tuesday, 26 March.

On Wednesday evening, 27 March, *Polarstern* reached South Georgia's Cumberland Bay and stayed there until Friday morning. Due to the prevailing wind from west to southwest a lee effect (Fig. 2.1) existed and was partly intensified by the orientation of the fjords. Once we observed a leap of wind force from Bft 2 to Bft 9 (and gusts around 60 knots) within a distance of only 100 m. On Good Friday, 29 March, *Polarstern* left South Georgia and set course for the South Sandwich Islands. At this time a low crossed the island and wind veered southeast. Due to the parallel coastline wind was accelerated up to Bft 6. On Easter Saturday, 30 March, a weak ridge crossed *Polarstern* and a low off Queen Maud Land built a trough towards South Sandwich Islands. Therefore on Easter Sunday, 31 March, wind veered southwest and increased Bft 6 to 7 combined with frequent snow showers.

Again a weak ridge followed but at the same time a storm formed west of Drake Passage and moved east. During the night to Wednesday, 3 April, the westerly wind increased up to Bft 7 to 8 and reached Bft 8 to 9 on Wednesday. Due to a swell of 5 to 6 m *Polarstern* sailed into the lee of Montagu Island during the night to Thursday. But dampened swell was combined with stronger winds at Bft 10 to 11 (gusts Bft 12) caused by jet like effects across and around the island (Fig. 2.2). Noon on Thursday *Polarstern* left Montagu. Wind rapidly abated to Bft 7 but a swell of 5 m was observed. During the night to Friday, 5 April, the storm moved away and wind abated to Bft 4.

On Sunday, 7 April, another storm reached Weddell Sea but weakened. It built a trough to the north which only for short times caused north-westerly winds up to Bft 8 and no significant swell could form. From Monday, 8 April, *Polarstern* operated at the northern edge of the low over Weddell Sea. Furthermore a high off Argentina moved southeast. Tuesday morning, 9 April, *Polarstern* left the South Sandwich Islands and set course for South Georgia again. Most of the time wind from west to northwest prevailed at hardly Bft 5 and swell decreased to 1 m. But moist air masses often caused mist or fog. The above mentioned high had strengthened and

become stationary north of South Georgia. It was the dominant feature during the second stay (until 12 April) of *Polarstern* at the island. Again local effects caused large differences: calm conditions within the fjords and locally up to Bft 9 due to acceleration of wind along the coast.

During the last part of the cruise towards the Falkland Islands wind changed often at maximum Bft 7. But on Sunday, 14 April, *Polarstern* had to cross an area of increasing swell (up to 5 m) caused by a storm off Bahia Blanca. On Tuesday morning, 16 April, 2013, *Polarstern* reached Port Stanley at northerly winds around Bft 7.

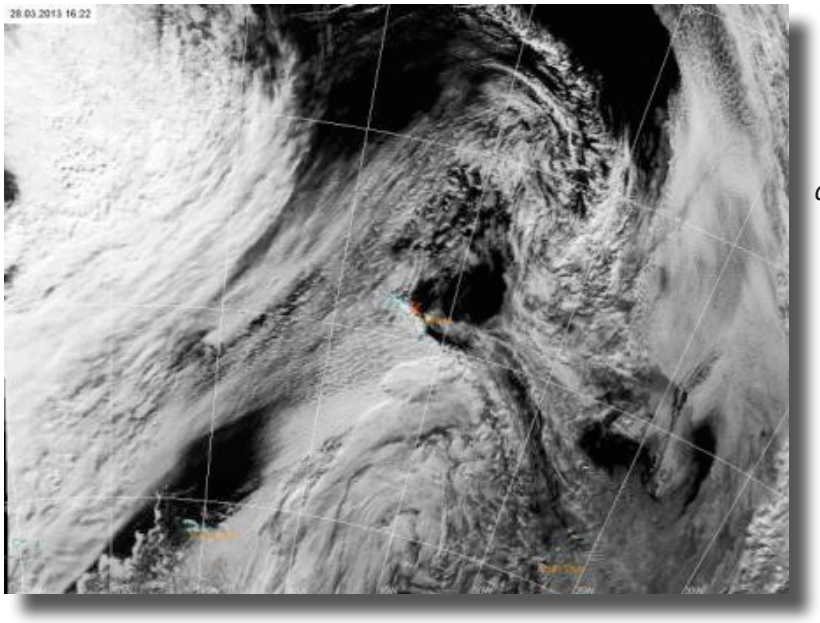

Fig. 2.1: Satellite image from 28 March of the working area. Note cloud distribution and no clouds in the lee of South Georgia.

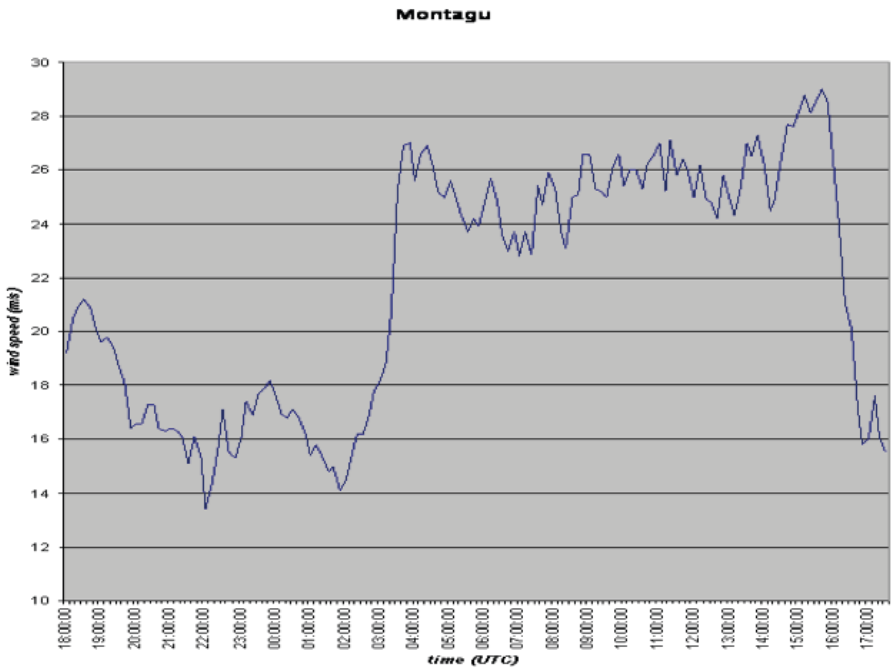

Fig. 2.2: Wind speed change in lee of Montagu Island

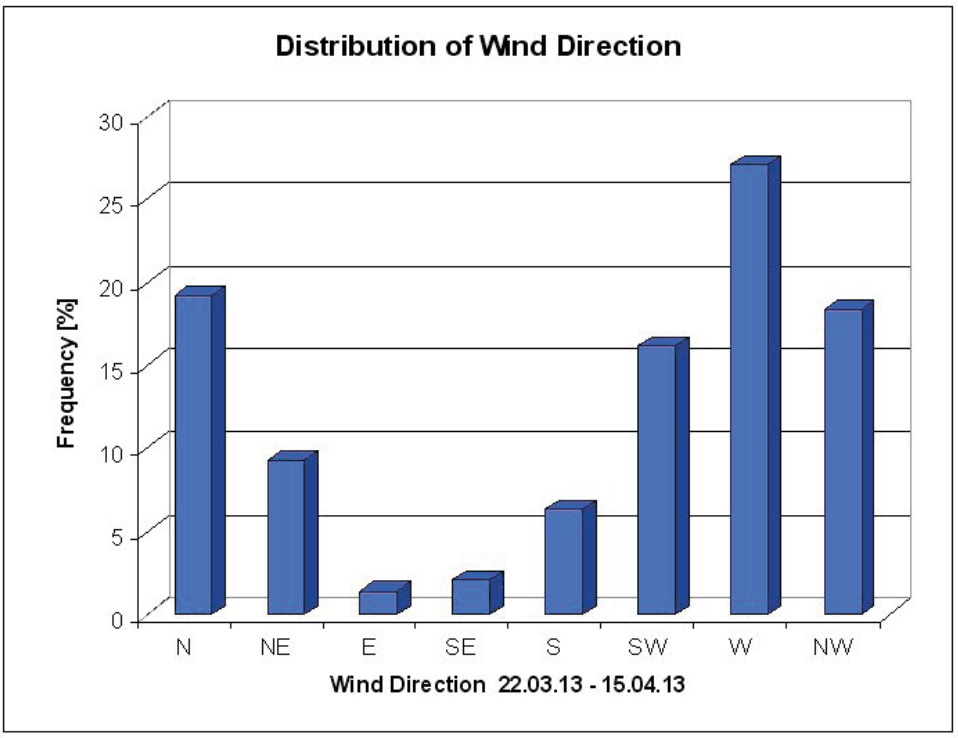

Fig. 2.3: Distribution of wind direction during ANT-XXIX/4

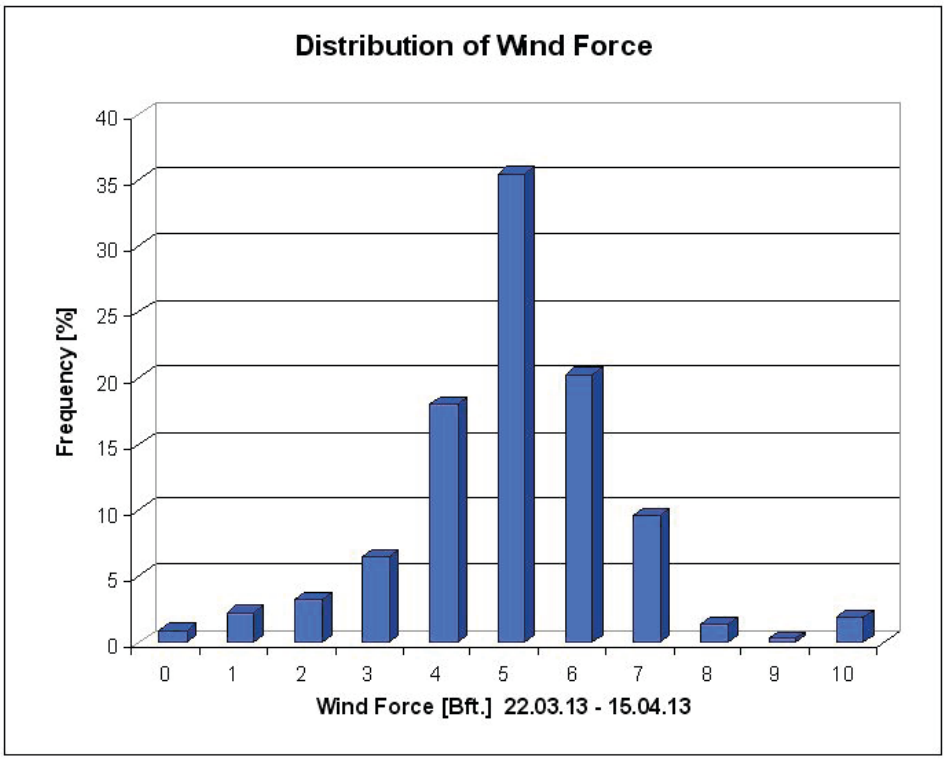

Fig. 2.4: Distribution of wind force during ANT-XXIX/4

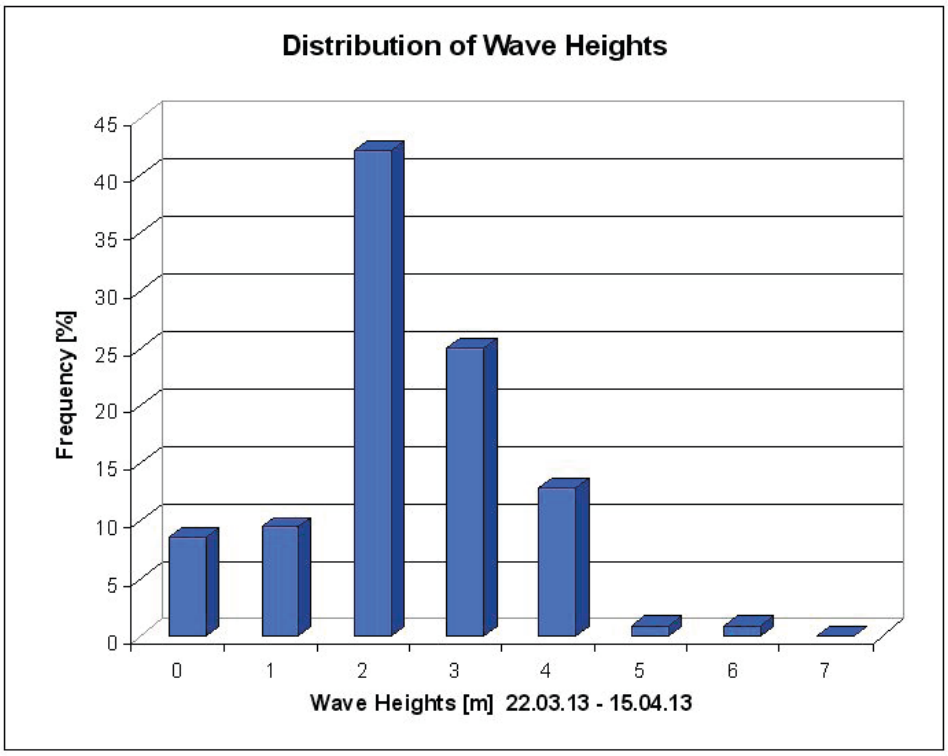

Fig. 2.5: Distribution of wave heights

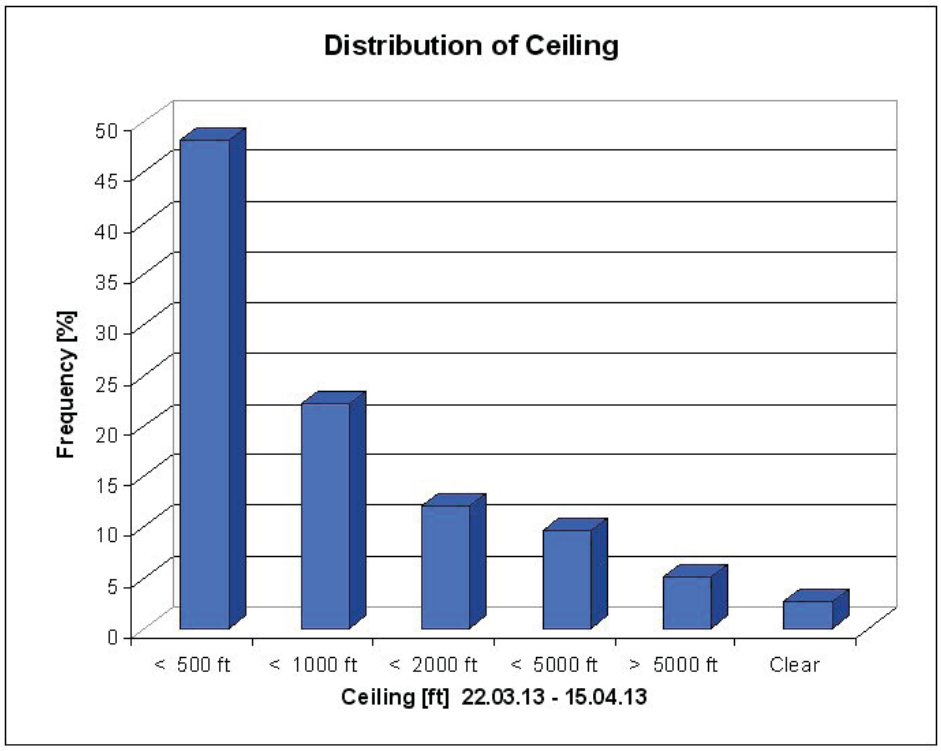

Fig. 2.6: Distribution of ceiling

3. MULTIBEAM ECHO-SOUNDING AND SURVEY

Alastair Graham[1], Paul Wintersteller[2], [1]BAS
Christian dos Santos Ferreira[2], Stefanie Oelfke[2], [2]MARUM
Tingting Wu[2], Miriam Römer[2]

Objectives

Multibeam bathymetric mapping underpins geoscientific investigations at sea, creating the platform from which multi-disciplinary marine science is conducted. As well as providing the main tool for contextualising and selecting stations for work, multibeam bathymetry offers a unique way to visualise the geomorphology of the submarine landscape, as well as the geological structure of the ocean floor. Collection of multibeam data also contributes to a wider effort to map unknown topography in unexplored parts of the world's oceans. In particular, it is increasingly used to improve our geological understanding in the vast areas of submerged land beneath the polar seas (Arndt et al. 2013).

Multibeam echo-sounder (MBES) mapping conducted on ANT-XXIX/4 contributed to each of the above scientific themes: site selection, geomorphology, structural geology and mapping of terrain in the Southern Ocean. Furthermore, under the broader scientific aims of ANT-XXIX/4, multibeam surveys addressed three specific objectives:

1) to investigate the presence, and constrain the locations and geological situation, of gas seeps in the Scotia Sea region, using bathymetry, sidescan sonar, and water-column information (South Sandwich work at sea and results section).

2) to map the geomorphology and shallow sedimentary architecture of the South Georgia shelf, to reveal new information on the history of ice-cap waxing and waning across the continental block (South Georgia work at sea and results section).

3) to provide the geophysical context for coring, in support of gas seep investigations, pore-water chemistry, sediment geochemistry, and Holocene and Quaternary palaeoenvironmental studies including records of climate, oceanographic and glacial change (both sites).

Work at sea

A major upgrade of the vessel-mounted ATLAS HYDROSWEEP DS3 MBES was applied at the beginning of the cruise. The new functionality allowed for recording of up to 313 hard-beams and 920 soft-beams, depending on the water depth. The upgrade also contained a new module to investigate the water column online. This so called ATLAS Hydro-Viewer has been installed on a second acquisition computer and is receiving the signal via UDP from the processing unit. The tool is essential when looking for gas flares while mapping the sea floor. We note that despite some initial performance issues, gas flares were found on the first trials of the DS3 on *Polarstern*.

The ATLAS HYDROSWEEP DS3 MBES was used for all multibeam survey. It is a 15 kHz deep-water system, with water-column imaging capability, and 2 x 2 degree resolution. The system was operated in conjunction with the ATLAS PARASOUND parametric sub-bottom profiler which uses the nonlinear parametric effect between two primary frequencies (about 18 kHz and 22 kHz) to produce a low frequency secondary signal, typically at 4 kHz (see Chapter 4).

Since the changes to the MBES system affected both hard- and software, a roll-/ pitch calibration was conducted on 26 March, right after leaving Argentinean waters. At the patch-test area, at 2,600 m water depth, a sound velocity profile (SVP) was taken alongside with a CTD and an SVP-probe (see chapter SVP). Both datasets were compared to estimate the errors between calculated and measured sound velocity. Since the errors were less than 0.03 % the SVP data from the probe were used to correct the MBES data for this patch test, and were considered reliable thereafter.

3.1 Patch test performance

As a first result we found differences of about 2 - 3 m/s between CTD/SVP and the surface sound velocity (SSV) in about 11 m water depth. The SSV is given by the hull-mounted SSV-probe (C-Keel). Due to this difference we used the profile to give the sound velocity at keel rather than the SSV-probe, while conducting the patch-test.

The mean depth of the patch survey area was about 2,600 meters. The standard deviation (SD) from roughly cleaned raw data of the whole swath up to 4.2-times coverage is 15.48 meters. According to the specification of ATLAS the DS3 system accuracy should be at a SD of 0.2 % of the water depth, which at 2,589 meters mean value is equal to:

2,589 * 0.002 = 5,178 m

Therefore the raw data has an accuracy level 3 times greater than maximum SD allowed for this system. Calculations based on a "well cleaned" dataset (free of big outliers and many spikes) were analyzed, and the SD value was 10.33 m.

Certainly the DS3 meets the specs of IHO 2nd order, while analyzing the problem why the system is not making the given specification the following two problems turned out:

a. There is a known heave problem on *Polarstern*, but still not solved. It is recommended to search for the reason. An additional technical report has been given to the shipping company Laeisz as well as to the AWI.

b. When opening the swath to 5-times coverage (about 135° swath width), it can be clearly seen, that outer beams at about more than 4 times coverage are upturned. (see Fig. 3.1.1) It is urgently recommended to ATLAS to improve their bottom detection. ATLAS already replied on the claim and is currently working on the problem. Later during the cruise a strong centre-section problem occurred in shallow waters. Indeed the bottom detection algorithm needs further investigations to solve this problem too (see chapter Data management).

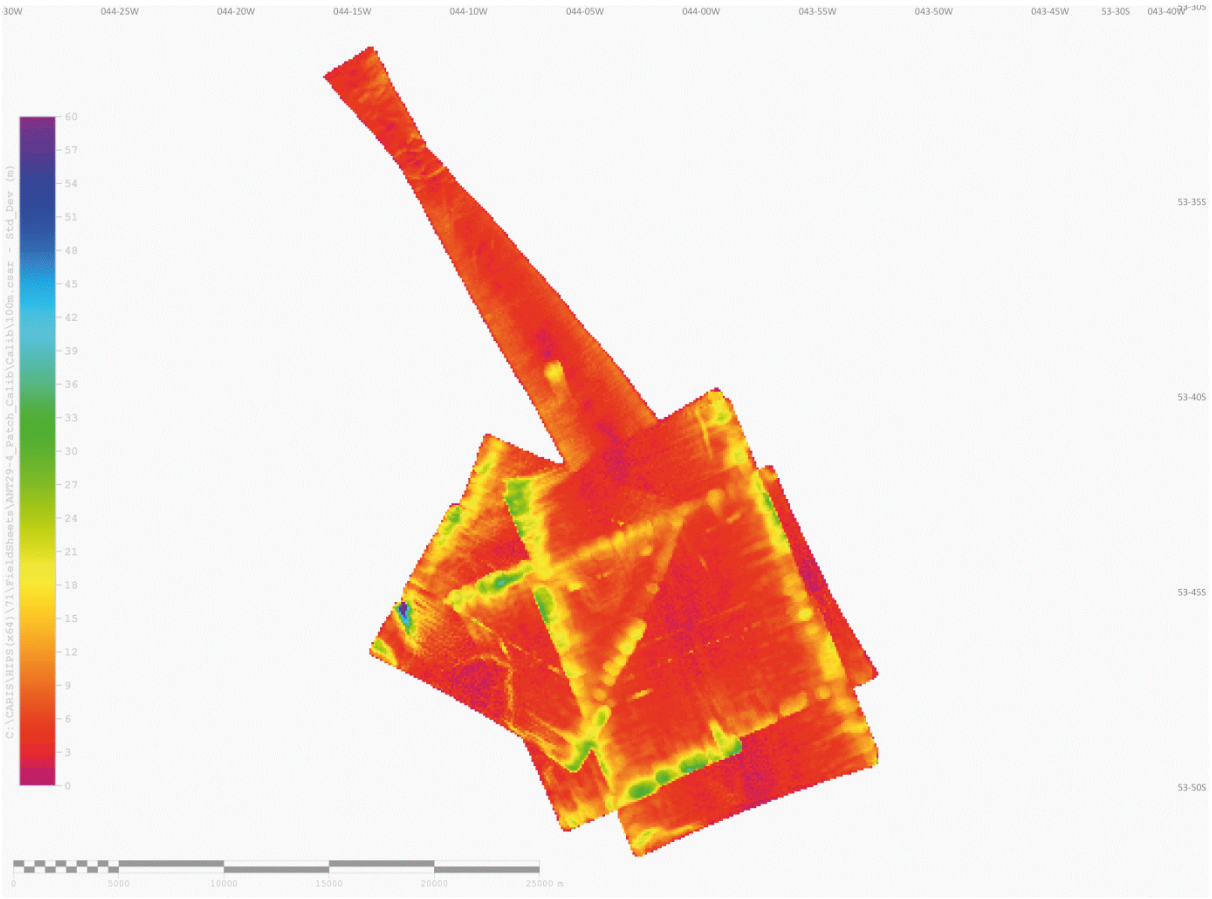

Fig. 3.1.1: Screenshot of the patch-test showing standard deviation (SD) in meters. Whereas most of the area is around or within the ATLAS specification, the upturned outer beams lead to SD below the specification. Also the influence of heave problems can be seen.

3.2 Water column flare-search, side scan and bathymetry acquisition

For the majority of the cruise, our main objectives required that multibeam, sidescan and PARASOUND were recorded continuously and at the same time. Since side scan data from MBES is improved by a large swath width, the MBES should be operated with an optimum setting of 4 - 6 times coverage. However, water column features can be best seen in the center zone of the swath when operating with 2 - 3 times the coverage and at a relatively low speed. Bathymetry on the other hand can be recorded up to 12 kn, and generally with a sweet spot in the 6 - 10 kn range which avoids noise generated by resonance from the propeller or other systems on the vessel. Thus, good settings that satisfy each of these individual requirements are sometimes hard to achieve, and often result in a trade-off depending upon the immediate work-at-sea task (e.g. mapping versus flare hunting).

Settings generally used on the cruise are described as follows:

3.2.1 Triggering of the ATLAS PARASOUND sub-bottom profiler (SBP)

The ATLAS PARASOUND PS3 can be triggered by ATLAS HYDROSWEEP DS3 and it is recommended to do so when investigating in the water column with the onboard MBES. The trigger output can be set in the *ATLAS HYDROSWEEP Control* window under *Sounder Environment* in the *Blanking Output* tab. Activate "*External Signal*

1", give a *Delay* of "*0 ms*" and a *Prolongation* of just "*1 ms*" in shallow water. Our experience is showing good results of a *Prolongation* of "*10 ms*" in deeper water.

The triggering only works when ATLAS PARASOUND is set to "*Transmission on Request*" under *Basic Settings* in *Transmission Sequence*. Once transmission on request is set, the *Trigger Options* "manual, external...." are available in the lower right of the window. Choose "*external line 1"* and HS-DS3 will trigger PARASOUND. Disadvantage for PARASOUND – it will work with more or less the ping rate of the MBES.

3.2.2 Settings for the ATLAS Hydro-Viewer

When opening the Hydro-Viewer by simply double-clicking the icon on the desktop, a tiny main window opens. Go to *File* and *Configuration* and follow the settings shown and described below (Table 3.2.1):

Tab. 3.2.1: Online/offline configuration for the Hydro-Viewer application

Hydro-Viewer Settings under Main Window

- *File*
- *Configuration*

Settings for Online Mode		*Settings for Offline Mode (Replay)*	
HMComManager		*HMComManager*	
Remoting	*Enable=FALSE*	*Remoting*	*Enable=TRUE*
Void-IO		*Void-IO*	
Enable=TRUE		*Enable=FALSE*	
XDR-UDP		*XDR-UDP*	
Enable=TRUE		*Enable=FALSE*	

To enhance the S/N contrast in the water column display, a so called "*Dynamic ClipDB*" and the "*Dynamic RangeDB*" can be set under *Profile*. Values of about "*35dB*" for the first and "*30dB*" for the later were found to be reasonable for most of the searches. The values may vary by depth.

PhysicalRenderHeightPix and *PhysicalRenderingWidthPix,* on the first page of the configuration file*,* represent the rendering settings of RAW-data to virtual display size, which gives opportunity to zoom into the swath-profile-view at least to a certain level. Since the program works with directX, the settings depend on the capabilities of the graphic card. We used "*2500 dpi"* for both. Zooming can be done with the mouse wheel by keeping the mouse in the middle of the window. The profile can be shifted with the left mouse button.

3.2.3 ATLAS HYDROSWEEP DS3 settings

During this cruise the following settings were used:

Transmission:	Single pulse
Pulse characteristic:	Frequency modulated Chirp With highest possible sample resolution (slider setting)

Swath coverage:	Usually 4 times the water depth, besides very shallow areas down to 300 m, where we used 5 times the water depth
Side scan:	Coverage by swath Sample distance: 0.1-8 m
PHF Receiver Amplification:	TVG (don't use automatic, in some cases manual showed better results)
Tranmission power:	Depth controlled
Shading:	No shading has been used
C-Keel:	When surveying small areas with a proper SVP, we used the profile rather than the SSV-probe (C-Keel-probe). On long distance and large survey lines we switched to the probe

The description of multibeam surveys at sea and preliminary results is divided between two broad geographic working areas: the first comprising the South Georgia shelf and the island's bays along its northern coast; the second focusing on the South Sandwich forearc region. Specific survey areas investigated for bathymetry and sub-bottom information during cruise ANT-XXIX/4 are highlighted on the basemap in Fig. 3.2.1.

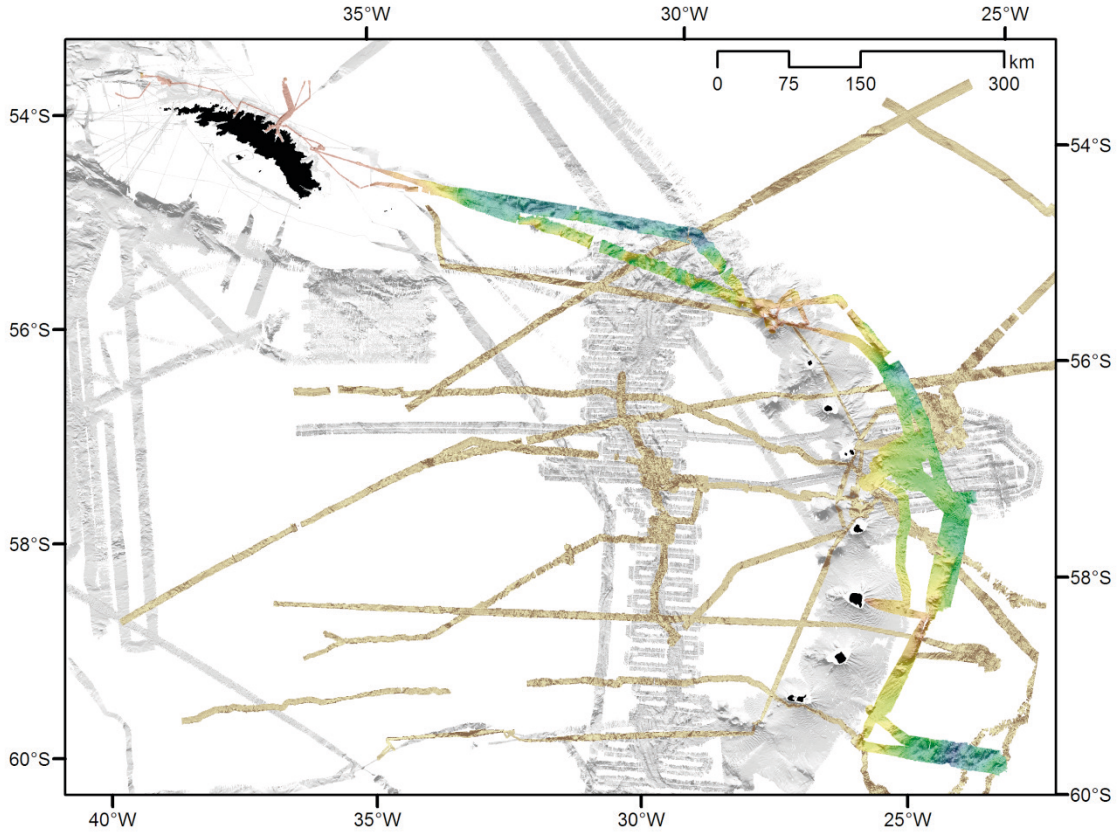

Fig. 3.2.1: Overview of the areas mapped during ANT-XXIX/4, shown with colours. The areas in grey are mapped during cruises of our colleagues from UK, whereas the brown tracklines are recorded on former Polarstern cruises.

3.3 Sound velocity profiles (SVP)

16 sound velocity profiles were taken during ANT-XXIX/4 with a maximum depth of 4,800 m. Eight of them had been calculated from CTD measurements (after Chen & Millero, 1977) the others had been acquired using *Polarstern's* VALEPORT MIDAS Sound Velocity Profiler along with MUC or OFOS. According to the sensor specifications the MIDAS SVP can operate up to 6,000 m water depth with an accuracy of ± 0.03 m/s. Due to the duration time of the OFOS dives the profile interval measurement was set to a value every 5 dBar by using VALEPORT DataLog Express Software.

The SVPs were applied to the ATLAS *Sensor Manager*, *HYSWEEP Survey–Corrections* and EIVA *NaviScan*. These corrections are not applied to the raw data files (.ASD, .HSX, .SBD) and must be reapplied using CARIS *HIPS and SIPS 7.1* – "Nearest in Distance" or "Nearest in Time" method for further post processing investigations. In order to extend the sound velocity profile the open source software MB-System and its tool *mblevitus* has been used for profiles up to 12,000 m water depth (Levitus, 1982).

The SVPs of the different areas represent the various environmental conditions regarding to e.g. melt water from the glaciers, very low sea surface temperatures and the distribution of salinity in the water column (Figs. 3.3.1 and 3.3.2). The 15 SVPs do not match for every condition in the different regions due to local effects and long distances during transits.

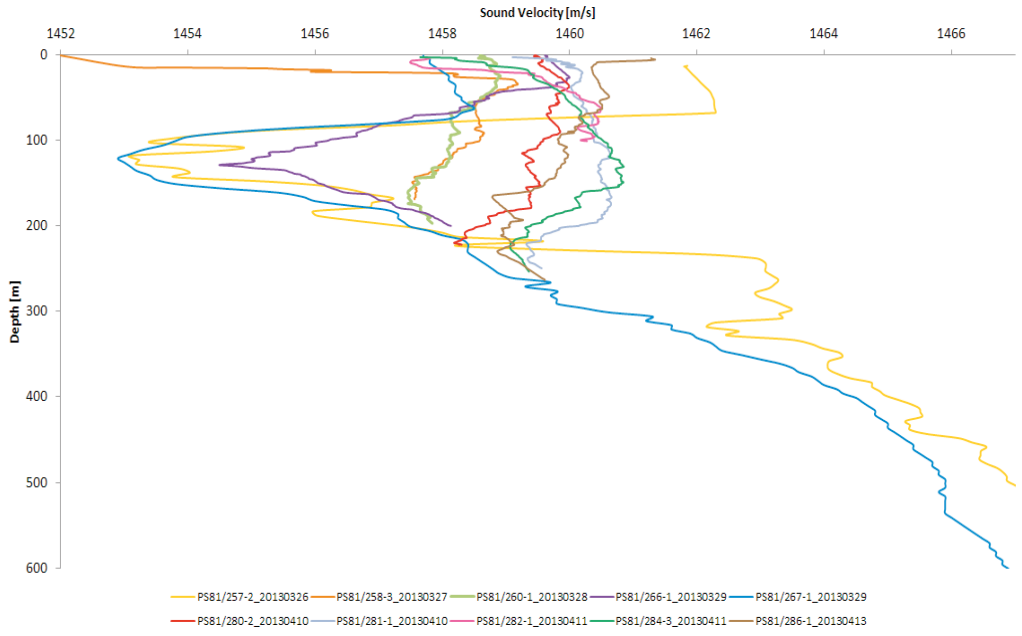

Fig. 3.3.1: SVPs off South Georgia, taken from CTD and MIDAS SVP Profiler

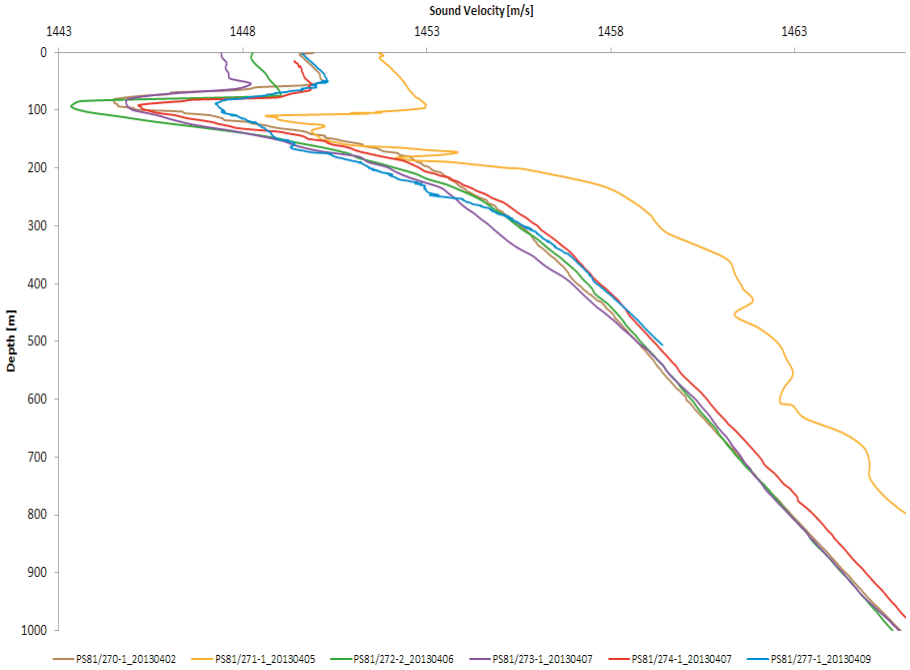

Fig. 3.3.2: SVPs off South Sandwich Islands, taken from CTD and MIDAS SVP Profiler

3.4 South Georgia

HS/PS survey tracks and a completed multibeam map on the South Georgia continental block are shown in figure 3.2.1. Work can be sub-divided into 5 distinct survey areas. In total, 1,763 km of survey lines were recorded on the shelf of South Georgia.

3.4.1 Cumberland Bay fjord

A major target of cruise ANT-XXIX/4 was to analyse the sedimentary records of the largest South Georgia fjord system, in Cumberland Bay. The 260 m deep fjord is in total 36 km long, 6 km wide, and made up of two separate tributaries: the Cumberland Bay West, and Cumberland Bay East. In and around the embayments, the sediments promised to reveal detailed histories of Holocene and Pleistocene environmental change, as well as new information on the history of ice cap advances and retreat in the sub-Antarctic over the last 10 - 20,000 years. High-resolution HYDROSWEEP (HS) multibeam bathymetry, sidescan, and PARASOUND (PS) sub-bottom profiler data would provide essential information on the geomorphology of the submarine environment, and necessary context for choosing suitable sites for gravity coring. As would later become apparent, the data would also prove key to identifying locations of gas seepage in the sediment-filled basins and fjords along the northern South Georgia coast. These were manifest in the form of flare signatures on both PS data, and in the water column imaging module on the DS3, and are discussed in chapter 4 (Subbottom Profiling and Plume Imaging) on the identification of seeps.

The bathymetry of Cumberland Bay fjord had already been mapped in detail by the Royal Navy ship HMS *Endurance*, during various survey campaigns since 2006. These data were presented in Hodgson, Graham, et al. (in review) in relation to the glacial geomorphology of the fjord environment. The excellent coverage around the island's shores meant there was not a need for extensive HS mapping in the South Georgia fjords during ANT-XXIX/4. Nevertheless, the acoustic stratigraphy of Cumberland Bay was not well known, with only 2 existing Kongsberg TOPAS profiles acquired for imaging shallow fjord sediments in Cumberland Bay East (data collected by A.G.C. Graham, British Antarctic Survey, on cruises JR224 in 2010 and JR257 in 2012). PS surveys could therefore provide new information on the three-dimensional sediment fill of the basins, and the internal stratigraphy of moraines marking the inner and outer limits of the two fjord tributaries. Moreover, acquisition of HS DS3 bathymetry in the bays, co-registered with existing Kongsberg EM120 bathymetry datasets from *Endurance*, would allow for direct comparison of the system accuracy, and highlight any problems with the recent HS calibration.

In total, we collected about 120-line km of PARASOUND data and mapped about 78 km² in the Cumberland Bay area during two separate working periods in the South Georgia region. In both the West and East bays, numerous along-fjord profiles were collected, while at the mouth of the bay, at least 6 parallel along-trough lines were acquired (Fig. 3.4.1).

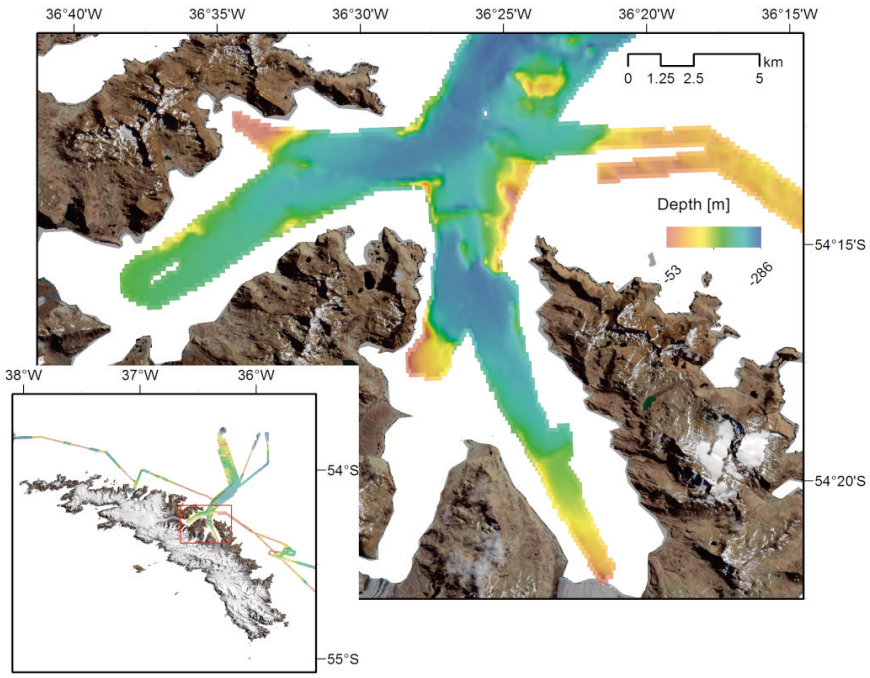

Fig. 3.4.1: Mapped area of the Cumberland Bay fjord

3.4.2 Cumberland Bay Trough

During periods of non-station work in Cumberland Bay, bathymetric survey was carried out from the coast towards the outer shelf to improve understanding of the regional shelf geology and glacial history. The specific target for HS and PS survey was an area of the outer continental block, ~30 nm northwest of Cumberland Bay. Previous work by Graham et al. (2008) had shown that this area formed a distinct N-S oriented glacial trough, connecting to a more prominent, NW-SE oriented trough (the Cumberland Bay Trough) that forms the offshore extension of the Cumberland Bay fjords. A compilation of singlebeam echo-sounder data acquired by fisheries vessels (the OLEX dataset) had already revealed numerous ridged features at the seafloor in this location, interpreted as glacier-formed moraines (marginal accumulations of sediment and debris transported by glacial ice, either subglacially, englacially or supraglacially, and deposited, typically, as irregular arcuate ridges at the glacier grounding line - (Graham et al. 2008)). However, the morphological detail, stratigraphic context, and distribution of these moraines was not known. Insight into past ice-cap extents, the number of past glacial advances, patterns of retreat and glacier dynamics could all be gleaned by studying the moraine field in more detail.

Parallel survey lines were thus acquired N-S over the moraine field over three separate mapping phases. In total, we collected -line km of multibeam and sub-bottom profiler data in the study area, covering a region of 322 km² in size (Fig. 3.4.2). To ensure a precise and complete grid, surveys were designed with a high degree of overlap (often to 100 %), to account for the noise already encountered in the inner swath-section of the ATLAS HYDROSWEEP DS3 system during prior observations in shallow water surveys within the Cumberland Bay. The overlap should also give opportunity to mosaic back scatter without nadir values.

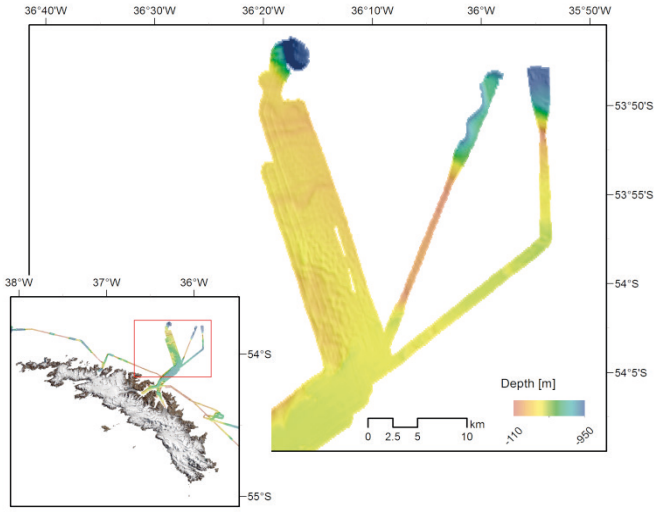

Fig. 3.4.2: Area mapped in the Cumberland Bay Trough

3.4.3 Royal Bay Trough

On our return track to Cumberland Bay to relieve the Jason Lagoon field party, *Polarstern* surveyed an area of the middle continental block at the mouth of Royal Bay (East of South Georgia; Fig. 3.4.3). Survey tracks were designed to investigate flare signatures observed on our initial transit line towards the South Sandwich Islands. These lie within the glacial trough that is the seaward extension of the Royal Bay fjord. A single survey line was also designed for crossing of an existing core site, BAS-GC666 (PI A.G.C. Graham) which will be the focus of a Masters study by Ove Meisel (University of Bremen). GC666 was obtained through a thick sequence of stratified trough infill sediments, possibly of Holocene age, but maybe even older. The core will be used to reconstruct palaeoenvironments and depositional environments through South Georgia's past.

PARASOUND data were collected along three main survey lines (48.5-line km) and a concurrent HS survey was carried out to map the trough bathymetry. A fourth line was acquired basinward in order to tie the acoustic stratigraphy of the three lines together, and to provide a tie line for correlation between a new gravity core site (station PS81/280-1) and the existing GC666 core location. Figure 3.4.3 clearly shows artefacts in the center zone of the HS DS3 records. They appear only in shallow depths (<500 m) and mainly in areas of weaker sediments.

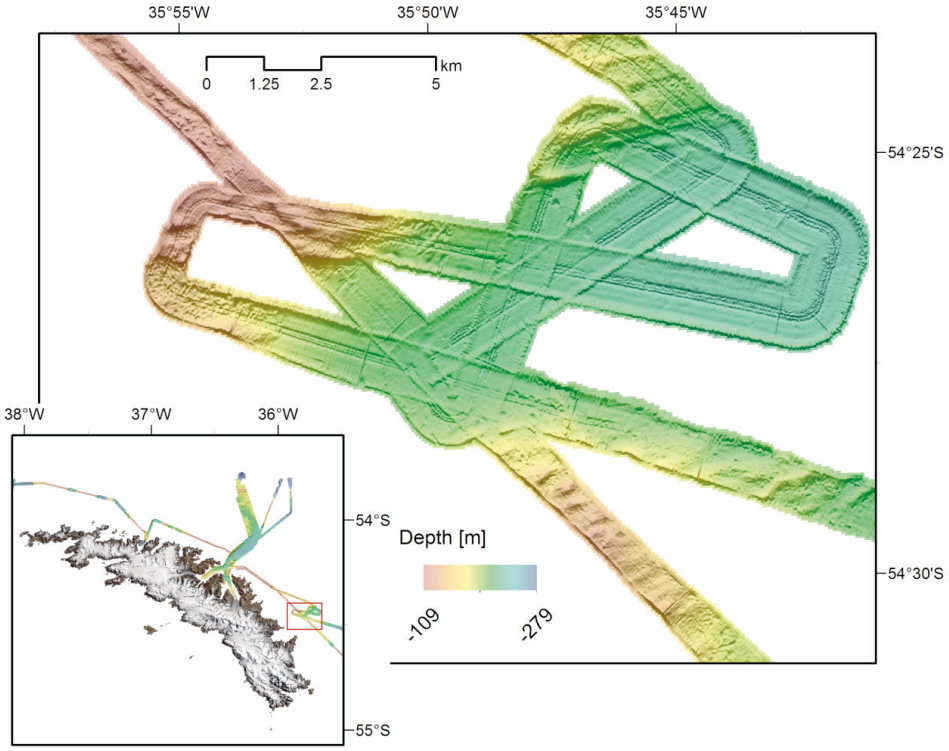

Fig. 3.4.3: MBES survey concurrent to ATLAS PARASOUND acquisition

3.4.4 Possession Bay

Our penultimate survey activity on the South Georgia shelf was to carry out HS/PS survey into and out of the fjord in Possession Bay, west of Cumberland Bay. As the deepest (380 m water depth) and most enclosed inner shelf embayment, the fjord was targeted for its potential as a coring site for future expeditions to the north South Georgia coastline. PS data were successfully acquired on 13.04 covering approximately 28-line-km, comprising an inward track and a reciprocal outward line. HYDROSWEEP data were obtained routinely along both tracks (Fig. 3.4.4), although the basin had already been extensively mapped by *Endurance*.

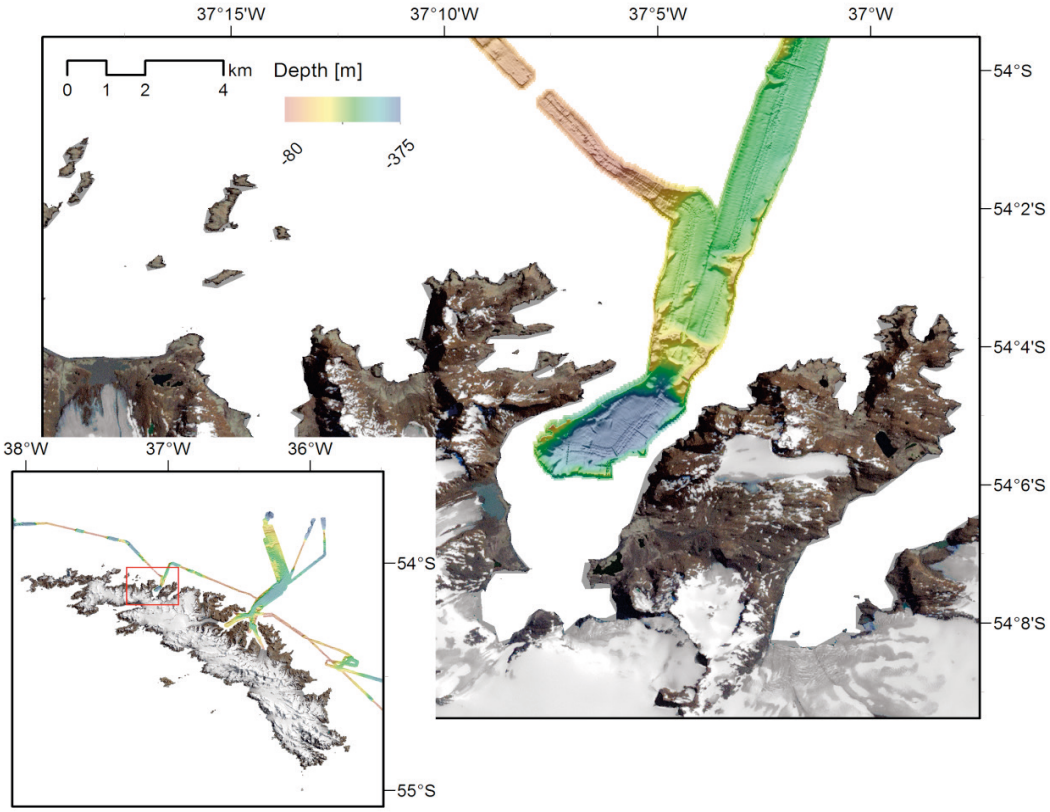

Fig. 3.4.4: PARASOUND survey at the Possession Bay

3.4.5 Unnamed trough, northwest of South Georgia

Leaving Possession Bay and heading west, the final survey on the South Georgia continental block was conducted in another, unnamed glacial trough to the northwest of Bird Island. This trough was investigated because (a) it's axis is sediment filled, and showed signatures of acoustic blanking consistent with the presence of gas and (b) it comprises the deepest known bathymetry anywhere on the South Georgia shelf. Thus, the site offered the greatest potential to form stable gas hydrates in the shelf sedimentary sequence.

The trough was also of additional interest with regard to the glacial history of the island: the sea floor at the heads of two smaller tributaries that combine to form the main trough is clearly drumlinised (ice-scoured by an overriding glacier), while the eastern flank of the trough, including a possible mid-trough moraine, have been lineated by the flow of glacial ice across their tops. The terminus of the trough is also characterised by several subtle arcuate end moraines, and a single large shelf-edge terminal moraine marks one or more of the larger ice-cap glaciations in the island's history. While this rich array of glacial geomorphology is evident in existing multibeam data, the age or facies context for these features is still entirely unknown.

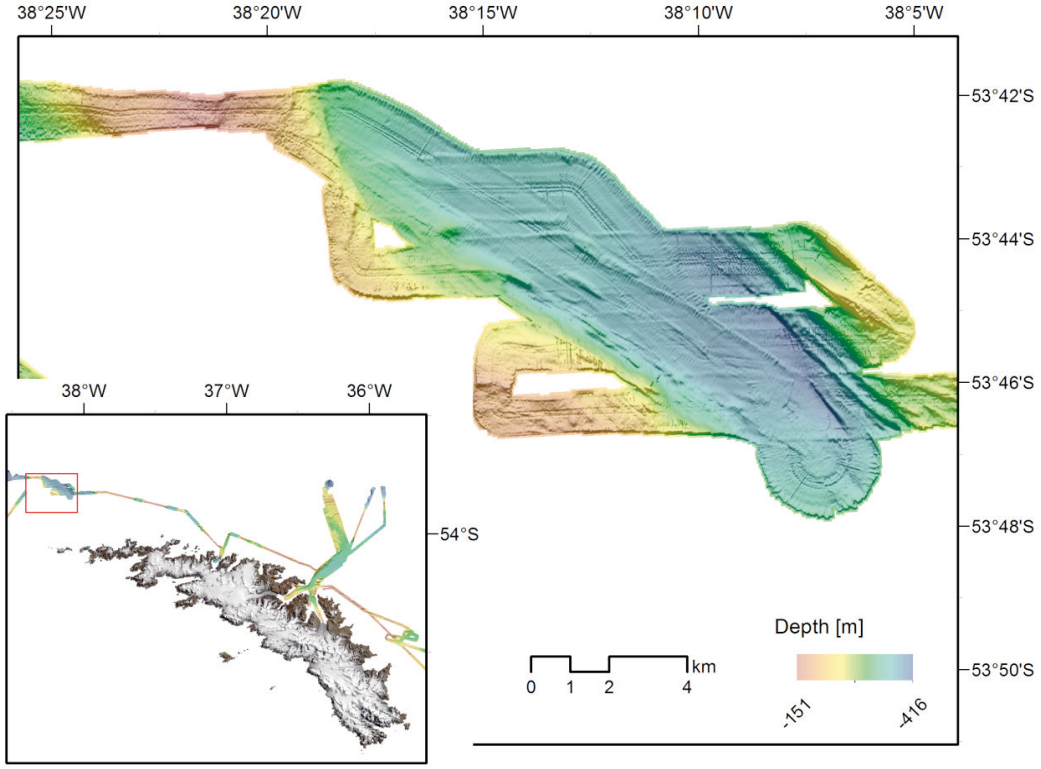

Fig. 3.4.5: HS survey of the unnamed trough

123-line km of PS data were acquired systematically to identify further zones of acoustic blanking, and to image gas flares emerging from the sea bed. In addition, the data formed the geophysical context for choosing core sites to investigate both the presence/absence of methane and/or hydrates, and past glacial depositional environments. HS survey data were also collected along the ship's course, to identify bathymetric features that might host gas seeps (such as small sea-floor mounds), and to produce a new detailed bathymetric chart of the largely unmapped central portion of the glacial trough (see above Fig. 3.4.5).

3.5 South Sandwich Islands

Work at sea around the South Sandwich Islands consisted of multibeam mapping and survey in 3 main areas: the northern region around Quest Caldera and Protector Shoal, the purposes of which were to explore the crests of submarine features and to search for signs of hydrothermal or cold-seep activity; the central region, where mapping of parts of the forearc were conducted, in order to search for evidence for seeps and to improve knowledge of the bathymetry in the region; and a southern part, the aim of which was to map a portion of the outer arc ridge/trench boundary.

In all three areas, dedicated multibeam survey was carried out over specific targets identified with pre-existing sidescan sonar/backscatter data, and normally consisted of 3 or more overlapping continuous survey lines. The completed maps for each sub-region are shown in Figures 3.5.1, 3.5.2, and 3.5.3. A total of 3233 km of PS and MBES survey lines were acquired with an average speed of 6.5 kn.

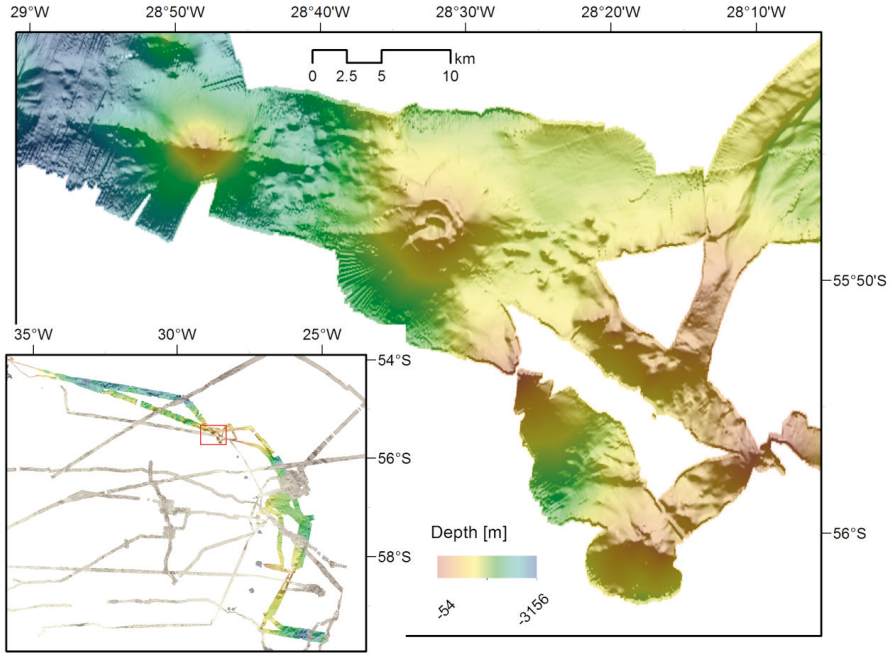

Fig. 3.5.1: Survey area around Quest Caldera and Protector Shoal

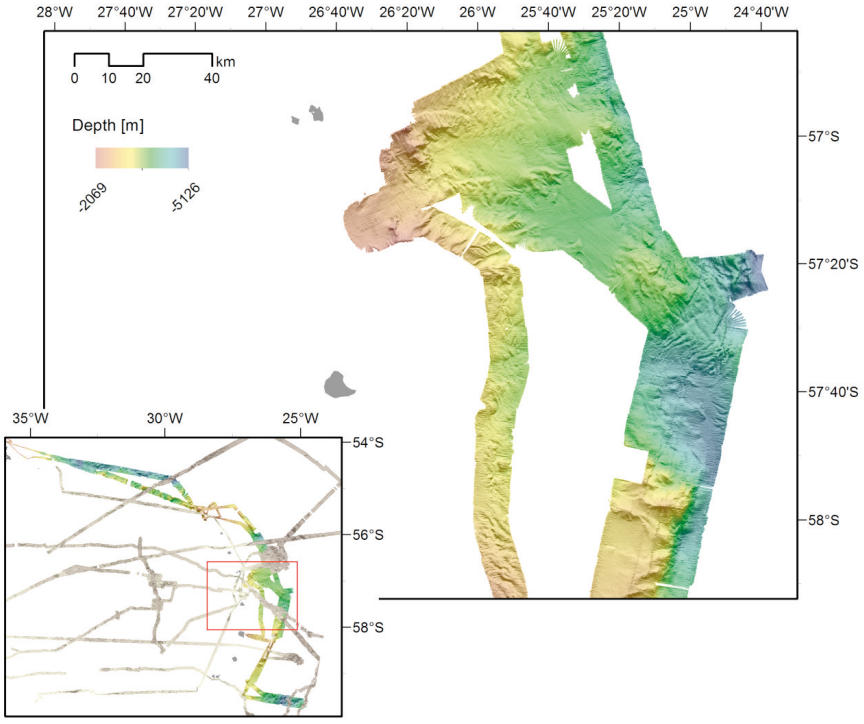

Fig. 3.5.2: Central South Sandwich Islands HS/PS survey

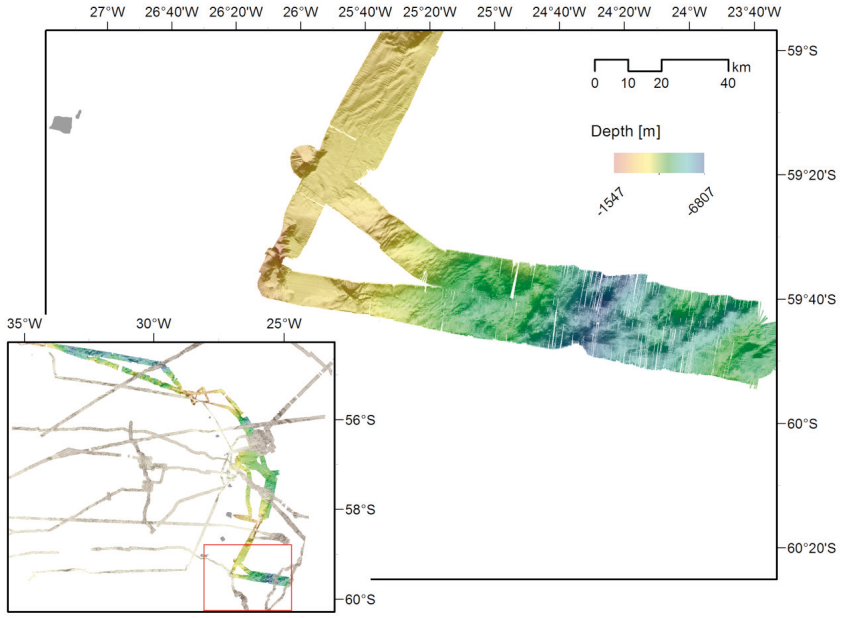

Fig. 3.5.3: Southern South Sandwich Island mapping while crossing the trench

Preliminary results

The most significant results from the South Georgia part of the cruise were forthcoming from Cumberland Bay, and can be summarised as follows:

Cumberland Bay fjord

Detailed mapping in the Cumberland Bay East has provided new high-resolution images of the moraines marking more recent glacial limits, which can be compared to existing multibeam datasets from the fjord.

PS data showed a thick stratified sedimentary infill, which we interpret to be characterised by glacigenic turbiditic layers (brighter amplitude flat-lying reflectors or thin, broadly distributed units with subtle pinch out), meltwater, rain out, and hemipelagic deposits. There are also type-cast examples of debris flows interlayered within the fjord sediment fill. These debris flow units are typical for fjord environments where steep slopes characterise the basin morphology (generally thought to be >1 degree) and where sedimentation rates are high due to sustained glacier sediment delivery. An interesting observation is that some of the brighter amplitude turbidite layers, and acoustically transparent debris flow lenses, occur at coeval horizons throughout the fjord stratigraphy. This may suggest a trigger for debris flow events, perhaps related to glacier frontal changes or to variability in the depositional environment (perhaps related to climate).

Because of excellent HS/PS coverage, we expect further analyses to reveal the 2.5 D shape and geometry of infill, the source and distribution of debris flows and the relationship of the various acoustic facies to the sedimentological units in cores, as well as their timing. In cores, we hope to identify any frontal changes based on grain size analyses, and variability in meltwater efflux over time using isotopic tracers. These sedimentological records can be tied back to the hydroacoustical information, and traced between core sites, where possible.

Cumberland Bay Trough

Newly mapped moraines on the outer shelf revealed former glacial limits in unprecedented detail, significantly improving upon the original imagery of these features in OLEX data. The weathering characteristics (morphological freshness) of the moraines will be studied in more detail, as will their size classification, geometry, and spatial distribution (Graham, Kuhn). However, an initial view of the features shows that they are heavily pockmarked or pitted, and occasionally iceberg scoured.

A surprise was the stratigraphic context for the moraine features, which suggested that some may be bedforms eroded into older pre-existing sedimentary strata. Furthermore, PS data showed a complex shallow stratigraphy with at least 2 major unconformities buried in the shallow sequence. One erosion surface underlies stratified sediments, and another seems to form the base to the most seaward moraine ridges. From these preliminary observations, it appears that at least two major glacial advances are recorded in the near-seabed sediments, and at least one cycle of advance/retreat is still expressed morphologically as a relatively fresh landscape at the sea-floor today. Other erosional surfaces were also imaged during work in the area offshore of Royal Bay. Additional work will focus on the study the PS data in more detail, alongside the new geomorphology, to interpret whether moraines were formed during ice advances or retreats, whether the relative event stratigraphy for the near-surface sediments can be resolved, and if possible ages

for the outer shelf features can be inferred. This information will ultimately provide the first palaeoglaciological information for the South Georgia offshore realm, and will be important for linking with southern hemisphere climate history, quantification of ice in the sub-Antarctic at the Last Glacial Maximum, and with implications for biological evolution of marine benthos in Antarctica through constraining the whereabouts of glacial refugia during glacial stages

Other South Georgia Troughs

Gas flares emitting from the sea-floor in Cumberland Bay, Cumberland Trough, and in troughs and bays on other parts of the shelf (e.g. the northwestern, unnamed trough, and the area around Royal Bay) were imaged in all geophysical/hydro-acoustic equipment onboard the ship. The finding of multiple sites of gas seepage is a major result of our hydroacoustic work from the cruise.

South Sandwich Islands

New and detailed maps of several volcanic seamounts in the northern island arc are an additional outcome from our investigations.

Multibeam data collected in the northern/central forearc region extend the mapping work of colleagues at the British Antarctic Survey (Phil Leat and others - (Leat et al. 2010)), and improve the imaging and knowledge of the structural form of the overall South Sandwich forearc. This includes maps of the distal part of so-called sediment wave fields east of Montagu Island, detailed bathymetry over geological structure (e.g. faults) in the deeper parts of the forearc, as well as improved understanding of the distribution and acoustic properties of any sediment cover in the study area. The lack of seeps in the forearc, although a disappointing result, is also a necessary finding and reveals previously unknown information about the structure and level of activity of this particular Southern Ocean arc.

Multibeam data in the southern extent of our survey region recorded new bathymetry in the South Sandwich trench which will improve bathymetric models for this region. The offset between our results and regional bathymetric grids was often more than +200 metres.

Data management and data quality

Almost 7TB of MBES data were recorded during this cruise. The enormous amount of data results mainly (>95 %) from water column recording. The primary high frequency (PHF) has been recorded in full sample resolution. At the time of writing, there is no way to set a distinct binning to reduce the quantity of stored data. For a longer cruise, the amount of data coming in is not sustainable from either a short-term or long-term storage perspective, and this is something we expect ATLAS to address in the near future, during further improvements to the system. Beside the MBES-PHF data all the acquired data has been saved on DL-Tapes and will be archived in PANGAEA Data Publisher for Earth & Environmental Science. The MBES-PHF data itself is stored on external hard drives. The decision on whether this data will be stored in the data base has not yet been made.

In comparison of data from before and after the upgrade of DS3 improvements in data density as well as the bottom detection algorithm are visible. The later still struggles with upturned outer beams and particular in shallow water, with a bottom-loss in the inner sector. As mentioned in chapter 3.1, ATLAS is currently working on a solution.

References

Arndt, J. E., H. W. Schenke, M. Jakobsson, F. O. Nitsche, G. Buys, B. Goleby, M. Rebesco, F. Bohoyo, J. Hong, J. Black, R. Greku, G. Udintsev, F. Barrios, W. Reynoso-Peralta, M. Taisei & R. Wigley (2013) The International Bathymetric Chart of the Southern Ocean (IBCSO) Version 1.0 – A new bathymetric compilation covering circum-Antarctic waters. *Geophysical Research Letters***,** n/a-n/a.

Graham, A. G. C., P. T. Fretwell, R. D. Larter, D. A. Hodgson, C. K. Wilson, A. J. Tate & P. Morris (2008) A new bathymetric compilation highlighting extensive paleo-ice sheet drainage on the continental shelf, South Georgia, sub-Antarctica. *Geochemistry Geophysics Geosystems,* 9.

Leat, P. T., A. J. Tate, D. R. Tappin, S. J. Day & M. J. Owen (2010) Growth and mass wasting of volcanic centers in the northern South Sandwich arc, South Atlantic, revealed by new multibeam mapping. *Marine Geology,* 275**,** 110-126.

Levitus, S, Climatological Atlas of the World Ocean, NOAA Professional Paper 13, U.S. Government Printing Office, Washington D.C., 173pp, 1982.

4. SUBBOTTOM PROFILING AND FLARE IMAGING

Gerhard Kuhn[1], Paul Wintersteller[2], [1]AWI
Miriam Römer[2], Ove Meisel[1], Stefanie Oelfke[2], [2]MARUM
Thomas Ronge[1], Tim Stoltmann[2], Steffen Wiers[1] [3]BAS, NERC
William Dickens[3], Christian Freksa[4], Norbert Lensch[1], [4]Uni Bremen
Birgit Glückselig[1], Chrispin Little[5], Britta Lüdke[1], [5]Uni Leeds
Benjamin Löffler[1], Inna Morgunova[6], Jiangong Wei[2] [6]VNIIOkeangeologia

Objectives

The most important tool on board for the identification, characterization and quantification of seafloor sediments and for gas flare and plume detection is the hull mounted PARASOUND DS III - P70 sub-bottom echosounder system (Atlas Hydrographic, Bremen, Germany).

We added subbottom profile lines to existing ones from former cruises ANT-X/5 (Gersonde, 1993), ANT-XI/2 (Gersonde, 1995), ANT-XXII/4 (Schenke & Zenk, 2005) with *Polarstern* in 1992, 1993/94, and 2005, and cruises JR224 (Larter et al. 2009), JR244 and JR257 with RRS *James Clark Ross* in 2009, 2011, and 2012, respectively, AWI and BAS collected marine geological and geophysical data sets from the Falkland Plateau, Scotia Sea, and from the South Georgia shelf (Graham et al. 2008).

Areal sediment distribution, sediment thickness and depositional facies were visualized by the PARASOUND system. Sea floor characterization, mapping the sub- and proglacial bedformes in the paleo-ice stream troughs and moraines will help us to interpret the history of local ice caps and their behaviour and interplay with sea level changes and marine sedimentation during past climate changes.

Some indications for elevated methane concentrations found in the water column on the South Georgia shelf (Larter et al. 2009) guided us to investigate gas bubble emissions producing so-called flares in hydroacoustic records during the cruise.

Work at sea and preliminary results

During cruise ANT-XXIX/4 a distance of nearly 4,600 nautical miles was profiled by the PARASOUND system (Fig. 1.1, cruise track). PARASOUND is a high-resolution sub-bottom echosounder, which operation is based on the parametric effect. Two high energy signals of ~19 (PHF) and ~23 kHz create two harmonics at difference frequency of ~4 (SLF) and frequency sum of ~42 (SHF) kHz in the water column above the sea floor. The PHF (19 kHz) can be used for imaging of gas bubbles in the water column. Opening angle of the transducer is ~4°, which corresponds to a footprint size of about 7 % of the water depth. The secondary low frequency (SLF) is variable from 0.5 to 6 kHz, which can be used for sub-bottom profiling, depending on the scientific objectives.

During the entire cruise the following settings were used: SLF Frequency 4 kHz, 2 or 1 periods/pulse length, rectangular pulse shape; and sensor operation mode "Quasi Equidistant Transmission" with time intervals between 1,000 and 2,000 ms between signal transmissions mostly used in water depths below ca. 1,500 m and "Single Pulse" in shallower waters. For noise reduction we used a synchronisation mode by triggering the PARASOUND signal from the HYDROSWEEP system in shallow waters.

At some geological stations, the SLF was set to 6 kHz for minimizing the noise generated by the ship's thrusters.

In order to get high vertical resolution and gas emission imaging the single pulse mode was chosen in Atlas Hydromap Control. The program Parastore is used for storing and displaying echographs. The settings applied in Parastore for PHF displaying are variable and dependent on the actual performance influenced by, e.g., water depth, water and weather conditions. Generally the filtering in the PHF window have been used to image gas emissions in the water column: Low pass: on, Iteration: 2, High cut: 1.The amplitude scale is also important for this purpose: Clip: between 1 and 200 mV, no Threshold, negative Flanks Suppression or Gain.

Two file formats were recorded: *.asd files, which can be replayed in Parastore contain data of the entire water column as well as the sub-seafloor. Parastore can also directly produce *.ps3 and *.sgy-files (SEG-Y files) recorded along with the auxiliary data. The depth range of the *.ps3 files was set identical to those of the online display window. We used *.ps3-files to plot the echograms in the program SENT for interpretation. *.ps3 and *.sgy-files can be produced also by replaying the *.asd files in Parastore.

The subbottom image profile and the water column PHF image were displayed online with the Parastore software on up to four monitor screens arranged side by side. Screenshots from these window displays were taken about every 2 hours (the time the window was renewed), saved and will be stored in the PANGAEA database. The resolution of these screenshot images is quite good and they superbly show the highly diverse sediment infill pattern in the glacial troughs of South Georgia. After minor image processing like conversion in black and white and colour reversal these screenshots are also printable (see Fig. 4.1). The displayed profile was taken crossing the outer Royal Bay glacial trough in south-easterly direction. Sediments were deposited on in-transparent bedrock following the pre-topography in concordance but also with clear onlap structures to the south. There are many zones of gas blanking and filled pockmarks. This blanking could perhaps form as well the lower boundary of the layered sediment reflectors. A disconformity is visible in about 10 m below surface shoaling in south-easterly direction (Fig. 4.1).

Numerous flares produced by gas bubble emissions were detected at the shelf north of South Georgia (Fig. 4.2). In total, about 130 individual anomalies representing gas bubble steams or gas pulses were found (Fig. 4.3 left), although the use of the single-beam echosounder restricts the detection coverage to only 7 % the water depth directly below the vessel. Online observations with the multibeam system at the end of the cruise have proven that there are probably more flares than those we crossed occasionally with the vessel and later post-processing will allow a more comprehensive view on how many flares are located at the shelf and in more detail how they are distributed. The example of a flare detected with the HYDROSWEEP system shown in Fig. 4.3 on the right illustrates that flares 200 m aside from the nadir could be recorded.

The first impression regarding the distribution of flares is a high sediment accumulation within the Cumberland Bay and outside the fjord most flares occur within the paleo ice-stream troughs connected to the fjords.

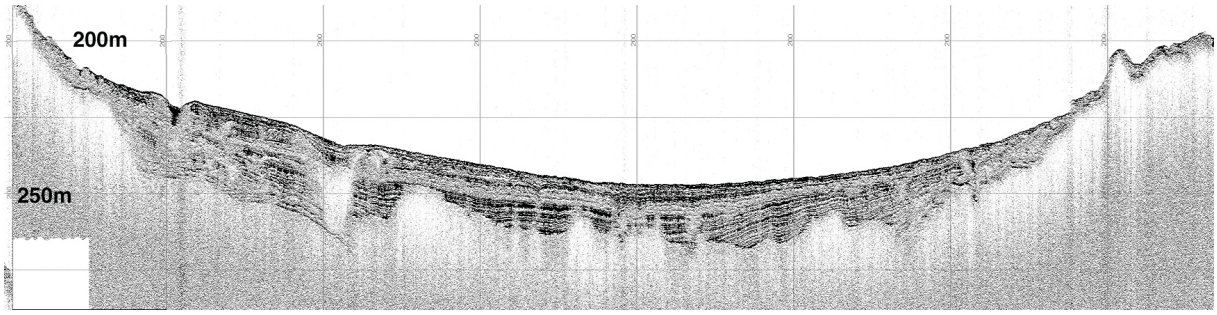

Fig. 4.1: Screenshot image of a subbottom profile from offshore Royal Bay taken on 29.03.2013 14:17 to 14:35 UTC from Lat. 54°26.16'S Long. 35°52.04'W to Lat. 54°28.46'S Long. 35°48.31'W, length of profile 5.9 km

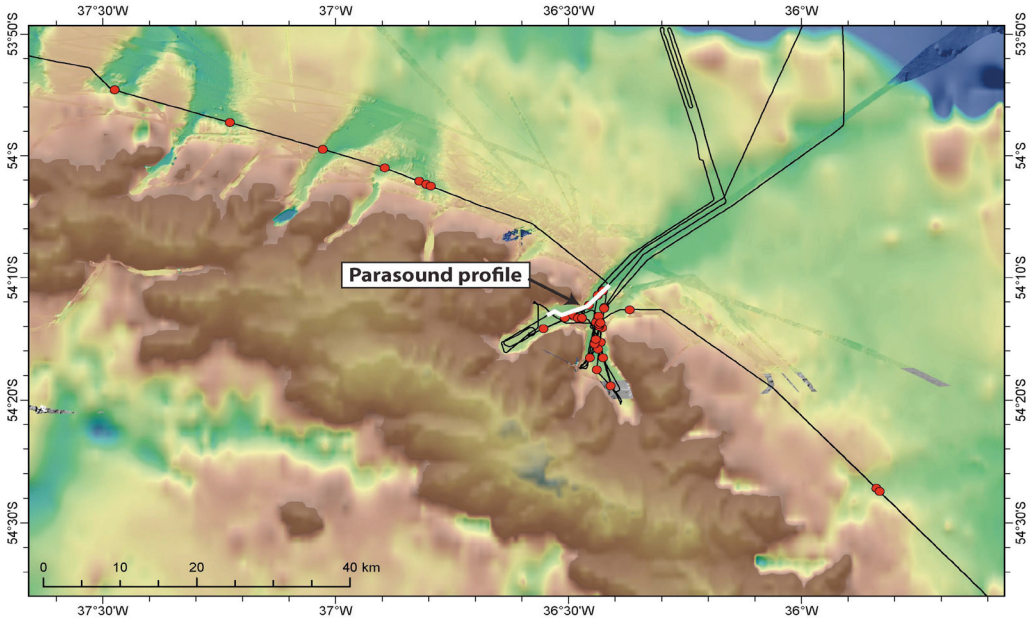

Fig. 4.2: Bathymetric map with the ship track and flare location (red points) detected until the 29.03.2013 north of South Georgia. The white line marks the position of the profile shown in Fig. 4.4.

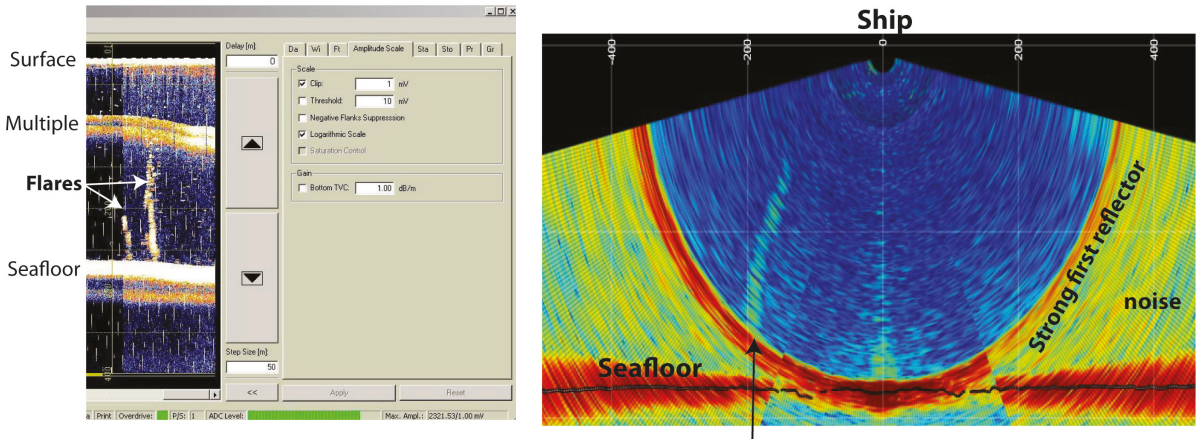

Fig. 4.3: Screenshot examples of flares recorded with the PARASOUND system (left) and with the HYDROSWEEP system (right)

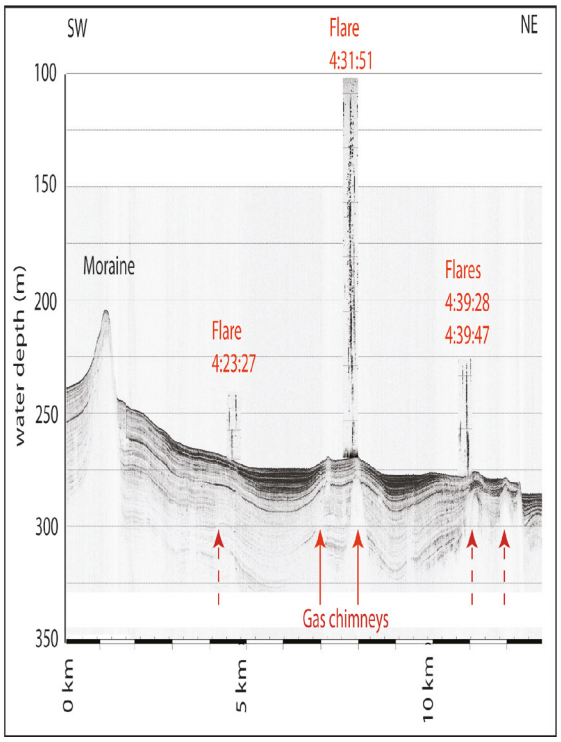

Fig. 4.4: PARASOUND SLF profile from Cumberland Bay West with trough-basin and moraine sediment fill and blanking zones representing gas chimneys. Parts of the PHF Profile above the sea floor show the detected gas flares in the water column reaching heights of up to 150 m.

Two software packages operate the PARASOUND system on a PC under Windows 7. ATLAS HYDROMAP CONTROL (Vers. 2.2.8.0) sets the control parameter, modes of operation and ranges of the echosounder. ATLAS PARASTORE-3 (Vers. 3.3.13.0)

is an acquisition, visualisation, processing, conversion, quality control, print and data storage software. With this software a replay of recorded data and further processing is possible as well. ATLAS HYDROMAP CONTROL SERVER (Vers. 2.1.3.0) runs in the background and provides the data exchange and communication with the signal processor unit and transceiver electronics. The software was running stable most of the time; timing errors made an exchange of the SPM unit necessary on 05 March. The spare part is working without an error annotation.

Data acquisition and storage of the PHF and SLF signal was switched on after leaving the 200 miles EEZ of Argentina on 23 March at 23:34 UTC and switched off on 16 April at 08:47 UTC before entering the 12 mile zone of Falkland Island. Both frequencies were stored in ASD (Atlas Sound Data) format. This is a raw file xml data format storing the complete sounding profiles. In addition, the SLF and PHF signals were stored as SEG-Y and PS3 format. Navigation data and general PARASOUND and PARASTORE-3 settings were stored in daily ASCII format files and printouts. SLF profiles were printed on DIN A4 pages and screenshots were taken and stored. During ANT-XXIX/4 the system was controlled by an operator around the clock, who took records of time, navigational data, basic settings and illustrated the sub-bottom profile by hand. At station work not relevant for geological sampling, the system was switched off.

Sub-bottom profiling is not only a tool for gathering information about sediment accumulation and erosion but it is also used for locating coring positions. PARASOUND was particularly useful for the identification of core sites on the South Georgia shelf, where a very patchy spatial distribution of sediments and a focussing of sediments in the paleo ice stream troughs were recorded (Fig. 4.3). The acoustic information from PARASOUND at each coring location can be compared with physical properties measured on the sediment cores with the multi-sensor core logger (MSCL, Chapter 7), thus allowing the correlation of acoustic data with core data.

During our cruise, ANT-XXIX/4, for the first time the PARASOUND and HYDROSWEEP system was successfully used to detect gas flares in subantarctic water.

Data management

Data were stored in a predefined manner (documented in the data handling manual on *Polarstern* intranet) and are already imported into PANGAEA Data Publisher for Earth & Environmental Science. Publications and perhaps one PhD thesis is planned to deal with these data. After publication and a moratorium time of 5 years after the cruise these data will be made publicly available.

References

Gersonde, R. (1993). Die Expedition ANTARKTIS X/5 mit FS "Polarstern" 1992 = The expedition ANTARKTIS X/5 of RV "Polarstern" in 1992. Berichte zur Polarforschung (Reports on Polar Research), Bremerhaven, Alfred Wegener Institute for Polar and Marine Research, 131, 167 p. hdl:10013/epic.10132

Gersonde, R. (1995). Die Expedition ANTARKTIS-XI/2 mit FS "Polarstern" 1993/94 = The expedition ANTARKTIS-XI/2 of RV "Polarstern" 1993/94. Berichte zur Polarforschung (Reports on Polar Research), Bremerhaven, Alfred Wegener Institute for Polar and Marine Research, 163 , 133 p. hdl:10013/epic.10164Gersonde, 1995

Graham, A. G. C., P. T. Fretwell, et al. (2008). A new bathymetric compilation highlighting extensive paleo-ice sheet drainage on the continental shelf, South Georgia, sub-Antarctica. Geochem. Geophys. Geosyst. 9(7): Q07011, 21 pages, doi:10.1029/2008GC001993.

Larter, R. D., Tyler, P. A., et al. (2009). Cruise report RRS *James Clark Ross* Cruise JR224 January to February 2009, Chemosynthetically-driven Ecosystems South of the Polar Front consortium programme. at:

https://www.bodc.ac.uk/data/information_and_inventories/cruise_inventory/report/9359/

Schenke, H. W. and Zenk, W. (2006). The Expeditions ANTARKTIS-XXII/4 and ANTARKTIS-XXII/5 of the Research Vessel "Polarstern" in 2005. Berichte zur Polar- und Meeresforschung (Reports on Polar and Marine Research), Bremerhaven, Alfred Wegener Institute for Polar and Marine Research, 537, 133 p. hdl:10013/epic.10542

5. OCEAN FLOOR OBSERVATION SYSTEM (OFOS)

Miriam Römer[1], Eberhard Kopiske[1], [1]MARUM
Katrin Linse[2], Yann Marcon[1], Crispin Little[3], [2]BAS, UK
Tingting Wu[1] [3]Leeds, UK

Objectives

Observations from previous expeditions to the forearc of the South Sandwich Islands and the shelf of South Georgia gave evidence for the presence of hydrothermal activity and methane seepage (Larter et al 2009, Rogers 2010). The plan for ANT-XXIX/4 was to deploy the OFOS system at locations identified as potential hydrothermal and seep targets by existing seismic data, and existing and new multi-beam and PARASOUND echosounder hydrocasts to verify the acoustic soundings by visual observations. The hydrothermal and seep geofuels (methane, sulfates, sulfides) not only can sustain chemotrophic life but also lead to precipitation of authigenic minerals, which is a process also influenced by microbial activity. Through OFOS observations we planned to (1) to characterise benthic macro- and megafauna as "normal" Antarctic fauna or as chemosynthesis dependent fauna, (2) to identify chemosynthetic microbial activity by the presence of white bacterial mats, (3) to detect precipitated authigenic minerals or chimney structures, and (4) to spot the release of gas bubbles from the seafloor. The main objective for the cruise was to identify targets of hydrothermal activity and fluid flow for a follow-up expedition.

Work at sea

The OFOS is a towed underwater camera system with a high-resolution digital camera (iSiTEC, CANON EOS 1Ds Mark III) owned by AWI. The three main components are a deck unit, the cable (single-mode-LWL-Faser) and an underwater unit. The underwater system is mounted in a steel frame with dimensions of 140L X 92W X135H cm. The camera, two flash lights (iSiTEC UW-Blitz 250, TTL driven), three Laser, four LED lights and a Tritech Altimeter are attached to the steel frame (Fig. 5.1). The deployment is controlled by the deck unit and five different software modules installed on a laptop computer control the operation of the components, and save the images and Posidonia positions.

The OFOS sled was deployed from the side of the *Polarstern* and towed at a speed of ~0.5 – 0.7 knots at a minimum distance of 1.5 m above the seafloor. This distance was maintained by a winch operator manually adjusting the cable length using visual seafloor observation on a live-view window, and by watching the altimeter display. In order to determine the position of the OFOS and to locate the positions of the images taken, a ship's ultra-short baseline system (USBL) Posidonia transponder was fixed to the frame of the OFOS.

As a backup system we sailed with the MARUM owned TV-sled frame and telemetry (Fig. 5.1). This TV-sled is a towed black-and-white camera system transmitting energy to the sled and the analogue video signal from the sled through the ship's coax cable. The main components are the video-data telemetry system consisting

of an underwater and a deck unit, a black-and-white camera system and a HID (high intensity discharge) light. The black-and-white video signal transmitted by the video-data-telemetry system is displayed in real time on monitors and recorded by a VCR. The electronic components of the system were manufactured by Oktopus GmbH (Kiel) and are property of the University of Hamburg (working group Prof. Matthias Hort). The underwater system is mounted in a steel frame with dimensions of 120L x 80W x 120H cm. The sled was also towed at a speed of 0.5 to 1 knots at a distance of about 3 m above the ground. This distance is maintained by a winch operator manually adjusting the cable length, such that a weight suspended 3 m below the sled is flying just above the seafloor. The length of the weight is ~25 cm and can be used for size estimation on the seafloor. The Posidonia transponder was also fixed to the frame during deployment.

The strategy for finding vents and seeps with the OFOS was, generally, to observe the seafloor in areas where there was ship-based evidence for fluid seepage or hydrothermal venting, e.g. when gas bubbles or plumes were detected as hydroacoustic anomalies in the PARASOUND or HYDROSWEEP echosounding systems, or where blanking in the sub-bottom profiler indicated high gas content in the sediment. In addition, we used previously obtained HAWAII side-scan sonar maps from the British Antarctic Survey to identify backscatter anomalies that may be indicative of methane seepage, such as the deposition of gas hydrates, chemosynthetic communities, or the precipitation of authigenic carbonates close to the sediment-seawater interface.

During each OFOS deployment we additionally fixed 3-6 MTLs (Miniaturized Temperature data-Logger) to investigate heat anomalies associated with hydrothermal venting or cold seeps. Details of the operation, acquisition and processing are given in chapter 8.

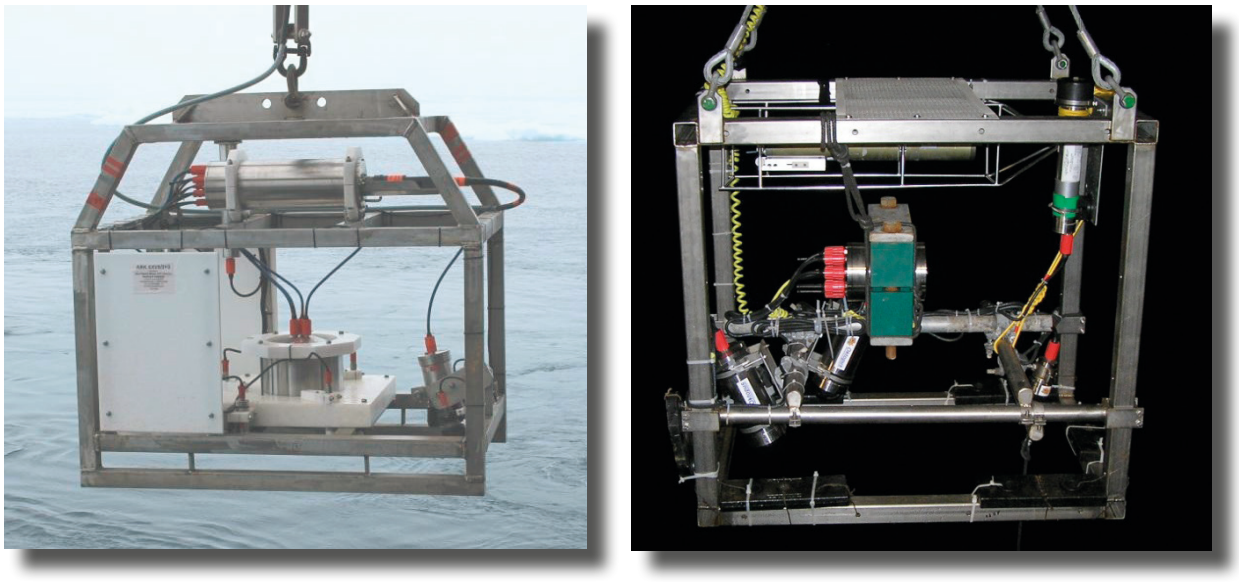

Fig. 5.1: On the left the OFOS underwater unit (owned by AWI) and on the right the TV-sled (owned by MARUM). Both systems were used during ANT-XXIX/4.

Preliminary results

In total, ten OFOS deployments were conducted during ANT-XXIX/4 in the Scotia Sea (Fig. 5.2, Table 5.1). Four of the deployments used the back-up MARUM TV-sled due to technical failure of the ship's fibre-optic cable, which was partly damaged during OFOS-3 and failed completely during OFOS-4 and OFOS-5. During these dives only low-quality black-and-white videos were recorded.

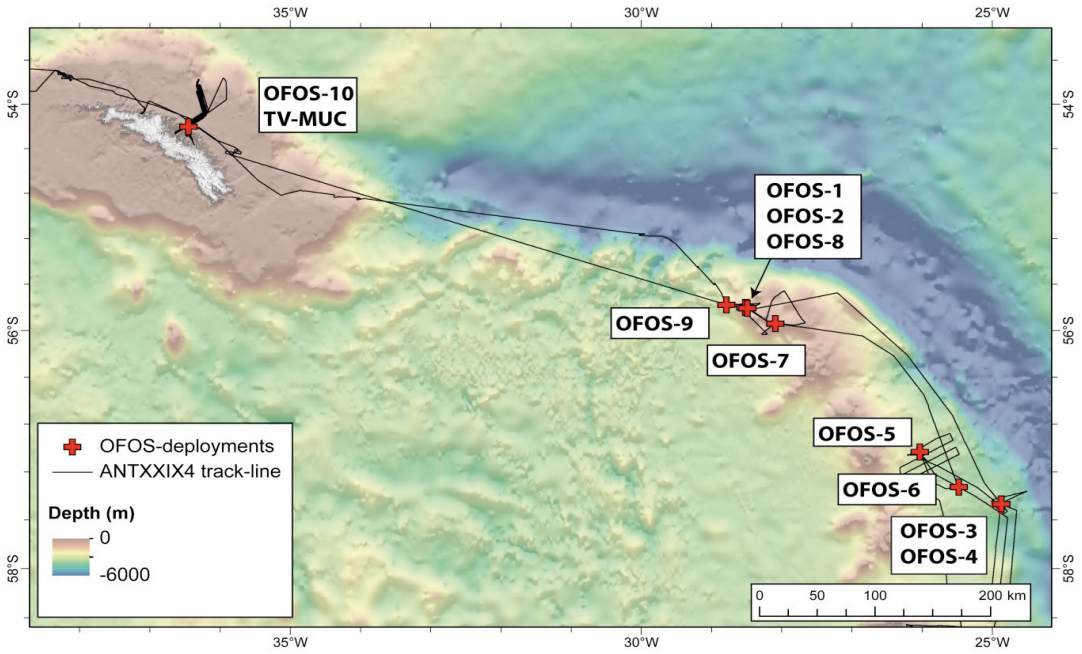

Fig. 5.2.: Overview map of OFOS deployments conducted during ANT-XXIX/4 in the Scotia Sea

The first two OFOS deployments and OFOS-8 were used to investigate the Quest caldera, where a temperature anomaly was detected directly during OFOS-1 and hydrothermal vent activity was visually confirmed during OFOS-8. Two other submarine volcanoes were investigated during OFOS-7 (Protector Shoal) and OFOS-9 (un-named volcano). Here there was no visual sign of hydrothermal activity, but locally elevated temperatures were found, indicative of some hydrothermalism at both volcanoes. Four OFOS dives were deployed in the fore-arc, although technical problems with the winch and then fibre-optic cable meant that OFOS-3 had to be aborted immediately on reaching the seafloor, and OFOS-4 and OFOS-5 lasted only 30 and 15 minutes, respectively. For OFOS-6 the MARUM TV-sled was deployed at a curious looking plume detected by the PARASOUND system, but its origin could not be confirmed because the OFOS could not be towed directly over the plume site. The last OFOS dive was in Cumberland Bay on the north side of South Georgia at a prominent flare identified in the hydroacoustic systems. Here gas bubbles were observed. Prior to this last OFOS dive a TV-MUC was used at another prominent flare in Cumberland Bay East to take a sample close to the gas emission site.

Data management

OFOS data obtained from this cruise will be uploaded to PANGAEA Data Publisher for Earth & Environmental Science archive.

Tab. 5.1.: Summary of OFOS deployments during ANT-XXIX/4

Deploy-ment	Area	Station-number	Date	Start					End					Attach-ments	Comments
				off deck	at bottom	Lon	Lat	Depth	from bottom	on deck	Lon	Lat	Depth		
OFOS-1	Quest	PS81/ 268-1	31.03.13	09:12	09:39	55°48.219	28°30.144	731	11:39	11:55	55°48.724	28°30.029	744	4 MTLs	
OFOS-2	Quest	PS81/ 268-2	31.03.13	11:21	12:37	55°48.008	28°31.488	731	15:11	15:29	55°49.366	28°32.136	950	4 MTLs	
OFOS-3	Forearc	PS81/ 269-1	01.04.13	14:38	15:58	57°28.111	24°53.055	3715	20:18	21:22	57°28.132	24°53.114	3708	SVP	Winch failure. Deploym. cancel. SVP worked
OFOS-4	Forearc	PS81/ 269-2	02.04.13	13:15	14:33	57°28.190	24°54.174	3659	15:27	16:37	57°28.285	24°54.174	3681	2 MTLs and SVP	Winch problem after 30 min, dive cancelled
OFOS-5	Forearc	PS81/ 273-1	07.04.13	09:33	10:35	57°02.028	26°02.221	3025	10:56	12:08	57°02.063	26°02.225	3026	3 MTLs and SVP	Optical signal failed
OFOS-6	Forearc	PS81/ 274-3	08.04.13	01:18	02:33	57°19.625	25°28.910	3723	04:10	05:18	57°19.644	25°29.053	3720	3 MTLs	MARUM TV-sled, Posidonia failed
OFOS-7	Protector Shoal	PS81/ 275-1	08.04.13	19:07	19:13	55°56.426	28°05.728	60	21:07	21:20	55°57.097	28°06.693	526	5 MTLs	MARUM TV-sled, no Posidonia
OFOS-8	Quest	PS81/ 276-1	08.04.13	23:04	23:23	55°48.542	28°29.687	716	01:30	01:44	55°48.652	28°29.516	717	5 MTLs	MARUM TV-sled
OFOS-9	Unnamed volcano	PS81/ 278-1	09.04.13	13:16	13:33	55°46.711	28°47.601	618	15:31	15:45	55°46.873	28°47.459	779	5 MTLs	MARUM TV-sled
OFOS-10	Cumberl. Bay Flare	PS81 285-1	11.04.13	23:26	23:36	54°12.138	36°27.187	265	00:59	01:05	54°12.202	36°27.344	264	5 MTLs	

5.1 OFOS-1 (PS81/268-1) at Quest caldera

Tab. 5.1.1: Basic data of OFOS-1/PS81/268-1 (extra equipment: 4 MTLs, taken on 31 March 2013 at Quest Caldera)

	Start down	Bottom view	End of dive	On deck
UTC	09:11	09:39	11:39	11:55
Positioning	Ship	Posidonia	Posidonia	Ship
Latitude Longitude	55°48.220'S 28°30.105'E	55°48.219'S 28°30.114'E	55°48.724'S 28°30.029'E	55°48.546'S 28°29.951'E
Water depth		724 m	744 m	

Survey tasks
Detecting vent structures or vent/seep related fauna

Key results

Surveying the rim of the Quest caldera showed typical Southern Ocean hard-rock seafloor fauna with sub-Antarctic and Antarctic species on old and slightly sediment covered volcanic rocks. No sign of active or inactive venting at the seafloor was found during the dive, but post processed temperature data showed an anomaly recorded when crossing over a seafloor depression, probably indicating hydrothermal activity in the close vicinity.

Technical description
Technical performance of the OFOS was generally very good. Due to strong southern winds we had to shorten the dive and stop shortly after WP3 because the ship was not able to manoeuvre in any direction downward into the caldera.

Dive description
The first OFOS deployment was performed at the Quest caldera (Fig. 5.1.1) and started at the rim of the structure in about 720 m water depth. The central part of the caldera is at, 1075 m, about 340 m deeper than the rim, and the distance from the rim to the centre is ~1.8 km. It was planned to survey along the rim and afterward down into the inner part of the caldera. However, we had to modify the original plan and divide the survey into two separate deployments, as the weather conditions changed and the ship had to move to the northwest of the caldera in order to allow surveying into the inner part of the caldera. Therefore, the first OFOS deployment took place only along the north-eastern rim of the caldera, and showed that the seafloor in this area is covered by volcanic blocks in all sizes from several centimetres to few meters. Soft sediments cover the areas between the blocks. Our general impression was that because of the thin veneers of sediment and abundant epifaunal coverage, the lava blocks seem to be old, with no evidence of fresh volcanic rock. An abundance of a variety of filter-feeding organisms was observed during the entire deployment, especially on elevated blocks. There were scattered areas with a large abundance of a white, branched octocoral, which in turn served as habitat for other organisms, such as filter feeding brittle stars and sponges. Other common fauna on the volcanic blocks were white seawhips, stick-shaped octocorals of the family Primoellidae, orange bottle-brush octocoral of the family Thourellidae, yellow sponges, bryozoans, yellow stalked crinoids and red brisingid starfish (*Freyella* sp.). Occasional red lithodid spider crabs of the genus

Paralomis were observed, representing a typical sub-Antarctic faunal element, as well as macrurid fish (rat-tails) and red *Nematocarcinus* shrimps, which are also found in the Antarctic. Between WP2 and WP3 we observed a steep-walled seafloor depression, several meters deep and about 10-20 m in diameter. Unfortunately, the distance to the seafloor became too large over this structure to take good images, but afterwards processed temperature records achieved from the 4 MTLs fixed on the frame of the OFOS indicate an obvious anomaly exactly corresponding to the time when passing the depression. The temperature suddenly became 0.35°C warmer, which may indicate that the OFOS was close to a hydrothermal active area.

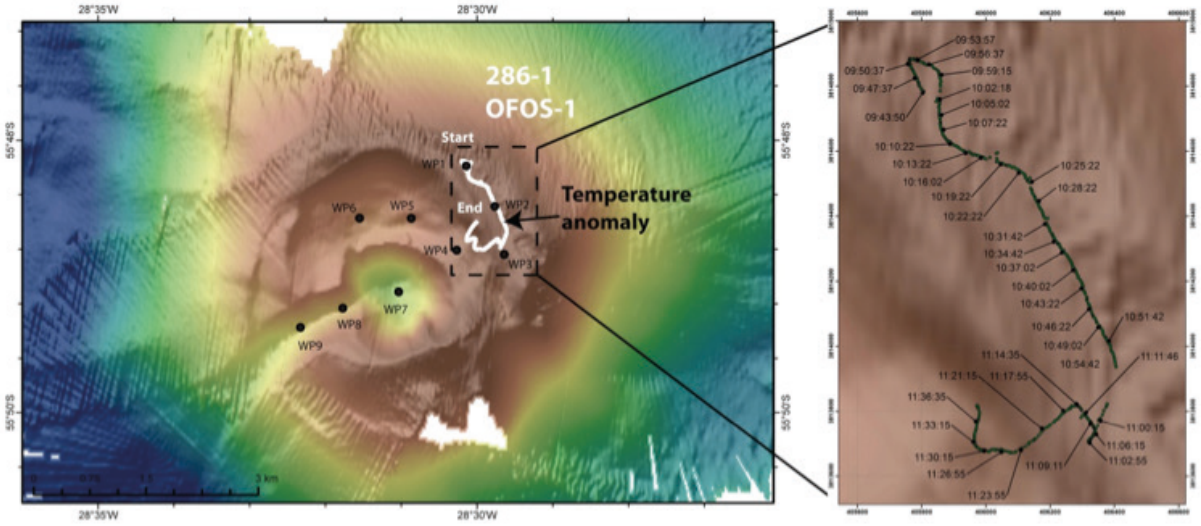

Fig. 5.1.1: Bathymetric map of the Quest caldera imaged during ANT-XXIX/4 with ATLAS HYDROSWEEP. The OFOS-1 track line is over the north-eastern rim of the structure. Due to strong winds from southwest, the dive was cancelled shortly after reaching WP3 in order to start a new dive from the other side of the caldera (OFOS-2).

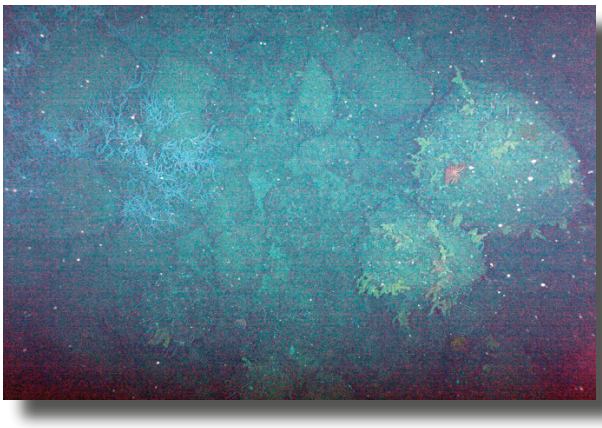

Fig. 5.1.2: Blocks of volcanic rocks covered with numerous octocorals and other epifauna

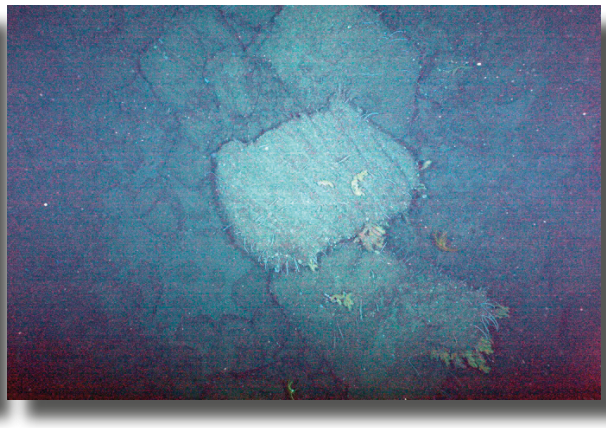

Fig. 5.1.3: Block of ropey lava from old lava flow

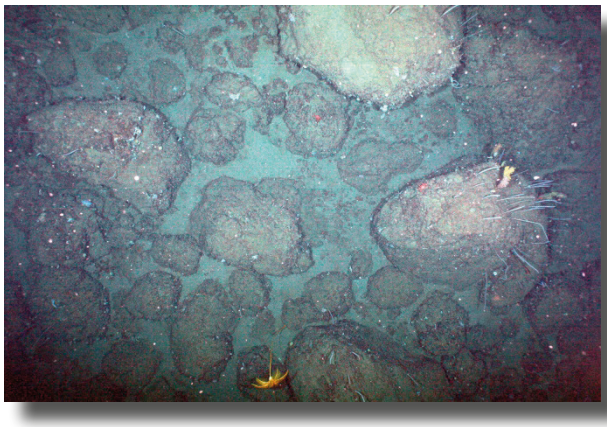

Fig. 5.1.4: Blocks of volcanic rocks with soft sediment between them. Stalked crinoids at bottom centre of image

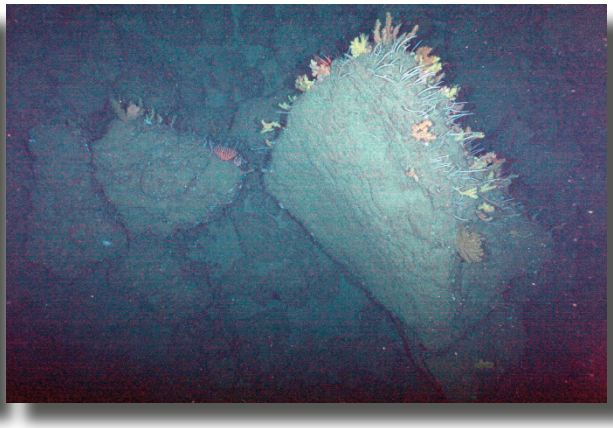

Fig. 5.1.5: Large block settled by numerous filter feeding epifaunal organisms

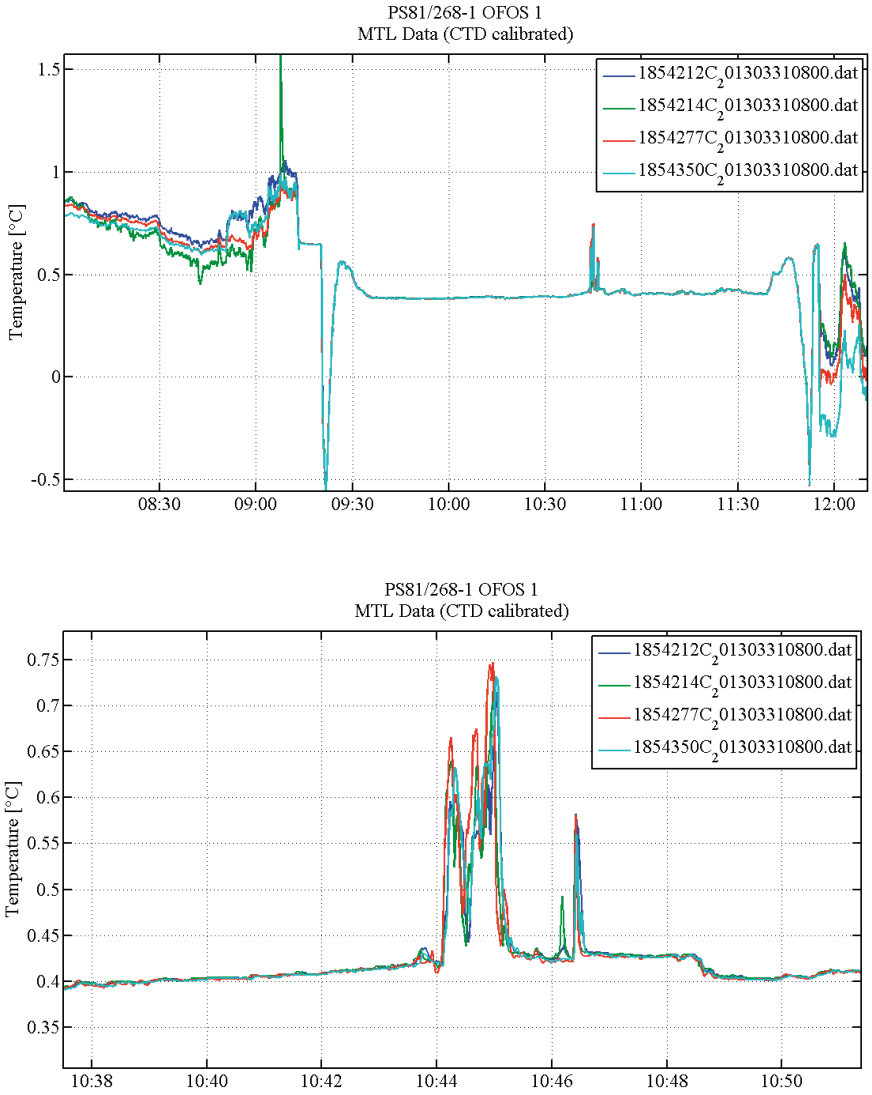

Fig. 5.1.6: The graphs showing the temperature measured with the MTLs during the entire OFOS deployment (above) and when passing the seafloor depression (below). The clear peak in temperature of ~0,35°C indicate hydrothermal activity in this area.

5.2 OFOS-2 (PS81/268-2) at Quest caldera

Tab. 5.2.1: Basic data of OFOS-2/PS81/268-2 (extra equipment 4 MTLs, taken on 31 March 2013 at Quest Caldera)

	Start down	Bottom view	End of dive	On deck
UTC	12:21	12:37	15:11	15:29
Positioning	Ship	Posidonia	Posidonia	Ship
Latitude Longitude	55°48.155'S 28°31.590'E	55°48.098'S 28°31.488'E	55°49.344'S 28°32.090'E	55°49.351'S 28°31.994'E
Water depth		734 m	927 m	

Survey tasks

Detecting vent structures or vent/seep related fauna

Key results

Surveying from the northern rim of the Quest caldera down to the central depression revealed no indication for vent activity.

Technical description

Technical performance of the OFOS was generally very good.

Dive description

The second OFOS deployment was at the Quest caldera (Fig. 5.2.1) following on from OFOS-1. The dive started at the rim of caldera to the west of OFOS-1 and observed similar geological features and animals. The faunal abundances and number of high density patches appeared to be higher than during OFOS-1, but no objective assessment has yet been done. The filter feeding fauna was less abundant on the inner caldera slope. On the floor of the first caldera plateau the sediment was covered in colourful gravel near to the slope, which gradually decreased in size and amount with increasing distance from the slope. The gravel served as attachment sites for a variety of sessile filter feeding animals, including seawhips, white branching fan-like octocorals, some sponges, bryozoans and serpulid worms. There were also a number of white infaunal anemones and orange epifaunal anemones. Rat-tail fish, *Paralomis* crabs and *Nematocarcinus* shrimp were present, but these increased in abundance where the gravel gave way to soft sediments. Here, holothurians (sea cucumbers) and their trails were seen.

The wall of the inner caldera was abrupt and had a talus slope descending into the inner caldera structure. Only few animals were observed at the slope. The floor of the inner caldera was similar to that of the outer caldera plateau, with gravel and soft sediment areas. The deepest part of the caldera had fewer seawhips, but *Nematocarcinus* was still abundant and occasionally larger fauna like rat-tails, holothurians and soft corals were seen. The ascending wall of the inner caldera close to WP8 was very steep and the winch operator had no time to stop OFOS hitting the wall of volcanic rocks. After that OFOS passed along the chute-like structure that runs SW from the nested caldera (Fig. 5.2.1). The seafloor here varied from sandy areas with scattered blocks, to talus slopes. The blocks were settled by occasional white branched, fan-like octocorals and stalked crinoids, and *Paralomis* crabs and *Nematocarcinus* shrimp were also present. Holothurians were less common. The dive ended at the deepest point.

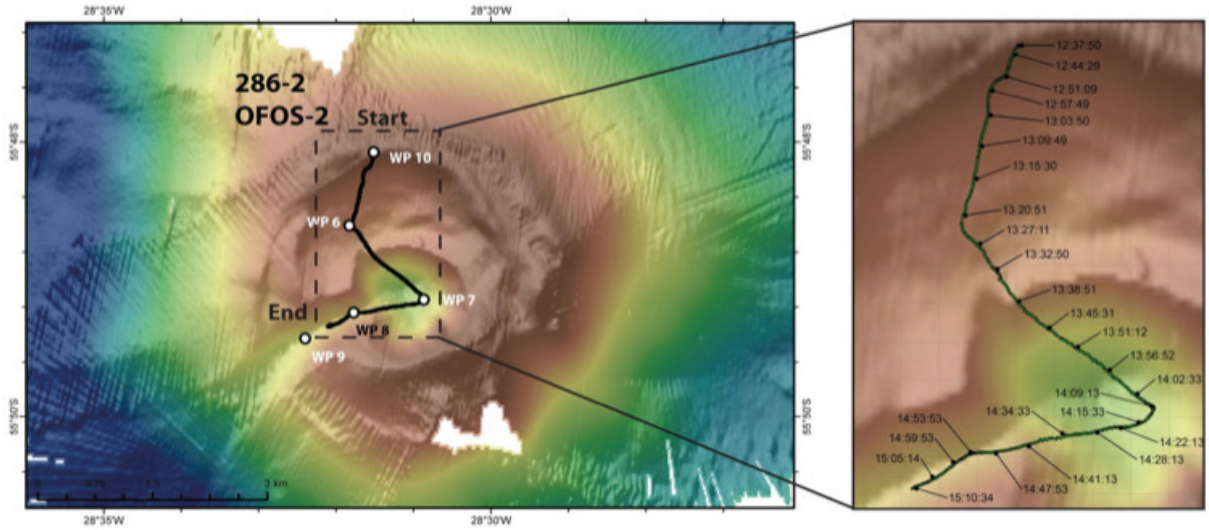

Fig. 5.2.1: Bathymetric map of the Quest caldera imaged during ANTXXIX/4 with ATLAS HYDROSWEEP. The OFOS-2 track line starting at the rim going down into the central part of the caldera and ending in the south-western chute-like trough.

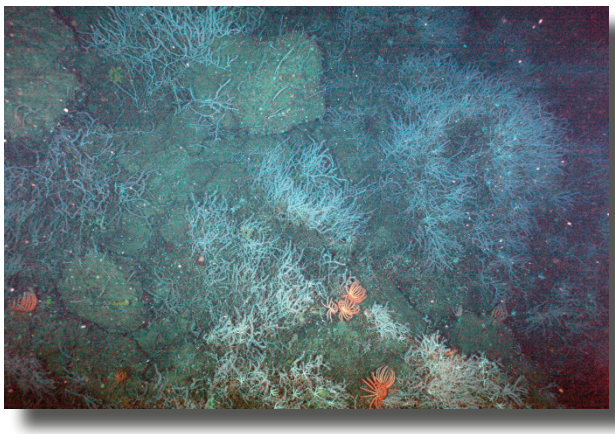

Fig. 5.2.2: Blocks of volcanic rocks on caldera rim covered with white octocorals, brisingid starfish and other epifauna

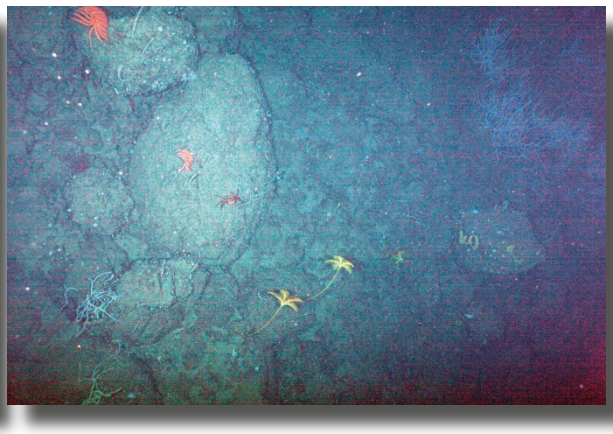

Fig. 5.2.3: Stalked crinoids attached to smaller blocks on crater rim

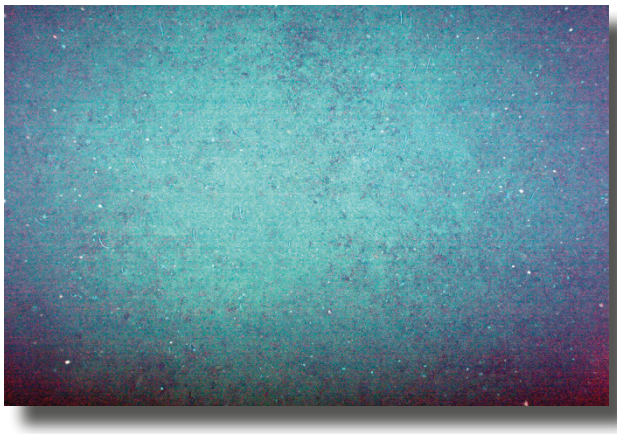

Fig. 5.2.4: Gravelly area on outer caldera plateau

Fig. 5.2.5: Area of soft sediment with phytoplankton debris on outer caldera plateau

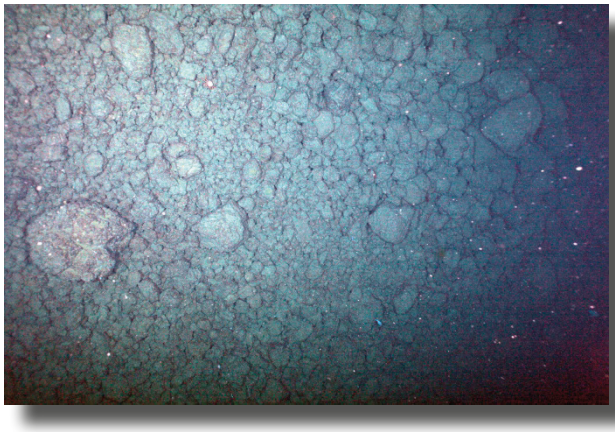

Fig. 5.2.6: Talus slope descending into inner caldera

Fig. 5.2.7: Nematocarcinus and holothurians on soft sediment on floor of inner caldera

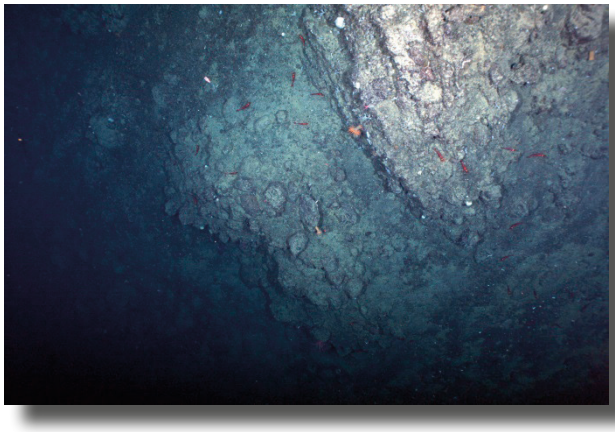

Fig. 5.2.8: Ascending wall of inner caldera

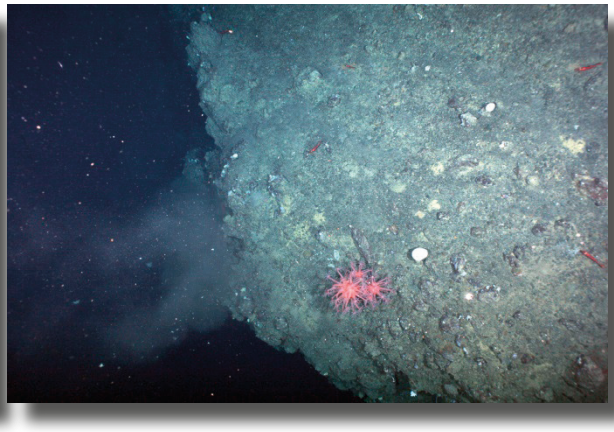

Fig. 5.2.9: Clang! OFOS hits the ascending wall of inner caldera

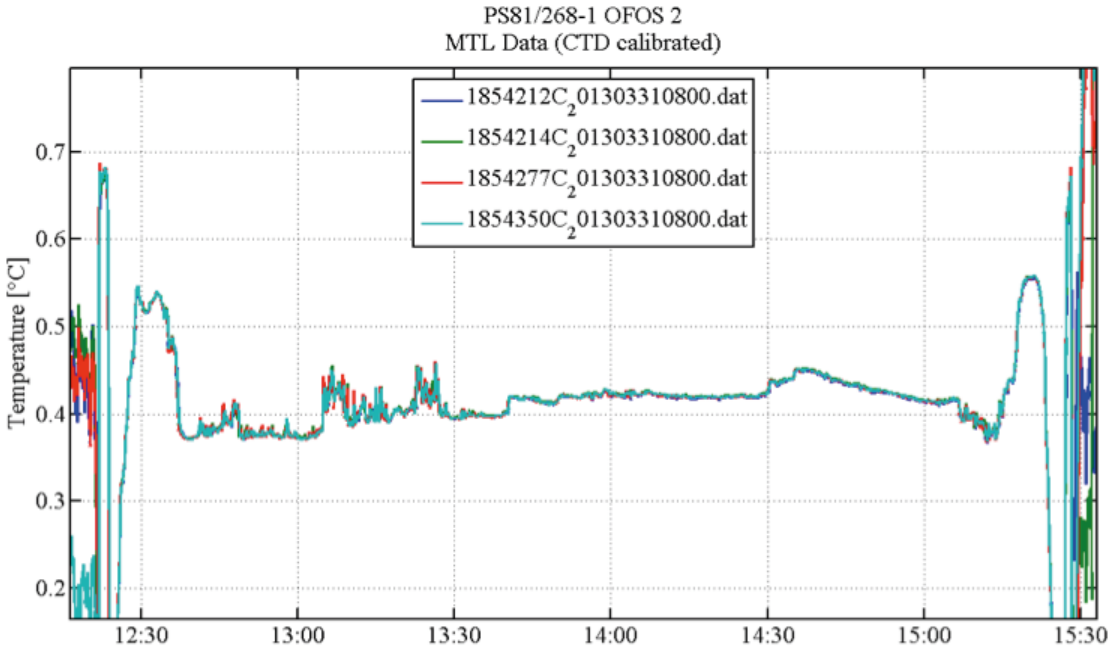

Fig. 5.2.10: Temperature measured with the MTLs during the entire OFOS deployment

5.3 OFOS-3 (PS81/269-1) at fore-arc

Tab. 5.3.1: Basic data of OFOS-3/PS81/269-1 (taken on 01 April 2013 at fore-arc)

	Start down	Bottom view	End of dive	On deck
UTC	14:38	15:58	-	21:22
Positioning	Ship	Posidonia	Posidonia	Ship
Latitude Longitude	57°28.212'S 24°53.139'W	57°28.111'S 24°53.084'W	-	57°28.158'S 24°53.365'W
Water depth		3726 m	3715 m	

Survey tasks
Detection of cold seeps structures

Key results
Only few seconds of bottom view showed soft sediments (grey to green) with scattered gravel, crossed by grazing traces (Lebensspuren) of sea cucumbers and other animals.

Technical description
Due to technical problems with the winch directly after reaching the seafloor, the dive was cancelled and the rest of the dive time had to be used for finding the error and testing with the OFOS at a depth between 3,000 – 3,500 m.

Tab. 5.3.2: Observation protocol

Time	**Observation**
14:40	OFOS at 20 m
14:45	Restart of OFOS software
14:49	Start to decent with 1 m/s
15:05	3,700 m depth
15:50	Rope speed to 0.7 m/s
15:53	Rope speed to 0.5 m/s
15:57	Seafloor visible
15:58	Sea cucumbers, Soft sediment
15:59	Cable problem
16:01	Lights off
16:15	Lights on
16:17	Lights off, lasers off
16:18	Lights and laser on or off for several times
16:23	3715 m cable out and straight up all cable in this point
16:24	seafloor back
16:26	OFOS coming up with 0.5 m/s
16:27	coming up with 1 m/s until 3,600 m cable length, then winch test

17:57	Restart dive
18:01	Decent with 1 m/s
18:06	Winch test in 3,400 m
21:06	750 m of cable out, coming up
21:22	OFOS on deck

5.4 OFOS-4 (PS81/270-1) at fore-arc

Tab. 5.4.1: Basic data of OFOS-4/PS81/270-1 (extra equipment: 2 MTLs, taken on 02 April 2013 at fore-arc)

	Start down	Bottom view	End of dive	On deck
UTC	13:15	14:33	15:27	16:37
Positioning	Ship	Posidonia	Posidonia	Ship
Latitude Longitude	57°28.263'S 24°54.399'W	57°28.190'S 24°54.383'W	57°28.285'S 24°54.174'W	57°28.594'S 24°53.899'W
Water depth		3,657 m	3,689 m	

Survey tasks
Detection of cold seeps structure

Key results
Smoothly sloping seafloor covered by soft sediment with numerous animal traces and inhabited by white brittle stars and small white anemones. While crossing some escarpments, the underlying volcanic material became visible proving that the mound structure is of volcanic origin covered by sediments.

Technical description

No technical problems during the first 30 minutes. But several error messages from the OFOS software indicated already that the connection was not perfectly established. Nevertheless, the system kept working when closing the error messages. After about 25 minutes on the seafloor the camera connection was lost for the first time, but was recovered after a restart of the system. But only a few minutes later the connection was lost again and could not be restarted. The LED at the OFOS deck unit indicated that there was no longer an optical connection and after checking possible solutions, we decided to cancel the dive and bring OFOS on deck.

Dive description
The fourth OFOS deployment was planned to investigate again the seafloor in the fore-arc area where high seafloor backscatter was observed in the HAWAII sidescan sonar map and confirmed during this cruise by HYDROSWEEP data. The deployment started on the slope of a morphologically elevated area in about 3,660 m water depth, at the northern part of the most prominent high-backscatter patch (Fig. 5.4.1). The seafloor appeared relatively flat and covered by gravelly soft sediments. The sediments were of mottled grey colour, crossed by numerous

darker-coloured moving traces of epibenthic organisms. Patches of greenish colours indicated sunken phytoplankton which probably acts as a food source for the epi- and infaunal benthic fauna. Brittle stars and white anemones were abundant at the sediment surface. Occasional holothurians were seen, together with their moving traces (Lebenspuren) and faecal pellets. One of the still images captured specimen of a deep-water serolid isopod genus, preliminary identified as *Acutiserolis*. These seafloor and faunal observations were similar to those noted during the ANDEEP II expedition in the South Sandwich Trench in 2002. A few small rocks of up to ~10 cm in diameter were also observed. After a few minutes travelling in south-eastern direction OFOS went over an escarpment of dark, glassy-looking rocks with several decimetre sized blocks, which we interpreted to be of volcanic origin. The scarp was a few meters high and may represent the leading edge of a lava flow running downslope from the top of the elevated area to the south. After passing the escarpment the seafloor was again flat, covered by sediments and inhabited by the same faunal assemblage of brittle stars and anemones, including a band of abundant anemones running a few metres from the scarp and parallel to it. Two more similar escarpments were passed over before the dive had to be aborted due to problems with the optical signal of OFOS. The observation time on the seafloor was therefore only about 25 minutes, covering about 200 m and an elevation change of ~30 m.

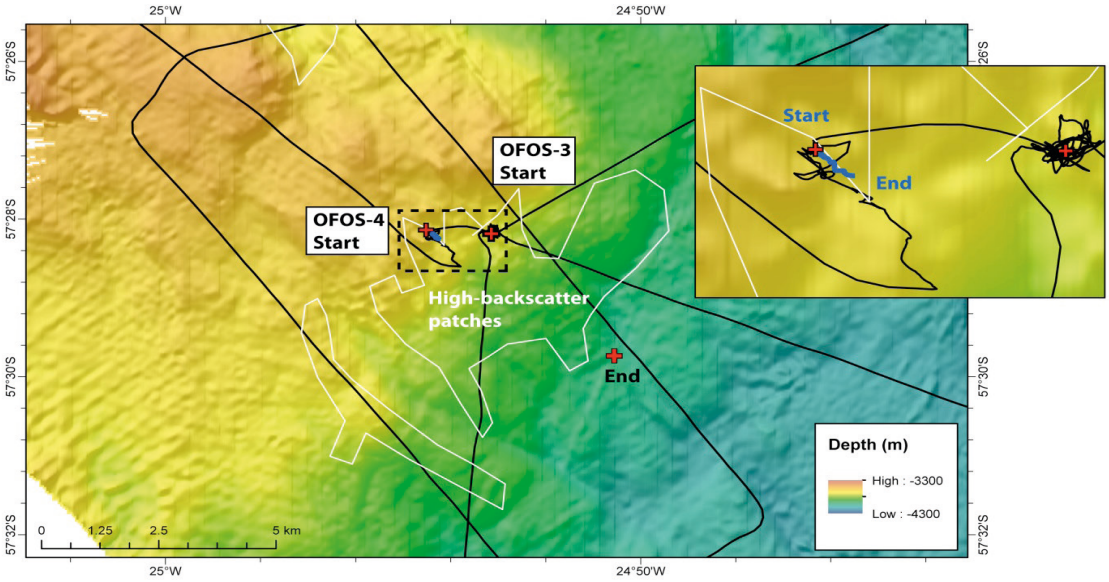

Fig. 5.4.1: Bathymetric map from ANT-XXIX/4 showing the high-backscatter patches mapped from the HAWAII-sidescan data (white outlined areas) and the planned OFOS Start and End points. OFOS-3 had to be cancelled due to technical problems and OFOS-4 was only ~25 minutes on the seafloor covering a line ~200 m in south-eastwards direction (blue line).

Fig. 5.4.2: Gravelly soft sediments with larger blocks, moving traces, white anemones and brittlestars

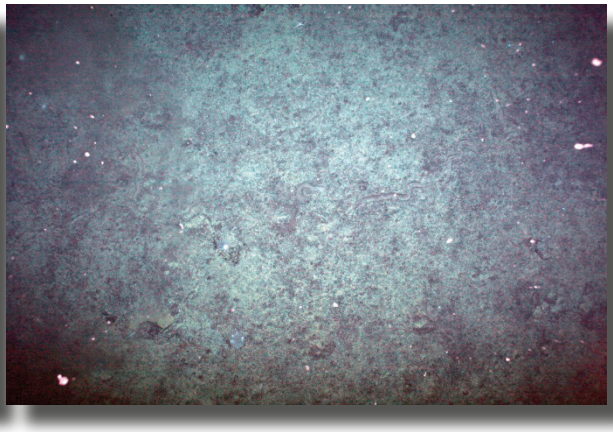

Fig. 5.4.3: Several metres long moving trace left to right centre

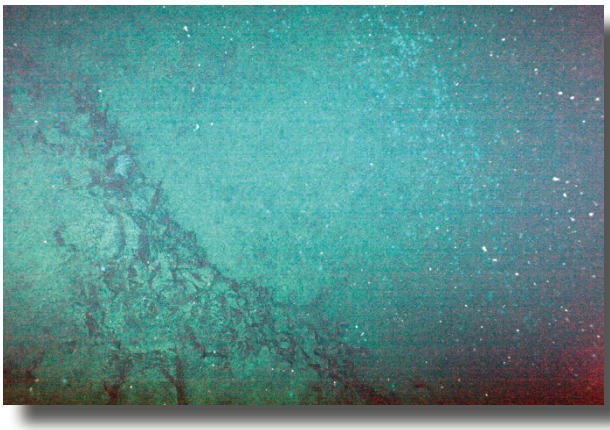

Fig. 5.4.4: First escarpment of glassy looking volcanic rock, and band of abundant white anemones

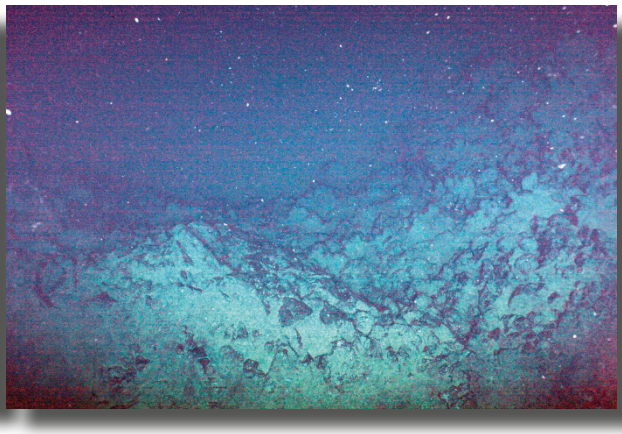

Fig. 5.4.5: Third escarpment of more brecciated volcanic rock

Tab. 5.4.2: Observation protocol

Time	Observation
13:45	OFOS at 1,397 m, going down 1 m/s, dive continued after successful winch test
13:57	OFOS at 2,000 m cable length, next winch test
13:57	Test successful, continue dive to 3,000 m cable with 1m/s
14:16	OFOS on 3,000 m cable length, next winch test successful
14:33	Sea Floor in sight soft sediment, gravel, brittle stars, traces
14:39	start with 0.5 Kn to WP2
14:43	Small scarp
14:45	Small scarp
14:46	Field of white discs

14:48	Starfish and scarp
14:51	Breccia and soft sediment
14:56	Camera connection problem
14:57	Connection fixed
14:59	Seafloor observable again
15:00	Camera problem, no live images, OFOS up by 10 m
15:19	Optical link failure
15:29	OFOS on way back to deck
16:36	OFOS on deck

5.5 OFOS-5 (PS81/273-1) at fore-arc

Tab. 5.5.1: Basic data of OFOS-5/PS81/273-1 (extra equipment 3 MTLs and SVP, taken on 07 April 2013 at fore-arc)

	Start down	Bottom view	End of dive	On deck
UTC	09:33	10:35	10:56	12:08
Positioning	Ship	Posidonia	Posidonia	Ship
Latitude Longitude	57°02.004'S 26°02.030'W	57°02.028'S 26°02.221'W	57°02.063'S 26°02.225'W	57°02.017'S 26°02.230'W
Water depth		3,031 m	3,026 m	

Survey tasks
Investigating the high seafloor backscatter patches

Key results
After only few minutes moving over the identified area of low seafloor backscatter the dive had to be aborted due to problems with the optical signal. The seafloor was covered in soft sediments with very little gravel, somewhat like that seen on OFOS dive 4, with visible brittlestars, sea cucumbers and the dark coloured grazing traces of sea cucumbers.

Technical description
After the last dive OFOS-4 when the fibre-optic cable failed, the subsequent ship board inspection suggested that the second fibre-optic was still working, allowing us to keep using the cable without a time-consuming cable repair, or switch to another cable. The dive started without technical problems, but the optical signal was lost after only 15 minutes on the seafloor and the dive had to be aborted. As for OFOS-4, during the dive the software sent several error messages first and shortly afterwards, with the LED indicating that the optical signal was turned off. Thus it appears that although the second optical fibre seemed to be OK when testing on-board, it was probably also already slightly damaged and broke entirely during the dive with the enhanced tension. After the dive the cable had to be entirely repaired (a process taking several days) meaning that the next OFOS deployments the MARUM TV-sled was used with a coax cable.

Dive description

The dive started at WP 1 and the OFOS was towed in the direction of WP2 in order to cross into the area of high seafloor backscatter identified in the HAWAII sidescan sonar map (Fig. 5.5.1 right). WP 1 is located in usual background backscatter and we expected to find a seafloor similar to that we observed during OFOS-4, and, indeed, the seafloor appeared relatively flat and covered in soft sediments mixed with a little gravel, but not as much as seen in OFOS-4. The greyish sediment was covered with a layer of darker phytodetritus. Large numbers of epi- and infauna were visible, including several species of brittlestars and at least two different species of large holothurians (one pale with tubercles on the body, and one dark), with the brittlestars and pale sea cucumbers being seen on every frame. Starfish were seen occasionally and a few rat-tail fish came in view. When the bow wave of OFOS pushed away the phytoplankton and top sediment layer, numerous polychaete tubes became visible. Based on the observed high abundance of motile and sessile fauna, this is a productive area. The OFOS moved only few tens of meters to the south and before reaching the area where high seafloor backscatter indicated a change of the seafloor characteristics, we got problems with the camera and error messages in the software. Unfortunately, the problem could not be solved and the dive had to be aborted after 15 minutes at the seafloor.

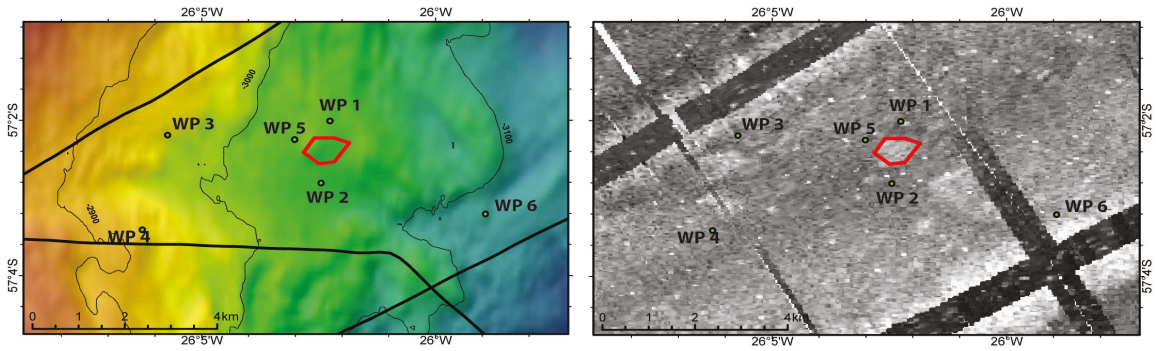

Fig. 5.5.1: Bathymetry map from ANT-XXIX/4 HYDROSWEEP data (left) and sidescan sonar map from deep-towed HAWAII system from an earlier cruise (right), with the waypoints planned for the OFOS-5 deployment. The dive actually started at WP1 but only covered few tens of metres, unfortunately not reaching the area indicated by high seafloor backscatter.

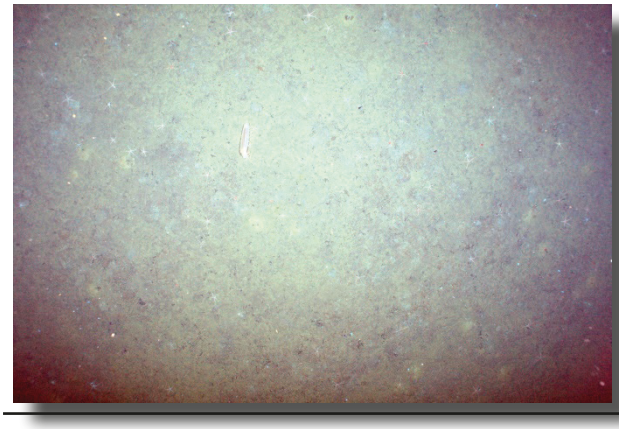

Fig. 5.5.2: Pale coloured sea cucumber grazing the flat seafloor covered with soft sediments

Fig. 5.5.3: Numerous brittlestars

Tab. 5.5.2: Observation protocol

Time	Observation
09:32	OFOS leaves deck
09:33	Camera on, lights on
09:39	Rope length is 149 m, rope speed 0.9 m/s
09:53	947 m, rope speed 1 m/s
09:56	Camera shooting in the raw mode
10:04	Jellyfish
10:15	Jellyfish
10:26	2,811 m depth, reducing rope speed to 0.5 m/s
10:32	Reducing rope speed to 0.3 m/s
10:35	Seafloor visible
10:37	Fish (rat-tail), brittle star
10:38	Sea cucumbers
10:38	Sea cucumbers
10:39	Soft sediment, with some stones
10:40	Sea cucumbers, brittle star
10:41	Sea cucumbers, brittle star
10:44	Changed picture format to jpeg mode
10:45	brittle star
10:47	Changed photo interval to 30 seconds
10:48	Sea cucumbers
10:50	Camera problem, restart software
10:57	OFOS is 7 m above seafloor
11:11	Cancel the dive due to communication problem

5.6 OFOS-6 (PS81/274-3) at fore-arc

Tab. 5.6.1: Basic data of OFOS-6/PS81/274-3 (extra equipment 3 MTLs, taken on 08 April 2013 at fore-arc)

	Start down	Bottom view	End of dive	On deck
UTC	02:33	02:33	04:10	05:18
Positioning	Ship	Posidonia	Posidonia	Ship
Latitude Longitude	57°19.605'S 25°29.072'W	57°19.625'S 25°28.910'W	57°19.644'S 25°29.053'W	57°19.536'S 25°29.178'W
Water depth		3,723 m	3,725 m	

Survey tasks
Investigating the source of the PARASOUND anomaly.

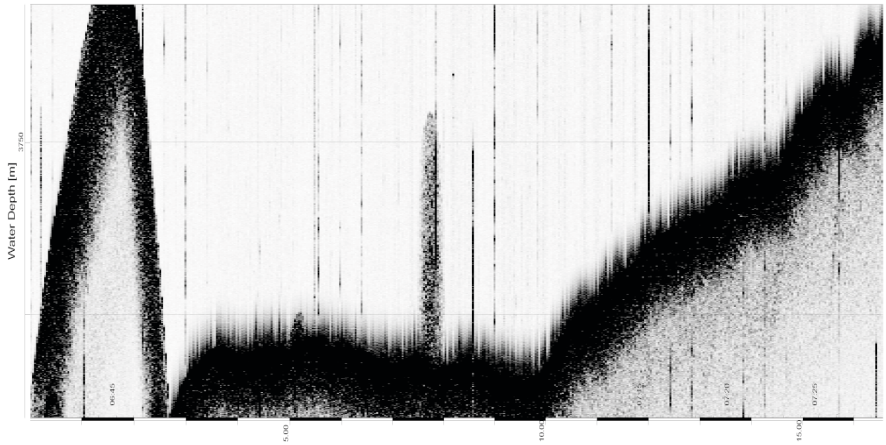

Fig. 5.6.1: PARASOUND echogram illustrating the anomaly detected in the water column reaching about 35 m from the seafloor

Key results
The seafloor area beneath the detected hydroacoustic anomaly is probably a seafloor depression surrounded by a rim of large volcanic blocks. Unfortunately, we could not manage to investigate depression using the OFOS, so the nature of the hydroacoustic anomaly remains enigmatic.

Technical description
This dive was performed with the MARUM TV-sled and telemetry. There were no technical problems during the deployment, but we lost the Posidonia connection after 20 minutes.

Dive description
During this deployment we tried to pass over the centre of the PARASOUND anomaly (Fig. 5.6.1) as often as possible to search for indications of seep or vent activity. The observations were impaired by the black and white images and a reduced picture resolution of the MARUM telemetry. Nevertheless, we were able to distinguish between areas of relatively flat, gravel and finer sediment covered

seafloor, and elevated areas with large blocks of volcanic rocks. The areas of soft sediment were similar to those seen in OFOS-4 dive, with abundant Lebensspuren, some holothurians and occasionally a rat-tail fish and large starfish, although the diversity appeared to be less. White round shapes were observed that could be anemones, or perhaps brittlestar discs. Three times the OFOS crossed areas with large rocks, some of which were dark coloured with clean fractured edges (?volcanic glass), others of which were much paler and appearing "spiky" at the edges. Several times we observed brisingids attached to these rocks. This area seem to be higher than the surrounding flat seafloor and additionally appears to represent a rim of a depression, probably located in the central part of this rocky area. Unfortunately, the OFOS could not be towed in the core of this area to prove this hypothesis. Generally it was very difficult to strategically map without Posidonia positioning and there was also a large shift between the last received Posidonia position and the first ship position (>100 m). Therefore, we may not have actually been surveying far to the NE of the target point (Fig. 5.6.2). Post dive analysis for the 3 MTLs showed no temperature anomalies (Fig. 5.6.3).

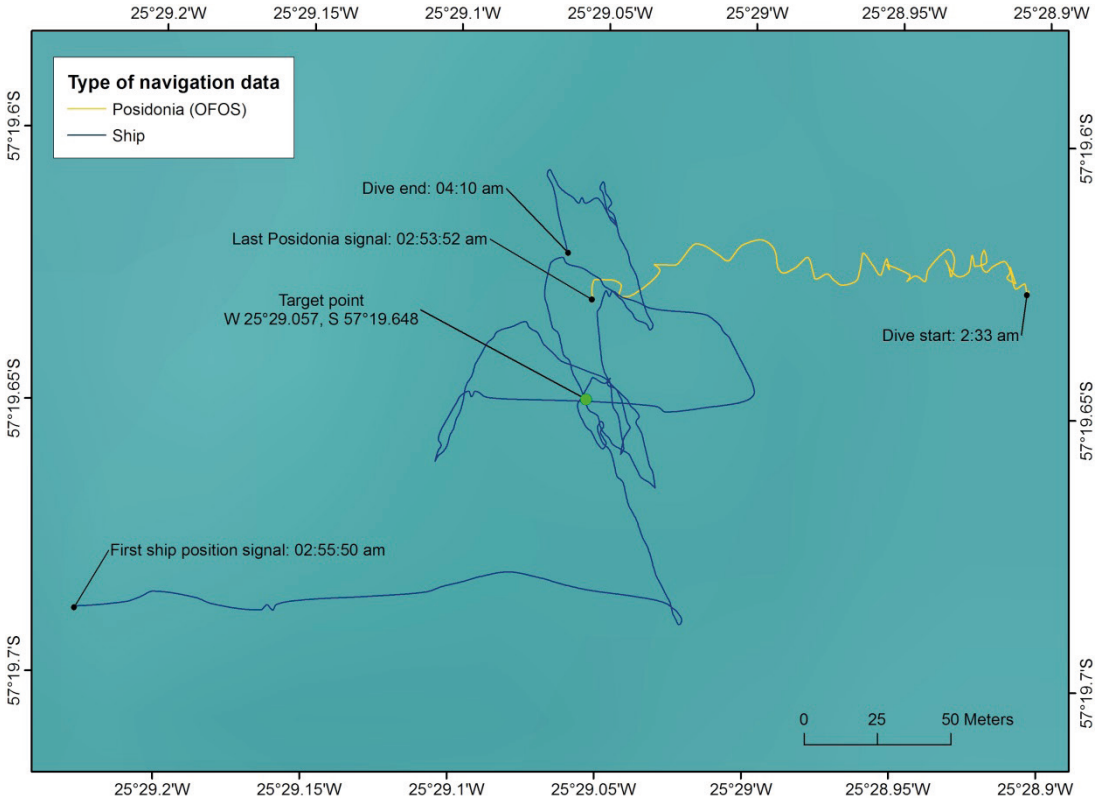

Fig. 5.6.2: OFOS-6 track lines, starting with working Posidonia positioning (yellow line) followed by the ship track after the Posidonia signal was lost. The green point marks the estimated central area of the hydroacoustic anomaly. Because of the uncertainty of the OFOS position we cannot be sure if we really surveyed over this point.

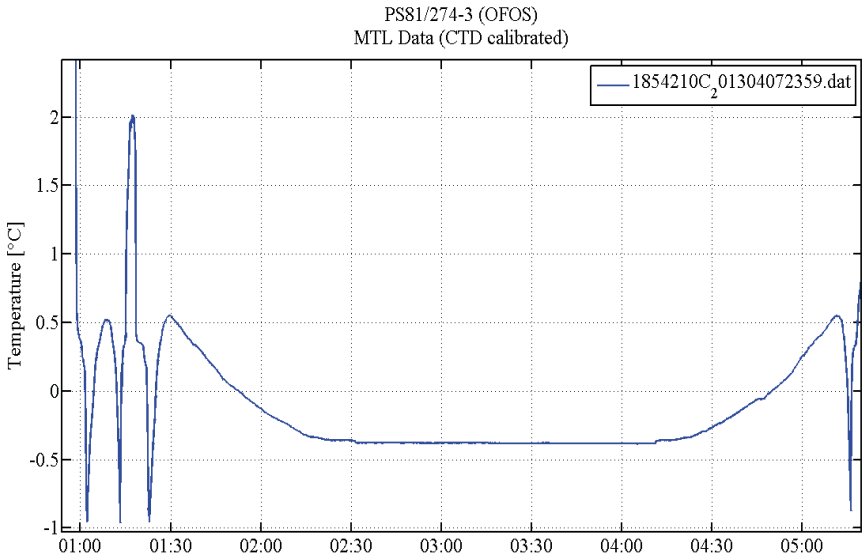

Fig. 5.6.3: Temperature vs time graph showing no temperature anomalies were recorded during OFOS-6

5.7 OFOS-7 (PS81/275-1) at Protector Shoal

Tab. 5.7.1: Basic data of OFOS-7/PS81/275-1 (extra equipment 5 MTLs, taken on 08 April 2013 at Protector Shoal)

	Start down	Bottom view	End of dive	On deck
UTC	19:07	19:13	21:07	21:20
Positioning	Ship	Posidonia	Posidonia	Ship
Latitude Longitude	55°56.424’S 28°05.728’W	55°56.426’S 28°05.728’W	55°57.097’S 28°06.693’W	55°57.064’S 28°06.589’W
Water depth		60 m	512 m	

Survey tasks
Investigating the top and flank of the submarine volcano at Protector Shoal and search for hydrothermal activity.

Key results
Lava flow structures on top of the submarine volcano and gravelly reworked material along the flank. No direct indication for hydrothermal activity, but the temperature sensors showed elevated values close to the end of the dive at the greatest depth.

Technical description

This dive was performed using the MARUM TV-sled and telemetry, because the fibre-optic cable for the AWI OFOS telemetry was being repaired. No problems during the entire dive with the connection or handling of the TV-sled. But, unfortunately, we had no Posidonia connection during the entire dive. (Afterwards we checked carefully and found out during the next dive that the entire Posidonia system had to be rebooted and then worked again.) Nevertheless, we had the impression that the OFOS was always very close behind the vessel (which was never moving faster than 0.5 kn) because the cable length was only few metres to tens of metres less than the water depth indicated from the multibeam system on the ship.

Dive description

The seafloor was visible very soon on this dive due to the shallow water depth at the top of Protector Shoal at ~55 m. Here were North-South running ridges about a metre apart of very pale coloured lava. Between the ridges were obvious parallel running cracks and darker coloured coarse grained sediment. No large animals or plants were visible at first, but as OFOS moved across the ridges to the West the seafloor surface changed to pitted lavas with angular collapse structures, and anchored in these were red or brown seaweeds (not distinguishable in the B/W video stream), up to 10 per square metre. The seaweeds appeared to have a broad single blade, which swung with the currents and seemed flexible. Moving towards WP2 the seafloor alternated between pitted lava with seaweeds and N-S running lava ridges, some of which had obvious ribs emanating at right angles to the ridges, but not reaching across to the next ridge. As the depth increased to below 66 metres no more seaweed was visible. At WP2 OFOS turned to the South and moved down-slope into the caldera. At first lava ridges were seen with a different orientation, roughly parallel to the direction of travel, but quite soon beyond 100 m these were lost and the seafloor consisted of a slope of gravel, sand and isolated lava boulders. From around 150 m large cidaroid urchins (pencil urchins) were commonly observed on gravelly sediment as well as occasional rat-tail fish, a couple of lithodid crabs, and a few anemones. The numbers of the cidaroids decreased with depth. At 500 m the gravel gave way to pitted lava again and this area may correspond to the recorded temperature anomaly (see Fig. 5.7.1 and 5.7.2). Shortly afterwards there was a potential winch problem and OFOS was raised to a safe depth, meaning contact with the seafloor was lost for 5 minutes. When contact was regained the seafloor was seen to be gravelly and as nothing further interesting was seen the dive was terminated.

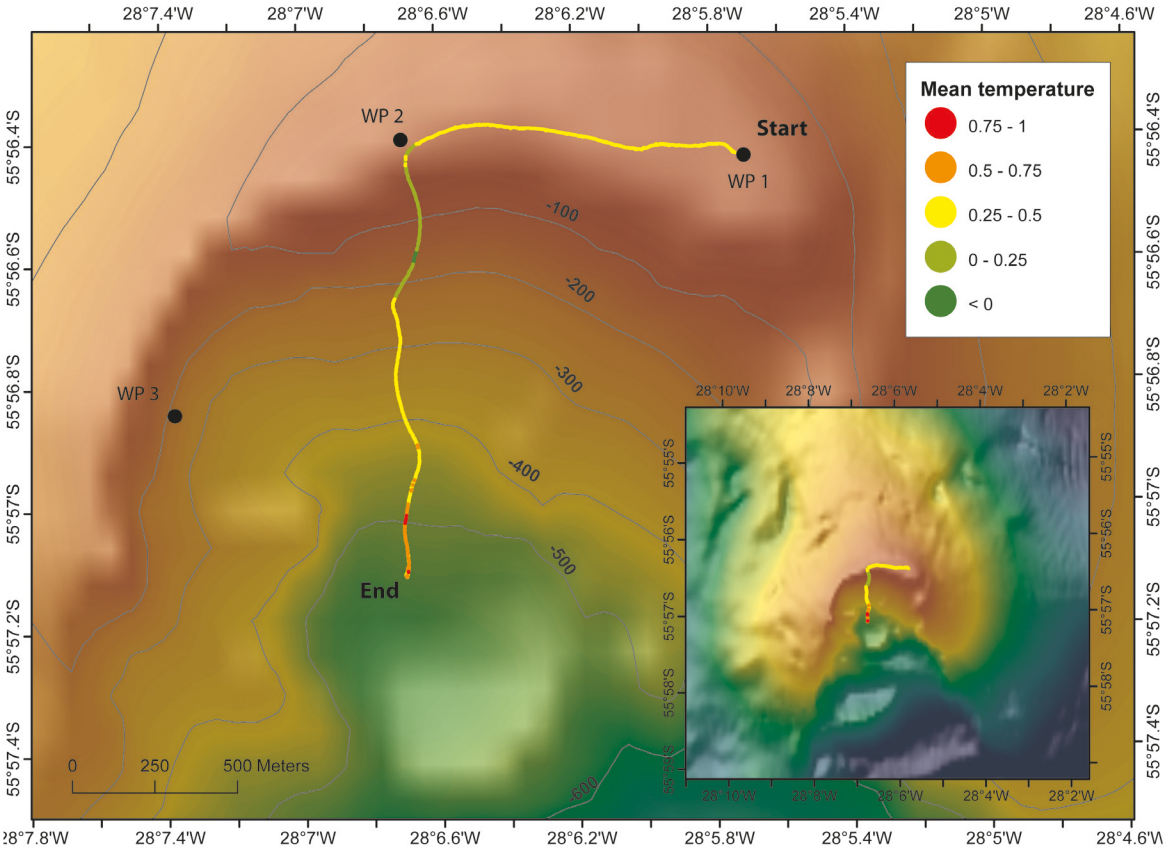

Fig. 5.7.1: Bathymetry map from ANT-XXIX/4 HYDROSWEEP data with OFOS dive track plotted. The track colour corresponds to the mean temperatures in the key.

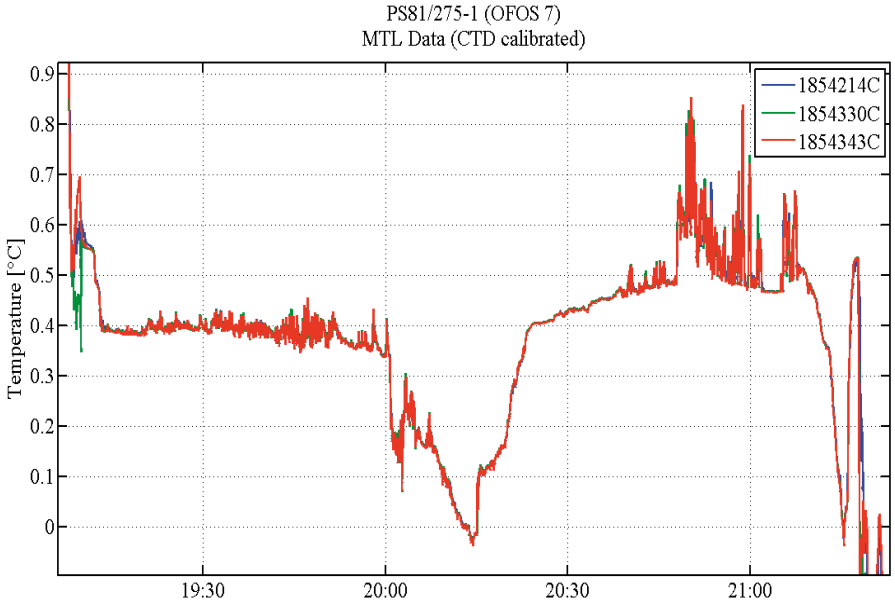

Fig. 5.7.2: Temperature measured with the MTLs during the entire OFOS deployment

5.8 OFOS-8 (PS81/276-1) at the rim of Quest caldera

Tab. 5.8.1: Basic data of OFOS-8/PS81/276-1 (extra equipment: 5 MTLs, taken on 08/09 April 2013 at the rim of Quest caldera

	Start down	Bottom view	End of dive	On deck
UTC	23:04	23:23	01:30	01:44
Positioning	Ship	Posidonia	Posidonia	Ship
Latitude Longitude	55°48.549'S 28°29.671'W	55°48.542'S 28°29.687'W	55°48.652'S 28°29.516'W	55°48.699'S 28°29.339'W
Water depth		718 m	701 m	

Survey tasks
Finding the hydrothermal active site that was detected by the temperature anomaly during the first OFOS deployment above a seafloor depression.

Key results

A depression ~20 m in diameter was surveyed intensively. This was the site of a small temperature anomaly identified in OFOS-1. Areas of low temperature venting were observed as small (metre square) patches of whitish precipitates/ microbial mat with small (less than 1 m tall) whitish chimneys and in one place an overhanging rock with microbial mat on underside. No shimmering water or black/ white smoke was visible at these two sites, but temperatures recorded with the MTLs showed elevated values of up to 2° C higher than surrounding background.

Technical description

This dive was again performed using the MARUM TV-sled and telemetry. The technical performance was very good, no problems during the entire dive. Posidonia was working well after a restart of the system on the way down to the seafloor at the beginning of the dive.

Dive description

During the decent of the OFOS through the water column at around 430 - 450 m 4 arms of a large, unknown cephalopod, probably an incirrate octopus, were seen across the video screen. Unfortunately, the VHS recorder was not switched on to record this. The observed animal seemed to be similar to the one detected during JC80 with ROV Isis at the E2 segment.

The seafloor first visible was the same seen during OFOS-1 and the beginning of OFOS-2 with large rocks covered with epifaunal animals (e.g. octocorals, brisingid starfish) with sediment in-between. After 23 minutes of the dive the seafloor dropped into a steep walled, elongated depression about 10 metres deep and OFOS was guided into this structure. Most of the rest of the dive was performed in this depression, establishing that it is 12 X 24 metres in size, with a NE-SW orientation (Figs. 5.8.1 and 5.8.2). The fauna of the rocks around the caldera rim mostly disappeared from the depression, but a few brisingid starfish were occasionally present and in some places patches of white sponges. In the depression at least 5 discrete patches of hydrothermal activity were found (Fig. 5.8.2). One in the SW of the depression was located at the base of a large rock with a prominent white

sponge. This area had whitish precipitates/microbial mat about 1 metre in extent with around 5 small (less than a metre tall) chimney structures with narrow lateral flanges. Another area at the NE of the depression was located close to the wall and consisted of a small mound of whitish precipitates/microbial mat about 1 metre in extent. Above this was a large overhanging rock and the underside of this rock also had the same whitish precipitates/microbial mat, presumably representing where buoyant hydrothermal flow was rising from the whitish patch below and intersecting the overhand of the rock above. Although whitish precipitates/microbial mat were observed, shimmering water was not seen, although the camera system would make it difficult to see this, even if present. No vent-endemic fauna typical of the Scotia back-arc vents, such as *Kiwa* crabs, stalked barnacles, peltospiroid gastropods or vesicomyid clams, were seen. After 1:40 h dive time the decision was made to leave the area and explore to the SE along the rim of the caldera. No further areas of venting were found and the seafloor and animals were similar to that already seen. Post dive analysis for the 5 MTLs showed elevated temperatures (up to 2.7° C) for most of the duration of the dive in the depression, but not outside it (Figs. 5.8.1, 5.8.2, and 5.8.3).

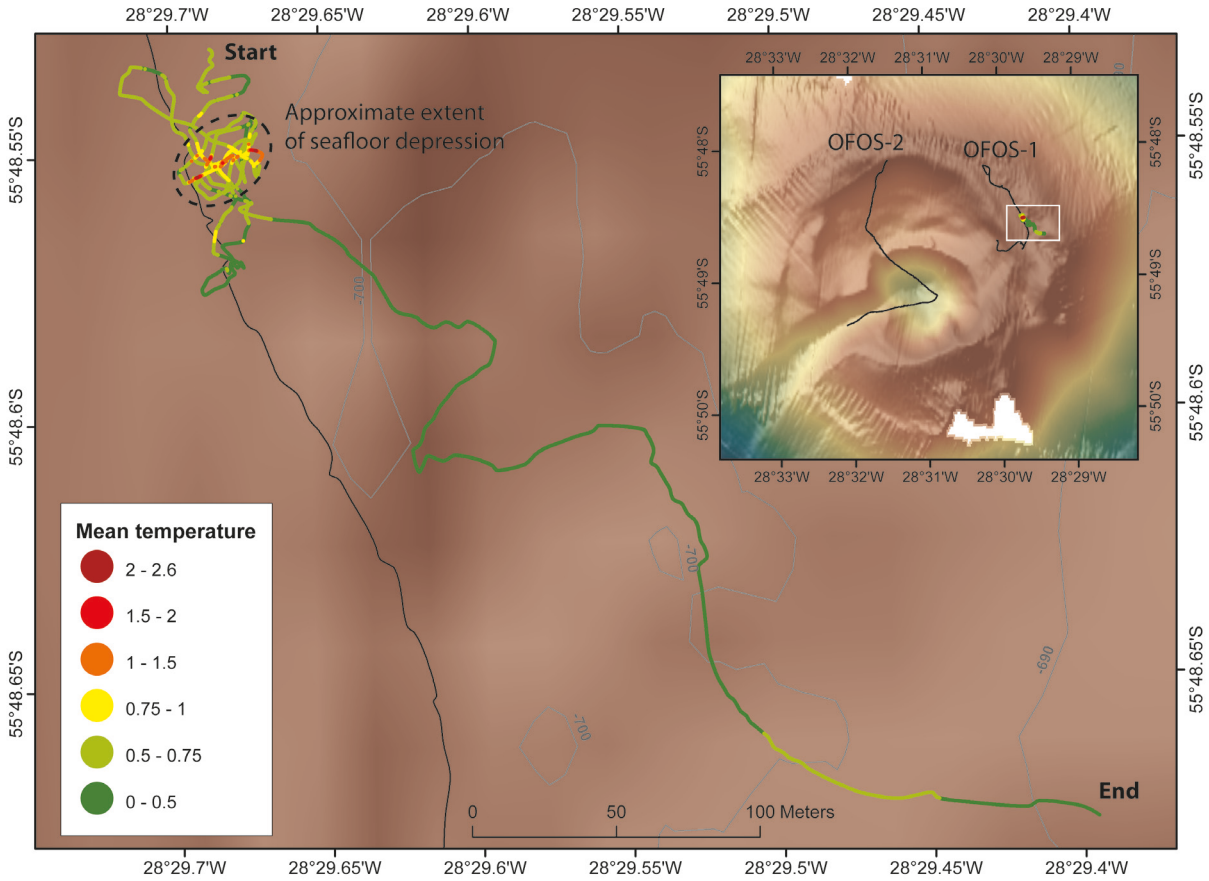

Fig. 5.8.1: Bathymetry map from ANT-XXIX/4 HYDROSWEEP data with OFOS-8 dive track plotted. The track colour corresponds to the mean temperatures in the key. Inset shows in addition the OFOS-1 and OFOS-2 dive tracks.

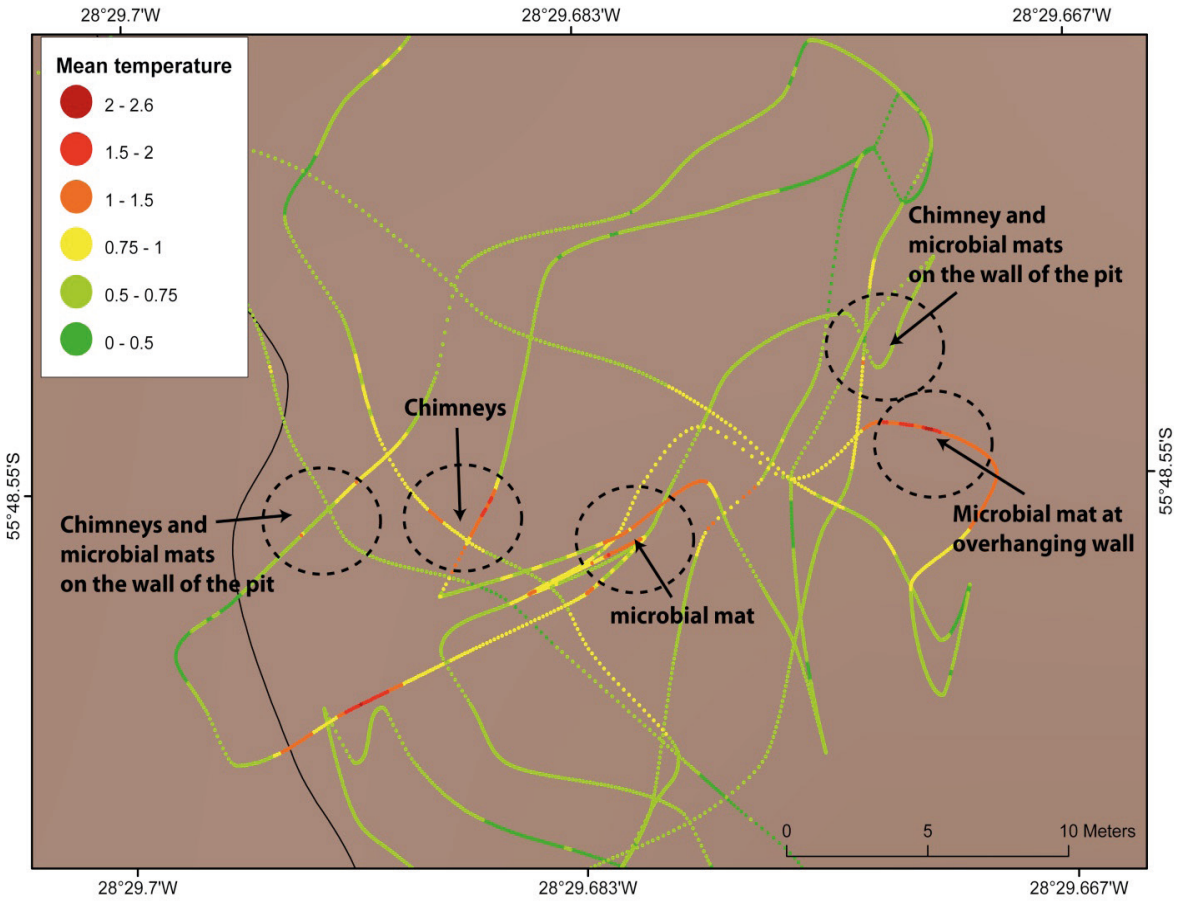

Fig. 5.8.2: Detail of the dive within and around the seafloor depression. Encircled are the areas where vent activity was detected.

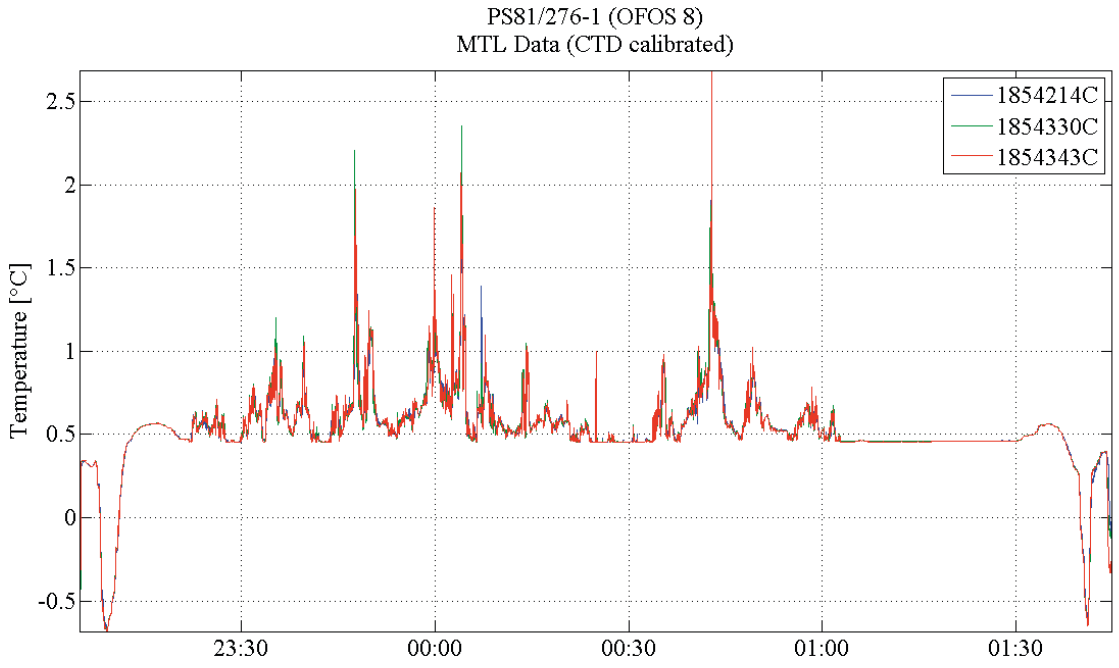

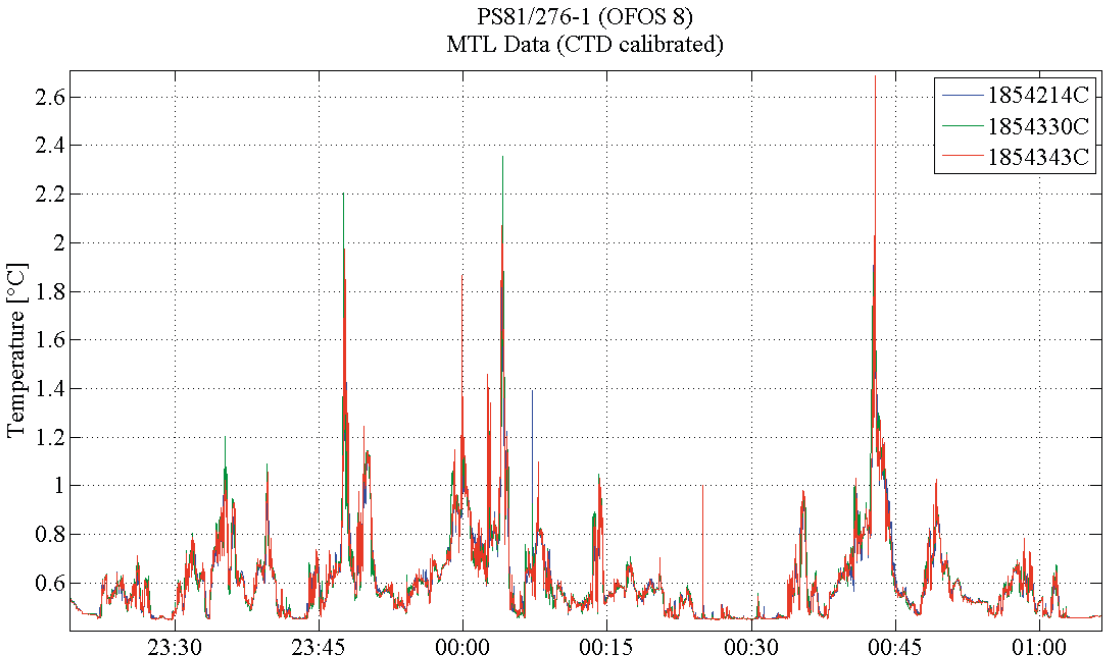

Fig. 5.8.3: Temperature measured with the MTLs a) see previous page, b) above, during the entire OFOS deployment

5.9 OFOS-9 (PS81/278-1) at unnamed submarine volcano

Tab. 5.9.1: Basic data of OFOS-9/PS81/278-1 (extra equipment 6 MTLs with new batteries, taken on 09 April 2013 at unnamed submarine volcano)

	Start down	Bottom view	End of dive	On deck
UTC	13:16	13:33	15:31	15:45
Positioning	Ship	Posidonia	Posidonia	Ship
Latitude Longitude	55°46.715'S 28°47.594'W	55°46.711'S 28°47.601'W	55°46.873'S 28°47.459'W	55°46.904'S 28°47.616'W
Water depth		613 m	792 m	

Survey tasks

Searching for hydrothermal activity on the saddle of the unnamed volcano, where a plume-like anomaly almost 100 m high was detected during an earlier hydroacoustic survey (Fig. 5.9.1).

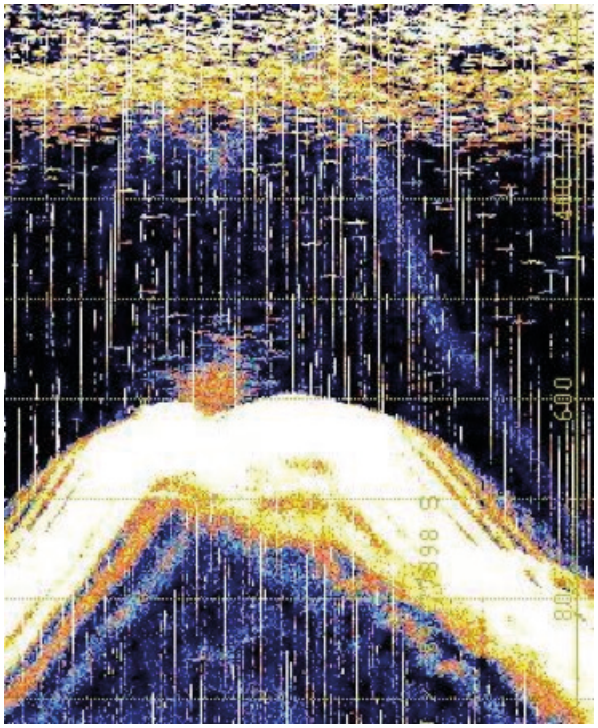

Fig. 5.9.1: Plume-like anomaly from PARASOUND in saddle of unnamed volcano

Key results

The top and the flanks of the volcano are formed of gravel and larger rock outcrops, which are colonized by crabs and abundant octocorals. There was no observable hydrothermal activity, but the temperature loggers clearly recorded two areas with elevated values close to the saddle between the two peaks of the volcano.

Technical description

This dive was performed with the MARUM TV-sled and telemetry. No technical problems during the deployment and the Posidonia connection worked during the entire dive.

Dive description

The OFOS dive started at WP 2 on top of the western peak of the volcano (Fig. 5.9.1). Volcanic rocks and gravel were observed in this area and numerous lithodid crabs were seen on the flat surface, but with no other obvious macro- or megafauna. From here OFOS headed eastwards over WP1 down-slope without much change in the seafloor characteristics. With increasing depth towards the middle of the double-topped volcano the crabs disappeared and no fauna was observed. Moving eastward up-slope to the eastern peak of the volcano there were many more large rocks and steep scarps of exposed lava, on which were attached brisingid starfish, large, actively feeding octocorals and stalked anemones. The top of the eastern peak had pale coloured lava flows, without visible fauna. During the decent ENE towards WP4 then the saddle between the peaks at WP1 the rock outcrops decreased and no fauna was seen. Approximately at the saddle exposed

volcanic rocks appeared again and while heading south to WP5 area the seafloor consisted of talus slopes of first decimetre-sized rocks and then smaller gravel. Numerous crabs were observed on the gravelly sediment (~625 m), with more than 10 crabs in the field of view. Further downslope on the southern side of the volcano the gravelly sediment with occasional larger blocks was colonised by numerous specimens of large, actively feeding octocorals (~620 m and deeper) with more than 50 individuals per field of view. These octocorals continued to be the dominant fauna down to 750 m. At depth and with the appearance of larger rocks, brisingids and erect octocorals were seen. The OFOS dive was terminated in around 800 m water depth after surveying ~1.1 km distance over 2 hours. Post dive analysis for the 6 MTLs showed elevated temperatures (up to 2 ° C) between WP1 and WP3, and WP1 and WP5 (Figs. 5.9.2 and 5.9.3), although there was no visual confirmation of these on the seafloor.

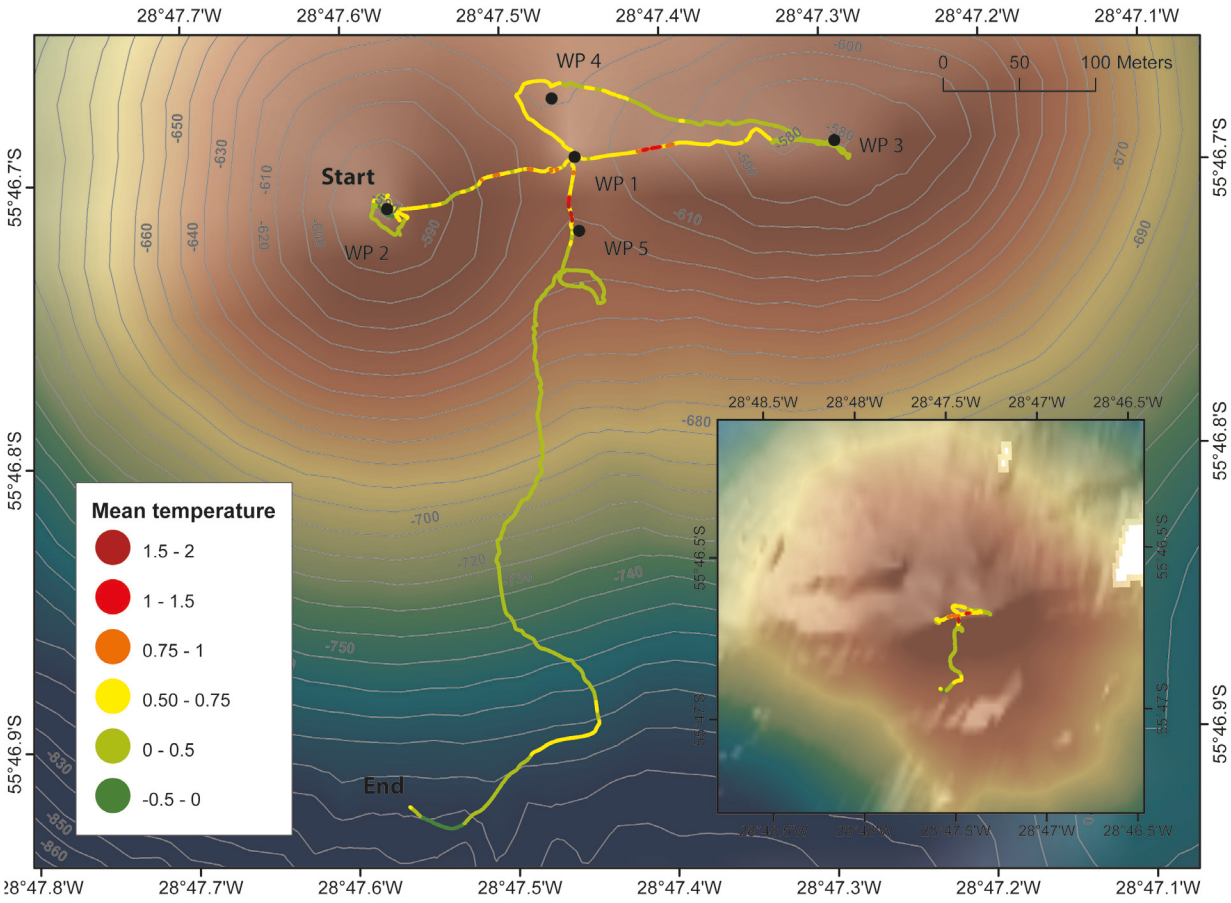

Fig. 5.9.2: Bathymetric map of the unnamed volcano with the track of OFOS-9. The colour indicates the mean temperature recorded during the dive with the temperature loggers. Between WP1 and WP3, as well as between WP1 and WP5 (both close to the saddle), the temperature is clearly elevated.

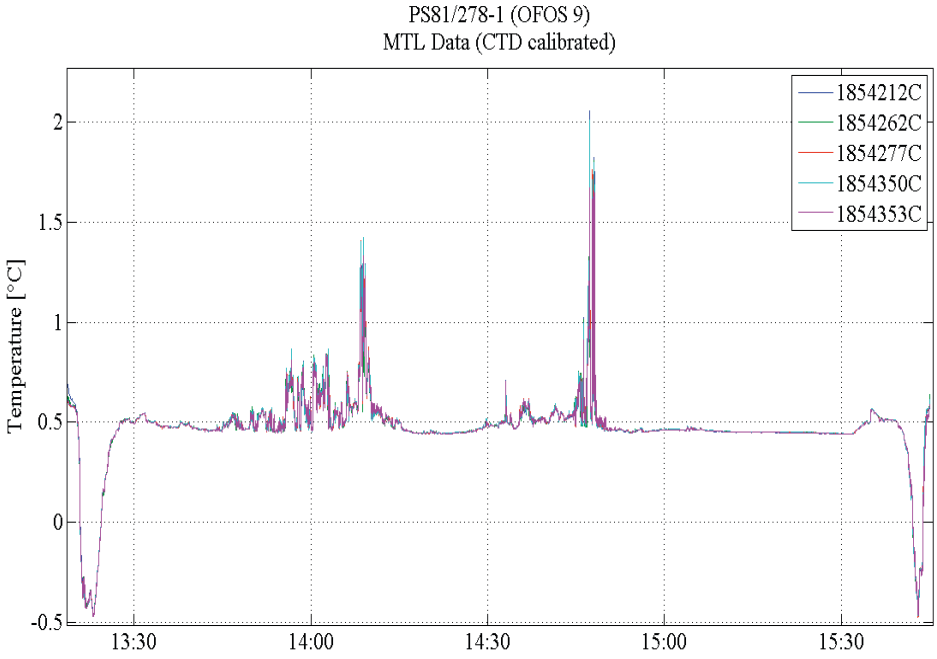

Fig. 5.9.3: Temperature plotted against the dive time of OFOS-9. The background temperature is around 0.5° C and was twice observed to be elevated to as much as 2° C.

5.10 OFOS-10 (PS81/285-1) at Cumberland Bay Flare

Tab. 5.10.1: Basic data of OFOS-10/PS81/285-1 (extra equipment 5 MTLs, taken on 11/12 April 2013 at Cumberland Bay Flare)

	Start down	Bottom view	End of dive	On deck
UTC	23:26	23:36	00:59	01:05
Positioning	Ship	Posidonia	Posidonia	Ship
Latitude Longitude	54°12.126’S 36°27.191’W	54°12.138’S 36°27.187’W	54°12.202’S 36°27.344’W	54°12.182’S 36°27.409’W
Water depth		265 m	260 m	

Survey tasks

Detecting the gas bubbles producing the Cumberland Bay Flare visible in the hydroacoustic systems.

Key results

Numerous single gas bubbles were observed emanating from the seafloor through small orifices in an area of few tens of meters in diameter, probably forming together the Cumberland Bay Flare. In addition, the same features were seen in an

area to the NW, where another flare became visible in the HYDROSWEEP system during the OFOS deployment.

Technical description

After the repair of the fibre-optic cable we were able to deploy the AWI OFOS again for this dive, and we had no problems during the entire deployment. The lack of swell in Cumberland Bay on the day allowed us to tow the OFOS only 1 - 2 m above the seafloor, which was necessary for seafloor observations in the turbid water conditions.

Dive description

The dive started directly on the location of the estimated centre of the Cumberland Bay Flare to investigate its origin. The camera visibility was very restricted due to the turbid water in the fjord, but, fortunately, calm weather conditions on the day allowed us to tow the OFOS very close to the seafloor, and we were able to see the bottom from ~2 m distance. The flat seafloor was covered with very soft sediments with extensive patches of detached kelp fronds (Figs. 5.10.1 to 5.10.6), many of which were partially covered in sediment. The epifaunal animals seen on the sediment included cidaroid sea urchins (*Ctenocidaris speciosa*) with epifauna (e.g. the bivalve *Lissarca notorcadensis*) on their spines, regular sea urchins (*Sterechinus* sp.), several species of asteroid starfish and sea cucumbers and large spiky sponges of the genus *Rosella*. One large raised seafloor area was colonized by large and small sea squirts, spiky *Rosella* sponges, octocorals (e.g. *Thouarella* sp.) and cidaroids (Figs. 5.10.1 to 5.10.6). Many benthic fish were seen, including nothothenids.

Numerous centimetre-sized holes in the seafloor were observed, and these could have been produced either by endo-benthic organisms (e.g. polychaete worms, bivalves) and/or represent the orifices of emanating gas bubbles (Figs. 5.10.1 to 5.10.6). After few minutes of the dive we identified rapidly ascending single gas bubbles, and we spent almost an hour in the area attempting to take pictures of these. However, with the downward looking camera it turned out to be impossible to take an in-focus picture of a bubble. Therefore, we took two videos from the screen. The gas bubbles did not emanate from distinct sources in form of bubble trains, but rather occurred as individual bubbles originating from various sources in an area of about 20 m in diameter. When traversing this area OFOS several times crossed over a site with whitish patches, with grey centres which are probably microbial mats and indicate areas of the most active and focussed seepage (Figs. 5.10.7 and 5.10.8, and Figs. 5.10.1 to 5.10.6). Interestingly, the whitish patches seem to be elevated and form small mounds (see Pictures). These features are similar to gas hydrate bearing seep sites, but as the Cumberland Bay Flare area is located in only 260 m water depth, and not in the estimated gas hydrate stability zone, we do not expect gas hydrate to occur here.

During the hour of surveying in this seep area, we could simultaneously observe a second flare in the HYDROSWEEP system, located about 40 m NW of the Cumberland Bay Flare (Figs. 5.10.7 and 5.10.8). We headed in the direction of this second flare and tried to detect the boundaries where gas bubbles occur producing the Cumberland Bay Flare and then detect the gas emission producing the second flare. In the area of the second flare we again observed rapidly ascending individual gas bubbles, and also mounds covered by microbial mats (see Figs. 5.10.1 to 5.10.6).

At the end of the dive we towed OFOS south-westward in order to move out of the flare areas, but we continued to some individual bubbles. However, some of these could have been floating small animals, a confusion caused as the tow speed was increased to about 0.5 kn. The dive finished in an area where blanking was observed in the sub-bottom profiler, perhaps an indication of more seep activity, although there was no corresponding flare in the water column. Nevertheless, we saw further gas bubbles in this area. Post dive analysis for the 5 MTLs showed no temperature anomalies for the duration of the dive (see Fig. 5.10.9).

References

Larter, R.D., P.A. Tyler, D.P. Connelly, J.T.P. Copley, A. Rogers, S.A. Bennett, C.F.A. Flouquet, A.G.C. Graham, A.M. Hilario, E.Z. Ramirez-Llodra, A.D. Beaton, D.R. Owsianka, V. Afanasayev, J.S.P. Cooper, P.J. Mason and D.D. Willis (2009) JR224 – Chemosynthertically-driven Ecosystems South of the Polar Front Consortium Programme. Cruise report. www.BODC.ac.uk

Rogers, A.D. (2010) JC42 - Chemosynthetic Ecosystems of the Southern Ocean (CHESSO) Cruise report. www.DODC.ac.uk

Fig. 5.10.1: Extensive mat of detached kelp fronds

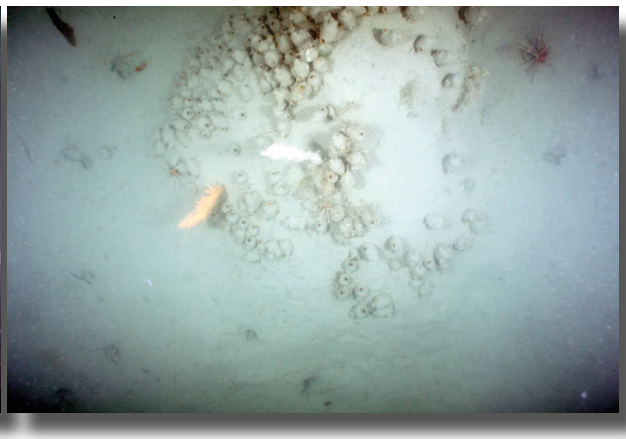

Fig. 5.10.2: Raised mound colonized by sea-squirts, octocorals and cidaroid sea urchins

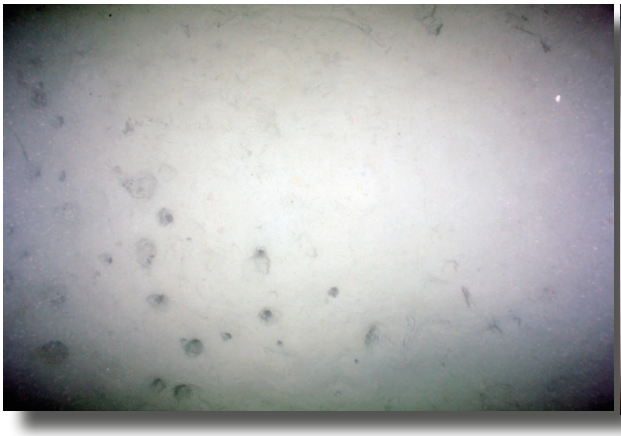

Fig. 5.10.3: Orifices in the seafloor, relating to endobenthic animals and/or emanating gas bubbles

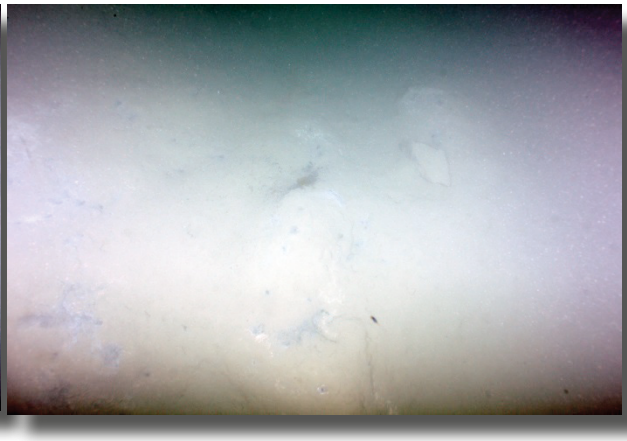

Fig. 5.10.4: Raised mounds with whitish and greyish sediment

Fig. 5.10.5: Raised mound with whitish and greyish sediment. Note detached kelp frond partially covered in sediment

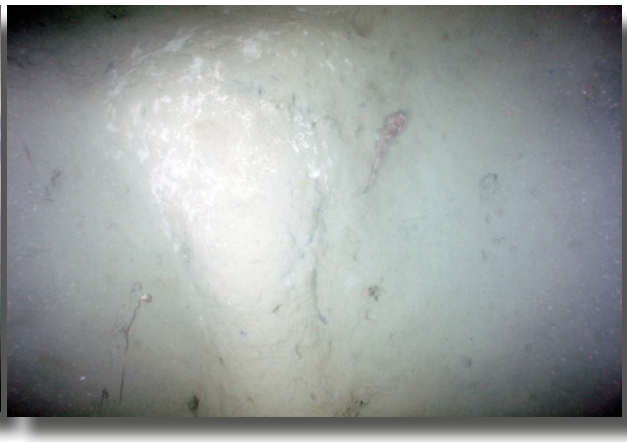

Fig. 5.10.6: Large raised mound with whitish and greyish sediment

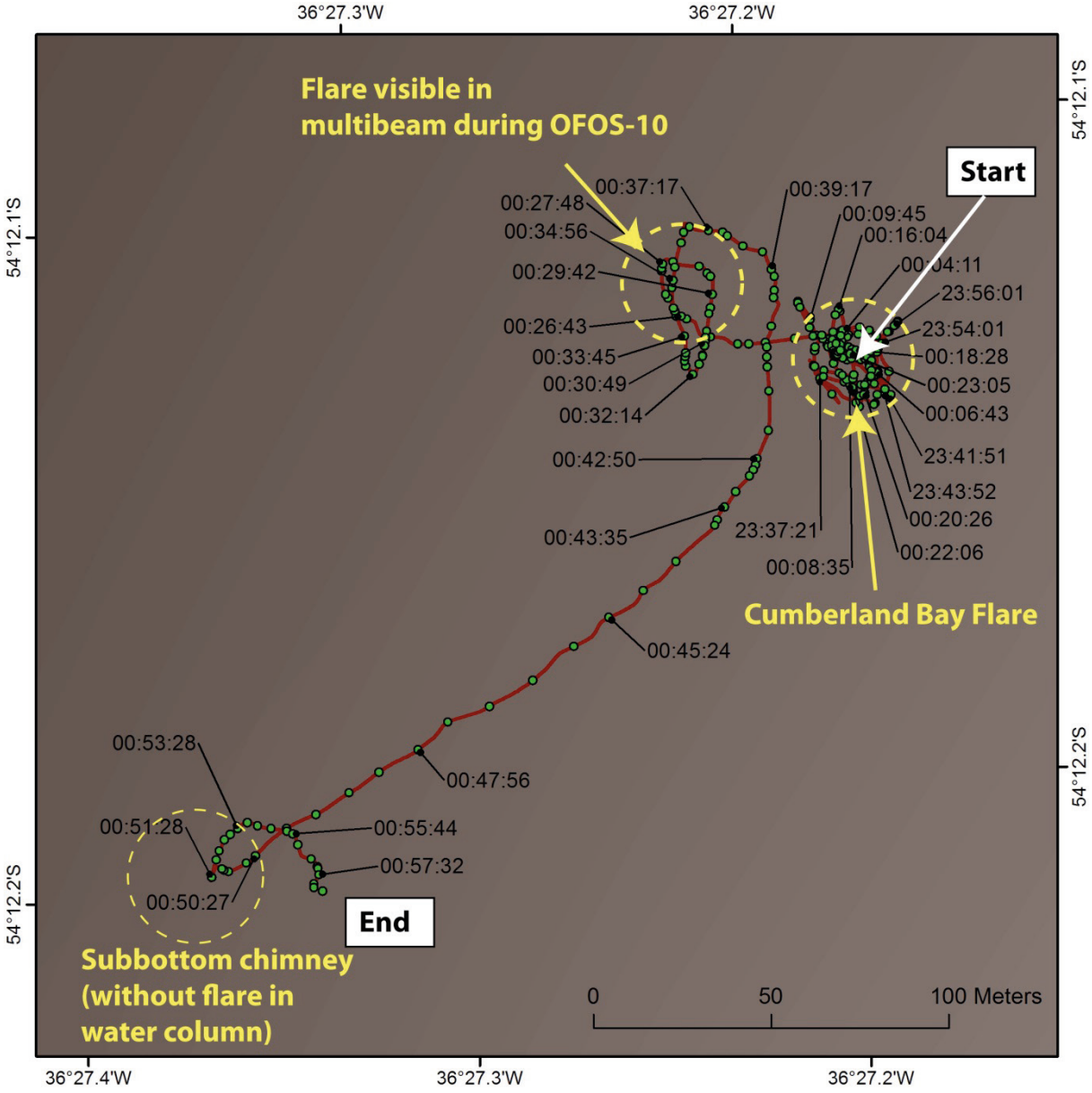

Fig. 5.10.7: Track line of the OFOS-10 deployment (red line) with the location of each photo taken (green points). The target areas are roughly outlined by the yellow circles. The dive started in the area of the Cumberland Bay Flare, passed over another flare northwest of it and finally ended about 200 m southwest, close to an area where another blanking in the subbottom indicated a gas chimney, although no corresponding water column flare was detected.

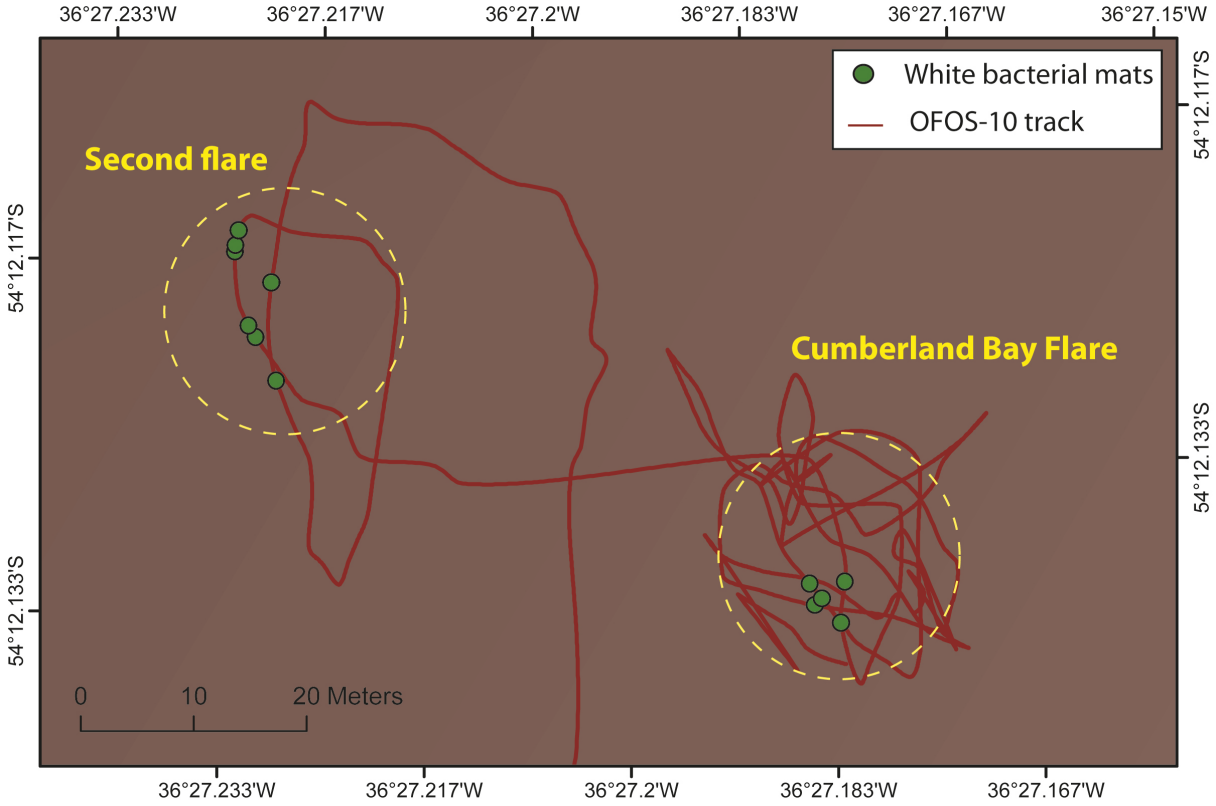

Fig. 5.10.8: Detail of the first part of OFOS-10 illustrating the locations of whitish sediment (most probably bacterial mats), which have been detected in both flare areas.

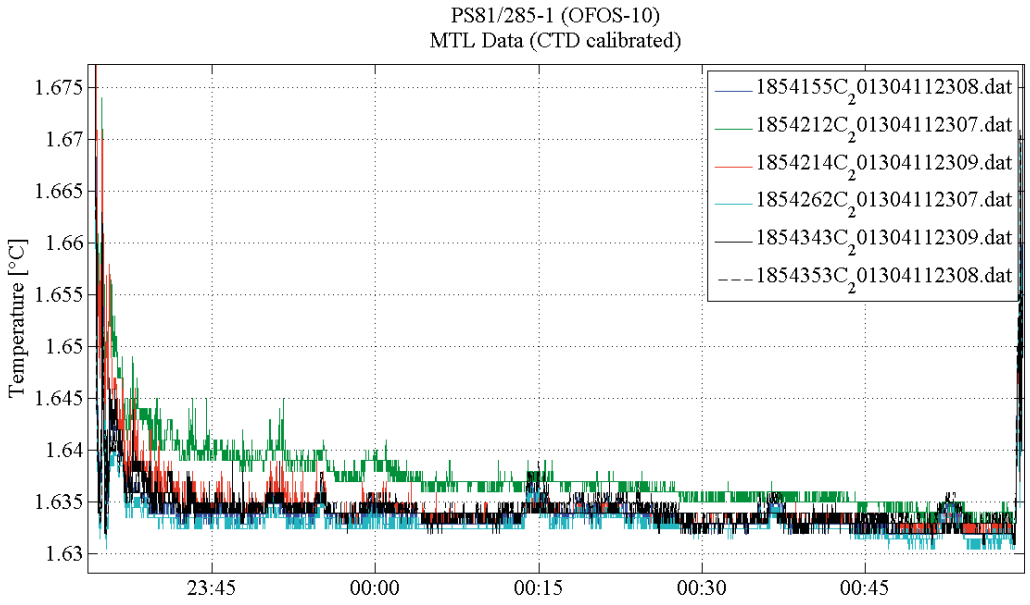

Fig. 5.10.9: Temperature measured with the MTLs during the entire OFOS deployment

6. LATE PLEISTOCENE SOUTH GEORGIA AND SCOTIA SEA MARINE SEDIMENTS

Gerhard Kuhn[1], Birgit Glückselig[1], Norbert Lensch[1], Britta Lüdke[1], Ove Meisel[1], Thomas Ronge[1], Steffen Wiers[1], Alastair Graham[2], William Dickens[2], Jenny Roberts[2], Jiangong Wei[3]

[1]AWI
[2]BAS
[3]MARUM

Objectives

Challenges at the forefront of Southern Ocean geoscientific investigations include establishing glacial and interglacial changes in the extent of Antarctic ice sheets, their sensitivity to melting by warm ocean currents reaching their margins, their impact on and response to sea level variations, their variability related to climate change impact and the reaction to shifts in the frontal system of the Antarctic Circumpolar Current (ACC), their impact on annual sea ice extent (Bintanja et al., 2013), the position of the southern westerlies (Lamy et al., 2010) and the possible influence of the ice sheets on Weddell Gyre dynamics and Antarctic Bottom Water (AABW) formation in the southern Weddell Sea (Huhn et al., 2013). Southern Ocean marine sediments provide key natural archives for addressing these problems, documenting glacial/interglacial paleoenvironmental changes and in some areas high-resolution records of the post Last Glacial Maximim (LGM) deglaciation.

South Georgia Island (SGI) is situated south of the Antarctic Circumpolar Current (ACC) and south of the Polar Frontal Zone today and therefore it is an ideal place to study the effects that climate changes had during the past glaciations of this island and the signals recorded in the surrounding seas. Diatom data from sediment cores discovered that at the LGM (21 000 years before present) Antarctic sea ice extent doubled and the Polar and sub-Antarctic Front shifted northwards 2° to 10° in latitude (Gersonde et al., 2005). This established a significant change to the environment at SGI, from polar Antarctic-like conditions during the LGM, to maritime sub-Antarctic conditions and high coastal productivity observed today.

The Western Antarctic Peninsula (WAP) with its maritime climate, off-coast islands, like the South Shetland and South Orkney Islands, and significant number of tidewater glaciers is a hotspot for global warming and glacier mass loss and thus a sensitive indicator for environmental changes. System change manifests in rapid retreat of glacier frontal position, break-up and disintegration of ice shelves and speed-up of inland ice masses, processes of deglaciation that had already started after the Last Glacial Maximum (LGM) (Weber et al., 2011), but for which the rates of change are largely unknown (Hillenbrand et al., 2013). Mean annual air temperatures on the WAP have increased by nearly 3°C since the middle of the last century (Turner et al., 2009), making it one of the most rapidly warming regions on Earth. If we want to know how the effects of persisting warming will effect the environment, we can use sub-Antarctic Islands like South Georgia, the Falkland Islands or southern Patagonia as potential analogues. Of primary interest, we would like to know the environmental impact of rapid recent changes on the local glaciers,

coastal primary productivity and sediment fluxes; how are the paleoenvironmental signals documented in the sediment archives, and whether the recent changes are unique or were preceded by other similar events during the Holocene.

During previous cruises ANT-X/5 (Gersonde, 1993), ANT-XI/2 (Gersonde, 1995), ANT-XXII/4 (Schenke & Zenk, 2005) with *Polarstern* in 1992, 1993/94, and 2005, and cruises JR224 (Larter et al., 2009), JR244 and JR257 (Allen, 2012) with RRS *James Clark Ross* in 2009, 2011, and 2012, respectively, AWI and BAS collected marine geological and geophysical data sets from the Falkland Plateau, Scotia Sea, and from the South Georgia shelf.

Extensive paleo-ice sheet drainage on this shelf was highlighted in a bathymetric compilation by Graham et al. (2008). During this cruise the target was to complete partially mapped areas and collect additional sediment cores and sediment surface samples for sedimentological, geochemical and micropaleontological work. The work was focused on previously selected sites and on sites selected from underway survey on the South Georgia shelf, in its coastal bays and troughs, in the Scotia Sea, and on the Falkland Plateau. Our investigations on the South Georgia shelf will address glacial changes and the climatic history of the island from the marine perspective, expanding upon the lake and shallow bay (not accessible with *Polarstern*) investigations carried out by Martin Melles and others (see Chapter 12).

The Antarctic Ocean is one of our most important climate amplifiers: First, the production of Antarctic deep water drives the Global Thermohaline Conveyer Belt, thus, climate. Second, the Antarctic deep water during glacial time was/ disputably still is, the largest marine sink of atmospheric CO^2. Employment of effective sensitive and in geological sense preservable proxies to obtain precise information on changes in the polar deep oceans physical to geochemical properties are essential to assess past, modern, and future physical to geochemical changes in bipolar deep-waters. In this respect, analyses on trace metal (Mg/Ca, U/Ca, B/Ca) ratios recorded in tests of foraminifers to estimate calcification temperatures, salinity variations, carbonate ion saturation, pH and alkalinity became common methods. However, for the Southern Ocean deep-sea benthic foraminifera calibration curves constrained by culture experiments are lacking. During this expedition we tried to retrieve multiple corers from 1,500 m water depth. The retrieved sediments will be transferred into 15 different aquaria including newly developed high-pressure aquaria. These aquaria will in different experimental set-ups be used to cultivate our most trusted paleodeep-water recorders at different temperatures and in waters with different carbonate chemistries to establish species-specific trace metal calibration curves for the Antarctic Ocean.

Target areas and main questions to be answered during the cruise were: Late Quaternary dynamics of South Georgia's ice cap and glaciers in relation to ACC changes

1. the LGM extent of the South Georgia ice cap
2. regional differences in post LGM deglaciation between South Georgia's outlet glaciers and the overall pattern of glacial retreat to present
3. the timing and forcing of deglaciation events by the ACC

Work at sea and preliminary results

The flow of the Antarctic Circumpolar Current (ACC), related oceanographic frontal systems, and bathymetrically controlled outflow regions of AABW make the Scotia Sea an area of particular interest for surface and bottom water paleoceanographic reconstructions. Near shore, on the continental shelf, the extent of inland ice caps and glacial-marine sediments deposited after the last and possibly from earlier glaciations were mapped by multibeam swath (see Chapter 3) and sub-bottom echo sounding profiles (see Chapter 4).

Surface and sediment core sampling was accomplished during the cruise and high sediment accumulation in some fjords and troughs superbly archive Holocene glacier behaviour and climate changes, which will be compared to the results from the lake drilling and terrestrial glacial-geomorphological work around Cumberland Bay West, South Georgia, supervised by Martin Melles (see Chapter 12).

Physical properties of all sediment cores taken were measured with a Multi-Sensor Core-Logger (MSCL) during the cruise (see Chapter 7).

For paleoenvironmental interpretations we need a profound knowledge of the age of the recovered sedimentary sequences. For ^{14}C-age determinations the reservoir effect by re-deposited ^{14}C-dead carbon has to be known and several techniques to date specific organic compounds will be applied to get a reliable chrono-stratigraphy in cooperation with Janet Rethemeyer's studies (see Chapter 11) and to get more paleoenvironmental information from stable isotopes of organic carbon and biogenic silica in cooperation with Melanie Leng (see Chapter 12).

Sub-bottom profiling is not only a tool for gathering information about sediment accumulation and erosion but it is also used for locating coring positions. PARASOUND was particularly useful for the identification of core sites on the South Georgia shelf, where a patchy spatial distribution of sediments had been recorded with a thick sediment section in the troughs formed by former ice streams and nearly no recent sediment cover in the areas between. The acoustic information from PARASOUND at each coring location can be compared with physical properties measured on the sediment cores with the multi-sensor core logger (MSCL), thus allowing the correlation of acoustic data with core data.

Multiple corer (MUC), mini corer (MIC), piston corer (PC) and gravity corer (GC)

During ANT-XXIX/4 a multiple corer (MUC) with 8 tubes of 10 cm and a mini corer (MIC) with 4 tubes of 6.7 cm diameter (deployed below the CTD rosette), was used at 13 sites to recover undisturbed surface sediments (Fig. 6.1, Appendix: station list). Two piston corers (PC), including two trigger corers (TC), and 18 gravity corers (GC) with a total core barrel length of 202 m were deployed to recover long sedimentary sequences (Fig. 6.1). The deployment of the gear types and the length of the coring devices were chosen based on lithological information derived from sediment acoustic profiles provided by the PARASOUND echosounding system. With the exception of three unsuccessful MUC (ø 10 cm) deployments (PS81/267-1, PS81/272-2, PS81/274-2), due to sandy bottom and only partial closure of the lower plugs, and two unsuccessful GC deployments (PS81/272-1 with sandy scoria pieces; PS81/287-1 with sticky diamicton), where the corer apparently fell over and did not intrude the barrel, respectively, all deployments were successful and resulted in a total core recovery of 143.7 m including 1.2 m core length recovered

with the TC. For core recovery and sections see Appendix 4 (station list) and 5 (core logs).

Three attempts for MUC sampling at exposed sites in water depth around 1,500 m were undertaken (PS81/267-1, PS81/277-7, PS81/277-8) for Jutta Wollenburg's (AWI) work on epizooic Cibicides-type foraminifers, filter-feeding unilocular animals with maxima abundances in areas of high current activities. The retrieved cores (unfortunately only five) were transferred into a cold laboratory and running at a site-alike bottom water temperature during the cruise. During the last day onboard the sediments and overlaying water were transferred into transfer-cores and storage systems. After the following expedition ANT-XXIX/5 these storage systems will be transferred into special cold boxes ensuring a site-alike temperature during the flight from Cape Town to Bremerhaven. In Bremerhaven the sediments will immediately be transferred into the respective aquaria and connected to respective supportive sea-water systems.

Two 20 m long piston corers (PC) were deployed to recover long sequences of both pelagic, biogenic opal rich sediments at site PS81/271-4 and hemipelagic-terrigenous sedimentary sequences.

The sediment cores taken with piston and gravity corers were cut onboard *Polarstern* into ≤1 m-long sections. After the measurement of physical properties with the multi-sensor core logger (see Chapter 7), PC and GC sections and subcores taken from the GBC, which were not opened onboard, were stored in a reefer container at a temperature of +4° C and will be transported to Bremerhaven from Cape Town in June.

Six GC corresponding to 38.5 core meters were opened and sub-sampled during the expedition. After opening and splitting, the sections were photographed. High-resolution colour reflectance and measurements of magnetic susceptibility (at 1-cm intervals using a point-sensor, see Chapter 7) as well as a sediment description were carried out on the archive halves. Sediment colours were determined using a "Munsell Soil Color Chart". Core descriptions are found in the appendix (A.5).

Sampling procedures of the cores followed standard methods at AWI and were exclusively carried out on the work halves. Sampling types and intervals (usually 5, or 10 cm) varied in response to the identified lithologies of the recovered sediments. The general sampling plan included sampling of a 25x10x1 cm sediment slab for X-raying. Samples (20 cm^3 in volume) for the determination of bulk parameters (water content, density, $CaCO_3$, total organic carbon, XRD, XRF, and opal content) were taken with syringes and stored in whirlpak bags, which were pre-weighed in the case of bulk samples. In addition to pore water samples, samples were taken for Fe-solid phases and geochemistry (see Chapter 9) and for compound analysis and dating of specific organic material and fractions (see Chapter 11). Further laboratory analyses on all cores will be carried out at AWI partly in close cooperation with BAS and the University of Cologne.

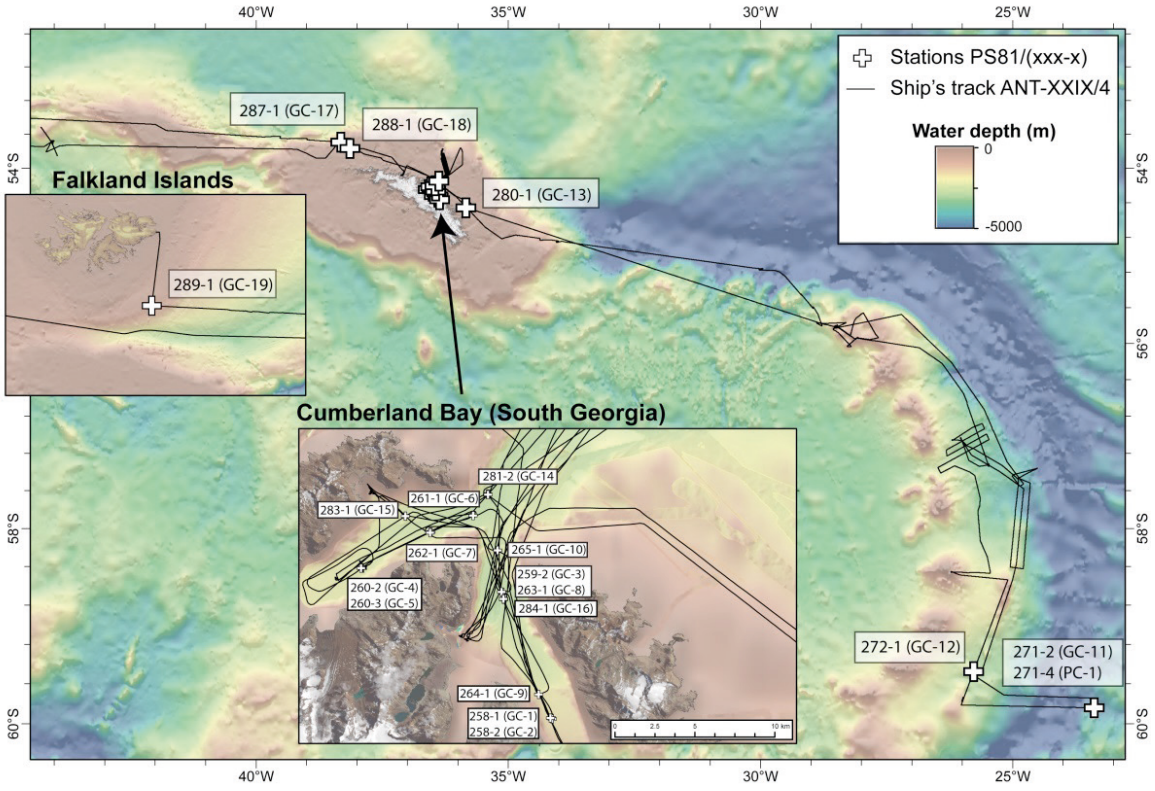

Fig. 6.1: Map of core locations

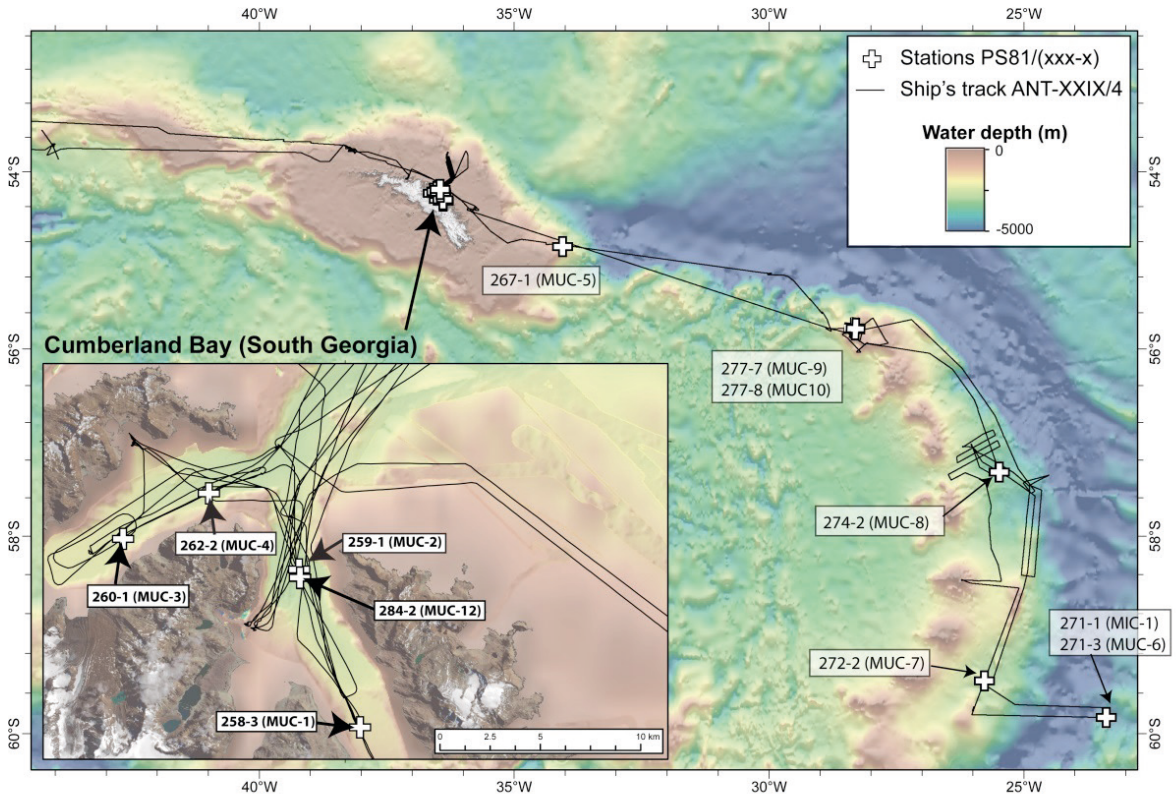

Fig. 6.2: Map of sediment surface samples

Data management and future work

Information regarding the lithological descriptions, metadata documentation, sample types and volumes will be made available via PANGAEA Data Publisher for Earth & Environmental Science database at AWI (http://www.pangaea.de). After analysis, verification and interpretation of the core logging data and analytical work on the samples the data will be made available in the database for internal access during a moratorial period for a PhD and master thesis and after publication.

Jutta Wollenburg's work is part of a bipolar DFG-project on the incooperation of trace metals in benthic deep-sea foraminifera. The results will be published in international journals within approx. 2 years after the expedition.

Ove Meisel will carry out a Master's degree thesis (supervised by GK and AG) on core GC666 recovered during cruise JR257 in 2010, on physical property data from core PS81/280-1 and surrounding bathymetric and sub bottom sediment echo-sounder profiles from one of South Georgia's glacial troughs (offshore of Royal Bay).

In collaboration with Alastair Graham (BAS), Sabine Kasten, Melanie Leng, Janet Rethemeyer and Martin Melles we will study the marine South Georgia sediment cores. Jenny Roberts (BAS) will conduct part of her PhD work on PS81/289-1 supervised by Victoria Peck (BAS) and in collaboration with Gerhard Kuhn (AWI).

References

Allen, C.S., et al. (Ed.) (2012). Marine Science Cruises JR257 and JR254E, report. British Antarctic Survey, unpublished cruise report. 105 pp.

https://www.bodc.ac.uk/data/information_and_inventories/cruise_inventory/report/jr257_254e.pdf

Bintanja, R., van Oldenborgh, G. J., Drijfhout, S. S., Wouters, B. & Katsman, C. A. (2013). Important role for ocean warming and increased ice-shelf melt in Antarctic sea-ice expansion. Nature Geosci 6, 376-379.

Gersonde, R. (1993). Die Expedition ANTARKTIS X/5 mit FS "Polarstern" 1992 = The expedition ANTARKTIS X/5 of RV "Polarstern" in 1992. Berichte zur Polarforschung (Reports on Polar Research), Bremerhaven, Alfred Wegener Institute for Polar and Marine Research, 131, 167 p. hdl:10013/epic.10132

Gersonde, R. (1995). Die Expedition ANTARKTIS-XI/2 mit FS "Polarstern" 1993/94 = The expedition ANTARKTIS-XI/2 of RV "Polarstern" 1993/94. Berichte zur Polarforschung (Reports on Polar Research), Bremerhaven, Alfred Wegener Institute for Polar and Marine Research, 163 , 133 p. hdl:10013/epic.10164Gersonde, 1995

Graham, A. G. C., P. T. Fretwell, et al. (2008). A new bathymetric compilation highlighting extensive paleo-ice sheet drainage on the continental shelf, South Georgia, sub-Antarctica. Geochem. Geophys. Geosyst. 9(7): Q07011, 21 pages, doi:10.1029/2008GC001993.

Hillenbrand, C.-D., Kuhn, G., Smith, J. A., Gohl, K., Graham, A. G. C., Larter, R. D., Klages, J. P., Downey, R., Moreton, S. G., Forwick, M. & Vaughan, D. G. (2013). Grounding-line retreat of the West Antarctic Ice Sheet from inner Pine Island Bay. Geology 41, 35-38.

Huhn, O., Rhein, M., Hoppema, M. & van Heuven, S. (2013). Decline of deep and bottom water ventilation and slowing down of anthropogenic carbon storage in the Weddell Sea, 1984–2011. Deep Sea Research Part I: Oceanographic Research Papers 76, 66-84.

Lamy, F., Kilian, R., Arz, H. W., Francois, J.-P., Kaiser, J., Prange, M. & Steinke, T. (2010). Holocene changes in the position and intensity of the southern westerly wind belt. Nature Geosci 3, 695-699.

Larter, R. D., Tyler, P. A., et al. (2009). Cruise report RRS James Clark Ross Cruise JR224 January to February 2009, Chemosynthetically-driven Ecosystems South of the Polar Front consortium programme. at:

https://www.bodc.ac.uk/data/information_and_inventories/cruise_inventory/report/9359/

Schenke, H. W. and Zenk, W. (2006). The Expeditions ANTARKTIS-XXII/4 and ANTARKTIS-XXII/5 of the Research Vessel "Polarstern" in 2005. Berichte zur Polar- und Meeresforschung (Reports on Polar and Marine Research), Bremerhaven, Alfred Wegener Institute for Polar and Marine Research, 537, 133 p. hdl:10013/epic.10542

Weber, M. E., Clark, P. U., Ricken, W., Mitrovica, J. X., Hostetler, S. W. and Kuhn, G. (2011). Interhemispheric Ice-Sheet Synchronicity During the Last Glacial Maximum. Science 334, 1265–1269.

7. MULTI-SENSOR CORE LOGGING AND OTHER PHYSICAL PROPERTIES MEASUREMENTS

Steffen Wiers[1], Gerhard Kuhn[1], Ove Meisel[1], [1]AWI
Thomas Ronge[1], William Dickens[2] [2]BAS

Objectives

Multi Sensor Core Logging has been performed as a first non-destructive measurement on all obtained sediment cores. In order to evaluate the influence of pore water extraction on the physical properties of the sediment, cores taken at the same station, one measured undisturbed and one measured after porewater extraction, have been compared. Additionally the measurements were used to compare and correlate cores taken in close position to each other.

In the region off South Georgia the measurements are used to identify the different sediment types and differentiate between basin and moraine sedimentation. This information is used to choose cores of high interest in terms of their expected depositional facies for splitting.

Sediment cores obtained at station PS81/271 contain biogenic opal rich sediments and show changes in the physical properties with thin volcanic ash layers, which might be used for dating purposes. Especially magnetic susceptibility measurements can be used for an identification of these ash layers.

Furthermore sound velocity and density measurements are used to calculate synthetic seismograms, which can be compared to sub-bottom profiling data obtained with the ATLAS PARASOUND sediment echo sounder during the cruise. This can then be used to calculate the true sediments thickness and distribution around coring stations and for core-to-core correlations.

Sub glacial depositions are often detected by high shear strength values. Therefore this parameter was taken on most of the split cores were such a deposition was expected. Visual colour reflectance in the spectral range from 400 to 900 nm (10 nm channels) was measured to use colour changes as an indicator for compositional changes. To calculate sediment fluxes and mass accumulation rates of specific compounds the water content and the sediment density will be measured on individual samples taken.

Work at sea

Physical properties of the sediments such as wet bulk density, p-wave velocity and magnetic susceptibility were detected on all the 143.7 m collected sediment cores with a GEOTEK multi-sensor core logger (MSCL). In addition, core diameter and temperature were measured for data processing and the calculation of additional values like porosity and seismic impedance. The parameters listed in the logger settings of the MSCL software (version 6) and given in Tab. 7.1 were used for calibration that was conducted after the Geotek MSCL manual and after Gunn & Best (1998) and Best & Gunn (1999). The AWI MSCL device (MSCL#14) was used for continuous whole-core measurement at 1 cm resolution.

In addition, magnetic susceptibility was measured with an F-sensor mounted to the MSCL at 1-cm intervals on the surfaces of all 38.52 m of splitted cores.

For example, density and magnetic susceptibility measurements of core PS81/265-1 are shown in Fig. 7.1. The core was taken from the outer moraine structure in Cumberland Bay East. Both parameters show elevated values in the lower part and after splitting this part was identified as a diamicton which was most likely deposited during glacial times. Wet bulk density is rising up to an average of about 2 g/cm^3 and magnetic susceptibility is almost twice the value of the upper part of the core. Peaks in susceptibility could be well correlated with big gravels transported by a glacier and found in the core after splitting. The downcore increase is also true for the density values which were strongly influenced by big stones which sometimes occupied up to one third of the liner.

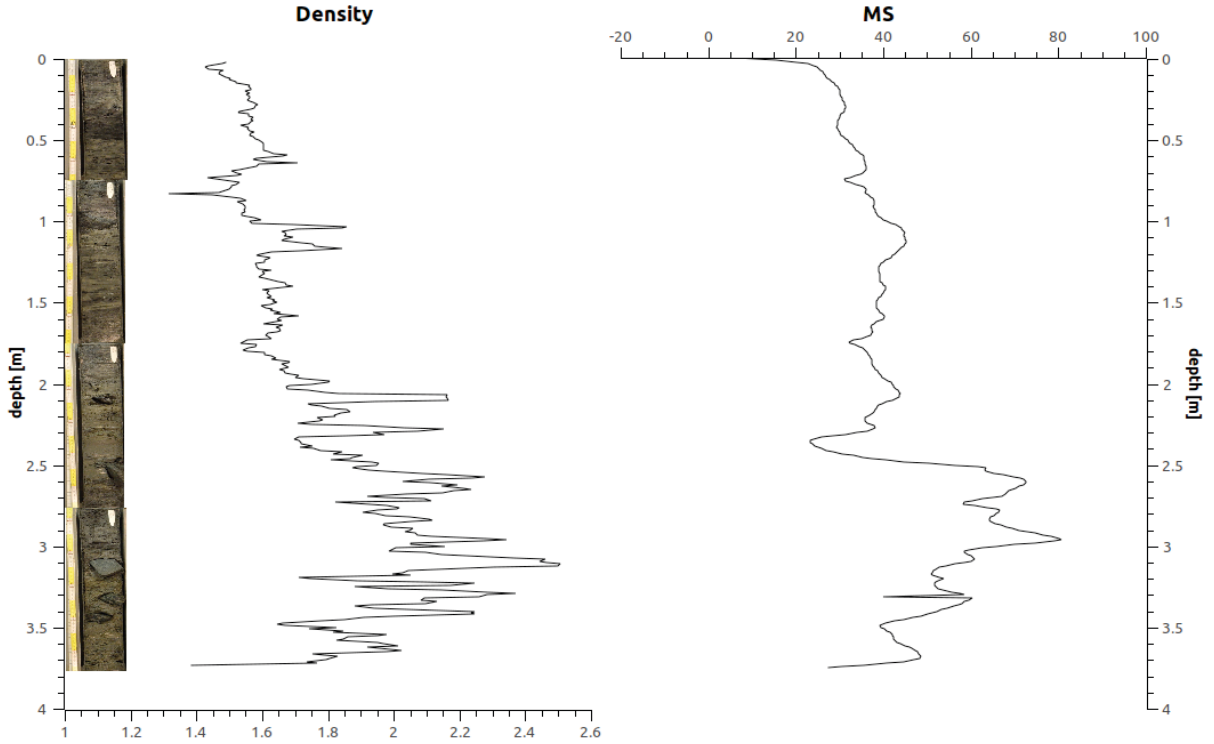

Fig. 7.1: Downcore changes in density (g/cm^3) and magnetic susceptibility (MS, 10^{-5} SI-units) of gravity core PS81/265-1. The facies change at 2.5 m is clearly visible in density and magnetic susceptibility showing that terrigenous input changed in composition during that time.

Quantitative measurements of diffuse spectral colour reflectance integrated over an area with a spot size of 1 cm diameter were carried out with a hand held CM-2002 spectrophotometer (Minolta Camera Co., Osaka, Japan). This system was used with the same settings as described in Balsam et al. (1998). The spacing of measurements was 1 cm. A clear plastic wrap covered the split core surface to avoid contamination. The calibration was done according to Minolta CM-2002 user's manual (Minolta Camera Co., 1991). Each data set contains the depth in core, CIE-lab L*a*b*, Munsell (Hue, Value, Chroma), the readings from each channel between 400 nm and 700 nm with 10 nm resolution (30 values), and CIE 1931 norm color values XYZ. The data together with calibration values are saved in ASCII files individually for each core.

The shear strength of sediments was measured with a hand held shear vane on the work halves of gravity cores (GC) PS81/264-1, 265-1, 284-1 recovered from the South Georgia shelf and from opal rich GC PS81/271-2.

Sediment samples were taken from all opened cores for water content, sediment density and further geochemical, sedimentological and mineralogical investigations.

Table 7.1: Sensors and parameter settings for measurements with the GEOTEK multi-sensor core logger during ANT-XXIX/4.

P-wave velocity and core diameter plate-transducers diameter: 4 cm transmitter pulse frequency: 500 kHz pulse repetition rate: 1 kHz recorded pulse resolution: 50 ns gate: 900 μs delay: 10 μs P-wave travel time offset: 7.62 μs (PC, 2*2.7 mm liner thickness, PS81/271 and 289) P-wave travel time offset: 7.60 μs (GC, 2*2.5 mm liner thickness, all other cores) temperature = 20 °C, salinity = 35 psu, not corrected for water depth and in situ temperature; calibrated with water core of known temperature and theoretical sound velocity
Temperature bimetal sensor, calibrated with Hg-thermometer
Density gamma ray source: Cs-137; activity: 356 MBq; energy: 0.662 MeV aperture diameter: 5.0 mm (PC + Trigger Core TC and GC) gamma ray detector: Gammasearch2, Model SD302D, Ser. Nr. 3047, John Caunt Scientific Ltd.; count time 10 s Gamma ray attenuation measurement and density calculation with equation type $y=Ax^2+Bx+C$, (Coefficients A, B, and C determined with measurements on calibration cores PC (PS81/271-4 and 289-1) A=0.0001, B=-0.0664, C=9.9804 GC cores (all other cores) A=0, B=-0.0675, C=9.9840
Fractional porosity Mineral grain density = 2.65, water density = 1.026
Magnetic susceptibility (MS) coil sensor: BARTINGTON MS-2C, Ser. Nr. 203 (100mm), Ser. Nr. 716 (140mm), and F-Sensor; nominal inner coil diameter: 10 (for PC) and 14 cm (for GC) coil diameter: 10.8 and 14.8 cm alternating field frequency: 565 Hz, count time 10 s, precision 0.1 * 10^{-5} (SI) magnetic field strength: ca. 80 A/m RMS Krel: 1.44 (PC, 8.46 cm core-ø); 1.56 (GC, 12 cm core-ø) coil sensor MS volume correction factor: 6.926 (PC), 6.391 (GC); for 10^{-6} (SI) F-sensor volume correction factor: 20 for 10^{-6} (SI)
Core thickness measurement Penny + Giles, Type HLP 190…, Ser #. 92730147, calibrated with distance pieces
Electrical resitivity measurements on GeoB device Inductive non contact sensor, averaging about 12 cm core length, calibrated with salty solutions. Porosity calculations after MSCL manual, Zero corrections after each section possible

Expected results

All physical property data still have to be corrected, and faulty values, e.g. at core section boundaries, have to be deleted. Also some values, like magnetic susceptibility, have to be processed, drift and volume corrected to obtain true, comparable values.

More geotechnical measurements will be done on the sediments of cores PS81/271-1 and -2 to study and compare the compaction behaviour of opal-rich sediments recovered in former drilling projects like ANDRILL.

Back at AWI, the individual samples will be weighed, freeze-dried and milled. Water content, bulk-, grain-, wet-, and dry-bulk-densities, and the porosity will be determined and corrected for salt content. In addition to these physical properties the geochemical and mineralogical composition of these samples will be measured.

Data management

All data will be stored in PANGAEA Data Publisher for Earth & Environmental Science after verification.

References

Balsam, W. L., Deaton, B. C. & Damuth, J. E. (1998). The effects of water content on diffuse reflectance spectrophotometry studies of deep-sea sediment cores. *Mar. Geol.* 149, 167-179.

Best, A. I. &Gunn, D. E. (1999). Calibration of marine sediment core loggers for quantitative acoustic impedance studies. *Mar. Geol.* 160, 137-146

Gunn, D. E. & Best, A. I. (1998). A new automated non destructive system for high resolution multi-sensor core logging of open sediment cores. *Geo-Marine Letters* 18, 70-77.

8. THERMAL PROPERTIES: *IN-SITU* TEMPERATURE, BOTTOM WATER TEMPERATURE AND THERMAL CONDUCTIVITY MEASUREMENTS

Ricarda Dziadek[1] [1]MARUM

Objectives

Temperature measurements are an important tool to detect fluid seepage sites. Especially *in-situ* measurements give detailed insight into transport processes of fluids or gas. Some processes may be distinguished:

- the advection of solids with fluids (mud flow),
- the advection of fluids through the sediments (pore-water advection),
- diffusion processes (chemical diffusion, conduction), or
- heat transported by rising gas bubbles without advection of pore water or mud.

Such processes may result in different shapes of temperature versus depth profiles:

- linear profiles indicating conduction of heat,
- concave profiles signify advective processes (mud flow, fluid advection), or
- unsteady profiles indicating that the heat transport may not be a simple one dimensional transport process but heterogeneous in space and time (Feseker et al., 2009a; Feseker et al., 2008).

During this expedition temperature measurements were realized by **M**iniaturized **T**emperature data-**L**ogger (MTL). The loggers record the temperature at present time with variable sampling intervals, depending on the duration of deployment. During this cruise the loggers were used as outriggers on gravity corer (Table 8.2; see also remarks in the station list A.4) or mounted on the TV-sled OFOS. The intention of the cruise report is to give an overview of the temperature measurements in the working area indicating major results.

Work at sea

Miniaturized Temperature data-Logger are autonomously operating precision thermometers for deep sea application. They were cooperatively developed by the section Meerestechnik/Sensorik at University of Bremen und the logging equipment company Antares. The accuracy is within the range of 5 – 1 mK, depending on the temperature range and precision up to 0.001 deg Kelvin. The housing is designed for an operation depth of 6000 m and sediment penetration. The sampling rate can be adjusted between 1 s and several minutes, yielding a registration time of 1 h

to 6 months. With a known distance these loggers were mounted on the gravity corer (see Fig. 8.1). During the sediment penetration, a steady time of 7 to 8 minutes was given, to let the sensors adjust to the ambient sediment temperature. This temperature, together with the known depth of the sensors, was later on board used to determine the temperature changes with depth, i.e. the geothermal gradient.

Between two and and six MTL were mounted on OFOS and sampled bottom water temperatures during all dives with an interval of 1s. Mounted diagonal (bottom and top of the OFOS frame) they successfully registered bottom water anomalies. In the station protocol (see Table 8.1) all deployments of the MTL sensors are compiled for OFOS dives as well as for the gravity corer.

KD2 Pro – thermal properties

The KD2 Pro, developed by Decagon Devices, Inc., enables to analyze thermal properties of the sediment (see Fig. 8.2). The operating environment for the handheld controller, powered by 4AA batteries, is 0 to 50°C. Its accuracy lies between 5 % from 0.2 - 2 W/m degK and ±0.01 W/mK from 0.02 - 0.2 W/ degK. The 6 cm single needle was used to obtain thermal conductivity values of one core. To identify the influence of the previous pore water sampling (every 20 cm), the sampling interval was set to 10 cm.

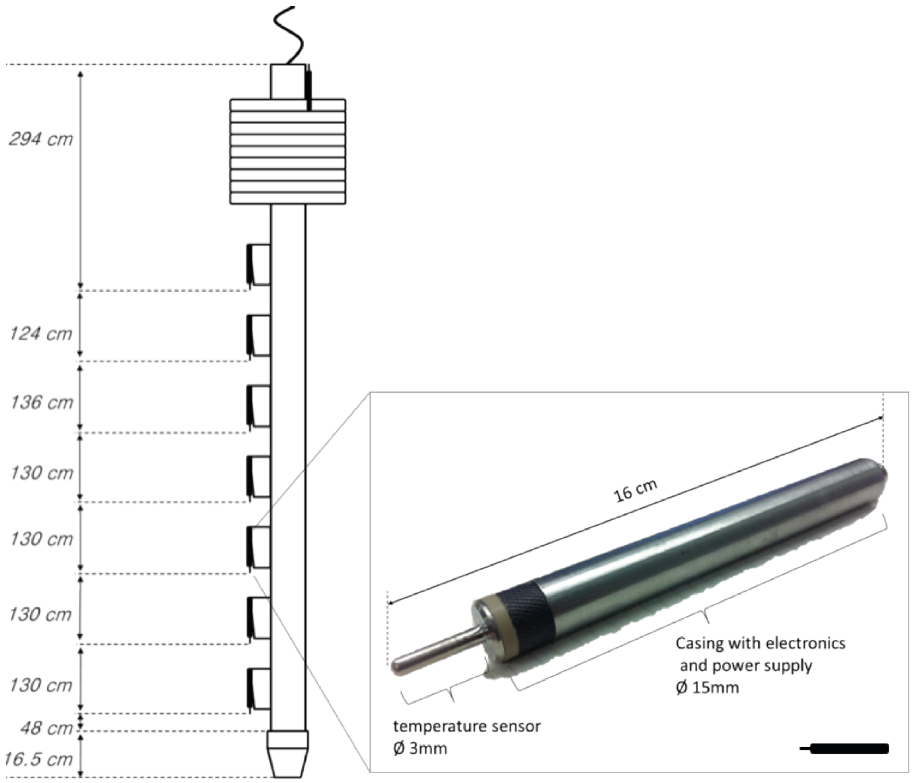

Fig. 8.1: Sensor mounting geometry on gravity corer

Tab. 8.1: Station protocol for MTL deployments mounted of either OFOS or the gravity corer. Ten loggers were calibrated during station PS81/257-2 with the CTD.

Date	Time (UTC)	Station	Latitude (S)	Longitude (W)	Penetration Time	Depth	Instrument	Comments	Area
26.03.13	04:31	PS81/257-2	53°41.530	44°03.440	05:30:00 - 07:22:04	2277	CTD-1	CTD CALIBRATION	
31.03.13	09:11	PS81/268-1	55°48.219	28°30.114	09:39:00 - 11:39:00	724	OFOS-1	OFOS Positions, T Anomaly	Quest Caldera
31.03.13	12:37	PS81/268-2	55°48.098	28°31.488	12:37:00 - 15:11:00	734	OFOS-2		Quest Caldera
01.04.13	14:38	PS81/269-1	57°28.111	24°53.055	14:38:00 - 21:22:00	3715	OFOS-3 / SVP-5		
02.04.13	13:15	PS81/270-1	57°28.190	24°54.174	13:15:00 - 16:37:00	3659	OFOS-4 / SVP-6	Logger 3: no data aquisition	Forearc
05.04.13	19:53	PS81/271-2	59°50.449	23°23.011	19:56:00 - 20:05:00	4794	Gravity Corer-11	core length: 9.40 m	Forearc
06.04.13	14:16	PS81/272-1	59°28.498	25°46.519	14:47:25 - 14:55:35	2870	Gravity Corer-12	no penetration	Forearc
07.04.13	16:08	PS81/274-1	57°19.680	25°29.009	18:01:00 - 21:14:00	3709	CTD-3	T anomaly	Forearc
08.04.13	01:18	PS81/274-3	57°19.625	25°28.910	02:33:00 - 04:10:00	3723	OFOS-6	Logger: 1,10 no data aquisition	Forearc
08.04.13	19:07	PS81/275-1	55°56.426	28°05.728	19:13:00 - 21:07:00	526	OFOS-7		Forearc
08.04.13	23:04	PS81/276-1	55°48.542	28°29.687	23:23:00 - 01:30:00	717	OFOS-8		Quest Caldera
09.04.13	13:16	PS81/278-1	55°46.711	28°47.601	13:33:00 - 15:31:00	779	OFOS-9		unnamed submarine volcano
10.02.13	18:50	PS81/280-1	54°27.440	35°50.503	18:55:18 - 19:03:06	237	Gravity Corer-13	6/8 MTL did not start logging	
11.04.13	00:58	PS81/281-2	54°12.149	36°27.210	01:02:50 - 01:10:11	260	Gravity Corer-14	activate now, #4,8 damaged	cumberland bay west
11.04.13	18:47	PS81/284-1	54°15.918	36°26.229	18:48:50 - 18:56:22	275	Gravity Corer-15	7 MTL did not start logging #7,9 damaged	cumberland bay east
11.04.13	23:26	PS81/285-1	54°12.138	36°27.187	23:36:00 - 00:59:00	265	OFOS-10	no obvious T anomaly	Cumberland Bay Flare
13.04.13	08:36	PS81/288-1	53°46.190	38°8.403	08:41:21 - 08:49:08	381	Gravity Corer - 17	8,10 previously bent	

Fig. 8.2: KD2 – Pro thermal properties analyzer. Picture shows handheld device, powered by 4 AA batteries, and the 6 cm single needle sensor. The sensor is directly inserted into the sediment.

Preliminary results

In-situ measurements

During four deployments with the gravity corer *in-situ* temperature measurements with the MTL were obtained and geothermal gradients were determined. The results are listed in Table 8.2.

Tab. 8.2

Station	Date	Time	Lat. S	Long. W	Water depth	Gradient
PS81/271-2	05.04.13	19:55	59°50.450	23°22.990	4794 m	14°C/km
PS81/281-2	11.04.13	01:02	54°12.140	36°27.210	260 m	52°C/km
PS81/284-1	11.04.13	18:48	54°15.910	36°26.230	275 m	46°C/km
PS81/288-1	13.04.13	08:41	53°46.170	38°08.420	381 m	32.25°C/km

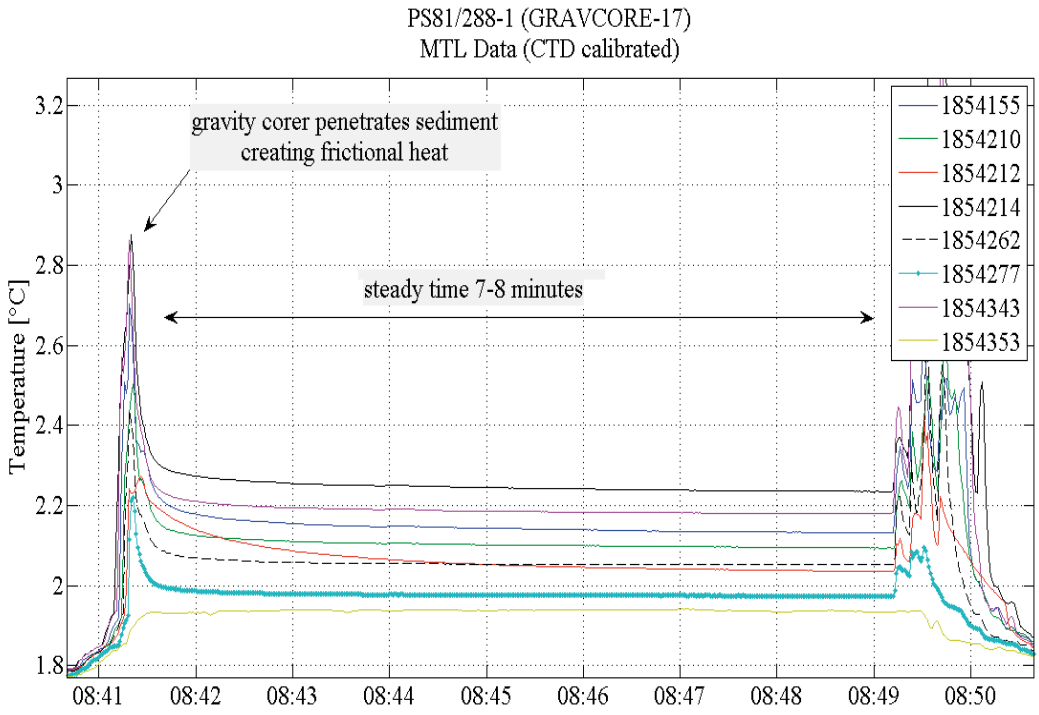

Fig. 8.3: MTL data for deployment PS/288-1 with the gravity corer (for details see Table 8.1). MTL 1854353 was mounted above the weight and there for measuring the water temperatures above the sea floor. It was dismissed for later determination of the thermal gradient. The penetration of sediment creates frictional heat, which is clearly seen in all loggers at 08:41:20 (UTC). During 7 minutes steady time the temperature decreases continuously until approximately 08:49:15 (UTC), when the gravity corer is lifted up again.For logger identification see legend.

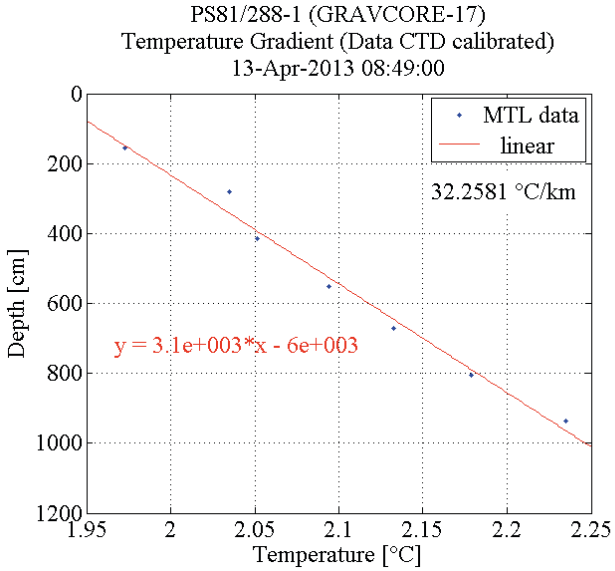

Fig. 8.4: All MTLs than clearly penetrated the sediment are used to calculate the geothermal gradient. At station PS81/288-1 gradient of 32.3°C/km was determined and indicates a normal conduction of heat.

Bottom water surveys: MTL mounted on OFOS

A further objective of this cruise was the study of heat anomaly associated with hot vents or cold seeps. Therefore the TV sled OFOS was equipped with several MTLs. Exemplary visualized in figure 8.5 are the datasets of four loggers deployed during PS81/268-1.

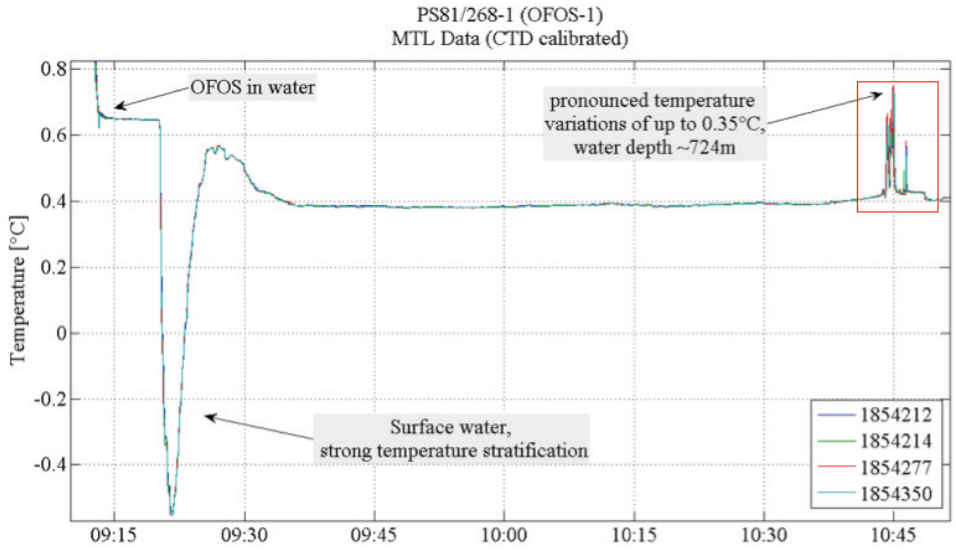

Fig.8.5: Four MTLs were mounted on OFOS deployment 1 at station PS81/268-1. The peak between 09:15:00 and 09:30:00 (UTC) is caused by stratification of the water column. Here, the surface water presents temperatures down to almost -0.6°C. Between 09:40:00 and 10:40:00 (UTC) the dive continues along the sea floor and the temperatures are stable at 0.4°C. At approximately 10:45:00 (UTC) a very pronounced temperature was detected by all four loggers (red square, for details see Fig. 8.6). Here temperature variations are as high as Δ0.35°C and in strong contrast to the rather stable temperatures of the ambient water.

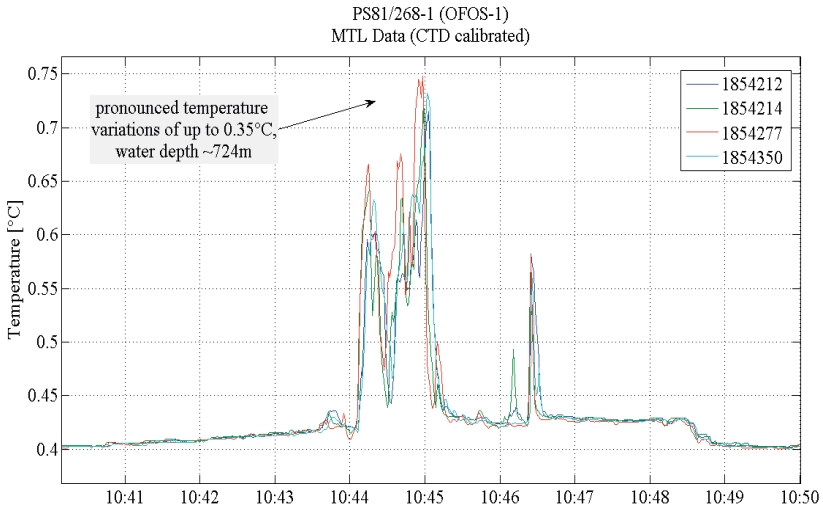

Fig. 8.6: Close up of the temperature anomaly detected by all four loggers between 10:43 and 10:49 (UTC). Small variations and offsets between the individual loggers can be explained by the mounting on OFOS on different locations, i.e. variations in distance to the heat source. Background temperature of 0.4°C is exceeded by up to Δ0.35°C.

Thermal conductivity measurements on core PS81/271-2

On core PS81/271-2 thermal conductivity measurements were conducted. High opal contents of this core result in very low values of the thermal conductivity scattered around 0.6 W/mK in depths of 250 – 910 cm. Within the upper 250 cm a larger deviation from the mean value can be observed. Values drop down to almost 0.4 W/mK and the reason for this is left to be discussed. The variations in temperatures can be explained by the environment in which the measurements were conducted. The core segments were stored in the cooling container, which has two separate rooms with different temperatures of approximately 6°C and 3°C. The third parameter r^2 visualized in figure 8.7 is an indicator of the quality of the measurements and should not be below 0.9950. A minimum value of 0.9994 and a mean 0.9997 demonstrate the a good quality of the measurements. Before these were conducted the sensor performance was verified with glycerin. At 20°C it has a known thermal conductivity of 0.285 W/mK at 20°C.

Together with the thermal gradient at this location (14°C/km) a heat flow of 8.4 mW/m² was calculated. Compared to values for heat flow depending on crustal age and sediment thicknesses compiled in figure 8.8 (Hasterok, 2011) this value is extremely low. The mean value for oceanic crust is 52 mW/m². A possible explanation for such a low value could be the highly porous diatom sediments at this location. Furthermore it needs to be emphasized, that this value could not be verified by other measurements at this location due to time issues.

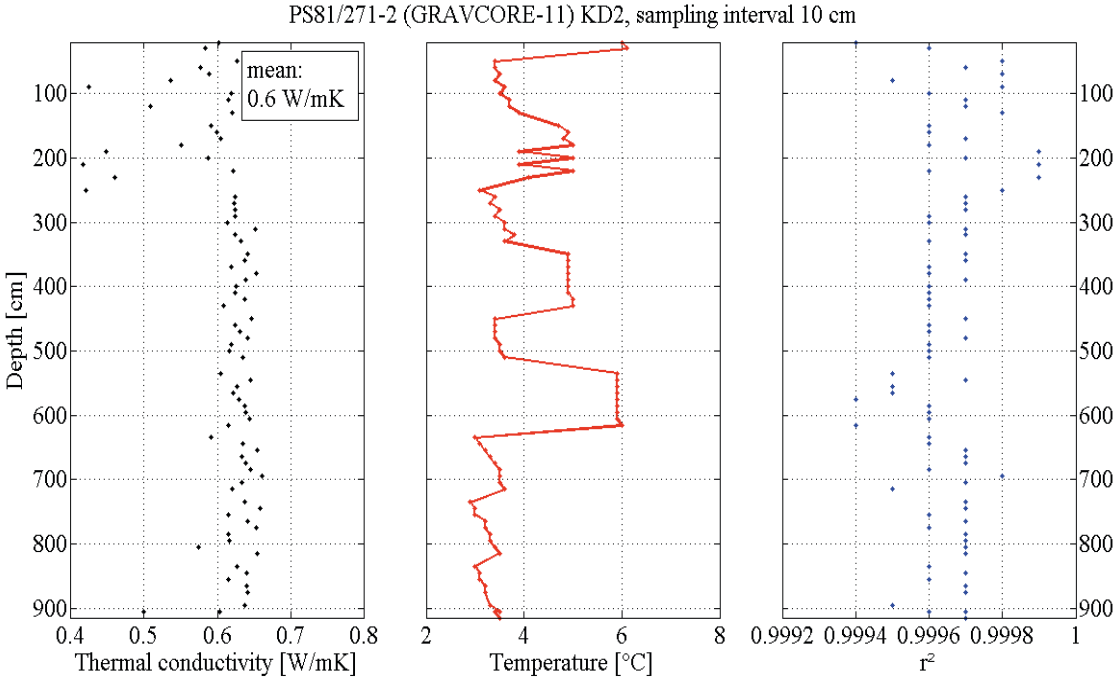

Fig. 8.7: Visualized are the results of thermal properties analyzed on opal core PS81/271-2 over 910 cm. Strong contrasts in the upper 250 cm are left to be discussed. Temperature variations are due to the storage of the core segments in cooling container at 3°C and 6°C. The mean value of the thermal conductivity of 0.6 W/mK is very low and could be explained be the high porosity of the core. Previous pore water sampling every 20 cm seemed to have no influence on the measurements. Yet sampling interval was set to 10 cm.

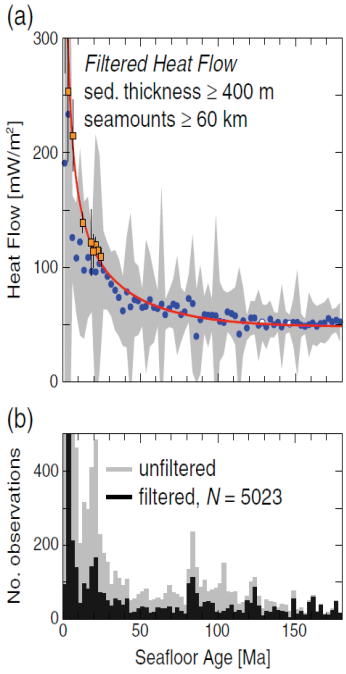

Fig. 5. Global filtering results with ≥400 m sediment cover and ≥60 km to the nearest seamount. (a) Heat flow versus age in 2.5 m.y. bins (open circles contain <10 sites) with one standard deviation (gray region). (squares) Site-specific analyzed data (Table 2). (b) Number of observations within each age bin, initial dataset in gray.

Fig. 8.8: Global filtering results with ≥ 400 m sediment cover and ≥ 60 km to the nearest seamount. (a) Heat flow versus age in 2.5 m.y. bins (open circles contain < 10 sites) with one standard deviation (gray region). (squares) Site-specific analyzed data (Table 8.2). (b) Number of observations within each age bin, initial dataset in gray. Heat flow with dependence on crustal ages decays over time to approximately 50 mW/m². Young oceanic crust at mid-ocean spreading centers has typically very high values of heat flow. The calculated value for station PS81/271-2 with 8.4 mW/m² is extremely low and needs more data for verification. A first interpretation could be the high porous, diatom sediments at this location. (Hasterok et al. 2011)

Data management

Raw data obtained from MTL deployments during this cruise will be uploaded to PANGAEA Data Publisher for Earth & Environmental Science in the following format:

yyyy mm dd HH MM SS Raw Res[Ohm] Temp[degC]

References

Feseker T, Dählmann A, Fouche, JP and Harmegnies F, (2009a) In-situ sediment temperature measurements and geochemical porewater data suggest highly dynamic fluid flow at Isis mud volcano, eastern Mediterranean Sea. Marine Geology 261: 128-137.

Feseker T, Foucher JP and Harmegnies F (2008) Fluid flow or mud eruptions? Sediment temperature distributions on Håkon Mosby mud volcano, SW Barents Sea slope. Marine Geology 247: 194-207.

Hasterok D., D.S. Chapman, E.E. Davis, Oceanic heat flow: Implications for global heat loss, Earth and Planetary Science Letters, Volume 311, Issues 3-4, 15 November 2011, Pages 386-395, ISSN 0012-821X, 10.1016/j.epsl.2011.09.044.

9. SEDIMENT GEOCHEMISTRY AND BIOGEOCHEMISTRY

Sabine Kasten[1], David Fischer[1], [1]AWI
Eva Kirschenmann[1], Benjamin Löffler[1], [2]MARUM
Patrizia Geprägs[2], Marta Torres[3] [3]OSU

Objectives

An important goal of this expedition was to understand biogeochemical processes operating within four distinct systems of the Scotia Sea/South Sandwich Plate. Our main targets were: 1) opal-rich sediments that characterize the incoming South American Plate; 2) pore-water/rock interactions at hydrothermal vents and at cold seep systems in the South Sandwich fore-arc and back-arc; 3) buried volcanoes and seamounts in the back-arc region, where fluid circulation within the upper igneous crust may be occurring and 4) methane seeps originating from localized high organic carbon sources off the South Georgia Island Fjords.

In general, we aim at using the chemical and isotopic composition of interstitial fluids in "normal" hemipelagic deposits as well as in locations of fluid discharge in the study area to trace fluid sources and the migration patterns as well as the impact that the particular composition and transport mechanisms have on geochemical and biogeochemical processes operating throughout the sediment column. Understanding and quantifying these complex interactions in the different depositional systems will enhance our understanding of subsurface biosphere processes and improve the quality of paleoenvironmental and paleoceanographic reconstructions from sedimentary archives. From a knowledge of characteristic diagenetic fingerprints associated with these biogeochemical processes, changes in fluid migration patterns with time may be inferred from analyses of solid phase samples, thus providing a record of the evolution of these dynamic environments through time.

Work at sea

During this cruise pore-water and solid-phase samples were collected from 5 multiple cores (MUC), 7 gravity cores (GC) and one long piston core (PC), as detailed in Table 9.1. Due to the hard-ground nature of the seafloor in the fore arc and volcano targets surveyed, only cores from the incoming plate (opal rich) and off South Georgia Island (carbon rich) were recovered. After arrival of the cores on deck of *Polarstern*, samples were transferred into a refrigerated container or laboratory (4°C). At each site two MUC cores were taken for oxygen measurements, pore-water extraction and solid-phase sampling.

Tab. 9.1: Sites investigated geochemically during this cruise, including parameters analysed on board and aliquots of samples taken and stored for further analyses in the home lab.

Station	Area	Device	Rhizon Sampling	Oxygen (microsensors)	Chlorinity	NH_4	Fe	PO_4	Si	HS^{-*}	SO_4, Cl* (1:50)	Trace metals* (acidified)	DIC, δ13DIC*	δ18O*	CH_4 (P. Geprags)	Sediment (stored under argon)	Sediment (frozen, -20°C)
PS81/258-1	Cumberland Bay East, close to glacier	GC	X	-	X	-	X	-	X	X	X	-	-	-	X	X	-
PS81/258-3	Cumberland Bay East, close to glacier	MUC	X	X	X	-	X	-	X	X	X	-	-	-	-	X	-
PS81/262-2	Cumberland Bay West	MUC	X	X	X	X	X	X	X	X	X	-	-	-	-	X	-
PS81/263-1	Grytviken Flare	GC	X	-	-	X	X	X	X	X	X	X	X	X	X	X	-
PS81/271-2	Sediment Basin E of Trench, opal-rich	GC	X	-	X	X	X	X	-	X	-	X	X	X	X	X	-
PS81/271-3	Sediment Basin E of Trench, opal-rich	MUC	X	X	-	X	X	X	-	X	-	X	X	X	-	X	-
PS81/271-4	Sediment Basin E of Trench, opal-rich	PC	X	-	X	X	X	X	-	X	-	X	X	X	X	X	-
PS81/280-1	"Background" site off South Georgia	GC	X	-	-	X	X	X	-	X	-	X	X	X	X	X	-
PS81/280-2	"Background" site off South Georgia	MUC	X	X	-	X	X	X	-	X	-	X	X	X	-	X	-
PS81/281-2	Cumberland Bay Flare	GC	X	-	-	X	X	X	-	X	-	X	X	X	X	-	-
PS81/284-1	Grytviken Flare	GC	X	-	-	X	X	X	-	X	-	X	X	X	X	X	-
PS81/284-2	Grytviken Flare	MUC	X	X	-	X	X	X	-	X	-	X	X	X	-	X	X
PS81/288-1	putative gas hydrate site	GC	X	-	X	X	X	X	-	X	-	X	X	X	X	-	-

Ex-situ oxygen measurements using amperometric microelectrodes were performed according to the technique described by Ziebis et al. (2012). Subsequently, pore water was retrieved by means of rhizons which have an average pore-size of 0.15 µm (Seeberg-Elverfeldt et al., 2005). Pore-water sampling was followed by on-board analyses of various pore-water constituents – including iron, ammonium, phosphate, silica and chloride. In addition pore-water subsamples were preserved and stored for the shore-based analyses of sulfate, chloride, hydrogen sulfide, total inorganic carbon, major and minor cation concentrations, as well as the stable isotopic composition of several of these constituents. Pore-water sampling from MUC cores was performed at a depth resolution of 1 (in the upper 10 centimeters) to 3 cm. From the gravity and piston cores, which were cut into 1 m long segments on deck, pore water was retrieved at 20 cm depth resolution by means of the rhizon samplers.

The concentration of dissolved species and their isotopic composition provide critical data for the identification of fluid sources, fluid/rock interactions, pathways of fluid migration, and plumbing of the system. In addition, geochemical data can help characterize the subsurface biosphere and aid in constraining mass balance inventories operating in this region.

Oxygen concentrations in the sediments were determined by use of amperometric Clark-type oxygen sensors with an internal reference and equipped with a guard cathode (Revsbech, 1989). The electrodes (Unisense, Denmark) were made of glass with a 6 cm long tip that was inserted into a hyperdermic needle (diameter 1.1 mm, length 50 mm) and had a response time of about 10 s. Signals were amplified and transformed to mV by a picoamperemeter, digitalized by an analogue/digital converter (ADC 216, Unisense, Denmark) and recorded by a computer using the software PROFIX (Unisense, Denmark). Measurements were performed at least 12 hours after core recovery in order to allow a temperature equilibration of the sediments at 4°C in the cold room. High-resolution (1 mm steps) vertical profiles of oxygen across the sediment/water interface were accomplished for MUC cores by use of a micromanipulator down to a maximum sediment depth of 6 cm.

Dissolved iron (Fe^{2+}) was detected photometrically (Dr. Lange photometer) at a wavelength of 565 nm. 1 mL of sample was added to 50 µL of Ferrospectral solution to complex the Fe^{2+} for colorimetric measurement.

Phosphate (PO_4^{3-}) was determined photometrically (Dr. Lange photometer) using the molybdenum blue method (Grasshoff et al., 1999). To 1 mL of sample 50 µL of an ammonium molybdate solution was added and spiked with 50 µL of an ascorbic acid solution. The phosphomolybdate complex was reduced to molybdenum blue and measured photometrically at 880 nm wavelength.

Silica was also measured photometrically (Dr. Lange photometer) as silica molybdate complex at 820 nm wavelength.

Ammonium was determined by a conductivity method.

High-precision chloride concentrations were acquired using a Metrohm titrator and silver nitrate ($AgNO_3$) solutions that were calibrated against repeated titrations of an IAPSO standard following the procedure of Gieskes et al. (1991). Repeated analyses of an IAPSO standard yielded a precision better than 0.3 %.

For the determination of **methane concentrations in sediments** the headspace technique was used. For this purpose 3 ml of sediment were taken using cut-off

syringes and transferred into 20 ml glass vials prefilled with 5 ml of 1 M NaOH. The sediment samples were taken from the gravity cores and one piston core (*c.f.* Table 9.1) from the bottom of freshly cut core segments directly on deck. Prior to gas chromatographic analysis, the samples were left for several hours at 20 °C and were shaken occasionally. The gas samples were analyzed onboard for their methane concentrations with a two-channel 6890N gas chromatograph (Agilent Technologies) according to the technique described by Pape et al. (2010). Methane is detected and quantified with a capillary column connected to a Flame Ionization Detector. Calibrations and performance checks of the analytical system were conducted regularly using commercial pure gas standards.

For the analyses of further dissolved pore-water species aliquots of the remaining pore water samples were 1) acidified with $HNO_{3\ (suprapure)}$ for the determination of major elements and trace metals by ICP-OES and ICP-MS, 2) immediately fixed using a 2.5 % zinc-acetate solution to precipitate and subsequently measure hydrogen sulfide, 3) stored without headspace in 2 ml glass vials for $\delta^{18}O$ analyses, and 4) poisoned with $HgCl_2$ for the determination of both the concentration and the stable carbon isotopic composition ($\delta^{13}C$) of dissolved inorganic carbon (DIC). For two MUC and two gravity cores subsamples for sulfate and chloride determinations were diluted 1:50 and stored at 4°C for on-shore ion chromatography (HPLC) analyses (*c.f.* Table 9.1).

In addition to the pore-water program, sediment samples were taken from the MUC and gravity cores and stored cooled (4°C) or frozen (-20°C) under argon. These samples will be used for detailed characterization of the solid constituents that can be used to trace ongoing and past biogeochemical and diagenetic reactions that characterize each of the geochemical environments targeted during this cruise. Analyses will include bulk sediment investigations by means of total acid digestion, sequential extractions and mineralogical methods. One of the cores (PS81/284-2) from the methane-rich sediments of the Cumberland Bay East at the so-called "Grytviken Flare" was also sampled for microbial analyses of the communities that may be responsible for the biogeochemical processes at play in this setting.

Preliminary results

Site PS81/271 is located in a basin-like setting east of the Sandwich Trench characterized by the accumulation of opal-rich sediments and was sampled by multiple corer, gravity corer and piston corer (Fig. 9.1). Oxygen penetration depth - as determined on MUC core PS81/271-3 – was around 4 cm. Below a distinct maximum in dissolved iron (Fe^{2+}) found at 6 cm depth, the sediments were sulfidic and characterized by high concentrations of ammonium of up to almost 1,700 µmol/l. Chloride concentrations showed a slight freshening with depth. Pore-water methane values were constant over depth with concentrations below 0.3 µmol/l.

In contrast to the opal-rich sediments east of the Sandwich Trench presented above (Fig. 9.1), the deposits sampled within and off the Cumberland Bay in northern South Georgia showed a much shallower oxygen penetration depth of only 4 mm on average. As an example the high-resolution oxygen profile and the depth concentration profiles of interstitial iron and phosphate obtained at site PS81/262-2 (MUC) in the Cumberland Bay West are displayed in Fig. 9.2. In accordance with the tenfold shallower oxic zone the concentrations of dissolved iron and phosphate in the surface sediments at this site are also significantly higher than at the opal-rich station PS81/271 (Fig. 9.1).

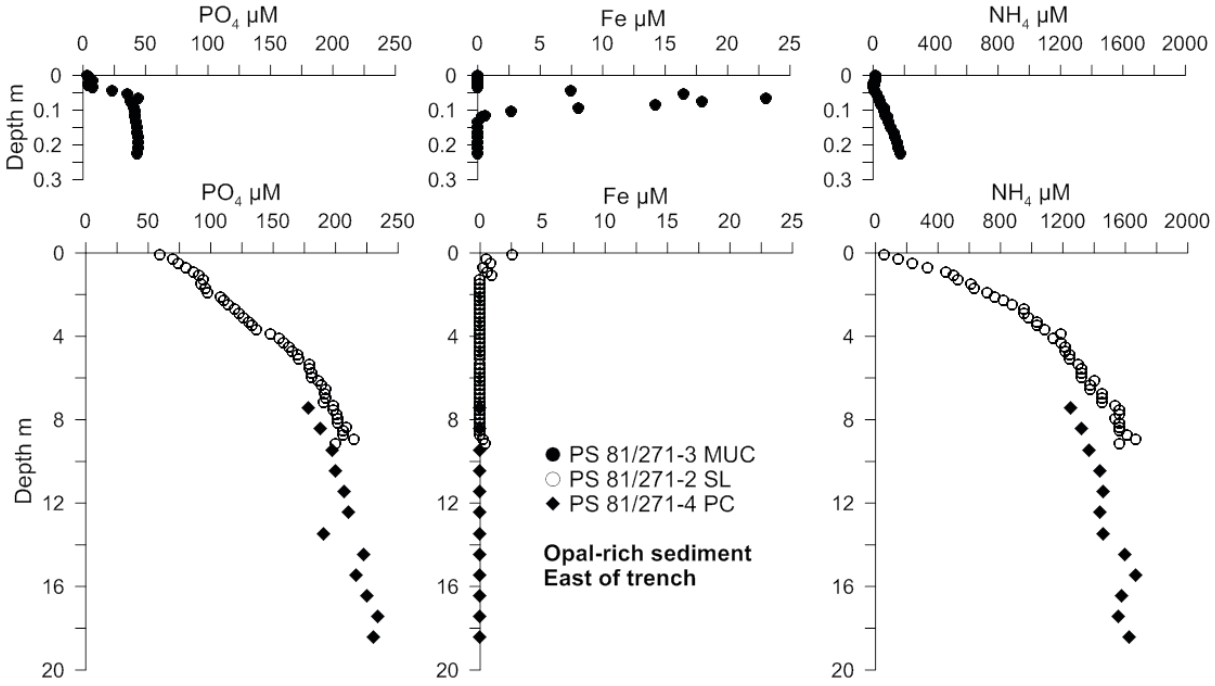

Fig. 9.1: Pore-water concentration profiles of phosphate, iron and ammonium from cores PS81/271-2 (GC), PS81/271-2 (MUC) and PS81/271-4 (PC)

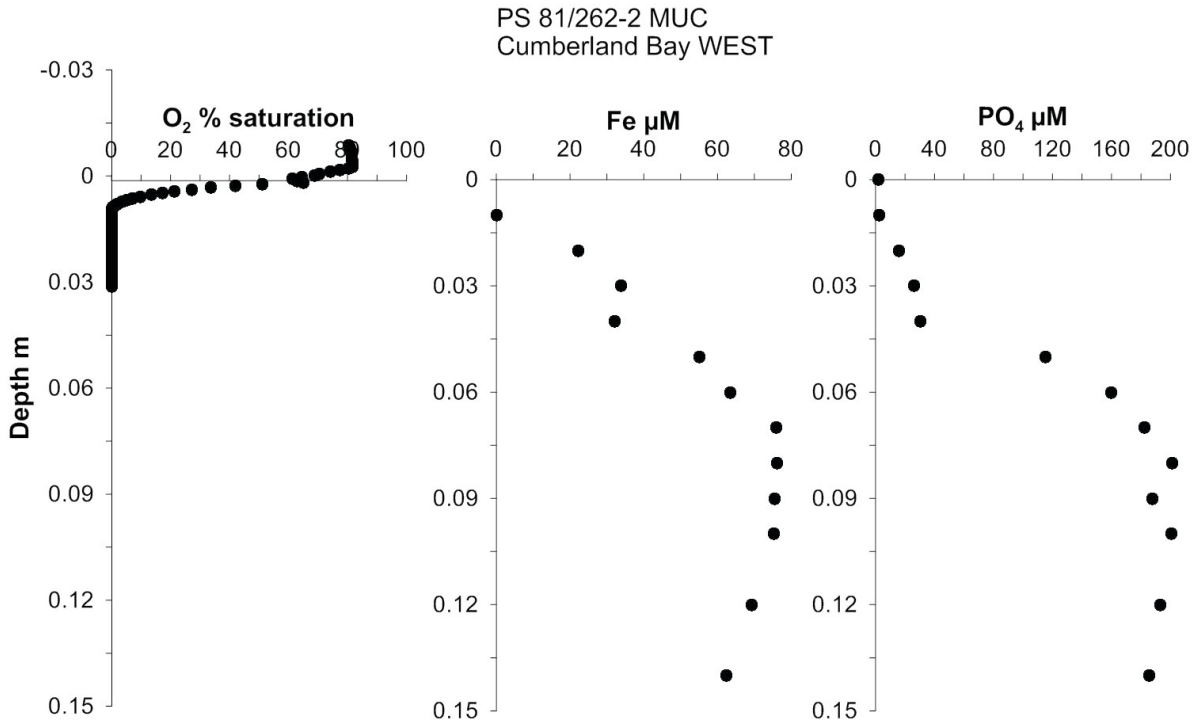

Fig. 9.2: Pore-water concentration profiles of oxygen, dissolved iron and phosphate at site PS81/262-2 (MUC) in the Cumberland Bay West

Station PS81/280 (Fig. 9.3) served as a "Background" site and was sampled outside the Cumberland Bay. Although a flare was found in the vicinity of this location the gravity and MUC cores PS81/280-1 and PS81/280-2 were taken at a distance from the potential centers of gas ebullition. The sediments only contained dissolved iron down to about 30 cm sediment depth and were sulfidic until the base of the core. The methane concentrations show highest values of up to 2.1 mmol/l at a depth of 8 m and then linearly decrease upward into the sulfate/methane transition, which at this site is located at a depth of around 5 m.

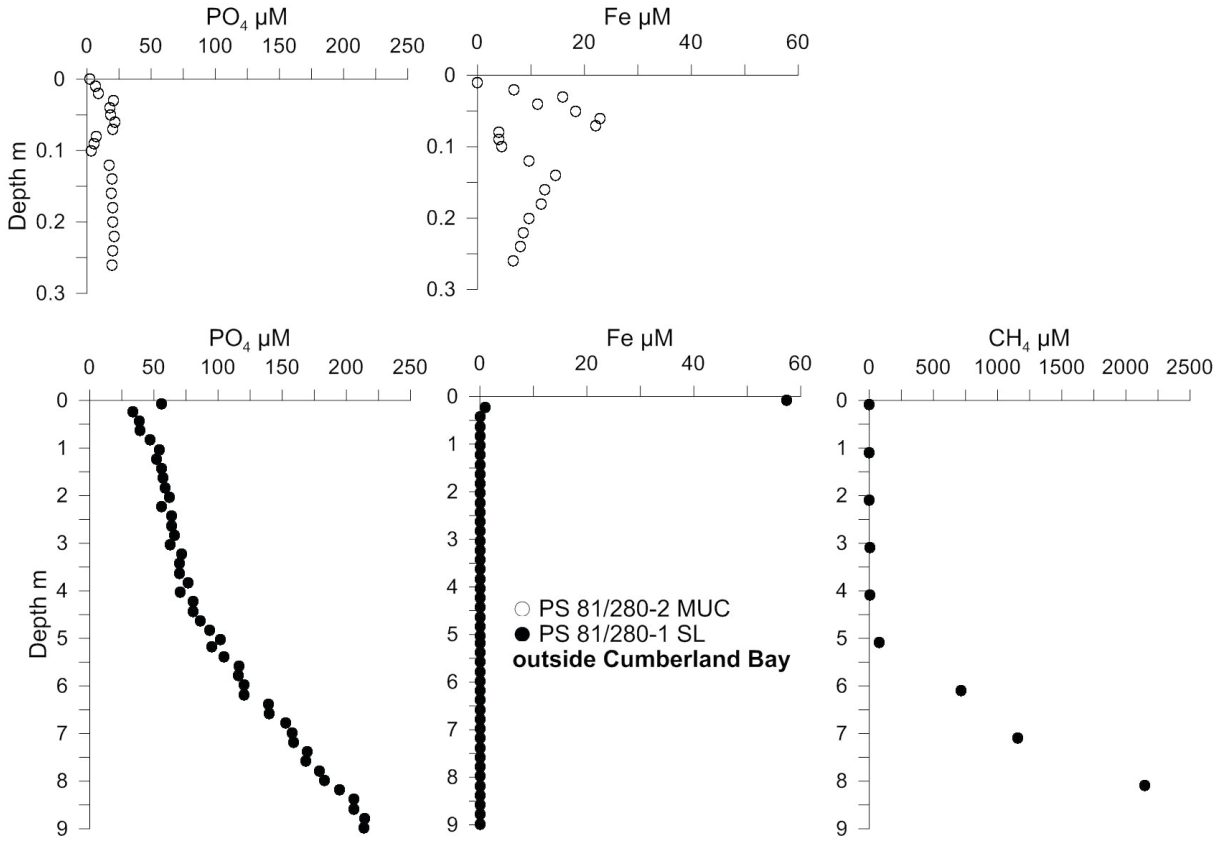

Fig. 9.3: Pore-water concentration profiles for the MUC and gravity cores retrieved at site PS81/280 outside Cumberland Bay ("Background site")

All sites sampled within the Cumberland Bay West and East – including site PS81/258 sampled close to the Nordenskjöld Glacier in Cumberland Bay East and all sites investigated close to gas flares - were characterized by high amounts of interstitial Fe^{2+} and a lack of hydrogen sulfide. As an example of these Fe-dominated Cumberland Bay sites, pore-water data for gravity core PS81/284 taken at the so-called "Grytviken Flare" are shown in Fig. 9.4. The sulfate/methane transition at this site is located at a relatively shallow depth of 2.5 m. Thus, although AOM-driven sulfate reduction definitely occurs at this site – as at all the investigated Cumberland Bay flare sites in general – a build-up of hydrogen in the pore water was not observed due to an inferred dominance of iron oxide reduction over sulfate reduction.

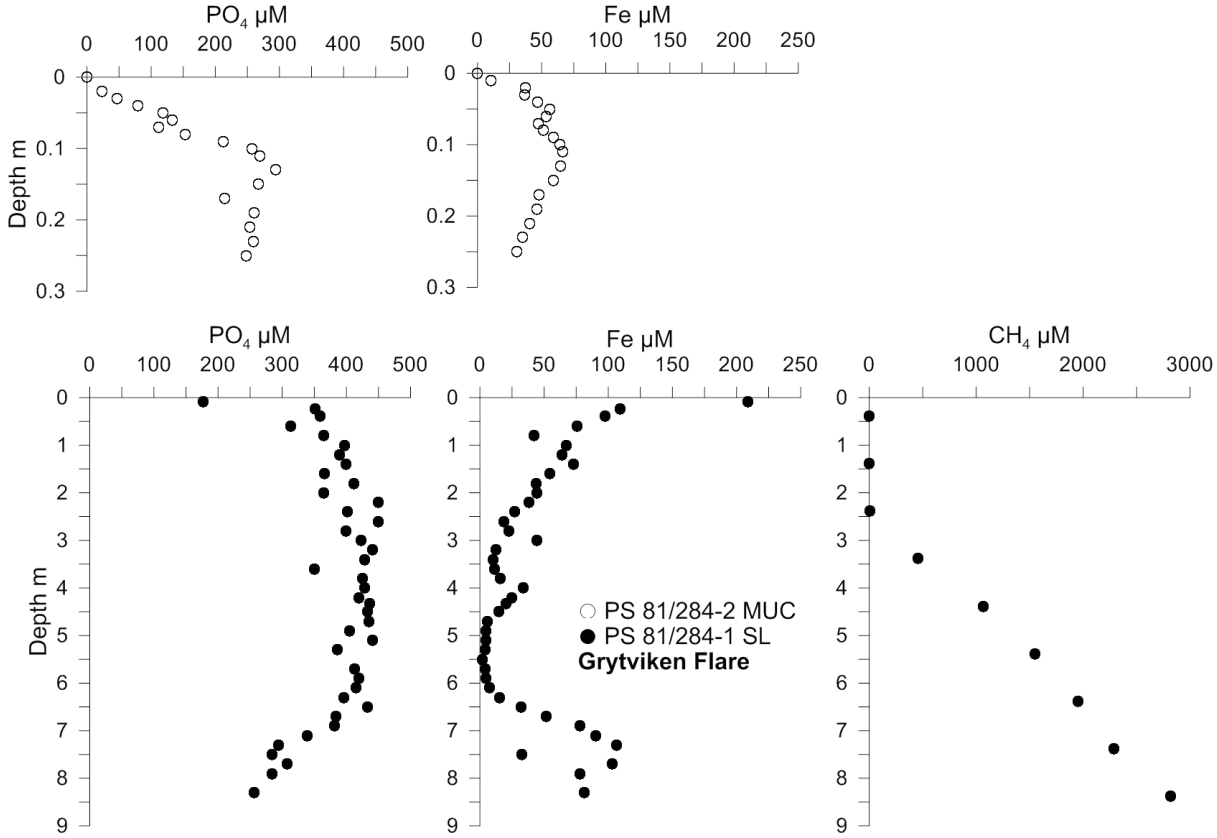

Fig. 9.4: Pore-water concentration profiles for the MUC and gravity cores retrieved at site PS81/284 in the Cumberland Bay East at the so-called "Grytviken Flare"

Due to appropriate temperature and pressure/water depth conditions Site PS81/288 located at the North-Western tip of the South Georgian archipelago was chosen as a potential gas hydrate site (Fig. 9.5). The sulfate/methane transition at this location was found at a very shallow depth of only 0.5 m and with values of more than 3 mmol/l the highest methane concentrations of all sites investigated during this cruise were found. However, gas hydrates could neither be found nor inferred on the base of infrared-camera inspections within the sampled sediment interval of about 7.6 m. However, the pore-water chlorinity profile displayed in Fig. 9.6 shows a slight increase in concentrations with depth, perhaps indicating the presence of gas hydrates at greater depth in the area.

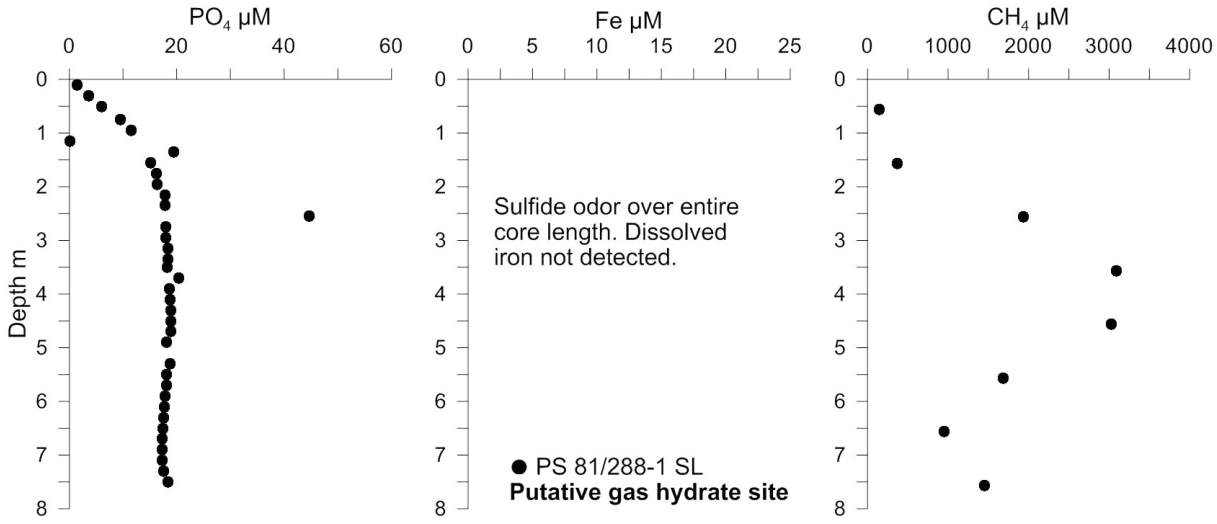

Fig. 9.5: Pore-water concentration profiles for gravity core PS81/288-1 retrieved at a putative gas hydrate site outside the Cumberland Bay

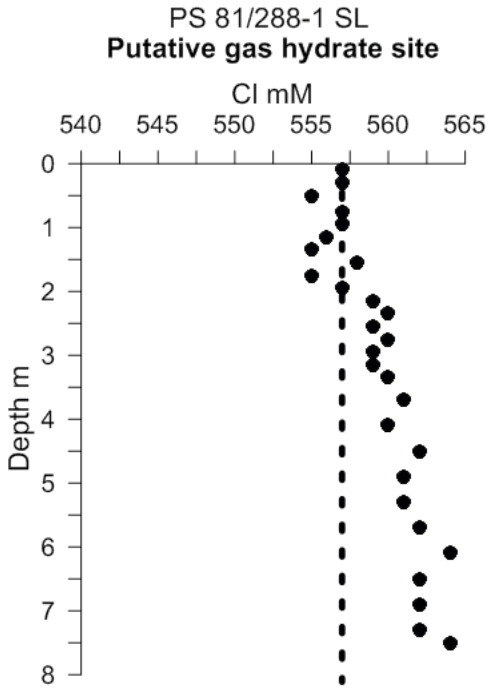

Fig. 9.6: Pore-water chlorinity profile from the putative gas hydrate site PS81/288

Data management

All information concerning the pore-water and solid-phase samples taken during this cruise will be implemented into PANGAEA Data Publisher for Earth & Environmental Science immediately after the end of the expedition. Data obtained and collected onboard and during subsequent analyses at the AWI, the MARUM/University of

Bremen and at Oregon State University will be submitted to PANGAEA and made publicly available after acceptance of the respective manuscripts in order to ensure long-term storage and availability for the scientific community.

References

Bodeï, S., Buatier, M., Steinmann, M., Adatte, T., Wheat, C.G. (2008) Characterization of metalliferous sediment from a low-temperature hydrothermal environment on the Eastern Flank of the East Pacific Rise. Mar. Geol., 250, 128-141.

Gieskes, J.M., Gamo, T., Brumsack, H. (1991) Chemical methods for interstitial water analysis aboard JOIDES Resolution. ODP Tech. Note, 15, doi:10.2973/odp.tn.15.1991.

Nürnberg, C.C., Bohrmann, G., Schlüter, M. (1997) Barium accumulation in the Atlantic sector of the Southern Ocean: Results from 190,000-year records. Paleoceanography, 12, 594-603.

Pape, T., Bahr, A., Rethemeyer, J., Kessler, J.D., Sahling, H., Hinrichs, K.U., Klapp, S.A., Reeburgh, W.S., Bohrmann, G. (2010) Molecular and isotopic partitioning of low-molecular weight hydrocarbons during migration and gas hydrate precipitation in deposits of a high-flux seepage site. chem. Geol., 269, 350-363.

Revsbech, N.P. (1989) An oxygen microelectrode with a guard cathode. Limnol. Oceanogr., 34, 472-476.

Seeberg-Elverfeldt, J., Schlüter, M., Feseker, T., Kölling, M. (2005) Rhizon sampling of porewaters near the sediment-water interface of aquatic systems. Limnol. Oceanogr. Methods, 3, 361-371.

Ziebis, W., McManus, J., Ferdelman, T., Schmidt-Schierhorn, F., Bach, W., Muratli, J., Edwards, K.J., and Villinger, H. (2012) Interstitial fluid chemistry of sediments underlying the North Atlantic gyre and the influence of subsurface fluid flow. Earth Planet. Sci. Lett. 323-324, 79-91.

10. BIOGEOCHEMISTRY OF THE WATER COLUMN

Susan Mau[1], Birgit Glückselig[1], [1]AWI
Patrizia Geprägs[2], [2]MARUM
Marta Torres[3], [3]OSU
Janet Rethemeyer[4] [4]Uni Köln

Objectives

Methane is a potent greenhouse gas: per unit mass, methane has a global warming potential that is 23 times higher than that of CO_2 over a 100-year timescale (Ramaswamy et al., 2001). Methane is produced in ocean sediment as well as in the water column. Despite of these methane sources only little of the gas actually escapes to the atmosphere. Only 4 – 15 Tg yr^{-1} CH_4 is emitted to the atmosphere from the ocean (Solomon et al., 2007) contributing only 0.7 – 2.5 % to the ~600 Tg CH_4 from all natural and anthropogenic sources. The low nanomolar concentration in the bulk of the ocean is thought to be maintained by microbial activity (Reeburgh, 2007).

This effective methane biofilter includes both anaerobic and aerobic microbial methane consumption in sediments and the water column. Anaerobic oxidation of methane (AOM) takes place at methane concentrations >0.5 – 5 μmol L^{-1} (Valentine, 2011). Below this concentration and in the oxic water column, aerobic methanotrophy controls methane emissions to the atmosphere. Physical, chemical, and biological factor and their interactions modulate the microbial oxidation of methane. In order to understand and predict the methane contribution of the ocean to the atmosphere in the future, it is essential to explore the cycle of methane in the ocean from its formation to its consumption and physical transport.

Within the Cumberland Bay, the hydrographic program aimed at understanding the degree of methane input from the sediments into the water column, and the fate of methane in this relatively shallow system. The distinct methane input from the sediments is undoubtedly oxidized within the water column, but this process is modulated by a complex circulation pattern driven by fresh water input from the glaciers and sea-bottom topography. To unravel the biogeochemical and hydrographic processes, we will utilize methane concentration and oxidation rate measurements, which will be analyzed in the context of conventional tracer data (temperature, salinity, $\delta^{18}O$, and nutrient distributions) complemented by reservoir dating using C-14 measurements.

In addition to investigations regarding the methane cycle in the ocean, plankton samples including the larger plankton fractions such as radiolarians, foraminifera, and dinoflagellates were collected for silicate isotope analysis from different water depths.

Work at sea

CTD deployment: The work at sea included sampling of the water column above or near methane seeps. Water samples were collected using the rosette sampler at seven stations (Fig. 10.1 and 10.2). Station PS81/257-2 and 271-1 were test station and reference station, respectively. The former was used to collect sound velocity for calibrating PARASOUND and HYDROSWEEP acoustics whereas the latter was used as a reference station without any methane seepage. The positions of PS81/274-1, PS81/281-1, PS81/282-1, PS81/284-3, and PS81/286-1 were chosen due to the proximity to acoustically imaged flares/plumes and PS81/277-1 was exclusively sampled for silicate isotopes.

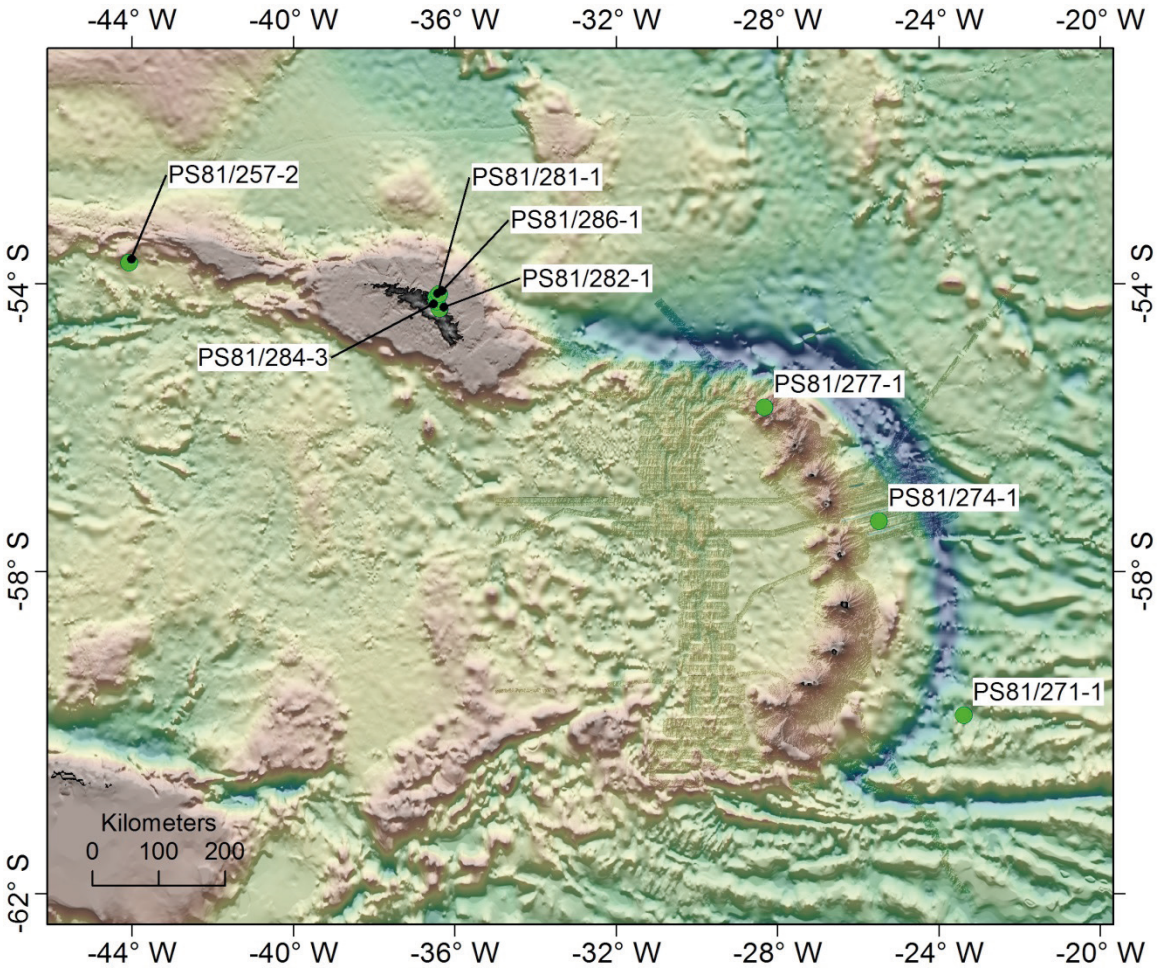

Fig. 10.1: Map of CTD/Ro stations during ANT-XXIX/4

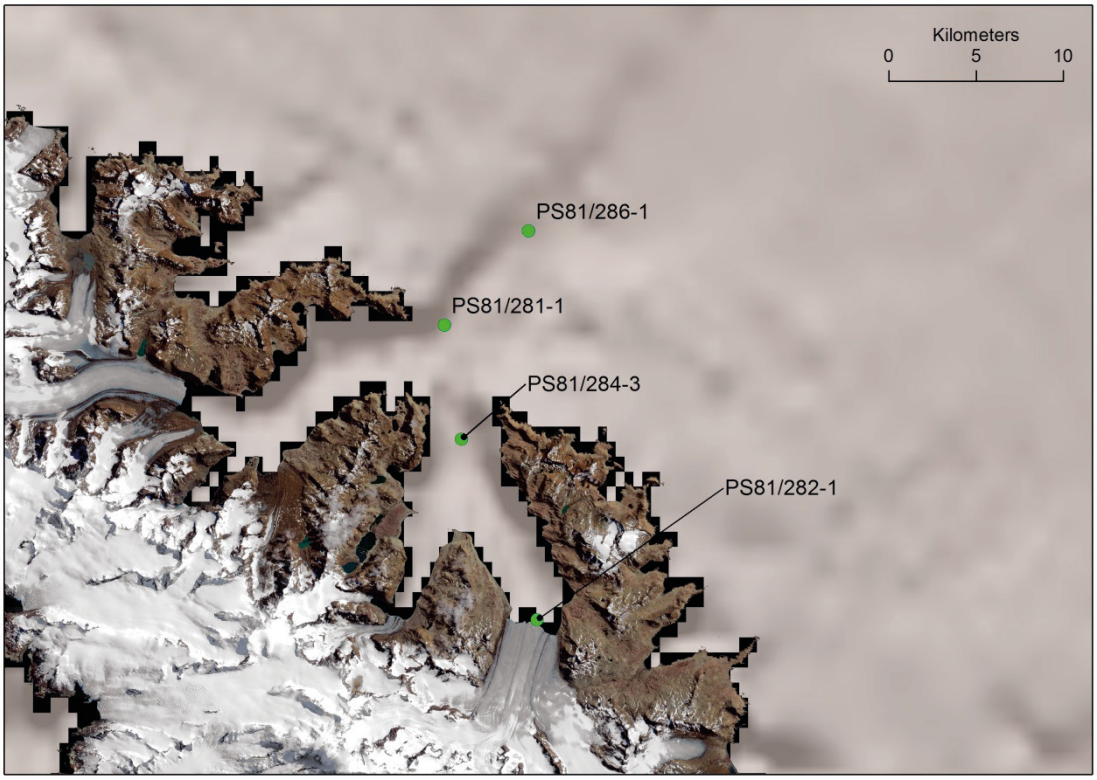

Fig. 10.2: Map of CTD/Ro stations in the Cumberland Bay, South Georgia

Water samples were taken for the following analysis which were partly completed on board, but mainly collected for shore-based analysis.

Methane concentration and isotopic ratio analyses: The gas samples were analyzed onboard for their methane concentrations with a two-channel 6890N (Agilent Technologies) gas chromatograph (GC); (Pape et al., 2010). Methane is detected and quantified with a capillary column connected to a Flame Ionization Detector, while permanent gases O_2, N_2, CO_2 were determined using a stainless steel column packed with mole sieve and coupled to a Thermal Conductivity Detector. Calibrations and performance checks of the analytical system were conducted regularly using commercial pure gas standards and gas mixtures. Water samples were taken immediately from the Niskin bottles; 750 ml of water was filled in pre-evacuated 1,000 ml sample bottles. This method is a modification of the vacuum degassing method described by Lammers and Suess (1994) and Rehder et al. (1999). The extracted gas was separated into two 20 ml glass vials, one of the vials was used for methane quantification on board and the other one will be used to determine carbon and hydrogen isotopes of methane onshore.

Methane oxidation rates were measured using radiotracers: A general outline of the radiotracer techniques is given here based on the more specific descriptions in Valentine et al. (2001) and Treude et al. (2003). $^{14}C\text{-}CH_4$ or $^{3}H\text{-}CH_4$ is added to the sample bottles by syringe whereupon displaced water can pass off through an additional needle. The bottles are shaken to equilibrate the tracer with the liquid phase. Then, the sample bottles are incubated for several hours in the

dark near *in-situ* temperatures. At the end of an incubation period, the uptake of CH_4 is either stopped by addition of an inhibitor or, in case of the ^3H-CH_4 tracer, the residual ^3H-CH_4 can be removed by purging with N_2-gas. This leaves the oxidation product (^3H-H_2O) behind. The ^{14}C-CO_2 produced can be recovered by acidifying the sample and trapping the stripped ^{14}C-CO_2 in vials. Label incorporated into cell carbon can be extracted by filtering the acidified and stripped sample. The recovered oxidation products are combined with a scintillation cocktail. The light that is produced from the excitation of the cocktail by the radioactivity of the sample is detected and converted to amplified electrical pulses by a photomultiplier tube. ^3H-CH_4 incubation and measurements were completed on board, but processing of the ^{14}C-CH_4 incubation products will be done in the home laboratory.

Further biogeochemistry analysis: to complement the dissolved methane and methane oxidation studies, samples were collected for shore based analyses of salinity, nutrients (nitrate, silica and phosphate), water ($\delta^{18}O$ and δD) and dissolved inorganic carbon ($\delta^{13}C$) isotopic composition, and a few selected samples were taken for trace element distributions (Tab. 10.1). Samples for nitrate and phosphate were immediately frozen, but a separate aliquot was taken for silica analyses, which was kept at 4°C. Samples for $\delta^{13}C$ were poisoned with $HgCl_2$. Samples for trace metal analyses were filtered through a 0.2 µm and acidified with ultrapure HNO_3.

Collecting further data sets: Salinity, temperature, and oxygen concentrations were measured using sensors of the CTD-unit. Wind and current data recorded on board are available for data correlation.

Silicate isotopes: Samples for silicate isotopes were taken at all CTD stations, except PS81/274 (flare, only bottom area) and PS81/282 (Cumberland Bay east, glacier). Silicate concentrations are expected to be very low in surface waters and the upper parts of the water column, as is typical for nutrients. The volume of water required for silicate isotope analysis is, therefore, greater at shallower depths. Thus 4 L were taken for silicate isotope samples above 500 m depth and 2 L below 500 m. All samples were decanted from the Niskin bottles using silicon-free tubing. The seawater was then filtered through 0.45 µm polycarbonate membrane filter and stored in a new set of 2 L plastic bottles at 4ºC.

Radiocarbon analysis: Water samples were also taken from selected stations and depth for radiocarbon analysis of dissolved organic and inorganic carbon, which will be measured at CologneAMS. These data will be used for the determination of reservoir effects.

Multinet: The multinet (Multinet B) was deployed at the station PS81/277 MN to collect plankton samples from different water depths. Different depth intervals were selected to sample the upper water column: 500 - 300 m, 300 - 200 m, 200 - 100 m, 100 - 50 m, and 50 - 0 m.

The multinet consists of a steel box with 5 net hoses, each with a mesh size of 55 µm. A frame with 5 net beakers (1 liter each) is attached on the lower end of the multinet. In order to collect larger plankton fractions such as zooplankton (radiolarians, foraminifera, dinoflagellates), the net beakers were equipped with 41 µm mesh size gaze.

The multinet was lowered with closed nets down to 500 m water depth at a maximum speed of 0.5 m/s. A board unit allowed for the opening and closing of the nets at selected water depth intervals, according to a pressure sensor installed on the device. Heaving of the device was done with a speed of 0.3 m/s. Since this area is known for its high marine primary productivity, the multinet was heaved 5 times to make sure to collect enough material for silicate isotopes measurement.

Back on board, the remaining plankton in the net hoses was washed into beakers. The plankton and remaining seawater were transferred into 1-liter bottles and stored at -20° C.

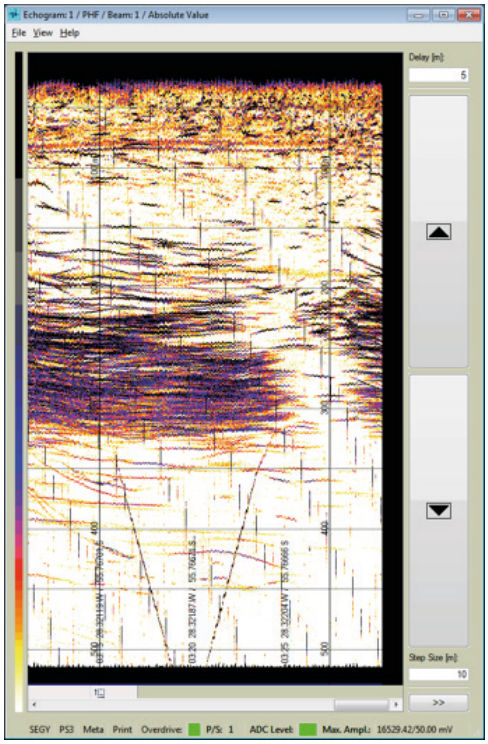

Fig. 10.3: PARASOUND image of the phytoplankton presences between 0-100 m and zooplankton accumulation between 100-300 m water depths at station PS81/277 sampled for silicate isotopes. The gap is due to the heave of the multinet (Screenshot taken during ANT-XXIX/4).

Preliminary results

Based on hydrographic data from Station PS81/257-2, we surmise that modified South Atlantic water with a temperature close to 1°C and a salinity of 34 PSU flows into the Cumberland Bay. Samples collected within the bay (Stations PS81/282-1 and PS81/284-3) clearly show the effect of glacial melt input evidenced as a fresh water lens in the upper 20 to 40 m water depth. A different and distinct water mass is present in the water column from 40 to ~100 meters, whereas the deepest waters in the bay have salinities reaching 34 PSU, likely a signal from the South Atlantic. These preliminary inferences will be further resolved by δ18O tracer data; however it is already apparent that the bay is highly stratified. Based on our CTD cast at Station 257-2, the oxygen content of the incoming South Atlantic water should have an oxygen concentration >6.5 ml/l. However, the deepest waters in the bay at Stations PS81/281-1, 284-3 an 286-1, which targeted distinct flares in the water column, show a distinct decrease in oxygen content below ~ 200

m, reaching values of 5 ml/l, which we attribute to *in-situ* aerobic oxidation of methane. No such low oxygen values were recorded in Station PS81/282-2, where no methane flares were detected and there is no high methane concentration observed in the water column. Methane oxidation rate data, coupled with carbon isotopic analyses, will be used to test this postulate.

Methane concentrations did not reach more than 6 nmol/L at stations near the Sandwich Islands, but elevated concentrations were observed in the Cumberland Bay (Fig. 10.4). Two CTD stations located in the proximity of the flares in the Cumberland Bay show methane concentration reaching up to 25.4 nmol/L at station PS81/281-1 and up to 55.6 nmol/L at station PS81/284-3 near the seafloor. The gas concentrations decrease within the first hundred meters above the seafloor where concentrations reach values of about 5 nmol/L or less (Fig. 10.4).

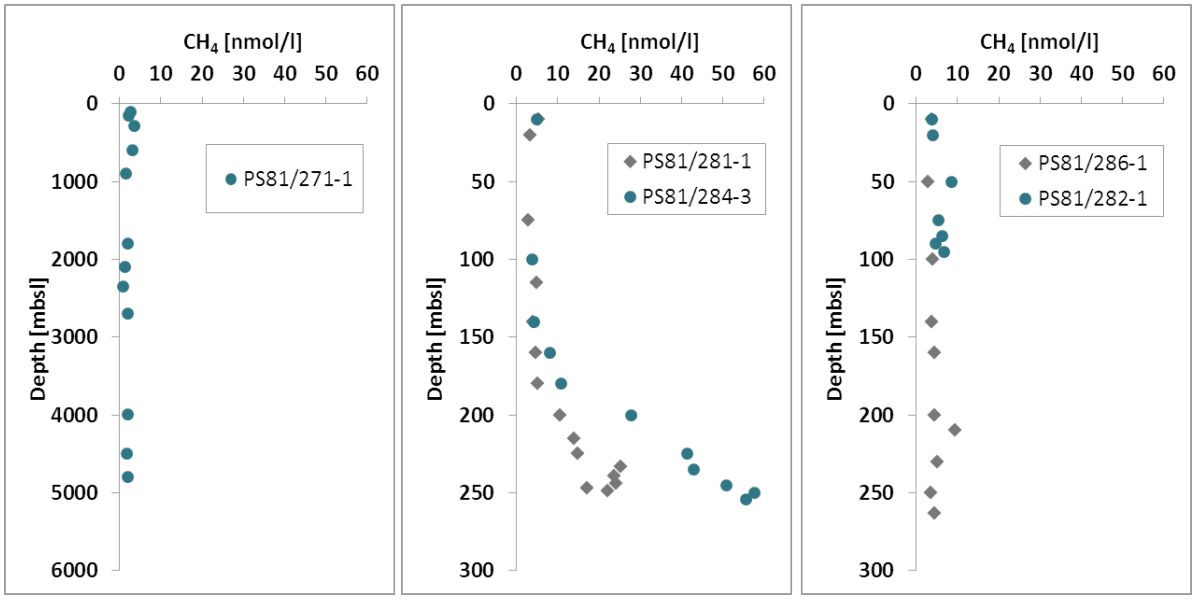

Fig. 10.4: Methane concentrations in the water column

Preliminary results regarding aerobic methane oxidation in the water column indicate that the turnover time of methane was generally very high ranging from 0.8 to 244 years. Even in the Cumberland Bay, where gas flares were observed, the turnover times ranged between 0.8 to 77 years, which is high in comparison to other seep sites offshore California or in the Svalbard area. Turnover times were highest near the seawater-atmosphere interface in the freshwater lens and near the seafloor (Fig. 10.5). However, at the station PS81/284-3 and 281-1 located within the flare field methane turnover times were more rapid than at station PS81/286-1, which is situated further away from methane seepage.

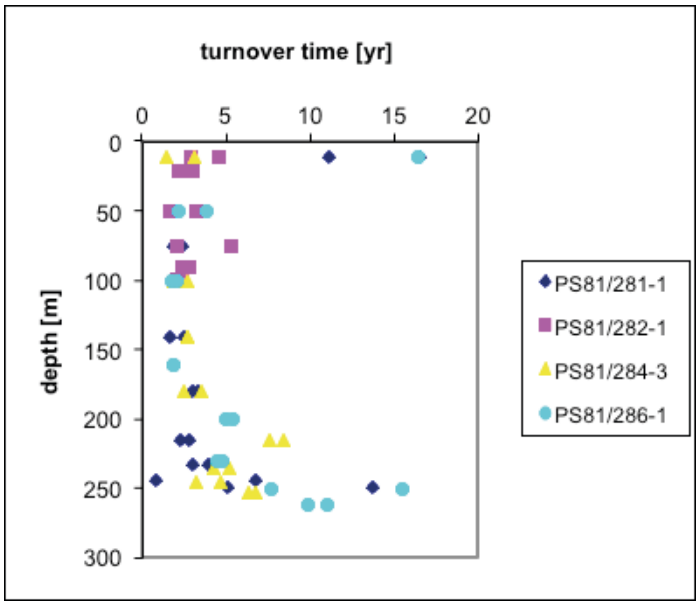

Fig. 10.5: Depth profiles of turnover times of the fours stations sampled in the Cumberland Bay

Data management

The acquired data will be published in peer-reviewed publications. Long-term archiving of the data will be assured through PANGAEA Data Publisher for Earth & Environmental Science at WDC Mare.

References

Lammers, S. and Suess, E., 1994. An improved head-space analysis method for methane in seawater. Mar. Chem., 47: 115-125.

Ramaswamy, V. et al., 2001. Radiative Forcing of Climate Change. In: C. Johnson, A. (Editor), Climate Change 2001: The Scientific Basis, Third Assessment Report of the Intergovernmental Panel on Climate Change. Cambridge University Press, Cambridge, pp. 349-416.

Reeburgh, W.S., 2007. Oceanic Methane Biogeochemistry. Chem. Rev., 107: 486-513.

Rehder, G., Keir, R.S., Suess, E. and Rhein, M., 1999. Methane in the Northern Atlantic controlled by microbial oxidation and atmospheric history. Geophys. Res. Lett., 26(5): 587-590.

Solomon, S. et al., 2007. IPCC Fourth Assessment Report (AR4) Climate Change 2007: The physical Science Basis. Cambridge University Press, Cambridge, United Kingtom, 996 pp.

Treude, T., Boetius, A., Knittel, K., Wallmann, K. and Joergensen, B.B., 2003. Anaerobic oxidation of methane above gas hydrates at Hydrate Ridge, NE Pacific Ocean. Mar. Ecol-Prog. Ser., 264: 1-14.

Valentine, D.L., 2011. Emerging topics in marine methane biogeochemistry. Annual Review of Marine Science(10.1146/annurev-marine-120709-142734).

Valentine, D.L., Blanton, D.C., Reeburgh, W.S. and Kastner, M., 2001. Water column methane oxidation adjacent to an area of active hydrate dissociation, Eel River Basin. Geochim. Cosmochim. Ac., 65(16): 2633-2640.

11. MOLECULAR COMPOSITION OF SEDIMENTARY ORGANIC MATTER AND RADIOCARBON DATING

Janet Rethemeyer[1] [1]Uni Köln
Inna Morgunova[2] [2]VNIIOkeangeologia

Objectives

Lipid biomarkers derived from aquatic and terrestrial organisms are helpful indicators for sedimentary and environmental changes, respectively. Different organic compounds like specific sterols, n-alkanes and n-carboxylic acids can serve as proxies for both sources and the processing of sedimentary organic matter. This methodology will be used to reconstruct changes in the deposition of terrigenous and aquatic organic matter in the Cumberland Bay area, South Georgia. The main aspect of this investigation is to derive source-specific information – complementing the sedimentological data by Wiers and Kuhn et al. (Chapter 7) – for the reconstruction of the deglaciation history of South Georgia. For example an increased proportion of terrigenous biomarkers relative to marine biomass-derived organic compounds into the Cumberland Bay sediments indicates an increase fluvial discharge during periods of rapid ice retreat. Ratios of different biomarkers may give further information on biogeochemical processes and redox conditions in the shallow fjords. The results of the marine sediment cores taken in the East and West Cumberland Bay sampled during this cruise (Table 11.1 and 11.2) will be compared with the sediment records from the Little Jason lagoon, West Cumberland Bay and the Jason and Allen lakes near this area investigated by Melles et al. (Chapter 12).

A further objective of the biomarker analysis is to provide information on the composition of the sedimentary organic matter as source of methane seepage in the Cumberland Bay area. A comparison of geochemical characteristics of sediments near seep sites (PS81/284-1, Grytviken Flare) with background sediments (PS81/259-1, PS81/280-2) both from the East Cumberland Bay can contribute to the determination of the origin of those anomalies. Zones of the active gas discharge are widespread in the global ocean mostly along the edge of continental shelfs and often connected with the fluids from the deep-strata or to the gas-hydrates distribution in the sediment. The comparative study of the collected samples from the South Georgia shelf with the data on the organic matter distribution in sediments obtained from the seep sites and active pockmark areas of the Arctic Ocean seas could provide the better understanding for the biogeochemical processes, gas sources and its migration patterns in different environments.

Sediment chronologies of both the marine and the lake cores taken during this cruise will be constructed based on radiocarbon analyses if possible of both aquatic and terrestrial materials. The aim is to derive information on local reservoir effects and its variability over time, which is rare for southern oceans. These analyses will also involve the dating of individual organic compounds of terrestrial origin if terrestrial macrofossils are absent.

Work at sea

Samples for lipid analysis were taken every 15 - 20 cm from the gravity cores listed in Table 11.1. Near-surface sediments were collected with a multicorer (Table 11.2), which were sampled in 2 cm intervals (Rethemeyer) and in larger intervals in accordance with the lithology of the sediment section (Morgunova). The samples were filled into pre-combusted glass jars or sterile plastic containers and stored and shipped cooled back to Cologne and St.Petersburg.

In the laboratory all sample material will be freeze-dried and will then be extracted with organic solvents to recover total extractable lipids. These will be separated into different compound classes, which will be analyzed by GC-MS. Radiocarbon dating will be performed with the 6 MV Tandetron AMS at the University of Cologne.

Tab. 11.1: Samples from gravity cores taken for lipid and radiocarbon analysis

Station	Instrument	Lat. (S)	Long. (W)	Water depth (m)	Rec. (m)	No of samples
PS81/258-1	GC-1	54°20.210	36°23.280	168	6.72	40 samples
PS81/260-2	GC-4	54°14.780	36°34.980	216	4.45	sampling at AWI
PS81/262-1	GC-7	54°13.490	36°30.710	234	8.79	sampling at AWI
PS81/263-1	GC-8	54°15.660	36°26.350	263	6.16	37 samples
PS81/264-1	GC-9	54°19.370	36°24.050	176	4.25	28 samples
PS81/265-1	GC-10	54°14.160	36°26.590	211	3.75	23 samples
PS81/284-1	GC-16	54°15.910	36°26.230	259	8.38	44 samples

Tab. 11.2: Multicorer samples taken for lipid analysis. All cores were sampled in 2 cm intervals; * these cores were sampled for later analysis in St. Petersburg in intervals different to 2 cm.

Station	Instrument	Lat. (S)	Long. (W)	Water depth (m)	Core length (cm)	No of cores
PS81/258-3	MUC-1	54°20.220	36°23.330	178	13.5, 38.0	2
PS81/259-1	MUC-2	54°15.680	36°26.260	262	13.0, 16.0*	2
PS81/260-1	MUC-3	54°14.800	36°34.930	216	23.5, 24.5	2
PS81/262-2	MUC-4	54°13.520	36°30.760	237	13.5	1
PS81/280-2	MUC-11	54°27.440	35°50.550	237	27.0, 29.0, 29.0*	3
PS81/284-2	MUC-12	54°15.928	36°26.220	269	30*	1

Data management

All results from the organic geochemical and radiocarbon analysis will be stored in in-house databases and will be submitted to PANGAEA Data Publisher for Earth & Environmental Science.

12. LATE QUATERNARY CLIMATIC AND ENVIRONMENTAL HISTORY OF SOUTH GEORGIA

Martin Melles[1], Ole Bennicke[2], [1]Uni Köln
Melanie Leng[3], Benedikt Ritter[1], [2]GEUS
Finn Viehberg[1], [3]BGS
Duanne White[4] [4]Uni Canberra

Objectives

The terrestrial geoscientific fieldwork carried out on the sub-Antarctic island of South Georgia (54 - 55° S, 36 - 38° W) aimed to obtain samples and data to provide a detailed insight into the climatic and environmental history of the island´s Lewin Peninsula (Fig. 12.1) since the Last Glacial Maximum some 20 ka ago. The research follows a multi-disciplinary approach, with investigations of shallow marine and limnic sediment records complimented by geomorphological and contemporary data. A wider picture in particular concerning the glacial history of South Georgia is expected from comparison of our data with those of the marine geophysical and geological results from the fjords and on adjacent shelf areas within the scope of the expedition ANT-XXIX/4 of *Polarstern* as well as with the minimal amount of data available in the literature.

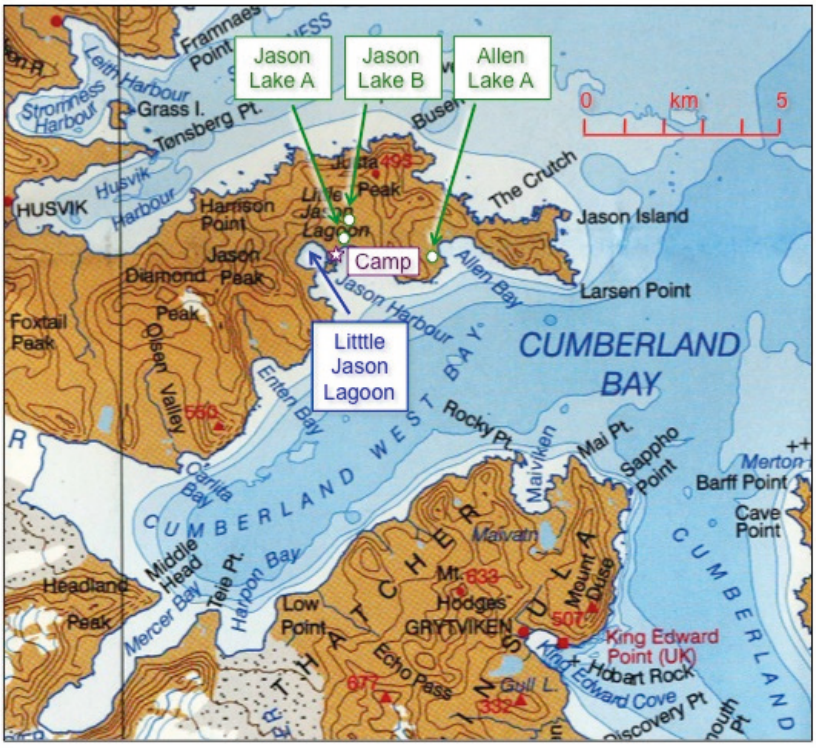

Fig. 12.1: Map of South Georgia´s Lewin Peninsula to the northwest of Cumberland Bay, with the locations of the field camp at Jason Hut (star) as well as Little Jason Lagoon and three unnamed lakes (here informally called Jason Lakes A and B and Allen Lake A), from which sedimentary records were cored (source map: British Antarctic Survey 2004).

Work on land

The fieldwork on South Georgia was carried out between 28 March and 11 April, 2013, from a field camp set up around the Jason Hut (maintained by the British Antarctic Survey) at the southeastern shore of Lewin Peninsula (Fig. 12.2). Transport from/to *Polarstern* and in the coastal waters was using a floatable coring platform (3.6 x 3.0 m) of the University of Cologne and a rubber boat provided by *Polarstern*.

Fig. 12.2: Temporary camp set up at the southeastern shore of Lewin Peninsula (for location see Fig. 12.1, photo: M. Leng)

Coring of Little Jason Lagoon

Little Jason Lagoon is an embayment at the southeastern shore of Lewin Peninsula (Fig. 12.1) and is isolated from Cumberland Bay to the south by a sill of about 0.5 to 1.5 m water depth (depending on tidal water level; Fig. 12.3). The catchment is extensively populated by seals but is also occupied by various sea birds including penguins, petrels and skuas. A bathymetric survey based upon point measurements of water depth employing a hand-held echosounder showed that the embayment is deepest (down to about 24 m water depth) along a SW-NE trending trough crossing the embayment's center (Fig. 12.4).

Sediment coring in Little Jason Lagoon took place from a floatable coring platform with coring equipment produced by the Austrian company UWITEC (www.uwitec.au; Fig. 12.5). Surface sediment samples from site Co1300 off the embayment and at site Co1301 in c. 8 m water depth within the embayment (Co1301; see Fig. 12.4), consist of gravelly sand and organic-rich sands, respectively (Table 12.1). In contrast, all samples taken from below 15 m water depth within the embayment comprise of black sapropel-type sediments (Co1302 to Co1305), in some parts overlain by a thin surface layer of buff coloured, presumably oxic sediments. This suggests that the redox boundary in deeper parts of Little Jason Lagoon today is close to the sediment/water interface.

Fig. 12.3: View from Lewin Peninsula towards south on Cumberland West Bay with Little Jason Lagoon towards the front (photo: D. White)

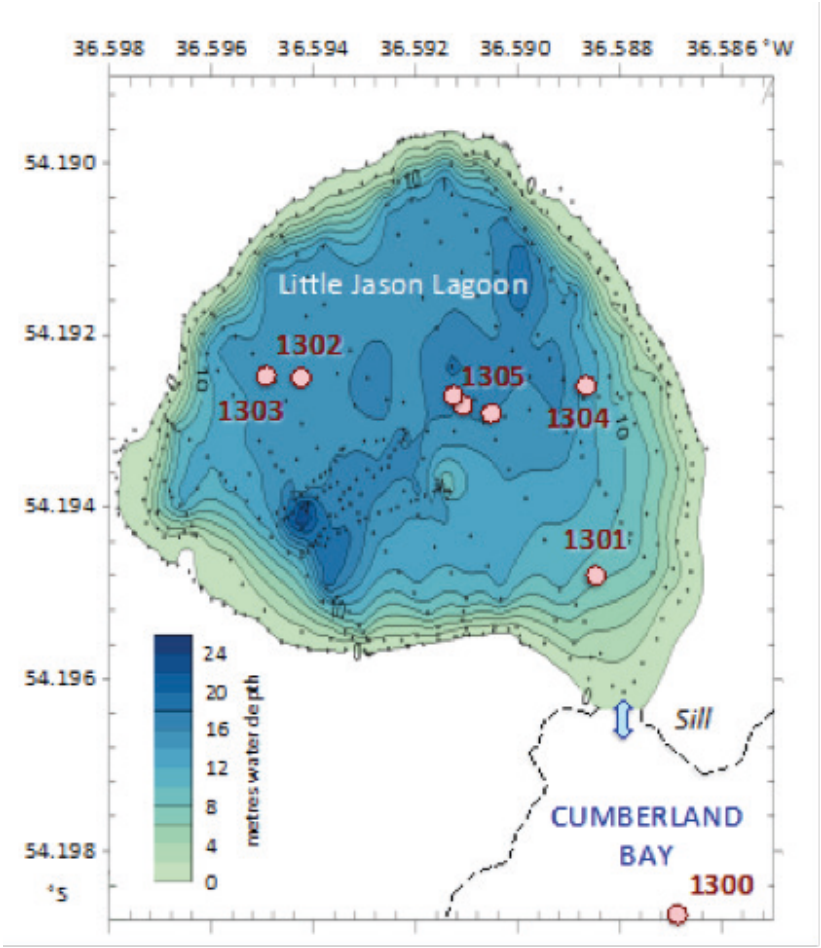

Fig. 12.4: Preliminary bathymetric map of Little Jason Lagoon, based upon point measurements of water depth (small dots), with the locations of sediment cores taken (red circles; for details see sample list in Tab. 12.1)

At site Co1305, the entire embayment sediment record down to its base (i.e. approximately 14.5 m sediment depth) has been recovered by GC (uppermost, water-rich sediments) and percussion piston corer (PC; Table 12.1). The core segments still need to be correlated to a composite record, based upon the core descriptions and variations in sediment proxies. This will take significant work due to differences in water depths over tidal cycles and some problems in the field with the release of the piston in the lowermost cores, however, once achieved it will likely result in a continuous record taking the large number of cores retrieved and minimum overlap between the PCs of 1 m.

Fig. 12.5: Coring at site Co1305 on Little Jason Lagoon (photo: M. Leng)

The sediment record recovered from the upper cores at site Co1305 comprise sapropels, with minor variations in sediment colour (variations of gray to black). A substantial gravel and sand content at the base of the record is thought to be due to high clastic sediment supply during deglaciation. The sharp transition from clastic to organic sedimentation suggests that anoxic conditions developed soon after deglaciation and persisted throughout the entire postglacial depositional history. Assuming deglaciation and formation of Little Jason Lagoon at the end of the last glacial, as suggested for most fjords of South Georgia (e.g., Clapperton et al. 1989, Bentley et al. 2007, Graham et al. 2008), our sediment record may provide the first complete postglacial palaeoenvironmental record from South Georgia with a temporal resolution that allows reconstruction of decadal/centennial events, which is essential if the climate is impacted by El Nino Southern Oscillation (a weather phenomena that is known to have impacted the western Antarctic Peninsula, Pike et al. 2013).

The investigations of the record Co1305 from Little Jason Lagoon shall focus on the dating of the deglaciation (minimum ages from radiocarbon dating of the basal sediments in the core composite; collaboration with J. Rethemeyer, Univ. Cologne), changes in relative sea level (e.g., reconstruction of salinity via diatoms, changes in the relative amounts of different types of organic matter entering the embayment), changes in plant and animal populations (e.g., quantification of seal hair, following Hodgson et al. 1998; arrival of pioneer and non native plants), and changes in climate (e.g., diatom oxygen isotopes from the lake sediments).

Tab. 12.1: Sediment cores recovered from Little Jason Lagoon and fresh-water lakes of Lewin Peninsula (GC = gravity corer, PC = piston corer, RC = Russian peat corer).

Station	Run	Gear	Date	Location	Latitude S	Longitute W	Water Depth (m)	Sediment Depth (cm)	Core Length (cm)	Storage	Description	Remarks
1300	-1	GC	March 30, 2013	Cumberland Bay W	54°11.924′	36°35.213′	21.0	0-4	4	bag	gravelly sand	off lagoon
1301	-1	GC	March 30, 2013	Little Jason Lagoon	54°11.687′	36°35.310′	7.8	0-16	16	liner	algae with sand	
1302	-1	GC	March 30, 2013	Little Jason Lagoon	54°11.550′	36°35.658′	15.8	0-38	38	liner	black sapropel	
1303	-1	GC	March 30, 2013	Little Jason Lagoon	54°11.548′	36°35.698′	15.7	0-30	30	liner	black sapropel	
1304	-1	GC	March 30, 2013	Little Jason Lagoon	54°11.555′	36°35.321′	15.8	0-26	26	liner	black sapropel	
1305	-1	GC	March 31, 2013	Little Jason Lagoon	54°11.575′	36°35.434′	15.7	0-17	17	liner	black sapropel after 1 cm	
1305	-2	GC	March 31, 2013	Little Jason Lagoon	54°11.575′	36°35.434′	15.7	0-18	18	liner	black sapropel after 1 cm	
1305	-3	GC	March 31, 2013	Little Jason Lagoon	54°11.575′	36°35.434′	15.7	0-2	2	glas	sapropel	for 14C/biomarker
1305	-4	GC	March 31, 2013	Little Jason Lagoon	54°11.575′	36°35.434′	15.7	0-2	2	bag	sapropel	for ostracods
1305	-5	GC	March 31, 2013	Little Jason Lagoon	54°11.575′	36°35.434′	15.7	0-20	20	liner	black sapropel	
1305	-6	PC	March 31, 2013	Little Jason Lagoon	54°11.575′	36°35.434′	15.7	0-210	210	liner	black sapropel	
1305	-7	PC	March 31, 2013	Little Jason Lagoon	54°11.575′	36°35.434′	15.7	0-240	240	liner	black sapropel	position/depth doubtful
1305	-8	GC	April 1, 2013	Little Jason Lagoon	54°11.568′	36°35.469′	19.6	0-35	35	liner	black sapropel	
1305	-9	PC	April 1, 2013	Little Jason Lagoon	54°11.568′	36°35.469′	19.6	0-222	222	liner	black sapropel	
1305	-10	PC	April 1, 2013	Little Jason Lagoon	54°11.568′	36°35.469′	19.6	134-456	322	liner	gray sapropel	
1305	-11	PC	April 1, 2013	Little Jason Lagoon	54°11.568′	36°35.469′	19.6	334-619	285	liner	gray sapropel	
1305	-12	PC	April 2, 2013	Little Jason Lagoon	54°11.562′	36°35.479′	19.6	534-628	294	liner	gray sapropel	
1305	-13	PC	April 2, 2013	Little Jason Lagoon	54°11.562′	36°35.479′	19.6	734-1030	296	liner	black sapropel	
1305	-14	PC	April 3, 2013	Little Jason Lagoon	54°11.563′	36°35.477′	19.1	934-1230	296	liner	gray above black sapropel	
1305	-15	PC	April 4, 2013	Little Jason Lagoon	54°11.562′	36°35.477′	19.1	1134-1424	290	liner	sapropel with gravel at base	piston problem (~1.8 m)
1305	-16	PC	April 4, 2013	Little Jason Lagoon	54°11.562′	36°35.477′	19.1	1134-1424	290	liner	sapropel with gravel at base	piston problem (~1.4 m)
1305	-17	PC	April 5, 2013	Little Jason Lagoon	54°11.562′	36°35.477′	19.2	1134-1420	286	liner	sapropel without gravel	piston problem (~0.8 m)
1305	-18	PC	April 6, 2013	Little Jason Lagoon	54°11.562′	36°35.477′	19.2	1034-1323	289	liner	sapropel without gravel	piston problem (~2.1 m)
1306	-1	GC	April 8, 2013	Jason Lake A	54°11.310′	36°34.717′	1.2	0-3	3	bag	organic mud	for ostracods
1306	-2	GC	April 8, 2013	Jason Lake A	54°11.310′	36°34.717′	1.2	0-26	26	liner	organic mud	
1306	-3	RC	April 8, 2013	Jason Lake A	54°11.310′	36°34.717′	1.2	40-140	100	half liner	organic mud	
1306	-4	RC	April 8, 2013	Jason Lake A	54°11.310′	36°34.717′	1.2	60-160	100	half liner	organic mud	
1306	-5	RC	April 8, 2013	Jason Lake A	54°11.310′	36°34.717′	1.2	20-120	100	half liner	organic mud	
1307	-1	GC	April 8, 2013	Jason Lake B	54°10.991′	36°34.832′	3.0	0-18	18	liner	organic mud	
1307	-2	GC	April 8, 2013	Jason Lake B	54°10.991′	36°34.832′	3.0	0-24	24	liner	organic mud	
1307	-3	RC	April 8, 2013	Jason Lake B	54°10.991′	36°34.832′	3.0	10-38	28	half liner	laminated clay	proglacial sediment
1308	-1	GC	April 9, 2013	Allen Lake A	54°11.520′	36°32.685′	1.1	0-19	19	liner	organic mud	
1308	-2	RC	April 9, 2013	Allen Lake A	54°11.520′	36°32.685′	1.1	67-167	100	half liner	organic mud	
1308	-3	RC	April 9, 2013	Allen Lake A	54°11.520′	36°32.685′	1.1	10-110	100	half liner	organic mud	
1308	-4	RC	April 9, 2013	Allen Lake A	54°11.520′	36°32.685′	1.1	116-216	100	half liner	organic mud	
1308	-5	RC	April 9, 2013	Allen Lake A	54°11.520′	36°32.685′	1.1	151-251	100	half liner	organic mud	

Coring of fresh-water lakes

Sediment coring of fresh-water lakes intended to retrieve sediment to provide complementary information on the deglaciation history (e.g., from radiocarbon dating of oldest postglacial deposits, Rosqvist and Schuber 2003) and on times of higher relative sea level (from marine/brackish stages to be identified for instance via diatom assemblages). Of particular importance are the lake sediment records for the reconstruction of the vegetation history (e.g., from pollen and spores), which can provide important information on the climate development on South Georgia (e.g., Birnie 1990), in particular if combined with other palaeoclimate proxies (Van der Putten et al. 2012). It may also be possible to understand climate change from the geochemistry of authigenic components in the sediments (e.g., diatom and or ostracod oxygen isotopes).

Coring of the lake sediments was undertaken using GC and the Russian peat corer (RC) from a small floating platform provided by the Geological Survey of Denmark (Fig. 12.6). This coring equipment and platform was sufficiently light to be carried to the lakes overland.

Fig. 12.6: Small platform used for the coring of fresh-water lakes, here with a gravity core retrieved on Jason Lake A

Coring was conducted in three lakes on Lewin Peninsula, located in the Jason and Allen Valleys (Fig. 12.1, Table 12.1). Jason Lake A is a shallow (up to 1.2 m water depth) lake with a sill presently at 2 m above the modern high tide mark. The lake is isolated from Cumberland West Bay by beach ridges today covered by peats occupied by tussock grass (Fig. 12.7). GC and RC coring resulted in a ca. 1.6 m thick sediment record that comprise organic-rich muds. The sediments postdate

the deglaciation and do not contain any marine muds. Hence, the record may be predominantly of value for the reconstruction of the coastal vegetation history during the past millennia.

Fig. 12.7: View from the east on Jason Lake A, showing Cumberland Bay West with the camp on the left and Little Jason Lagoon in the background (photo: F. Viehberg)

Jason Lake B, a lake of less than 100 m diameter (Fig. 12.8), is located a few hundred meters to the north of Jason Lake A in Jason Valley. It is situated at around 100 m higher altitude, beyond the settlement area of seals. This may explain the rather thin sediment succession cored in the central lake part at ca. 3 m water depth. The record comprises 0.2 m of organic-rich sediments above ca. 0.2 m of laminated clays. The latter were probably deposited during the time of deglaciation, when glaciers still existed in the catchment of Jason Lake B. The record due to its restricted thickness is of limited value for the reconstruction of the deglacial history, however, it may provide important information on the time of deglaciation and on the annual climate variability during this period.

Fig. 12.8: View towards the southwest on Jason Lake B, with Cumberland West Bay being visible in the background (photo F. Viehberg)

The longest lake sediment record (2.5 m) was recovered from Allen Lake A. This lake is located at a 24 m above sea level in Allen Valley, in an area heavily populated by seals. The record consists of organic-rich muds throughout. It thus has potential to provide information on the environmental development of Allen Valley during most of the time since deglaciation with a particularly good time resolution.

Fig. 12.9: View of Allen Lake A from the northwest, with the small coring platform in the lake center and Allen Bay of Cumberland Bay in the background (photo: D. White)

Geomorphology

Geomorphic mapping and sampling were conducted to compile a history of glacier and ice sheet fluctuations, and also to provide the geomorphic and landscape context for the interpretation of the lake and marine sediment core data. The field program aimed to map out moraine sequences and construct a relative age history, whilst also taking samples for absolute dating. Special emphasis was placed on determining if the outer peninsulas had been overrun by a major ice sheet, and if so, the timing and magnitude of such ice expansion.

Geomorphic mapping

Geomorphic mapping was conducted through foot and small boat based field traverses, focussed mainly on the valleys surrounding Jason Bay (Fig. 12.10). The mapped region was surveyed at a traverse spacing of approximately 0.5 km. Steep and difficult terrain hampered access to the higher parts of the landscape, but peaks to 570 m above sea level were investigated.

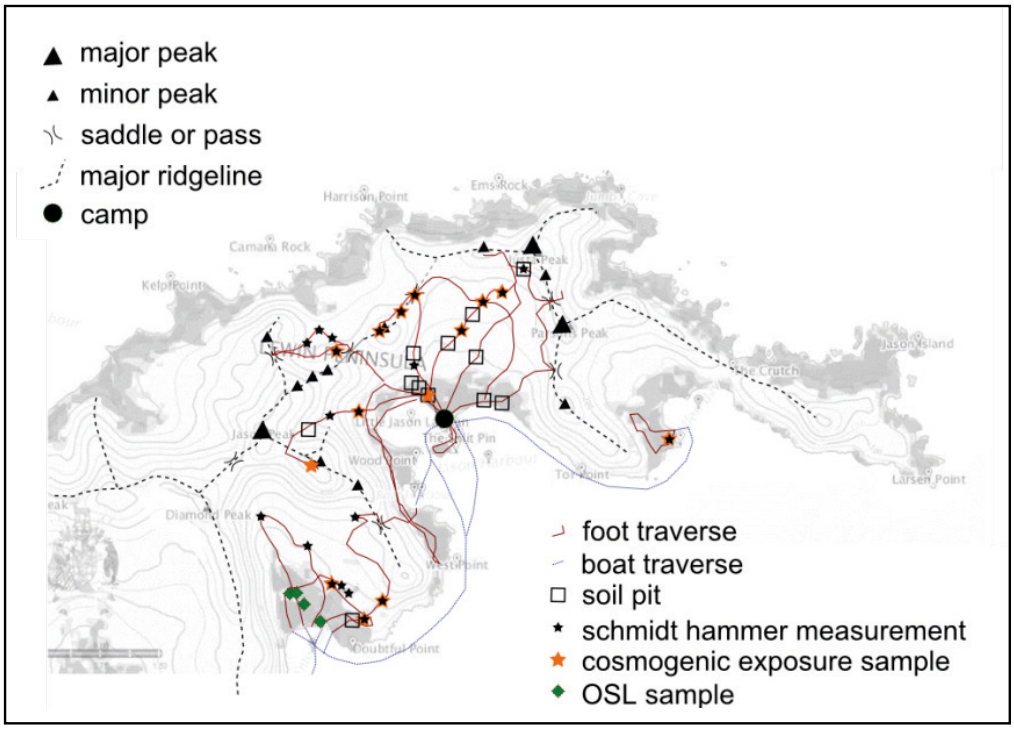

Fig. 12.10: Sketch map of geomorphic surveys and sampling conducted on Lewin Peninsula

Relative age histories were compiled largely through geomorphic cross-cutting and position relationships and rock hardness measurements using a Schmidt Hammer (e.g., White et al. 2009). Previous work had emphasised the utility of soil development (e.g., Clapperton et al. 1989, Bentley et al. 2007) and lichenometry (Roberts et al. 2010) as indicators of moraine age, but reconnaissance surveys indicated that these were not directly applicable in the context of the present study. Lichens were either not present (youngest moraines) or had reached full size (oldest 3 moraine sets). Soil development was strongly affected by altitude or geomorphic position, limiting its effectiveness as a comparator across sites.

Twenty-seven subglacially rounded and striated cobbles or boulders were collected for cosmogenic exposure dating from the three oldest moraine sets identified (Table 12.2). The youngest, by correlation with the relative age criteria presented by Clapperton et al. (1989), was deposited in the past few hundred years and thus too young to accurately date using cosmogenic exposure dating. Bedrock samples were also collected at five sites. Geomorphic observations and Schmidt hammer results indicated that most moraines above c. 100 m altitude were geomorphically unstable and thus samples on these features were unlikely to produce an accurate age of ice retreat. Thus, subglacial cobbles and boulders sited on stable bedrock sites were preferentially collected in the upland areas (Fig. 12.11, Table 12.2). Exposed bedrock was rare at lower altitudes, so samples were collected from moraine crests where solifluction lobes were absent, and that had been colonised and thus stabilised by vegetation.

Tab. 12.2: List of samples taken during the geomorphological field work on South Georgia

Site ID	Collection time	Latitude (° S)	Longitude (° W)	Altitude (m)	Cosmo erratics	Cosmo bedrock	OSL	Sedi-ment
9	29/03/2013 16:07	54.18027	36.59139	292		1		
10	29/03/2013 16:48	54.17783	36.58939	229		1		
11	29/03/2013 17:37	54.17830	36.58216	165		1		
32	30/03/2013 12:31	54.18573	36.56876	126				1
34	30/03/2013 13:54	54.18145	36.57731	145	1	1		
35	30/03/2013 15:12	54.18364	36.57396	147	1			
36	30/03/2013 16:20	54.18158	36.58146	149	1			
38	31/03/2013 14:03	54.17263	36.57605	378	1			
51	1/04/2013 15:07	54.21552	36.59677	107	1			
52	1/04/2013 15:49	54.21593	36.59656	101	1			
53	1/04/2013 16:19	54.21376	36.59541	117	1			
54	1/04/2013 16:29	54.21372	36.59547	121	1			
62	2/04/2013 12:41	54.18929	36.58924	19	2			5
63	2/04/2013 15:22	54.18782	36.59186	57				4
64	2/04/2013 15:58	54.18715	36.59263	76				3
72	3/04/2013 15:01	54.18565	36.60632	282	1			
73	3/04/2013 15:34	54.18485	36.60601	272	1			
74	3/04/2013 16:08	54.18493	36.60583	280	1			
75	3/04/2013 16:08	54.18483	36.60567	279		1		
80	4/04/2013 11:56	54.21346	36.61509	15			2	3

Site ID	Collection time	Latitude (° S)	Longitude (° W)	Altitude (m)	Cosmo erratics	Cosmo bedrock	OSL	Sedi-ment
81	4/04/2013 14:55	54.21344	36.61454	6			1	
95	4/04/2013 17:30	54.21713	36.60054	64	1			
96	4/04/2013 17:59	54.21745	36.60069	62	1			
100	5/04/2013 12:49	54.19130	36.60043	112	1			
101	5/04/2013 13:35	54.19147	36.60204	122	1			
102	5/04/2013 13:36	54.19141	36.60223	122	1			
118	7/04/2013 13:11	54.22692	36.73095	14	4			1
119	7/04/2013 15:07	54.21322	36.60881	42	1			
120	7/04/2013 16:00	54.21338	36.60877	45	1			
121	7/04/2013 16:00	54.21340	36.60867	45	1			
131	7/04/2013 18:01	54.21609	36.61096	0			1	
136	7/04/2013 18:49	54.21497	36.61339	-2			1	
238	9/04/2013 16:22	54.19446	36.54399	44	1			
239	9/04/2013 16:55	54.19446	36.54393	41	1			
240	9/04/2013 16:55	54.19447	36.54393	41	1			

Fig. 12.11: Subglacial cobbles resting on bedrock at cosmogenic sample site 073 (photo: O. Bennike)

Raised shorelines in Enten Valley and Jason Valley (Figs. 12.1, 12.12, and 12.13) were also surveyed and sampled for optically stimulated luminescence (OSL; Table 12.2). Surveying was conducted using a measuring tape and clinometer. The raised beaches themselves were the primary targets, but the high-energy (shingle-dominated) nature of the beaches, and quartz-poor lithologies on South Georgia prevented direct dating of these features. Thus, OSL sampled beach dunes directly behind raised beaches were collected as an indicator of maximum sea levels at these sites (Fig. 12.14).

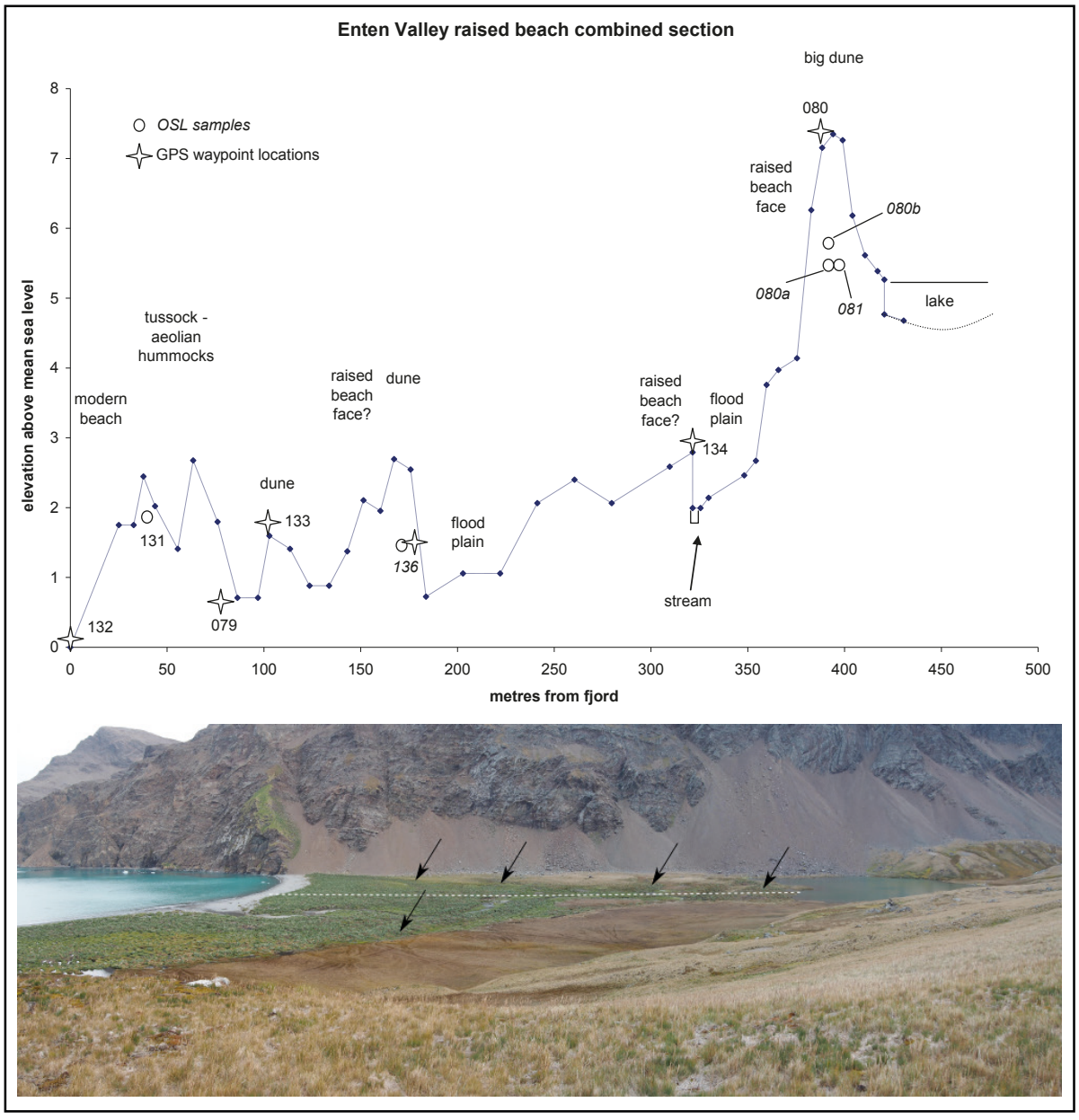

Fig. 12.12: Tape and clino survey (dotted line) across the raised beaches (arrowed in photo) in lower Enten Valley (photo: D. White)

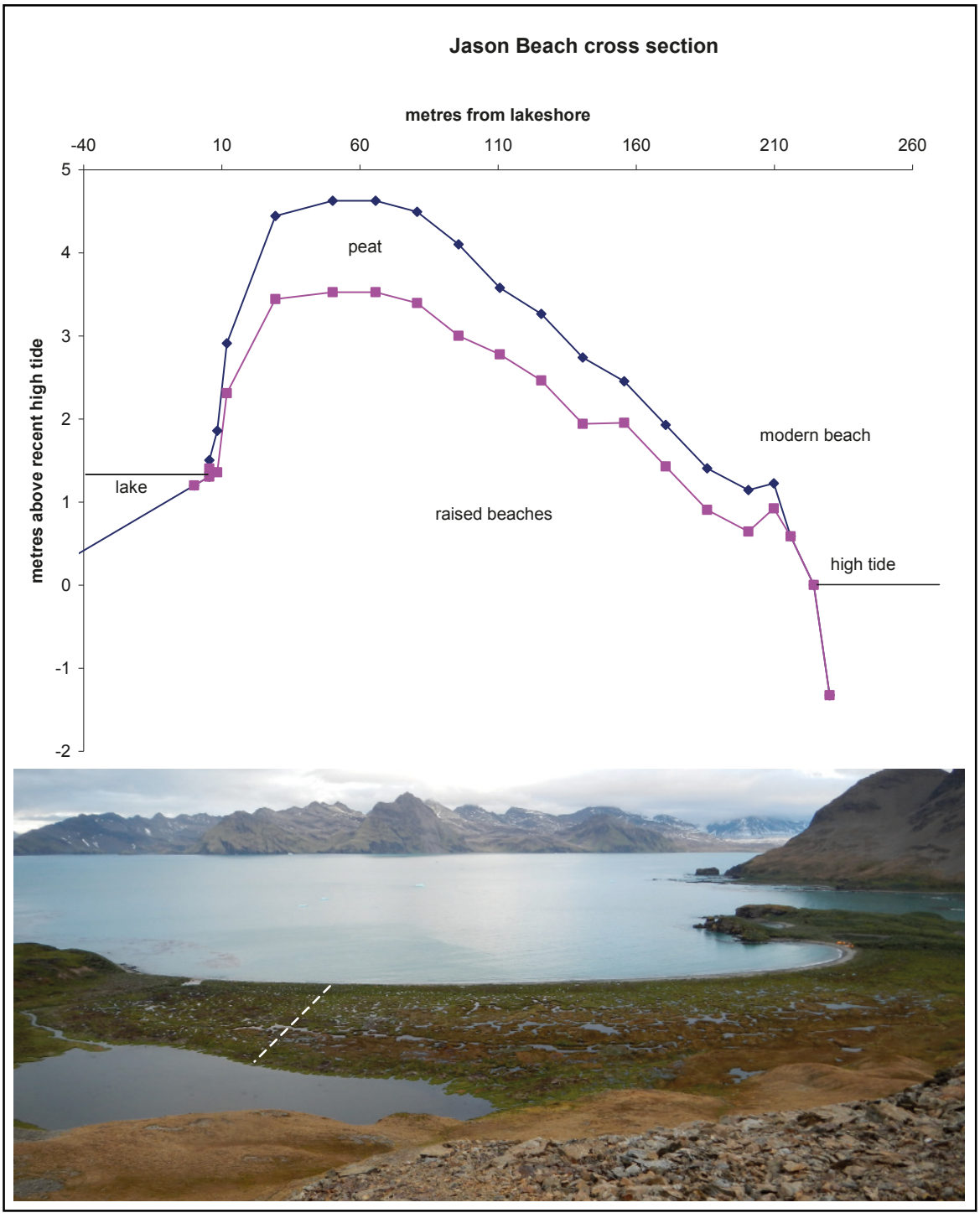

Fig. 12.13: Tape and clino survey (dotted line) across the raised beaches at Jason Valley. Dotted line describes position of survey (photo: D. White)

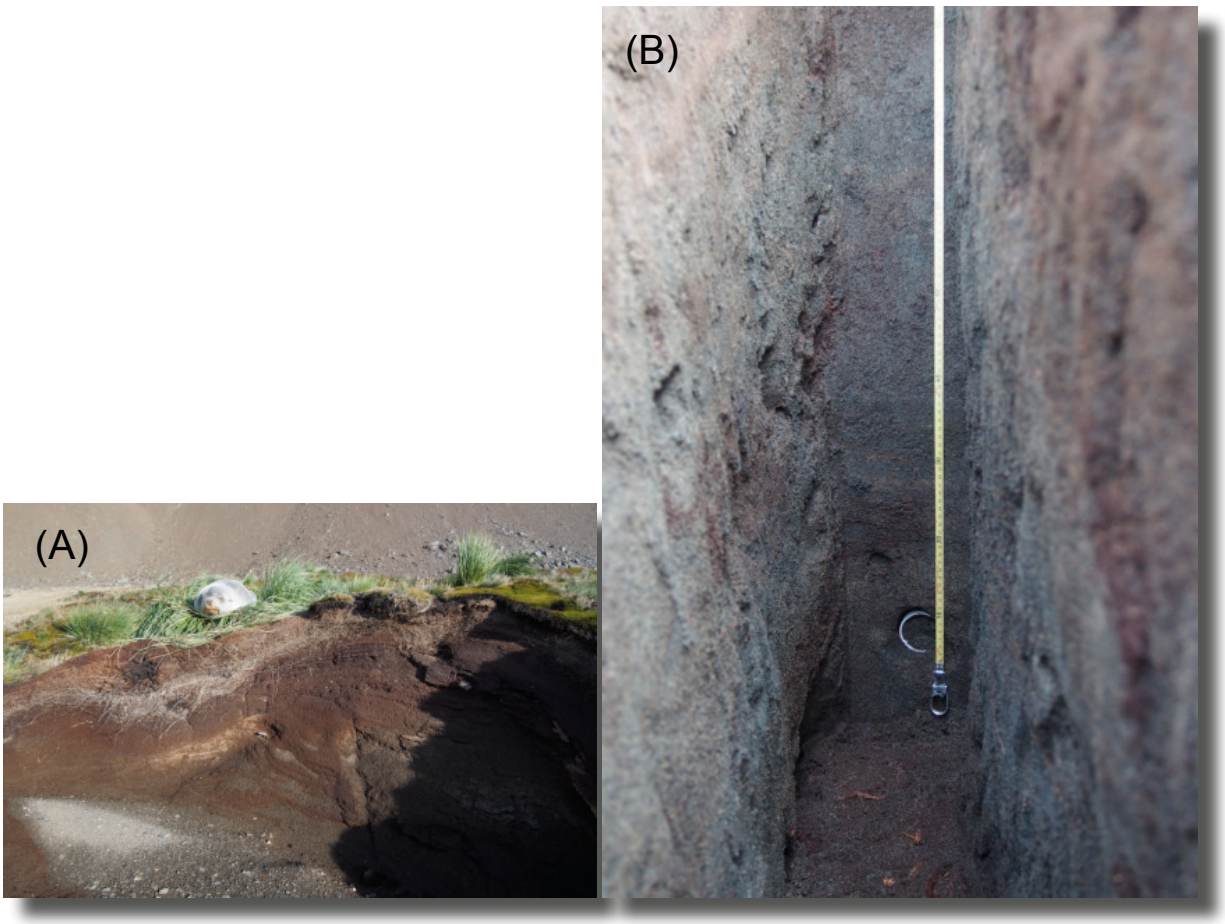

Fig. 12.14: Sample site 080, showing (A) the upper section of the large dune in Enten Valley, with cross bedding dipping right, away from the modern ocean. (B) shows location of OSL sample 080a in trench through grey, un-oxidised dune sands two metres directly below the fur seal in (A) (photo: D. White).

Preliminary results

Moraines and other glacial deposits from four major periods of deposition were discovered and mapped in the study area (Fig. 12.15).

The youngest, least weathered deposits, correlating to the stage 5 (12-19th Century) deposits described by Clapperton et al. (1989) were found only in the high cirques above 300 m above sea level. Soils on these moraines were slightly oxidised, but no horizonsation had developed. Some reduction in rock hardness had occurred compared to fresh debris (Table 12.3).

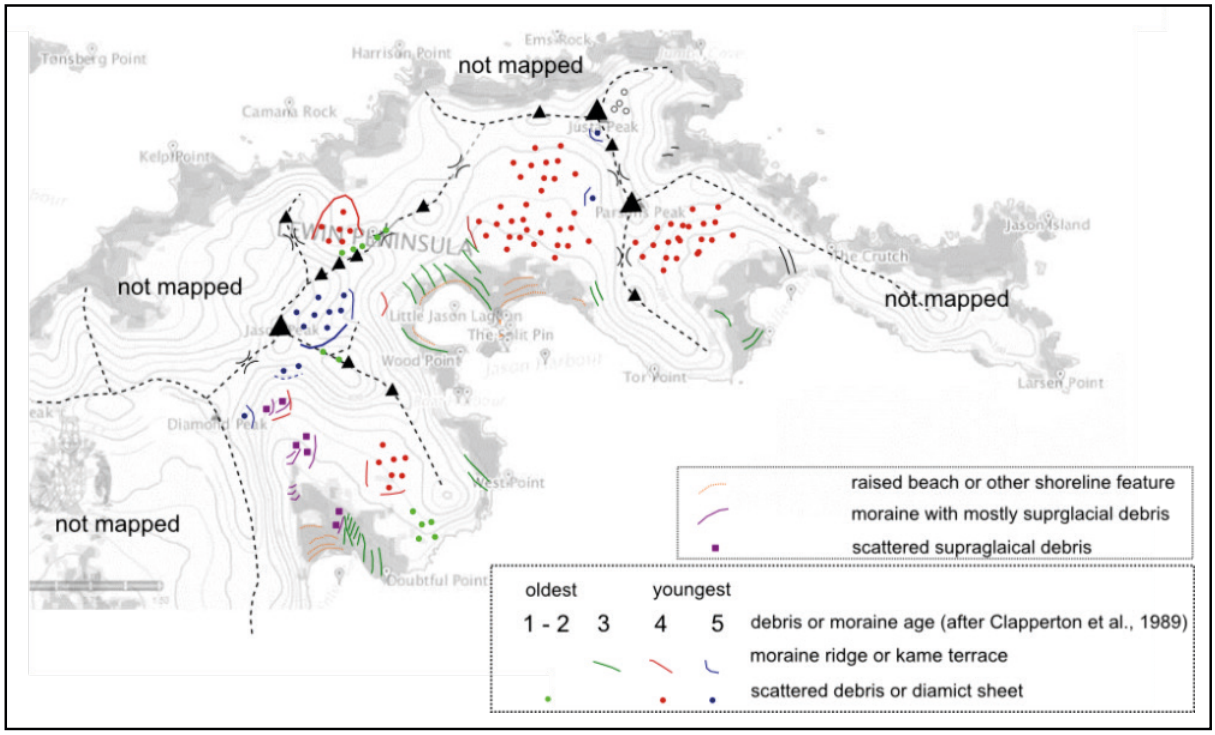

Fig. 12.15: Sketch map of glacial limits and raised shoreline locations on outer Lewin Peninsula

Tab. 12.3: Schmidt Hammer rebounds for subglacial boulders on stable sites on Lewis Peninsula, grouped by moraine set based on characteristics from Clapperton et al. (1989). Fresh erratics were collected from debris approximately 100 m in front of Neumayer Glacier. The right-hand column refers to the number of sites studied, at each of which 30 boulders were measured.

Moraine set	Mean	n
Fresh	56.8	1
5	51.2	3
4	34.4	9
3	29.3	6
1 -2	26.9	3

The second youngest deposits, correlating to stage 4 (Neoglacial) deposits from Clapperton et al. (1989), were found in each valley. The altitude of the lowest moraine varied with valley, ranging from ~30 m in eastern Jason Bay, to 100 m in the small valley directly north of Little Jason Lagoon. Some soil development had occurred, with a distinct oxidised horizon present to ~10 cm in areas above significant vegetation colonisation. Subglacial cobbles in stable sites had moderate strength reduction, with Schmidt Hammer rebounds ranging from 32-37 (Table 12.3). Contrarily, moraine crests were much less stable, returning Schmidt Hammer rebounds of ~45.

The third youngest deposits (correlating with stage 3 [Lateglacial] from Clapperton et al. 1989) reflect an event where valley glaciers had expanded down to at least modern sea level. Moraines were found on the outlet of each of the major valleys. Relative age measurements for this unit were complicated due to the presence of significant vegetation, but Schmidt Hammer rebounds were substantially lower than those from the earlier stages.

The last, oldest stage was only represented by strongly weathered debris that were rare, but found at most stable sites outside the limits of the subsequent glacial expansions described above. This included the summit of the peak (at 570 m) between Enten and Jason Valleys. No distinct moraines from this event were preserved.

Raised shorelines were found in most major valleys, but only at relatively low altitudes (Fig. 12.15). Distinct raised beach deposits were found at 3 and 4 m above modern sea level at Jason and Enten Valleys respectively. Bevelled platforms previously interpreted as raised marine terraces (e.g. Bentley et al., 2007) surrounded Little Jason Lagoon, but no distinct marine or shoreline sediments were preserved on the summits of these features, so they could not be conferred a distinct marine origin.

Contemporary sampling

We undertook a survey to look at the current types of land and aquatic plants and soils (especially the fine grained glacial moraine sediment) to define geochemical 'end-member' values (carbon isotopes, compound specific, and radiocarbon signatures) (Table 12.4A) of components that could have entered the lagoon and lakes in the past. There are broad plant zones with increasing altitude from large tussock grass at sea level to tiny mosses and bryophytes on the high slopes. The mosses and bryophytes are so called pioneer plant types as they prefer thin soils and rocky landscapes, and can endure harsh, high altitude weather conditions. Looking for signals about how the proportions of the various plant communities have changed through time will tell us about how the landscape has changed under changing climates. We assume that immediately after the glaciers retreated the pioneer plant communities would soon have developed, but with warmer and wetter conditions other species would have arrived, and the pioneers would migrate to the steeper slopes. Since evidence for actual plants in the sediments maybe restricted to a few seeds, pollen grains and plant fragments we will also be looking for climate signals in the modern plants mainly in the form of their carbon isotope and compound specific signatures. If these compounds are preserved in the tiny fragments of plant material we can extract from the core sediments then we may be able to identify the dominant sources of organic material into the lake and hence environmental change. The contemporary plants will also be investigated for their modern radiocarbon values, this is especially important for obtaining good chronological control on the lagoon and lake sediments. This is potentially a

significant issue for the aquatic plant remains preserved in the sediments as aquatic plants can use carbon from a variety of sources and incorporate 'old' carbon from dissolution of the inorganic carbon components in the rocks.

We have also collected water samples (rain, ponds, lakes, lagoon, marine) for oxygen, hydrogen and carbon isotope ratios (Table 12.4B). These data will define the hydrological state of the various water bodies from which the cores were taken. If we can extract for example oxygen isotopes from tiny shells in the sediments then we have the possibility of investigating changes in hydrology. In the lagoon this will most likely be a function of the varying proportions of marine to freshwater which will be a function of sea level, temperature and wetness of the climate through time. In the lakes the oxygen isotope variations will most likely be a function of the amount of rainfall.

Tab. 12.4: The contemporary (A) vegetation and rock samples and (B) water samples used to define modern 'end member' values for the geochemical signatures of the organic matter and waters in the lagoon and lakes

(A) Organic and Rock samples	Locality description	$^{13}C/^{12}C$ (BGS)	^{14}C, compound Spec. (Cologne)
LJL-1v	mixed moss + soil, E lagoon	Y	Y
LJL-2v	meadow grass + soil, E lagoon	Y	Y
LJL-3v	tufted fescue + soil	Y	Y
LJL-4V	mixed moss + soil, E lagoon on moraines	Y	Y
LJL-5a	seal excrement	-	Y
LJL6-v	mixed sea weed from E lagoon margin	Y	Y
LJL7-a	bryozoans & shells on sea weed, E lagoon shore	Y	Y
LJL8-a	seal bones and teeth		Y
LJL9-v	tussock grass + soil from E lagoon by hut	Y	Y
LJL10-r	moraine from E lagoon, carbonate?		Y
LJL11-r	moraine from E lagoon, carbonate?	Y	Y
LJL12-p	peat from on top of moraine at 1m depth (old)	Y	Y
LJL13-v	highest altitude veg + soil, fellfield? E lagoon	Y	Y
LJL14-v	small mosses on scree at high altitude	Y	Y
LJL15-r	modern scree matrix, carbonate?	Y	Y
LJL16-v	marine macroalgae from low tide level	Y	Y
LJL-17v	modern kelp weed from marine	Y	Y
1308-1 (Allan Lake A)	catchment veg 1	-	Y
1308-1 (Allan Lake A)	catchment veg 2	-	Y
1308-1 (Allan Lake A)	lake surface sediment	-	Y
1308-1 (Allan Lake A)	peat	-	Y

(B) Water samples	Locality description	O, H, C isotopes (BGS)	^{14}C (Cologne)
LJ1	outside lip of lagoon, marine water with icebergs	Y	-
LJ1(a)	ice berg	Y	-
LJ2	inside lagoon sill	Y	-
LJ3	lagoonal surface water	Y	Y
LJ4a	lagoonal bottom water samples from gravity corer	Y	-
LJ4b	lagoonal surface water	Y	-
LJ5	inflow to lagoon, streams to N	Y	Y
LJ6	inflow to lagoon, streams to N	Y	Y
LJ8	marine water from Jason Harbour	Y	Y
SL-1	small lake water to east of lagoon	Y	Y
LE	Lake Enten (duck)	Y	-
rain1	6.4.13 Northerly	Y	-
rain2	6.4.13 Northerly	Y	-
rain3	6.4.13 Northerly	Y	-
rain4	6.4.13 Northerly	Y	-
rain5	6.4.13-7.4.13 overnight rain	Y	-
ice	Neumayer glacier ice	Y	-
lake	Allan Bay lake 9.4.13	Y	-
ice	Glacial ice	Y	-

Data management

All metadata relating to sample sites will be stored in the database PANGAEA Data Publisher for Earth & Environmental Science (www.pangaea.de) on short notice. These data sets will be complemented by the analytical data obtained on the sample material, latest when they are published. The majority of field samples will be stored at the University of Cologne; some of the samples and in most cases sample aliqouts will be distributed to the institutions participating in our South Georgia project.

References

Bentley, M.J., Evans, D.J.A., Fogwill, C.J., Hansom, J.D., Sugden, D.E., Kubik, P.W. (2007): Glacial geomorphology and chronology of deglaciation, South Georgia, sub-Antarctic. - Quaternary Science Reviews, 26, 644–677.

Birnie, J. (1990): Holocene environmental change in South Georgia: evidence from lake sediments. - Journal of Quaternary Science, 5, 171-187.

British Antarctic Survey (2004): South Georgia, 1:200 000 scale map. BAS (Misc 12A), Cambridge, British Antarctic Survey.

Clapperton, C.M., Sugden, D.E., Birnie, J., Wilson, M.J. (1989): Late-glacial and Holocene glacier fluctuations and environmental change on South Georgia, Southern Ocean. - Quaternary Research, 31, 210-228.

Graham, A.G.C., Fretwell, P.T., Larter, R.D., Hodgson, D.A., Wilson, C.K., Tate, A.J., Morris, P. (2008): A new bathymetric compilation highlighting extensive paleo–ice sheet drainage on the continental shelf, South Georgia, sub-Antarctica. – Geochemistry, Geophysics, Geosystems, 9, 1-21.

Hodgson, D.A., Johnston, N.M., Caulkett, A.P., Jones, V.J. (1998): Palaeolimnology of Antarctic fur seal *Arctocephalus gazella* populations and implications for Antarctic management. - Biological Conservation, 83, 145-154.

Pike, J., Swann, G.E.A., Leng, M.J., Snelling, A.M. (2013): Glacial discharge along the west Antarctic Peninsula during the Holocene. – Nature Geosciences, 6, 199-202.

Roberts, S.J., Hodgson, D.A., Shelley, S., Royles, J., Griffiths, H.J., Deen, T.J., Thorne, M.A.S. (2010): Establishing lichenometric ages for nineteenth- and twentieth-century glacier fluctuations on South Georgia (South Atlantic). - Geografiska Annaler, 92A, 125-139.

Rosqvist, G.C. and Schuber, P. (2003): Millennial-scale climate changes on South Georgia, Southern Ocean. - Quaternary Research, 59, 470-475.

Van der Putten, N., Verbruggen, C., Björck, S., de Beaulieu, J.-L., Barrow, C.J., Frenot, Y. (2012): Is palynology a credible climate proxy in the Subantarctic? - The Holocene, 22, 1113-1121.

White, D., Bennike, O., Harley, S., Fink, D., Kiernan, K., McConnell, A., Wagner, B. (2009): Geomorphology and glacial history of the Rauer Group, East Antarctica. - Quaternary Research, 72, 80-90.

13. AT-SEA DISTRIBUTION OF SEA BIRDS AND MARINE MAMMALS, REPRESENTATIVES OF THE OCEANS' FOOD CHAINS' HIGHER TROPHIC LEVELS

René-Marie Lafontaine[1], Roseline C. Beudels-Jamar[1], [1]PolE
Gerald Driessens[1], Griet Nijs[1], Henri Robert[1],
(not on board: Claude L. Joiris)

Background and objectives

The main objectives of PolE long-term studies of the quantitative at sea distribution of seabirds and marine mammals in polar marine ecosystems are, on the one hand, to contribute to a better understanding of the mechanisms influencing their distribution (water masses, fronts, pack ice, ice edge and eddies) and, on the other hand, to try and detect spatial and temporal evolutions in these distributions with special attention to possible consequences of global climatic changes. As they constitute the upper trophic levels in the food chain, sea birds and marine mammals distribution reflects prey abundance, zooplankton, krill, nekton and small fish, and is thereby a reflection of the ecology and the biological production of the whole water column. Improved knowledge of their distribution constitute therefore one of the best way to identify and localize areas of high biological productivity, and to detect temporal changes.

Probably most important of all is the need, currently on top of the international agenda of the world conservation community, to develop a coherent and ecologically representative network of marine protected areas (MPA) in the international waters including all seas falling under the jurisdiction of the Antarctic Treaty. Less than 1% of the world's seas are now under any form of protected area designation. The tools necessary to identify the most important areas, and to delineate them, are still debated and largely missing. If the role of seabirds in MPA designation has been widely recognized, using seabird distribution data is still not integrated into MPAs designation process. Furthermore, very few MPAs have been established for seabirds conservation. In order to identify marine biological hotspots, information on seabirds foraging ranges, and at-sea density estimates, such as those collected on board *Polarstern*, will be hard to get, but essential data.

In the Antarctic and Sub-Antarctic regions, biological studies carried out so far focused mainly on the Weddell Sea and the Ross Sea, as well as, to a lesser extent, the Amundsen and Bellingshausen seas. The area covered by this ANT-XXIX/4 *Polarstern* mission is a poorly studied one, in particular for sea birds and marine mammals and therefore deserves particular attention.

Work at sea

Birds and mammals were recorded by transect counts from the bridge, 18 meters above sea level, without width limitation. Animals are detected with naked eye, observations being confirmed and detailed with binocular and/or telescope. Each count lasts 30 minutes with a 120° angle in front of *Polarstern*. Counting was done on a continuous basis during all movements of the ship (transects), visibility conditions allowing. We conducted a total of 730 counts (2 x 365); simultaneous counts were done on each site of the bridge in order to allow comparison between data obtained from different observation platforms. Nine helicopter flights, when weather conditions allowed it, where performed in order to identify whales and other large cetaceans density and distribution. Transects were established along the same route, or on perpendicular axes, as that of the ship.

Preliminary results

During ship transects, a total of 35,700 birds of 40 sea birds species were counted, with a mean number of 52 birds per counting period. The three most common species observed, representing nearly two-third of the total number of individuals, were the Antarctic Prion, *Pachyptila desolata,* with 17,616 individuals counted (46% of the total of birds observed), the Chinstrap Penguin, *Pygoscelis antarctica*, with 4,484 individuals (11.6%) and the White-chinned Petrel, *Procellaria aequinoctialis,* with 2,125 individuals (5.5%).

Important differences in bird species composition and density were noted between the rich South West Atlantic Shelf (FKLD or Patagonian Shelf), the Antarctic convergence zone, the vicinity of South Georgia and the sea over the South Sandwich Trench.

Of particular notice, an important aggregation of marine birds and mammals was noted on 29 March just East of South Georgia, at the edge of the shelf. We observed there a "feeding bonanza" of more than seventeen thousands Antarctic Prions (associated with large numbers of Antarctic Fur Seals and whales). Nearly 88% of all our observations of Antarctic Prions for the whole cruise were made during 4 counting ½ hour periods only, when we approached and travelled through this large aggregation.

As for the marine mammals, 13 different species were identified during our counting from the boat or during successful helicopter flights. Humpback Whale *Megaptera novaeangliae* with 122 individuals was the most commonly observed whale during this leg. One Sperm Whale, *Physeter macrocephalus*, 23 Southern Right-Whales, *Eubalaena australis,* 25 Fin Whales, *Balaenoptera physalus*, 9 Southern Bottle-nosed Whale, *Hyperoodon australis*, 3 Killer Whales, *Orcinus orca*, and 30 Long-finned Pilot Whales, *Globicephala melas*, were also observed. Smaller cetaceans were also seen, included Commerson Dolphin, *Cephalorhynchus commersonii*, in Magellan Channel, two large groups of Southern Right Whale Dolphins, *Lissodelphis peronii,* as well as 2 species of *Lagenorhynchus* dolphins, Dusky and ca 30 Hourglass Dolphins.

South-American Fur Seals, *Arctocephalus australis,* were spotted near the ship on the Patagonian shelf and Antarctic Fur Seals, *Arctocephalus gazelle,* around South Georgia and South Sandwich islands. The latter was very abundant (more than two thousands individuals) at the feeding bonanza described above.

A small number of Elephant Seals, *Mirounga leonina*, was also observed in the water in South Georgia bays, very close to their breeding colonies.

Some interesting behaviour was also noted, in particular the Southern Right-Whales, regularly observed at close proximity of icebergs or very close to the ship when in station. This attraction for large objects has been noted before (Shirihai 2006) but has not been explained. It could be related to search for food resources or shelter.

The aggregation of whales, fur-seals and prions observed just east of the South-Georgia shelf on 29 March could not be relocated two weeks after. Is it a very short term phenomenon or did we pass just at the end of it? Further research will reveal if there are clear correlations with oceanographic and biological parameters, such as water quality parameters, seafloor topography, plankton blooms or krill or fish concentrations. This knowledge can then be used for the mapping of ecologically important or vulnerable areas.

Data management

The main topic in the utilization of results will concern water masses, fronts and eddies. Due to specific calibration of the eco-sounder, detection of water column zooplankton and fish was not possible during this leg. Evaluation of prey abundance was therefore not feasible.

Results will be included in our PolE data base, made accessible to anyone interested in collaboration (crjoiris@gmail.com), and published within the year after the expedition in an international journal.

References

Joiris, C.R. and Dochy, O. (submitted) A major feeding ground for fin whales, southern fulmars and grey-headed albatrosses around the South Shetland Islands, Antarctica. Polar Biol.

Joiris, C.R. (2000) Summer at-sea distribution of seabirds and marine mammals in polar ecosystems: a comparison between the European Arctic seas and the Weddell Sea, Antarctica. J. Mar. Syst. 27: 267-276.

Joiris, C.R., (1991) Spring distribution and ecological role of seabirds and marine mammals in the Weddell Sea, Antarctica. Polar Biol. 11: 415-424

Shirihai, H. (2006). Marine mammals of the World. Collins, London. 384 pp.

A.1 TEILNEHMENDE INSTITUTE / PARTICIPATING INSTITUTIONS

	Address
ATLAS HYDROGRAPHIC	ATLAS ELEKTRONIK GmbH Sebaldsbruecker Heerstr. 235 28309 Bremen Germany
AWI	Stiftung Alfred-Wegener-Institut für Polar- und Meeresforschung in der Helmholtz-Gemeinschaft Postfach 120161 27515 Bremerhaven Germany
BAS/NERC	British Antarctic Survey Natural Environmental Research Council Madingley Road, High Cross Cambridge Cambridgeshire CB3 0ET United Kingdom
BGS/NERC	British Geological Survey Natural Environmental Research Council Nicker Hill Keyworth Nottingham, NG12 5GG United Kingdom
DWD	Deutscher Wetterdienst Geschäftsbereich Wettervorhersage Seeschifffahrtsberatung Bernhard Nocht Str. 76 20359 Hamburg Germany
GEUS	Geological Survey of Denmark and Greenland Øster Voldgade 10 1350 Copenhagen K Denmark
HELISERVICE	HeliService international GmbH Am Luneort 15 27572 Bremerhaven Germany

	Address
IMMH	Internationales Maritimes Museum Hamburg Kaispeicher B Koreastr. 1 20457 Hamburg Germany
MARUM	Zentrum für marine Umweltwissenschaften Universität Bremen Leobener Str., MARUM 28334 Bremen Germany
OSU	Ocean Ecology and Biogeochemistry Oregon State University 104 CEOAS Administration Building Corvallis, OR 97331-5503 USA
PolE	Laboratory for Polar Ecology Rue du Fodia 18 1367 Ramillies Belgium
Uni Bremen	Universität Bremen Bibliothekstr. 1 28359 Bremen Germany
Uni Canberra	Institute for Applied Ecology University of Canberra ACT 2601 Australia
Uni Köln	Institut für Geologie und Mineralogie Universität Köln, Zülpicher Str. 49a 50674 Köln Germany
Uni Leeds	School of Earth and Environment Maths/Earth and Environment Building The University of Leeds Leeds. LS2 9JT United Kingdom

	Address
Visual Drugstore	Visual Drugstore GmbH Gysslingstr. 72 80805 München Germany
VNIIOkeangeologia	All-Russian Research Institute for Geology and Mineral Resources of the World Ocean Angliyskiy av., 1 Saint Petersburg, 190121 Russia

A.2 FAHRTTEILNEHMER / CRUISE PARTICIPANTS

Name/ Last name	Vorname/ First name	Institut/ Institute	Beruf/ Profession
Bennike	Ole	GEUS	Fieldwork, South Georgia
Beudels	Roseline	PolE	Biologist
Bohrmann	Gerhard	MARUM	Chief Scientist
Dickens	William	BAS, NERC	Geologist
Driessens	Gerald	PolE	Biologist
Dziadek	Ricarda	MARUM	Student, geosciences
Ewert*	Jörn	ATLAS	Engineer
Ferreira	Christian	MARUM	Technician, bathymetry
Fischer	David	AWI	Geochemist
Freksa	Christian	Uni Bremen	Computer scientist
Gepraegs	Patrizia	MARUM	PhD Student, chemistry
Glueckselig	Birgit	AWI	Technician, multinet
Graham	Alastair	BAS, NERC	Geologist
Kasten	Sabine	AWI	Geochemist
Kern	Markos	Visual Drugstore	Media/NG, Web-Log
Kirschenmann	Eva	AWI	Student, geochemistry
Kopiske	Eberhard	MARUM	Technician, TV-sled
Kuhn	Gerhard	AWI	Geologist
Lafontaine	René-Marie	PolE	Biologist
Leng	Melanie	BGS, NERC	Fieldwork South Georgia
Lensch	Norbert	AWI	Technician
Linse	Katrin	BAS	Biologist
Little	Crispin	Uni Leeds	Biologist
Loeffler	Benjamin	AWI	Geochemist
Luedke	Britta	AWI	Technician
Marcon	Yann	MARUM	Geologist
Mau	Susan	AWI	Biologist
Meisel	Ove	AWI	Student, geosciences
Melles	Martin	Uni Köln	Fieldwork South Georgia
Miller	Max	DWD	Meteorologist
Morgunova	Inna	VNIIOkeangeologia	CTD
Neuhoff	Holger, von	IMMH	Media/NG, Web-Log
Nijs	Griet	PolE	Biologist
Oelfke	Steffi	MARUM	MSc student, geology
Rethemeyer	Janet	Uni Köln	Geochemist
Ritter	Benedikt	Uni Köln	Fieldwork South Georgia
Robert	Henri	PolE	Biologist

Name/ Last name	Vorname/ First name	Institut/ Institute	Beruf/ Profession
Roberts	Jenny	BAS	Geologist
Roemer	Miriam	MARUM	Geologist
Ronge	Thomas	AWI	Geologist
Sonnabend	Hartmut	DWD	Meteorologist
Stoltmann	Tim	MARUM	Student, geosciences
Torres	Marta	OSU	Geochemist
Viehberg	Finn	Uni Köln	Fieldwork South Georgia
Wei	Jiangong	MARUM	Geologist
White	Duanne	Uni Canberra	Fieldwork South Georgia
Wiers	Steffen	AWI	Student, geology
Wintersteller	Paul	MARUM	Geologist
Wu	Tingting	MARUM	Geophysicist
Lindner	Roland	HeliService	Helipilot
Schwabe	Sascha	HeliService	Helipilot
Möllendorf	Carsten	HeliService	Heli technician

*Jörn Ewert disembarked on March 29 at King Edward Point South Georgia

A.3 SCHIFFSBESATZUNG / SHIP'S CREW

No.	Name	Rank
1	Schwarze, Stefan	Master
2	Grundmann, Uwe	1. Offc.
3	Farysch, Bernd	Ch. Eng.
4	Fallei, Holger	2. Offc.
5	Langhinrichs, Moritz	2. Offc.
6	Peine, Lutz G.	2. Offc.
7	Pohl, Klaus	Doctor
8	Hecht, Andreas	R. Offc.
9	Grafe, Jens	2. Eng.
10	Minzlaff, Hans-Ulrich	2. Eng.
11	Holst, Wolfgang	3. Eng.
12	Scholz, Manfred	Elec. Eng.
13	Himmel, Frank	ELO
14	Hüttebräucker, Olaf	ELO
15	Nasis, Ilias	ELO
16	Riess, Felix	ELO
17	Loidl, Rainer	Boatsw.
18	Reise, Lutz	Carpenter
19	Bäcker, Andreas	A.B.
20	Brickmann, Peter	A.B.
21	Gladow, Lothar	A.B.
22	Hagemann, Manfred	A.B.
23	Lamm, Gerd	A.B.
24	Scheel, Sebastian	A.B.
25	Schmidt, Uwe	A.B.
26	Wende, Uwe	A.B.
27	Winkler, Michael	A.B.
28	Preußner, Jörg	Storek.
29	Elsner, Klaus	Mot-man
30	Pinske, Lutz	Mot-man
31	Schüll, Norbert	Mot-man
32	Teichert, Uwe	Mot-man
33	Voy, Bernd	Mot-man
34	Müller-Homburg, R.-D.	Cook
35	Martens, Michael	Cooksmate
36	Silinski, Frank	Cooksmate
37	Czyborra, Bärbel	1. Stwdess

No.	Name	Rank
38	Wöckener, Martina	Stwdess/Kr.
39	Arendt, René	2. Steward
40	Gaude, Hans-Jürgen	2. Steward
41	Möller, Wolfgang	2. Steward
42	Silinski, Carmen	2. Stwdess
43	Sun, Yong Sheng	2. Steward
44	Yu, Kwok Yuen	Laundrym.

A.4 STATION LIST PS 81

	Date	Time (UTC)				Instrument	Begin / on seafloor				End / off seafloor				Rec.	Remarks
Station	2013	Begin	on ground	off off	End		Position	Latitude S	Longitude W	Water depth (m)	Latitude S	Longitude W	Water depth (m)		(m)	Penetration depth, sections,……
PS81/ 257-1	26.03.13	04:31			19:20	HS-calibr.	S	53°44.900	44°12.610	2603	53°44.538	43°54.252	2600			
PS81/ 257-2	26.03.13	05:30	05:39	07:21	07:22	CTD-1 / SVP-1	S	53°41.530	44°03.440	2278	53°41.520	44°03.510	2277			20 water samples
PS81/ 258-1	27.03.13		21:21			GC-1	S	54°20.210	36°23.280	168					6,72	GC 10m long, penetration 7m
PS81/ 258-2	27.03.13		22:11			GC-2	S	54°20.240	36°32.320	163					9,18	GC 10m long, penetration 10.5m
PS81/ 258-3	27.03.13		23:36			MUC-1 / SVP-2	S	54°20.220	36°23.330	178					6 x 0.4	SK: 0.47, 0.18; JaR: 0.38; BG: 0.38; GK: 0.39; Archiv frozen: 0.42
PS81/ 259-1	28.03.13		01:12			MUC-2	S	54°15.680	36°26.260	262					8 x 0.1	IM: 0.16; JaR: 0.13, 0.13; JeR: 0.10; BG: 0.15, 0.10; GK: 0.12; Archiv frozen: 0.12
PS81/ 259-2	28.03.13		02:11			GC-3	S	54°15.660	36°26.350	265					11,85	GC 15m long, penetration 12.5m
PS81/ 260-1	28.03.13		19:14			MUC-3 / SVP-3	S	54°14.800	36°34.930	216					7 x 0.2	JaR: 0.24, 0.25; JeR: 0.2; BG: 0.19, 0.25; GK: 0.24; Archiv frozen: 0.26
PS81/ 260-2	28.03.13		19:53			GC-4	S	54°14.780	36°34.980	216					4,45	GC 15m long, banana
PS81/ 260-3	28.03.13		21:09			GC-5	S	54°14.800	36°35.020	212					5,12	GC 10m long
PS81/ 261-1	28.03.13		22:15			GC-6	S	54°12.900	36°28.110	263					3,62	GC 10m long
PS81/ 262-1	28.03.13		23:03			GC-7	S	54°13.490	36°30.710	234					8,79	GC 10m long, penetration 10m

		Time (UTC)						Begin / on seafloor			End / off seafloor				
	Date		on	off		Instrument	Posit-ion	Latitude	Longitude	Water	Latitude	Longitude	Water	Rec.	Remarks
Station	2013	Begin	ground	off	End			S	W	depth (m)	S	W	depth (m)	(m)	Penetration depth, sections,…….
PS81/ 262-2	28.03.13		23:44			MUC-4	S	54°13.520	36°30.760	237				7 x 0.2	SK: 0.14; JaR: 0.15; JeR: 0.13; BG: 0.15; GK: 0.15, 0.15; Archiv frozen 0.19
PS81/ 263-1	29.03.13		00:57			GC-8	S	54°15.660	36°26.350	263				6,16	GC 10m long, penetration 10m
PS81/ 264-1	29.03.13		02:01			GC-9	S	54°19.370	36°24.050	176				4,25	GC 5m long, penetration 5m
PS81/ 265-1	29.03.13		03:10			GC-10	S	54°14.160	36°26.590	211				3,75	GC 5m long
PS81/ 266-1	29.03.13	05:24	05:31	05:31	05:35	SVP-4	S	54°00.440	36°12.660	248,6	54°00.390	36°12.770	247,3		The probe went down to 200m (based on rope length information). Max. depth reached at: 54°00.400 S, 36°12.770 W, 435.5m water depth.
PS81/ 267-1	29.03.13	21:47	22:24		22:47	MUC-5 / SVP-5	S	54°51.360	34°02.940	1320				0	TV-MUC. No penetration
PS81/ 268-1	31.03.13	09:12	09:39	11:39	11:55	OFOS-1	P	55°48.219	28°30.144	731	55°48.724	28°30.029	744		4 temperature loggers (MTL), Area: Quest Caldera. A temperature anomaly was recorded by all four loggers
PS81/ 268-2	31.03.13	11:21	12:37	15:11	15:29	OFOS-2	P	55°48.008	28°31.488	731	55°49.366	28°32.136	950		4 temperature loggers (MTL), Area: Quest Caldera

	Date	Time (UTC)				Instrument	Position	Begin / on seafloor			End / off seafloor			Rec.	Remarks
Station	2013	Begin	on ground	off	End			Latitude S	Longitude W	Water depth (m)	Latitude S	Longitude W	Water depth (m)	(m)	Penetration depth, sections,……
PS81/ 269-1	01.04.13	14:38	15:58	20:18	21:22	OFOS-3 / SVP-6	P	57°28.111	24°53.055	3715	57°28.132	24°53.114	3708		Failure (problem with the winch during the whole dive). SVP worked.
PS81/ 270-1	02.04.13	13:15	14:33	15:27	16:37	OFOS-4 / SVP-7	P	57°28.190	24°54.174	3659	57°28.285	24°54.174	3681		2 temperature loggers (MTL), Area: forearc. Optical signal failed after a short time on the seafloor.
PS81/ 271-1	05.04.13	15:22	17:02	18:28	18:30	CTD-2 / MIC-1	S	59°50.460	23°22.955	4792	59°50.431	23°23.050	4795	3 x 0.3	24 water samples. Sediment: SM: 0.25; GK: 0.27; Archive frozen 0.25 The target location was the location of a former core PS2283.
PS81/ 271-2	05.04.13		19:55			GC-11	S	59°50.450	23°22.990	4804				9,26	GC 10m long, 4 temperature loggers (MTL) mounted on the corer. Measured gradient: 14 °C/km.
PS81/ 271-3	05.04.13		23:01			MUC-6	S	59°50.430	23°23.030	4802				4 x 0.5	SK 0.45, 0.46; BG: 0.45; Archive frozen 0.57
PS81/ 271-4	05.04.13		02:22			PC-1	S	59°50.390	23°23.050	4797				18,48	PC 20m long, penetration 20m, TC 0.1-1.1m

		Time (UTC)						Begin / on seafloor			End / off seafloor				
	Date		on	off		Instrument	Posit-ion	Latitude	Longitude	Water	Latitude	Longitude	Water	Rec.	Remarks
Station	2013	Begin	ground	off	End			S	W	depth (m)	S	W	depth (m)	(m)	Penetration depth, sections,…….
PS81/ 272-1	06.04.13		14:47			GC-12	S	59°28.510	25°46.560	2869				0,14	GC 10m long, 7 temperature loggers (MTL) mounted on the corer but almost no penetration
PS81/ 272-2	06.04.13		16:33			MUC-7 / SVP-8	S	59°28.480	25°46.590	2872				0	No recovery, all corers empty
PS81/ 273-1	07.04.13	09:33	10:35	10:56	12:08	OFOS-5 / SVP-9	P	57°02.028	26°02.221	3025	57°02.063	26°02.225	3026		3 temperature loggers (MTL), Area: forearc. Optical signal failed after a short time on the seafloor.
PS81/ 274-1	07.04.13	16:08	18:01	21:14	21:17	CTD-3	P	57°19.680	25°29.009	3709	57°19.661	25°29.186	3725		24 water samples. Posidonia navigation is available to track CTD dive
PS81/ 274-2	07.04.13		22:41			MUC-8	S	57°19.600	25°29.090	3715				0	No recovery, all corers empty
PS81/ 274-3	08.04.13	01:18	02:33	04:10	05:18	OFOS-6	P	57°19.625	25°28.910	3723	57°19.644	25°29.053	3720		3 temperature loggers (MTL), Area: forearc, potential flare. This dive was done with the MARUM TV-Sled.
PS81/ 275-1	08.04.13	19:07	19:13	21:07	21:20	OFOS-7	S	55°56.426	28°05.728	60	55°57.097	28°06.693	526		5 temperature loggers (MTL), Area: Protector Shoal. This dive was done with the MARUM TV-Sled, Posidonia did not work during the entire dive.

	Date	Time (UTC)				Instrument	Position	Begin / on seafloor			End / off seafloor			Rec.	Remarks
Station	2013	Begin	on ground	off	End			Latitude S	Longitude W	Water depth (m)	Latitude S	Longitude W	Water depth (m)	(m)	Penetration depth, sections,.....
PS81/ 276-1	08.04.13	23:04	23:23	01:30	01:44	OFOS-8	P	55°48.542	28°29.687	716	55°48.652	28°29.516	717		5 temperature loggers (MTL), Area: Quest Caldera. This dive was done with the MARUM TV-Sled, Chimney-like structures and temperature anomalies were observed.
PS81/ 277-1	09.04.13	03:04	03:19	03:33	03:34	CTD-4	S	55°46.000	28°19.290	1413	55°46.010	28°19.280	1414		16 water samples. No Posidonia
PS81/ 277-2	09.04.13	03:55	04:13	04:44	04:44	MN-1	S	55°46.020	28°19.340	1404	55°46.050	28°19.310	1416		
PS81/ 277-3	09.04.13	04:55	05:15	05:47	05:47	MN-2	S	55°46.030	28°19.250	1415	55°46.000	28°19.310	1397		
PS81/ 277-4	09.04.13	05:56	06:17	06:48	06:48	MN-3	S	55°45.970	28°19.300	1415	55°45.990	28°19.290	1416		
PS81/ 277-5	09.04.13	07:00	07:22	07:46	07:46	MN-4	S	55°45.990	28°19.240	1426	55°46.070	28°19.180	1413		
PS81/ 277-6	09.04.13	08:05	08:32	09:01	09:05	MN-5	S	55°45.970	28°19.240	1415	55°45.990	28°19.260	1414		
PS81/ 277-7	09.04.13		09:54			MUC-9	S	55°45.970	28°19.210	1433				5 x 0.2	BL: 0.157, 0.155, 0.156; 0.114; 0.151
PS81/ 277-8	09.04.13		10:59			MUC-10	S	55°45.940	28°19.180	1429				1 x 0.04	BG: 0.04

		Time (UTC)						Begin / on seafloor			End / off seafloor				
	Date		on	off		Instrument	Posit-ion	Latitude	Longitude	Water	Latitude	Longitude	Water	Rec.	Remarks
Station	2013	Begin	ground	off	End			S	W	depth (m)	S	W	depth (m)	(m)	Penetration depth, sections,…….
PS81/ 278-1	09.04.13	13:16	13:33	15:31	15:45	OFOS-9	P	55°46.711	28°47.601	618	55°46.873	28°47.459	779		5 temperature loggers (MTL), Area: Unnamed submarine volcano This dive was done with the MARUM TV-Sled.
PS81/ 279-1	10.04.13	11:08	11:18	11:38	11:38	MN-6	S	54°41.673	34°35.655	1275	54°41.718	34°35.585	1277,7		Station for the bird watcher group
PS81/ 280-1	10.04.13		18:55			GC-13	S	54°27.440	35°50.53	236				9,09	GC 10m long, 8 temperature loggers (MTL) mounted on the corer. 5 MTL loggers failed to start recording, and 1 failed during the coring.
PS81/ 280-2	10.04.13		19:49			MUC-11 / SVP-10	S	54°27.440	35°50.550	237				8 x 0.3	SK: 0.30, 0.26; JaR: 0.27, 0.29; BL 0.05; IM 0.05-0.29; BG: 0.27; GK: 0.30; Archiv frozen: 0.29
PS81/ 281-1	10.04.13	23:50	00:09	00:30	00:30	CTD-5	P	54°12.124	36°27.201	255	54°12.110	36°27.250	257		24 water samples. Target: Cumberland Bay Flare
PS81/ 281-2	11.04.13		01:02			GC-14	S	54°12.140	36°27.210	261				8,64	GC 10m long, 8 temperature loggers (MTL) mounted on the corer. Measured gradient: 52.6 °C/km

	Date	Time (UTC)				Instrument	Begin / on seafloor				End / off seafloor			Rec.	Remarks
Station	2013	Begin	on ground	off	End		Position	Latitude S	Longitude W	Water depth (m)	Latitude S	Longitude W	Water depth (m)	(m)	Penetration depth, sections,.....
PS81/ 282-1	11.04.13	11:27	11:33	11:43	11:45	CTD-6	S	54°21.910	36°21.950	109	54°21.920	36°21.870	111		24 water samples. No Posidonia. Target: Cumberland East near glacier
PS81/ 283-1	11.04.13		17:19			GC-15	S	54°12.920	36°32.280	193				4,66	GC 5m long, penetration 5m
PS81/ 284-1	11.04.13		18:48			GC-16	S	54°15.910	36°26.230	259				8,38	GC 10m long, penetration 10m. 8 temperature loggers (MTL) mounted on the corer (1 failed to record).Measured gradient: 46.9°C/km
PS81/ 284-2	11.04.13	20:21	20:34	21:47	21:57	MUC-12	P	54°15.928	36°26.220	269	54°15.930	36°26.221	269	8 x 0.3	TV-MUC. SK 0.30, 0.25; BL: 0.29, 0.27; BG: 0.28, 0.27; GK: 0.24; Archiv frozen 0.26, Cores taken at S54°15.930, W36°26.221
PS81/ 284-3	11.04.13	22:13	22:15	22:44	22:45	CTD-7	P	54°15.916	36°26.230	269	54°15.942	36°26.216	270		24 water samples.
PS81/ 285-1	11.04.13	23:26	23:36	00:59	01:05	OFOS-10	P	54°12.138	36°27.187	265	54°12.202	36°27.344	264		5 temperature loggers (MTL), Area: Cumberland Bay Flare
PS81/ 286-1	12.04.13	19:03	19:06	19:31	19:32	CTD-8	S	54°08.988	36°22.421	272	54°09.010	36°22.330	272		24 water samples. No Posidonia.
PS81/ 287-1	13.04.13		07:13			GC-17	S	53°41.710	38°19.350	240				0,03	GC 5m long

		Time (UTC)						Begin / on seafloor			End / off seafloor				
	Date		on	off		Instrument	Posit-ion	Latitude	Longitude	Water	Latitude	Longitude	Water	Rec.	Remarks
Station	2013	Begin	ground	off	End			S	W	depth (m)	S	W	depth (m)	(m)	Penetration depth, sections,…….
PS81/ 288-1	13.04.13		08:41			GC-18	S	53°46.170	38°08.420	374				7,56	GC 10m long, 8 temperature loggers (MTL) mounted on the corer. Measured gradient: 32 °C/km
PS81/ 289-1	16.04.13		01:59			PC-2	S	53°00.275	57°53.250	671				12,39	PC 20m long, 15 m penetration, from 2.10 to 3.10 m liner imploded, TC 0.22 m

OFOS	Ocean floor observation System
GC	Gravity Corer
PC	Piston corer
GKG	Box corer
DR	Dredge
MUC	Multicorer
CTD/RO	CTD/rosette
HS_PS	HYDROSWEEP/ PARASOUND survey
MIC	Mini Corer
SVP	Sound Velocity Profile
MN	Multi-Net

* P = POSIDONIA S = ship position T = target position

Sediment (MUC, MIC) sampling by:

SK: Sabine Kasten (porewater, geochemistry)

JaR: Janet Rethemeyer (14C-dating, lipids)

JeR: Jenny Roberts (benthic foraminifers)

BG: Birgit Glückselig (silicate microfossils)

GK: Gerhard Kuhn (sedimentology, bulk geochemistry)

IM: Inna Morgunova (DOM)

A.5 PS81 CORE DESCRIPTIONS

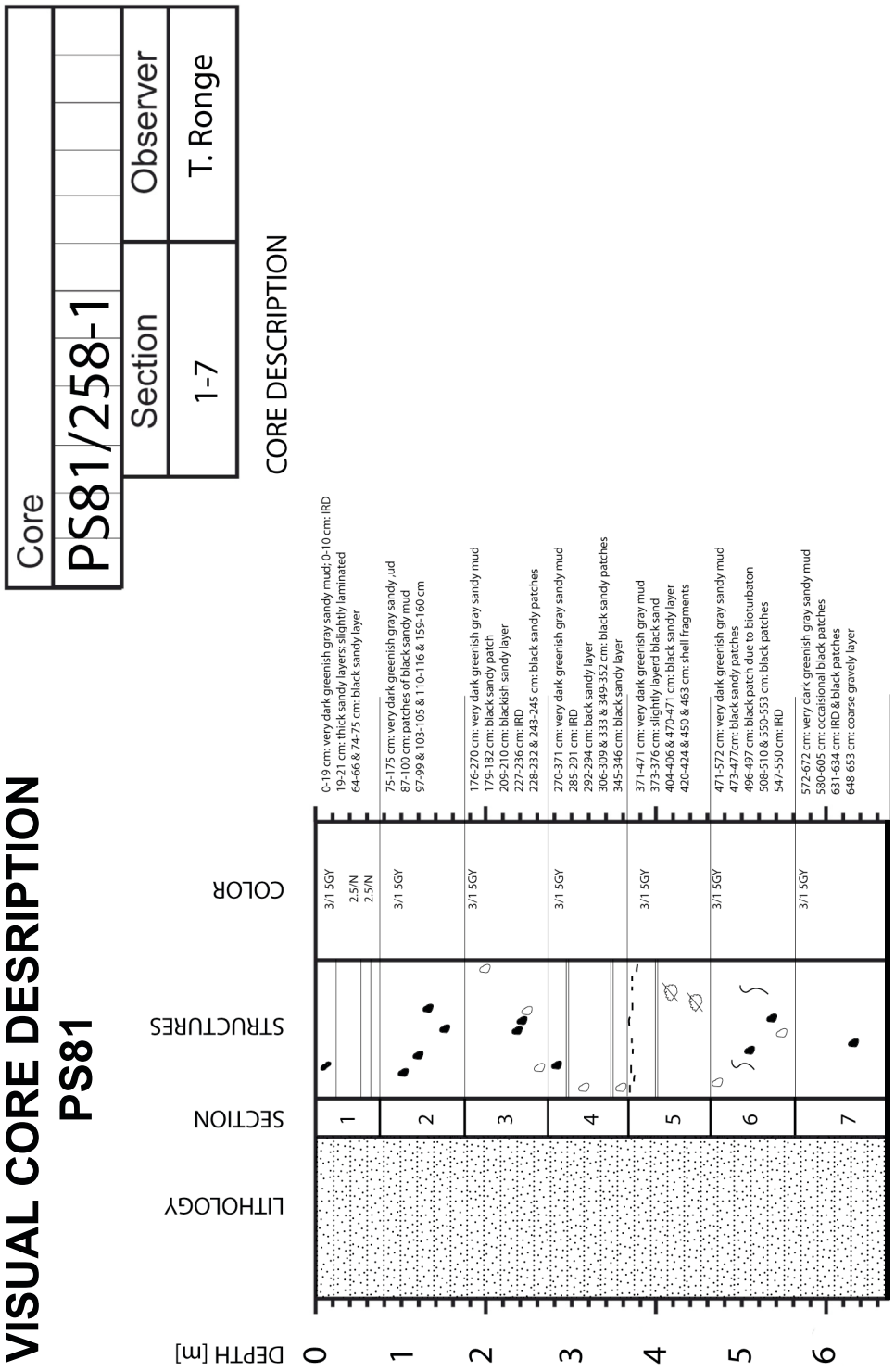
VISUAL CORE DESRIPTION
PS81
Core
PS81/258-1
Section
1-7
Observer
T. Ronge
CORE DESCRIPTION
DEPTH [m]
LITHOLOGY
SECTION
STRUCTURES
COLOR
0-19 cm: very dark greenish gray sandy mud; 0-10 cm: IRD
19-21 cm: thick sandy layers; slightly laminated
64-66 & 74-75 cm: black sandy layer
75-175 cm: very dark greenish gray sandy ,ud
87-100 cm: patches of black sandy mud
97-99 & 103-105 & 110-116 & 159-160 cm
176-270 cm: very dark greenish gray sandy mud
179-182 cm: black sandy patch
209-210 cm: blackish sandy layer
227-236 cm: IRD
228-232 & 243-245 cm: black sandy patches
270-371 cm: very dark greenish gray sandy mud
285-291 cm: IRD
292-294 cm: back sandy layer
306-309 & 333 & 349-352 cm: black sandy patches
345-346 cm: black sandy layer
371-471 cm: very dark greenish gray mud
373-376 cm: slightly layerd black sand
404-406 & 470-471 cm: black sandy layer
420-424 & 450 & 463 cm: shell fragments
471-572 cm: very dark greenish gray sandy mud
473-477cm: black sandy patches
496-497 cm: black patch due to bioturbaton
508-510 & 550-553 cm: black patches
547-550 cm: IRD
572-672 cm: very dark greenish gray sandy mud
580-605 cm: occaisional black patches
631-634 cm: IRD & black patches
648-653 cm: coarse gravely layer

VISUAL CORE DESCRIPTION
PS/81

Core	
PS81/264-1	
Section	Observer
1-5	T. Ronge

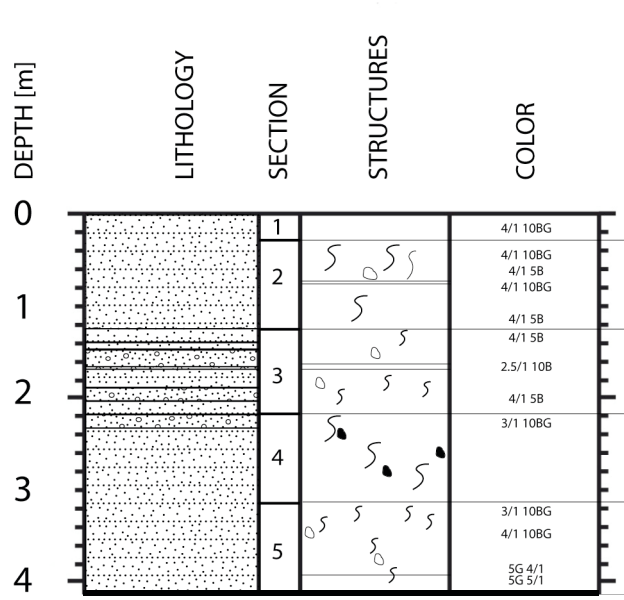

CORE DESCRIPTION

0-25 cm: dark greenish gray mud; 23-25 cm black patches

25-103 cm: dark greenish gray mud; moderate bioturbation indicated by black & dark bluish gray patches
61-70 cm: black patch & dark bluish gray layer
103-125 cm: dark bluish gray mud; slight bioturbation

125-173 cm: slightly bioturbated dark bluish gray sandy mud
135-138 & 191-195 cm: black patch
142-144 & 155-157 &179-183 & 215-221 cm: very coarse sandy to gravely layers
173-179 cm: bluish black mud
215-218 cm: IRD

225-227 cm: gravely layer
227-325 cm: very dark greenish gray sandy mud; moderate biotrubation indicated by black patches
256-257 & 267-269 & 315-318 cm: IRD

325-336 cm: severly bioturbated, very dark greenish gray mud
336-415 cm: severly bioturbated dark greenish gray mud
350-370 cm: section showing an accumulation of black patches
377-379 & 400-402cm: black patch
410-411 cm: black layer

VISUAL CORE DESCRIPTION
PS/81

Core	
PS81/271-2	
Section	Observer
1-10	T. Ronge

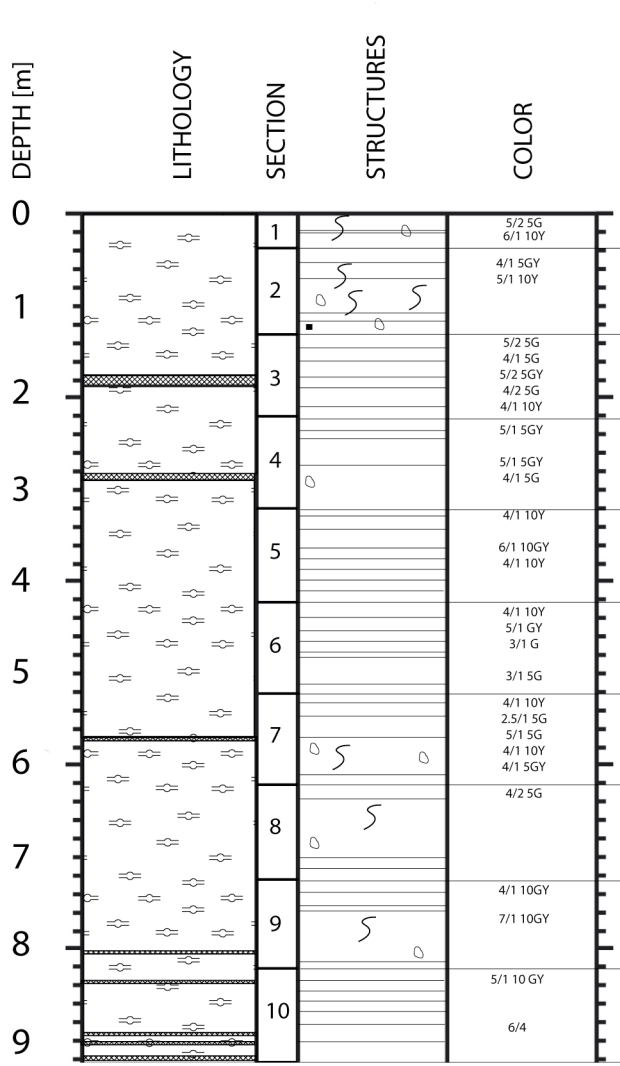

CORE DESCRIPTION

0-16cm slightly bioturbated grayish green diatom ooze (DO); 16-18cm greenish gray DO; 16-30cm severly bioturbated DO; 30-31cm greenish black DO (ash?)
30-38cm dark greenish gray DO with bioturbated black patches
38-42cm dark greenish gray DO; 42-58cm bioturbated greenish DO
58-60cm greenish black DO (ash?); 60-90cm bioturbated greenish gray DO; 73-76cm & 88-89cm black patch
90-92cm very dark grayish green DO; 92-99cm bioturbated greenish gray DO; 99-112cm very dark grayish green DO
112-118cm olive gray DO; 118-138cm bioturbated greenish gray DO; 118-120cm black patches / layers; 130-131cm fragment of volcanic glas

138-143cm grayish green DO; 143-146cm dark greenish gray DO; 146-151cm greenish gray DO; 151-152cm olive gray DO; 152-155cm greenish black DO
155-170cm grayish green DO several layers of greenish black DO
170-178cm greenish black DO; 178-181cm dark greenish gray ash layer; 181-191cm light gray DO
191-200cm dark greenish gray DO; 200-212cm olive bioturbated DO; 210-211cm black layer of DO
211-216cm pale yellow DO; 216-238cm greenish gray DO

238-287cm layered greenish gray DO layers - dark greenish gray
287-304cm fine laminated greenish gray ash/mud
304-332cm greenish gray DO
415-318cm darker patch of DO
332-338cm dark greenish gray DO

338-382cm layerd dark greenish gray DO, several layers of dark greenish gray & greenish black DO
382-384cm greenish gray DO
384-438cm layerd dark greenish gray DO, mm to cm thick layers of darker & olive gray & light greenish gray DO

438-449cm layered dark greenish gray DO
449-452cm less fluffy, greenish gray DO
452-456cm les fluffy very dark greenish gray gray DO
456-493cm laminated greenish gray DO
493-501cm very dark greenish gray DO; 501-526cm laminated greenish gray to dark greenish gray DO

526-529cm dark greenish gray DO; 529-531cm greenish black DO; 531-601cm greenish gray DO, several cm thick layers; 560-562cm very dark gray DO
566-572cm very dark greenish gray DO; 584cm mm thick black layer; 585-591cm dark patches - slightly bioturbated
601-612cm dark greenish gray DO; 612-613cm greenish black DO
613-626cm slightly layerd dark greenish gray DO

626-666cm grayish green DO, dark layers @ 634-635cm; 642-643cm & 658-659cm
666-677cm bioturbated grayish green DO
677-681cm cm thick dark green layers; 681-726cm grayish green DO; 687cm dark patch - bioturbation; 691-693cm dark green layer
693-700cm minor bioturbation
706-709cm very dark greenish gray layer

726-826cm layerd dark greenish gray DO
728-729cm dark DO; 747-749cm dark DO layer; 753-754 light greenish gray layer; 765-766cm dark layer; 771-779cm slightly bioturbated
780-781cm dark layer; 785-789cm dark layer
802-807cm dark DO layer; 808-809cm dark patch
811cm black layer - ash?

826-926cm layerd greenish gray DO
836-837cm light greenish gray layer; 854-855cm pronounced ash/lapilli layer; 864-868cm dark greenish gray layer
879-881cm pale olive layer; 881-887cm dark layer
889cm dark patch; 902-904cm ash/lapilli layer; 906-907cm ash/lapilli layer
916-919cm ash/lapilli layer

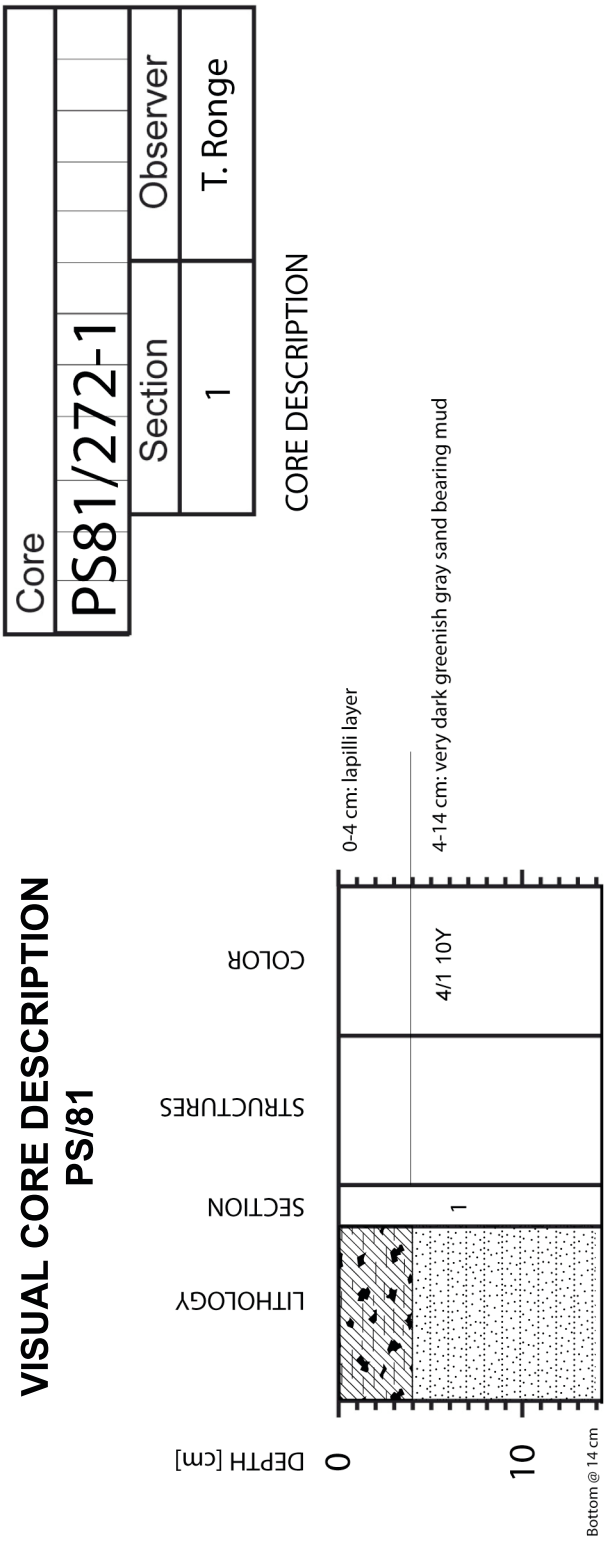
Core
PS81/272-1
Section
1
Observer
T. Ronge
CORE DESCRIPTION
VISUAL CORE DESCRIPTION
PS/81
LITHOLOGY
SECTION
STRUCTURES
COLOR
DEPTH [cm]
0
10
1
4/1 10Y
0-4 cm: lapilli layer
4-14 cm: very dark greenish gray sand bearing mud
Bottom @ 14 cm

VISUAL CORE DESCRIPTION
PS81

Core		
PS81/284-1		
	Section	Observer
	1-9	T. Ronge

CORE DESCRIPTION

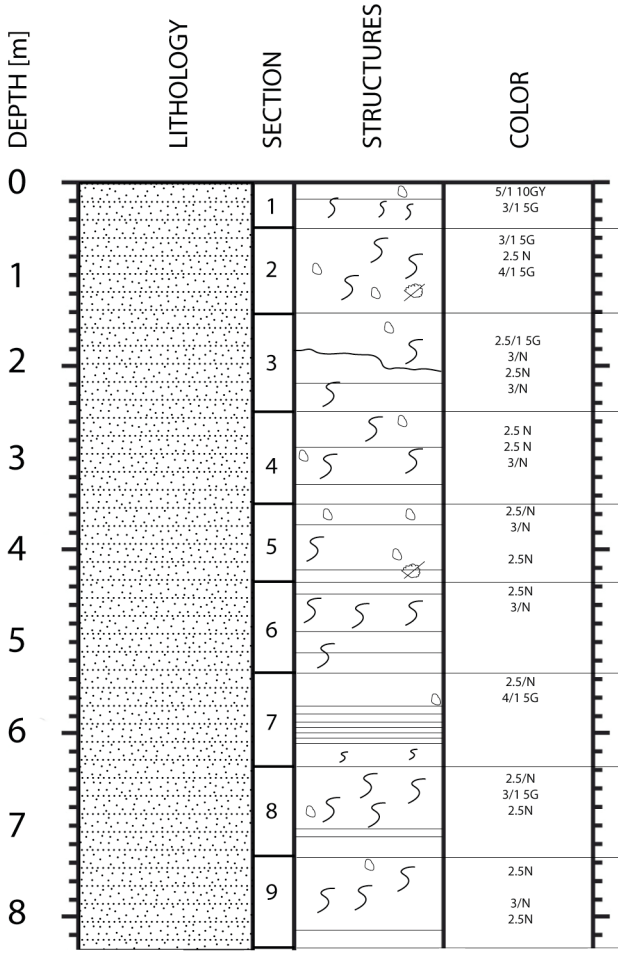

0-7cm greenish gray mud
7-48cm severly bioturbated very dark greenish gray mud

48-122cm severly bioturbated very dark greenish gray mud
75cm IRD
119-121cm black patch; 122-148cm moderatly bioturbated greenish gray mud
133-135cm shell fragments

148-180cm bioturbated greenish black mud
153-155cm & 162-168cm black patches
180-200cm bioturbated very dark gray mud
200-213cm black mud
213-248cm severly bioturbated very gray mud

248-273cm bioturbated black mud; 266-267cm
273-319cm bioturbated black mud, slightly lighter than preceeding section, several holes - gas?
277-278cm black layer
288-294cm black patches
319-348cm severly bioturbated very dark gray mud

348-370cm bioturbated black mud; 365-366cm outgassing structure
370-404cm very dark gray mud, occaisional outgassing channels; 377-384cm black patches; 390-392cm IRD
404-405cm black layer; 405-426cm severly bioturbated very dark gray mud; 417-424cm black patch
417-419cm IRD; 426-438cm bioturbated black mud; 435-436cm shell fragment

438-441cm bioturbated black mud
441-466cm severly bioturbated very dark gray mud
466-510cm slightly bioturbated very dark gray mud
505-515cm IRD
510-538cm severly bioturbated very dark gray mud

538-548cm black mud
548-571cm bioturbated dark greenish gray mud; 562-568cm IRD
571-615cm dark greenish gray mud; several ca. 1cm spaced black layers - ash?
615-638cm bioturbated very dark gray mud

638-685cm severly bioturbated black mud
652-658cm black patches
685-701cm bioturbated dark greenish gray mud
701-738cm bioturbated black mud
719-724cm black & dark gray patches

738-770cm severly bioturbated black mud, several black patches
738-740cm IRD
770-801cm bioturbated very dark gray mud
801-838cm moderatly bioturbated black mud

A.6 CTD STATIONS, WATER DEPTHS AND SAMPLES

PS81/257-2	**CTD-1 / SVP-1**	**26.03.13**
Lat	53°41.530	
Long	44°03.440	
Depth	2278	

20 water samples

Sampler	**True depth**	**CH4**	**CH4 oxi**	**Si**	**Chl**
1	2200.0	X		X	
2	2200.0				
3	2003.0			X	
4	1752.0			X	
5	1500.7			X	
6	1500.7			X	
7	1250.8			X	
8	1001.2			X	
9	700.9	X	X		
10	700.9			X	
11	500.0			X	
12	301.2			X	
13	201.7			X	
14	152.6			X	X
15	99.7			X	X
16	90.7				X
17	71.0				X
18	49.9			X	X
19	30.1				X
20	9.5				X
21	9.5				X
22	9.5				
23	9.5				
24	9.5				

PS81/271-1 CTD-2 / MIC-1 05.04.13

Lat 59°50.460

Long 23°22.955

Depth 4792

24 water samples. Sediments recovered in 3 out of the 4 MIC corers.

The target location was the location of a former core PSX15 GC2283.

Sampler	True depth	CH4	CH4 oxi	Si	Chl	Nutrients	Microbiol	14C	O2
1	4786.0	X	X			X			X
2	4786.0						X		X
3	4766.0	X	X			X			X
4	4731.0	X				X		X	X
5	4499.7	X		X		X			X
6	3995.0	X		X		X			X
7	3599.5	X		X		X			X
8	3300.0	X		X		X			X
9	3003.0	X	X	X		X			X
10	2700.8	X		X		X		X	X
11	2349.3	X		X		X			X
12	2100.5	X		X		X			X
13	1800.2	X		X		X			X
14	1503.0	X		X		X			X
15	1198.0	X	X	X		X		X	X
16	902.0	X		X		X			X
17	600.0	X		X		X			X
18	400.0	X	X	X		X			X
19	285.2	X	X	X		X			X
20	285.2						X		X
21	150.7	X		X	X	X		X	X
22	104.5	X		X	X	X			X
23	50.3	X	X	X	X	X			X
24	50.3						X		X

PS81/274-1	**CTD-3**	**07.04.13**
Lat	57°19.680	
Long	25°29.009	
Depth	3709	

24 water samples. Posidonia navigation is available to track CTD dive

Sampler	True depth	CH4	CH4 oxi	Si	Chl	Nutrients	Microbiol.	14C	Metals
1	3711.0						X		
2	3711.0		X						
3	3698.0								
4	3698.0								
5	3696.0								
6	3705.0								
7	3704.0								
8	3706.0								
9	3706.0								
10	3707.0								
11	3706.0								
12	3697.0								
13	3690.0								
14	3685.0								
15	3702.0						X		
16	3702.0		X			X			X
17	3703.0					X			X
18	3703.0					X			X
19	3699.0		X			X			X
20	3696.0		X			X			X
21	3686.0		X			X			X
22	3684.0		X			X			X
23	3676.0		X			X			X
24	3666.0		X			X			X

PS81/277-1	CTD-4	4/9/2013
Lat	57°19.680	
Long	25°29.009	
Depth	1412	

Sampler	True depth	CH4	CH4 oxi	Si	Chl	Nutrients	Microbiol.	14C	Metals
1	500.1			X					
2	500.1								
3	500.1								
4	301.2			X					
5	301.2								
6	301.2								
7	201.3			X					
8	201.3								
9	201.3								
10	100.5			X					
11	100.5								
12	100.5								
13	50.3			X					
14	50.3								
15	50.3								
16	10.0			X					
17	10.0								
18	10.0								
19	10.0								
20	10.0								
21	10.0								
22	10.0								
23	10.0								
24	10.0								

PS81/281-1	CTD-5	10.04.13
Lat	54°12.124	
Long	36°27.201	
Depth	255	

24 water samples. No Posidonia.
Target: Cumberland East near glacier

Sampler	True depth	CH4	CH4 oxi	Si	Chl	Nutrients	Microbiol.	14C	Metals	18O	13C	Salt
1	249.2						X					
2	249.2	X	X	X		X			X	X	X	X
3	247.0	X				X				X	X	X
4	244.0	X	X			X			X	X	X	X
5	238.9	X				X				X	X	X
6	233.6	X	X			X			X	X	X	X
7	224.7	X				X				X	X	X
8	215.1	X	X			X				X	X	X
9	200.5	X		X		X				X	X	X
10	189.3					X				X	X	X
11	180.0	X	X			X				X	X	X
12	170.4					X				X	X	X
13	159.5	X				X				X	X	X
14	149.9			X		X				X	X	X
15	140.2	X	X			X			X	X	X	X
16	131.0					X				X	X	X
17	115.3	X				X				X	X	X
18	100.1			X		X				X	X	X
19	75.3	X	X			X			X	X	X	X
20	50.2			X		X				X	X	X
21	30.3					X				X	X	X
22	19.8	X				X				X	X	X
23	10.8	X	X	X		X			X	X	X	X
24	10.8						X					

PS81/282-1	**CTD-6**	**11.04.13**
Lat	54°21.910	
Long	36°21.950	
Depth	109	

24 water samples. No Posidonia.
Target: Cumberland East near glacier

Sampler	True depth	CH4	CH4 oxi	Si	Chl	Nutri ents	Micro biol.	14C	Metals	18O	13C	Salt
1	99.2						X					
2	99.2	X	X			X			X	X	X	X
3	95.3	X				X				X	X	X
4	90.4	X	X			X			X	X	X	X
5	85.0	X				X				X	X	X
6	80.3					X				X	X	X
7	74.8	X	X			X			X	X	X	X
8	69.5					X				X	X	X
9	59.7					X				X	X	X
10	50.1	X	X			X			X	X	X	X
11	39.9					X				X	X	X
12	29.9					X				X	X	X
13	19.8	X	X			X			X	X	X	X
14	9.8	X	X			X			X	X	X	X
15	9.8						X					
16	9.8											
17	9.8											
18	9.8											
19	9.8											
20	9.8											
21	9.8											
22	9.8											
23	9.8											
24	9.8											

PS81/284-3	CTD-7	11.04.13
Lat	54°15.916	
Long	36°26.230	
Depth	269.0	

24 water samples.

Sampler	True depth	CH4	CH4 oxi	Si	Chl	Nutrients	Micro-biol.	14C	Metals	18O	13C	Salt
1	253.7						X					
2	253.7	X	X			X				X	X	X
3	249.8	X		X		X				X	X	X
4	245.1	X	X			X				X	X	X
5	235.3	X	X			X				X	X	X
6	225.2	X				X				X	X	X
7	215.4	X	X			X				X	X	X
8	200.1	X				X				X	X	X
9	189.7			X		X				X	X	X
10	179.9	X	X			X				X	X	X
11	170.2					X				X	X	X
12	160.2	X				X				X	X	X
13	150.2					X				X	X	X
14	140.0	X	X			X				X	X	X
15	129.8			X		X				X	X	X
16	114.4					X				X	X	X
17	100.3	X	X	X		X				X	X	X
18	75.0					X				X	X	X
19	50.2			X		X				X	X	X
20	30.1					X				X	X	X
21	20.1					X				X	X	X
22	10.1	X	X			X				X	X	X
23	10.2						X					
24	10.2			X								

PS81/286-1	**CTD-8**	**12.04.13**
Lat	54°08.988	
Long	36°22.421	
Depth	272	

24 water samples. No Posidonia.

Sampler	True depth	CH4	CH4 oxi	Si	Chl	Nutri ents	Micro biol.	14C	Metals	18O	13C	Salt
1	262.5						X					
2	262.5	X	X			X		X	X	X	X	X
3	262.5					X				X	X	X
4	259.0					X				X	X	X
5	250.5	X	X	X		X			X	X	X	X
6	240.5					X				X	X	X
7	230.2	X	X			X				X	X	X
8	220.0					X				X	X	X
9	210.0	X				X				X	X	X
10	200.0	X	X	X		X			X	X	X	X
11	179.3					X				X	X	X
12	160.0	X	X			X			X	X	X	X
13	150.0			X		X				X	X	X
14	140.7	X				X				X	X	X
15	119.9					X				X	X	X
16	100.4	X	X	X		X			X	X	X	X
17	80.5					X				X	X	X
18	60.0					X				X	X	X
19	50.0	X	X	X		X			X	X	X	X
20	40.0					X				X	X	X
21	19.9			X		X				X	X	X
22	10.6	X	X			X		X	X	X	X	X
23	10.6						X					
24	10.6											

Die "Berichte zur Polar- und Meeresforschung" (ISSN 1866-3192) werden beginnend mit dem Heft Nr. 569 (2008) als Open-Access-Publikation herausgegeben. Ein Verzeichnis aller Hefte einschließlich der Druckausgaben (Heft 377-568) sowie der früheren **"Berichte zur Polarforschung"** (Heft 1-376, von 1981 bis 2000) befindet sich im open access institutional repository for publications and presentations (**ePIC**) des AWI unter der URL http://epic.awi.de. Durch Auswahl "Reports on Polar- and Marine Research" (via "browse"/"type") wird eine Liste der Publikationen sortiert nach Heftnummer innerhalb der absteigenden chronologischen Reihenfolge der Jahrgänge erzeugt.

To generate a list of all Reports past issues, use the following URL: http://epic.awi.de and select "browse"/"type" to browse "Reports on Polar and Marine Research". A chronological list in declining order, issues chronological, will be produced, and pdf-icons shown for open access download.

Verzeichnis der zuletzt erschienenen Hefte:

Heft-Nr. 656/2012 — "The Expedition of the Research Vessel 'Sonne' to the Manihiki Plateau in 2012 (So 224)", edited by Gabriele Uenzelmann-Neben

Heft-Nr. 657/2012 — "The Expedition of the Research Vessel 'Polarstern' to the Antarctic in 2011 (ANT-XXVIII/1) ", edited by Saad El Naggar

Heft-Nr. 658/2013 — "The Expedition of the Research Vessel 'Polarstern' to the Arctic in 2012 (ARK-XXVII/2)", edited by Thomas Soltwedel

Heft-Nr. 659/2013 — "Changing Polar Regions - 25th International Congress on Polar Research, March 17-22, 2013, Hamburg, Germany, German Society for Polar Research", edited by Eva-Maria Pfeiffer, Heidemarie Kassens, and Ralf Tiedeman

Heft-Nr. 660/2013 — "The Expedition of the Research Vessel 'Polarstern' to the Arctic in 2012 (ARK-XXVII/1)", edited by Agnieszka Beszczynska-Möller

Heft-Nr. 661/2013 — "The Expedition of the Research Vessel 'Polarstern' to the Antarctic in 2012 (ANT-XXVIII/3)", edited by Dieter Wolf-Gladrow

Heft-Nr. 662/2013 — "Climate Change in the Marine Realm: An international summer school in the framework of the European Campus of Excellence", edited by Angelika Dummermuth and Klaus Grosfeld

Heft-Nr. 663/2013 — "The Expedition of the Research Vessel 'Polarstern' to the Arctic in 2012 (ARK-XXVII/3)", edited by Antje Boetius

Heft-Nr. 664/2013 — "Russian-German Cooperation SYSTEM LAPTEV SEA: The Expeditions Laptev Sea - Mamontov Klyk 2011 & Buor Khaya 2012", edited by Frank Günther, Pier Paul Overduin, Aleksandr S. Makarov, and Mikhail N. Grigoriev

Heft-Nr. 665/2013 — "The Expedition of the Research Vessel 'Polarstern' to the Antarctic in 2013 (ANT-XXIX/3)", edited by Julian Gutt

Heft-Nr. 666/2013 — "The Expedition of the Research Vessel 'Polarstern' to the Antarctic in 2013 (ANT-XXIX/5)", edited by Wilfried Jokat

Heft-Nr. 667/2013 — "The Sea Ice Thickness in the Atlantic Sector of the Southern Ocean", by Axel Behrendt

Heft-Nr. 668/2013 — "The Expedition of the Research Vessel 'Polarstern' to the Antarctic in 2013 (ANT-XXIX/4)", edited by Gerhard Bohrmann